Functional analysis of the unconventional prefoldin URI-1 in Caenorhabditis elegans

Inauguraldissertation

zur
Erlangung der Würde eines Doktors der Philosophie
vorgelegt der
Philosophisch-Naturwissenschaftlichen Fakultät
der Universität Basel

von

Christine Parusel
aus Frankfurt am Main, Deutschland

Zürich, 2005

Genehmigt von der Philosophisch-Naturwissenschaftlichen Fakultät auf Antrag von Prof. Dr. Denis Monard, Prof. Dr. Wilhelm Krek und Prof. Dr. Michael O. Hengartner.

Basel, den 20. September 2005

Prof. Dr. Hans-Jakob Wirz
Dekan

Table of Contents

This thesis is dedicated to

my grandfather,

Alois Parusel,

who died as I was 18
on the 25. Feb. 1993 at the age of 88

and my grandmother

María Fernandez de la Puente,

who died during my PhD studies
on the 26. Jan 2004 at the age of 94

I will always remember you

Acknowledgments

To my supervisor Prof. Dr. Wilhelm Krek for the opportunity of doing this work in his laboratory. I appreciate having been given the freedom to largely run my own research. His trust and support made this doctoral work possible.

Thanks to Prof. Dr. Michael O. Hengartner and Prof. Dr. Denis Monard for supporting me through this doctoral thesis and critical reading of the thesis. I appreciate the time and effort and especially the flexibility concerning the arrangement of the defense appointment.

I would like to take this opportunity to extend my sincere gratitude to Prof. Dr. Monica Gotta whose support, patience and motivation influenced this doctoral thesis greatly. I am grateful for all the helpful discussions, for teaching me how to write and present science, and for her engaged personal support.

A big thank to Dr. Ian J. Frew, for all the input and support and especially for getting me through the last days of this thesis writing.

Thanks to Dr. Yandong Shi who helped me to think in genetic terms and Dr. Jean-Claude Labbé for help with the mutant.

Finally, I would like to thank all members of the Gotta and the Krek labs for helpful discussions and Andrea Bucceri from the Thoma lab for help with the UV experiments.

Last but not least, I would like to thank my friends who have stood by me. Thank you Dr. Beatrix Otte, David Lehmann, Jasenka Knezovic, Rea Wieland, Rebecca Raddatz and Dr. Silke Robatzek.

The apoptotic cell corpse and HUS-1::GFP foci counts described in this thesis were performed by our collaboration partner Dr. Ekat A. Kritikou.

1 Summary

URI is a conserved unconventional member of the prefoldin family of molecular chaperones that, at the biochemical and biological level, is multifunctional. It interacts with several proteins with key roles in transcriptional control, including the RPB5 core subunit of RNA pol II and the TIP49/TIP48 ATPases, components of various chromatin-remodeling complexes. More recently, URI has also been shown to interact with the parathyroid tumor suppressor parafibromin, a component of the PAF1 complex involved in histone methylation and cell cycle control. Notably, there is evidence from functional studies in yeast and human cells that URI acts downstream of the target-of-rapamycin (TOR) and the insulin-sensitive PI3K signaling pathways to control rapamycin-sensitive transcriptional programs. Thus, it appears that URI participates in signaling circuits dedicated, at least in part, to the integration of diverse metabolic and hormonal cues to control cell growth and division.

This thesis demonstrates that the *uri-1* orthologue in *C. elegans* is highly expressed at the mRNA and protein level in the germ line and is critically important for germ cell proliferation. More specifically, we observed that URI-1-deficient cells arrest at prometaphase of the mitotic division cycle and display DNA breakage, as evidenced by TUNEL staining and the appearance of HUS-1::GFP foci formation, implying that one or more functions of URI-1 might be linked, directly or indirectly, to the suppression of DNA damage and cell cycle arrest. Moreover, *uri-1* +/- mutants or cells depleted of URI-1 function display an increased germ line apoptosis in the meiotic compartment. Notably, the latter is a p53-dependent phenomenon, which in turn demonstrates that it is the result of endogenous genotoxic DNA damage. These results, taken together, imply key roles for *C. elegans* URI-1 in signaling circuits dedicated to genomic integrity control and the suppression of cell cycle arrest and apoptosis.

2 Introduction

2.1 Cell growth and cell proliferation

Unicellular organisms are limited by the nutrients from the environment and usually divide as often as growth permits. In contrast, cells in multicellular organisms are typically immersed in excess nutrients. In this setting, cell proliferation is regulated by limiting extracellular signals, namely growth factors and mitogens that drive cell growth and cell division, respectively (Conlon and Raff, 1999).

Cell growth (an increase in cell size and mass) does not rely on cell cycle progression. This is evidenced by the observation that in a variety of cell types cell growth continues even when the cell cycle is blocked (Conlon et al., 2001; Fingar et al., 2002; Hemerly et al., 1995; Mitchison and Creanor, 1971; Neufeld et al., 1998; Sheikh et al., 1995; Swann, 1957; Weigmann et al., 1997). Conversely, blocking cell growth by nutrient or growth factor deprivation results in a cell cycle arrest, usually in G_1 (Pardee, 1974; Prescott, 1976; Temin, 1971). Similarly, abundant nutrients or overactivation of growth signaling pathways can impel cell cycle progression, typically abbreviating the length of the G_1 phase (Backman et al., 2002; Rupes, 2002; Saucedo and Edgar, 2002). The dependency of the cell cycle on cell growth is thought to be established by size requirements for the major cell cycle phase transitions, thereby governing the time spent by cells in G_1 phase and/or G_2 phase (Jorgensen and Tyers, 2004). Thus, cell growth and the cell cycle are coordinated but separable processes (Swann, 1957) and can be regulated independently by distinct extracellular signals. Both processes are controlled by the TOR and the Insulin/IGF signaling pathways. These interconnected signal transduction pathways are known to regulate cell growth and cell proliferation in response to nutritional cues in a variety of organisms (Backman et al., 2002; Junger et al., 2003; Kozma and Thomas, 2002; Manning and Cantley, 2003; Puig et al., 2003; Saucedo and Edgar, 2002).

2.2 TOR pathway

One central element in the control of cell growth and cell proliferation in response to nutritional cues is the serine/threonine protein kinase TOR (target of rapamycin), a member of the phosphatidylinositol 3-kinase-related kinase (PI3K-related kinase) family

(for review see (Harris and Lawrence, 2003)). TOR is part of a nutrient–sensing complex (Kim and Sabatini, 2004) that is active in the presence of sufficient nutrients and has been implicated in growth control via its regulation of translation initiation (Thomas and Hall, 1997). Translation rate is believed to communicate cell size to the cell cycle (Prescott, 1976; Unger and Hartwell, 1976).

TOR is highly conserved from yeast to mammals, although metazoans, flies and humans possess only one TOR gene (Oldham et al., 2000; Zhang et al., 2000), whereas *S. cerevisiae* and *S. pombe* yeast each have two TOR genes (Weisman and Choder, 2001). The yeast TOR proteins (TOR1 and TOR2) have overlapping roles in cell cycle progression, but TOR2 was found to have essential effects on cytoskeletal organization that are not shared with TOR1 or inhibited by rapamycin (Barbet et al., 1996; Schmidt et al., 1998; Schmidt et al., 1996; Zheng et al., 1995).

Most of the functions of TOR are specifically inhibited by the antifungal macrolide rapamycin, originally isolated from a bacterial strain of *Streptomyces hygroscopicus* (Abraham and Wiederrecht, 1996). Rapamycin binds directly to the prolyl isomerase FKBP12 (FK506-binding protein) and this complex then binds to TOR1 and TOR2 (Brunn et al., 1997; Chen et al., 1995). Rapamycin treatment of yeast cells resembles disruption of both TOR1 and TOR2 (Heitman et al., 1991; Helliwell et al., 1994; Kunz et al., 1993), resulting in cell cycle arrest in early G1, glycogen accumulation, sporulation, characteristic transcriptional changes (Beck and Hall, 1999; Cutler et al., 1999), increased autophagy, decreased amino acid import, and a 90% inhibition of mRNA translation (Barbet et al., 1996; Heitman et al., 1991; Noda and Ohsumi, 1998; Zarr et al., 1998; Zheng and Schreiber, 1997), phenotypes that are also observed with nutrient starvation, consistent with a role of TOR in nutrient sensing. Activated TOR leads to the phosphorylation of the 40S ribosomal kinase p70 S6K, the translational repressors 4E-BPs and also controls the activity of a set of phophatases like the yeast Pph21p/Pph22p/Sit4p through phosphorylation. These phosphatases subsequently dephosphorylate downstream effectors such as the GATA transcription factor Gln3p (Cutler et al., 2001). Thus, in addition to its effect on the phosphorylation state of proteins involved in translational control, TOR signaling regulates the abundance of the components of the translation machinery at both the transcriptional and translational level (Raught et al., 2001).

2.2.1 Regulation of protein synthesis

Protein synthesis is regulated in many instances at the initiation phase, the stage during which a ribosome is recruited to the 5′ end of an mRNA and positioned at a start codon (Raught et al., 2001). The eukaryotic ribosomes rely on a number of translation initiation factors to specifically recognize and bind to the 5′ end of an mRNA, the 5` MeGTP-cap. The cap binding protein eIF-4E (eukaryotic translation initiation factor 4E) is a component of the eIF-4F complex, which also contains the scaffold protein eIF-4G and the RNA helicase eIF-4A. eIF-4E recruits the mRNA to the eIF-4G scaffold. The RNA helicase eIF-4A, along with the cofactor eIF-4B, then unwinds the secondary structure in the mRNA 5' UTR, facilitating the ability of the 43S pre-initiation complex (consisting of the 40S ribosomal subunit, eIF-3, and a ternary complex of eIF-2, GTP, and initiator methionyl-$tRNA_i^{Met}$) to scan the mRNA until an AUG start codon in the proper sequence context is encountered (Gingras et al., 1999b; Raught et al., 2001). The interaction between eIF4E and eIF4G is regulated by a family of translation repressor peptides, the eIF4-binding proteins (4E-BPs), which compete with eIF4G for binding to eIF-4E (Bernal and Kimbrell, 2000; Lin et al., 1994; Miron et al., 2001; Pause et al., 1994; Poulin et al., 1998). In nutrient-starved or stressed mammalian cells, 4E-BPs are dephosphorylated and compete with the eIF4G proteins for an overlapping binding site on eIF4E (Gingras et al., 1999b). They thereby regulate the availability of eIF-4E and subsequently regulate the translation of mRNAs processing a 5` MeGTP-cap (Gingras et al., 1999b).

Translational initiation is also regulated by the general amino acid control, a pathway responsible for regulating amino acid homeostasis in response to starvation and stress in yeast. The Gcn2p kinase contains a regulatory domain whose sequence resembles histidyl-tRNA synthetase and which binds uncharged tRNAs that accumulate when amino acids are scarce with higher affinity then the corresponding charged tRNA (Dong et al., 2000). This interaction is believe to induce a conformational change that overcomes an intrinsic defect in the adjacent kinase domain and thereby activates GCN2 (Abastado et al., 1991; Dong et al., 2000; Qiu et al., 2002; Wek et al., 1995; Zhu et al., 1996; Zhu and Wek, 1998). GCN1 is necessary for activation of GCN2 by uncharged tRNAs, and it is thought that GCN1 acts as a chaperone to transport uncharged tRNAs that enter the A-site of ribosomes to the tRNA-binding domain of GCN2 for kinase activation (Kubota et al., 2001; Marton et al., 1997; Sattlegger and Hinnebusch, 2000; Vazquez de Aldana et al., 1994). Activated GCN2

stimulates the translation of the primary regulator of global amino acid control GCN4 by phosphorylating the α subunit of translation initiation factor 2 (eIF2α), its only known substrate (Dever et al., 1992; Hinnebusch, 1997; Hinnebusch and Natarajan, 2002).

eIF2 is responsible for binding the initiator methionyl-$tRNA_i^{Met}$ (Met-$tRNA_i^{Met}$) in an ATP-dependent manner and delivering this charged methionyl initiator tRNA to the initiation codon of the 40S ribosomal subunit in the form of a ternary complex (eIF2-GTP-Met-$tRNA_i^{Met}$). The pre-initiation complex binds the 5' end of mRNA and migrates downstream. When the initiator AUG codon is encountered, the eIF2-bound GTP is hydrolyzed and eIF2 is released from the ribosome in an inactive eIF2-GDP complex, with the subsequent formation of the 80S elongating ribosome. The eIF2-GDP complex must be recycled by the guanine nucleotide exchange factor eIF2B (Hinnebusch, 1994; Vazquez de Aldana et al., 1994). Phosphorylation of the α subunit of eIF2 at serine 51 converts eIF2 from a substrate to an inhibitor of eIF2B, which is limiting in the cell. The inhibition of GDP/GTP exchange on eIF2 reduces the GTP-bound form of eIF2, impedes ternary complex formation and subsequently has a profound inhibitory effect on overall protein synthesis.

Although the decrease in ternary complex levels represses general protein synthesis, it paradoxically specifically stimulates translation of GCN4 mRNA (gene specific translation), a mechanism involving upstream open reading frame (uORF), bypassing and translation reinitiation (Hinnebusch, 1997). A specialized reinitiation mechanism involving four short open reading frames in the GCN4 mRNA leader serves to repress GCN4 translation under non starvation conditions and derepress it in response to eIF2α phosphorylation in starved cells (Dong et al., 2000). When cells are growing under non-starvation conditions, ribosomes translate the first uORF, reinitiate at uORFs 2-4, and are unable to recognize the GCN4 start codon (Hinnebusch, 1997). The first uORF is the least inhibitory and is required for the ability of ribosomes to bypass the translational barrier imposed by the remaining three uORFs (Mueller and Hinnebusch, 1986). A large amount of data supports a scanning/reinitiation model in which ribosomes translate the first uORF but remain mRNA-bound thereafter. While moving further downstream, reinitiation at the inhibitory uORF4 precludes subsequent reinitiation at GCN4. In amino acid starved cells, the reduction in ternary complex levels is thought to delay rebinding of ternary complexes to ribosomes scanning downstream of uORF1. Consequently, many ribosomes bypass the inhibitory uORF4 before acquiring a ternary complex, thus permitting recognition of the

GCN4 start codon and translation of the mRNA of the GCN4 gene (Abastado et al., 1991; Dever et al., 1992; Mueller and Hinnebusch, 1986; Wek et al., 1995). The transcriptonal activator Gcn4p binds to specific DNA-binding motif sequences (GCN4-protein-responsive elements) that are present in the promoter regions of its target genes and thereby upregulates the expression of hundreds of genes, the majority involved in amino acid biosynthesis needed to adapt to starvation conditions (Natarajan et al., 2001; Qiu et al., 2001).

It is intriguing to speculate that translational regulation mediated by eIF2α phosphorylation and uORFs has been conserved throughout eukaryotic evolution to regulate the production of specific transcription factors. Like in yeast, mammalian GCN2 has been shown to be required for adaptation to deprivation of specific amino acids in mice (Harding et al., 2000; Zhang et al., 2002). In mammals, GCN2 regulates translation of the mRNA for the transcription factor ATF4 (activating transcription factor 4) in response to limitation of amino acids. Although there is no GCN4 ortholog in mammalian cells, ATF4 is induced by eIF2α phosphorylation under amino acid starvation conditions though a mechanism of translation reinitiation similar to that described for yeast GCN4 (Jiang et al., 2004; Vattem and Wek, 2004). ATF4 is known to enhance the expression of additional transcriptional regulators that together contribute to expression of a large number of genes involved in metabolism, redox chemistry and apoptosis (Harding et al., 2000; Jiang et al., 2004). Thus, key elements of the mechanism of nutritient control of transcription and translation have been highly conserved throughout evolution.

2.2.2 Translational regulation by TOR

In mammalian cells, mTOR positively regulates protein synthesis in part by modulating the activities of components of the translational machinery, including the 40S ribosomal kinase p70 S6K (S6K) and the translation initiation factor 4E-binding protein (4E-BP1) (Avruch et al., 2001; Di Como and Arndt, 1996; Lawrence and Abraham, 1997)(Figure A). TOR stimulates translation initiation under nutrient-rich conditions partly through the phosphorylation of 4E-BP1. Phosphorylation of 4E-BP1 promotes its dissociation from eIF-4E, enabling binding of eIF-4E to eIF4G and subsequent recruitment into the eIF-4F complex (Gingras et al., 2001). This inhibits cap-dependent translation, linking the activity of 4E-BPs intimately to nutrient availability.

The translational activation of mTOR target mRNAs is expected to promote cell growth and proliferation. The effect of mTOR on cell cycle progression in mammalian cells is mediated at least in part by the increased translation of mRNAs encoding positive regulators of cell cycle progression, such as cyclin D1 and c-Myc and by decreased translation of negative regulators thereof, such as the cyclin-dependent kinase inhibitor p27.

Another major downstream target of mTOR is the S6K, which phosphorylates the major ribosomal protein S6, leading to translational up-regulation of those ribosomal mRNAs that possess a 5` terminal oligopyrimidine tract (5` TOP), and mRNAs coding for other components of the translation machinery, thereby enhancing the overall translation capacity of cells (Meyuhas, 2000; Pullen and Thomas, 1997). Thus, through the S6Ks, TOR signaling activates the translation of ribosomal protein mRNAs and thereby controls cell size (Leicht et al., 1996; Mahajan, 1994).

The S6K gene family is conserved through species with worms and flies possessing only one gene, whereas mammals have two genes (S6K1 and S6K2) (Shima et al., 1998); Thomas, 2002 #493; Volarevic, 2001 #492}. Both S6K and 4EBP1 contain a conserved five amino acid sequence TOS (TOR signaling) motif that is believed to function as a docking site and which is crucial for their regulation by the mTOR pathway (Schalm et al., 2003).

The rapamycin-sensitive TOR cascade also mediates translation control by crosstalking to the general amino acid control in yeast. Inhibiting TOR with rapamycin promotes the dephosphorylation of Gcn2p through a mechanism involving the phosphatase complex Tap42p-Sit4p (Harris and Lawrence, 2003), a direct target of TOR. This dephosphorylation has been shown to increase the affinity of Gcn2p towards uncharged tRNAs, thereby leading to Gcn2p activation without increase in uncharged tRNA levels (Cherkasova and Hinnebusch, 2003; Kubota et al., 2003). In the presence of adequate nutrients, TOR stimulates the association of type 2A and type-2A-related protein phosphatases (like Pph21p/Pph22p/Sit4p) with the regulatory subunit TAP42 by direct phosphorylation of TAP42 (Di Como and Arndt, 1996), thereby inhibiting the phosphatases (Di Como and Arndt, 1996; Jiang and Broach, 1999; Schmidt et al., 1998). Upon nutrient starvation, or in the presence of rapamycin, dephosphorylated Tap42p dissociates from Pph21p/22p and/or Sit4p and relieves Tap42p inhibition of Pph21p/Pph22

and/or Sit4p. The activated Pphs and/or Sit4p subsequently dephosphorylate downstream effectors (Cutler et al., 2001) including the Gcn2p kinase which becomes activated, ultimately leading to inhibition of translation initiation through phosphorylation eIF2α (Cherkasova and Hinnebusch, 2003). Thus, rapamycin stimulates eIF2α phosphorylation by GCN2 with attendant induction of GCN4 mRNA translation (Cherkasova and Hinnebusch, 2003; Valenzuela et al., 2001). Moreover, the putative TOR regulated eIF4E-associated protein Eap1p constitutes another interface between the two pathways (Matsuo et al., 2005). TOR inactivation derepresses Eap1p, which functions downstream of Gcn2p to attenuate Gcn4 translation via a mechanism independent of eIF4E-binding. Thus, the effect of rapamycin is an apparent paradox. Rapamycin activates Gcn2p to induce Gcn4 translation on one hand, but derepresses Eap1p to attenuate the translation on the other hand. A plausible explanation may be that Eap1p contributes a negative feedback loop to fine-tune the cellular response to nutritional stress. In response to mild starvation, such as that for amino acids, general amino acid control pathways are activated to stimulate amino acid biosynthesis utilizing available carbon and nitrogen sources. However, when starvation becomes more severe and causes depletion of raw materials for biosynthesis, it is reasonable for the cells to cease the global amino acid control and activate autophagy instead. Indeed, nitrogen starvation was reported to repress Gcn4 translation (Grundmann et al., 2001). Thus, the TOR pathway simultaneously regulates the abundance and activity of the translation machinery in both unicellular and multicellular organism.

2.2.3 Transcriptional regulation by TOR

In addition to its well characterized function in translational control, TOR regulates transcription of genes involved in ribosomal biogenesis (Powers and Walter, 1999; Zaragoza et al., 1998) and nutrient response (Beck and Hall, 1999; Bertram et al., 2000; Cardenas et al., 1999; Hardwick et al., 1999). This additional mechanism by which TOR regulates cell growth and proliferation works by excluding transcriptional activators from the nucleus. For example, in yeastin the presence of adequate nitrogen the GATA transcription factors Gln3p and Gat1p are phosphorylated in a TOR-dependent manner and thereby tethered to the cytoplasmic Ure2 protein and thus excludes from the nucleus. Cytoplasmic retardation of the transcription factors prevents the transcriptional activation of their nitrogen-regulated target genes (Beck and Hall, 1999; Bertram et al., 2000). The phosphorylation state of Gln3p is controlled not only directly by TOR-mediated phosphorylation, but also by the TOR-regulated Tap42p-Sit4p phosphatase complex. Upon

nutrient limitation or rapamycin treatment, dephosphorylated Tap42p dissociates from the TOR controlled, type 2A-related phosphatase Sit4p and relieves Tap42p inhibition on Sit4p. The activated Sit4p subsequently dephosphorylates the GATA transcription factor Gln3p (Cutler et al., 2001). Dephosphorylated Gln3p is released from URE2 and translocated into the nucleus where it binds GATA sequences upstream of nitrogen catabolite repression sensitive genes and activates their transcription (Beck and Hall, 1999). In addition to Gln3p, TOR inhibits the nuclear localization and activation of several other nutrient-response transcription factors, such as Msn2p, Msn4p (Beck and Hall, 1999; Komeili et al., 2000). Thus, the TOR signaling pathway broadly controls nutrient metabolism by sequestering several transcription factors in the cytoplasm and thereby preventing their access to the nucleus (Beck and Hall, 1999).

In mammalian cells, mTOR regulates binding of the serine/threonine protein phosphatase PP2A (homologue of yeast Sit4p, Pph21p/22) to the immunoglobulin-receptor-binding protein α4 (homologue of yeast Tap42p) (Duvel et al., 2003; Schmelzle and Hall, 2000) and thereby plays a critical role in regulating the activity of the phosphatases (Wera and Hemmings, 1995). Several additional serine/threonine protein phosphatases, like PP4 and PP6, have been identified as components of the mTOR signaling pathway in mammalian cells (Dennis et al., 1999), but whereas control of protein phosphatases by TOR is clearly linked to the regulation of transcription and protein stability in yeast, the cellular functions of protein phosphatases controlled by mTOR remain to be elucidated.

2.2.4 TOR functions in two independent, evolutionarily conserved complexes

In yeast, the combination of proteins that associate with TOR1 and TOR2 define rapamycin-sensitive and insensitive complexes, referred to as TORC1 and TORC2 respectively. Yeast TOR complex 1 (TORC1) contains LST8 (lethal with sec thirteen), KOG1 (kontroller of growth 1) and either TOR1 or TOR2, whereas the mammalian TORC1 (mTORC1) is comprised of TOR in association with the proteins Raptor (regulatory associated protein of mTOR) (homolog of *S. cerevisiae* KOG1) and GβL (homolog of *S. cerevisiae* LST8), both of which are rapamycin-sensitive regulators of cell growth (Hara et al., 2002; Kim et al., 2002a; Loewith et al., 2002). The FKBP12-rapmycin complex is able to bind to TOR1 or TOR2 in TORC1 (mTOR in mTORC1) and thereby inhibit TORC1 signaling (Loewith et al., 2002). Raptor appears to serve as an mTOR scaffold protein, the binding of which to mTOR substrates is necessary for effective

mTOR-catalyzed phosphorylation. For example, Raptor binds the TOR substrates 4E-BP1 and S6K and presents them to mTOR for phosphorylation, thus promoting mRNA translation (Choi et al., 2003; Nojima et al., 2003; Schalm et al., 2003). Binding of TOR to Raptor or Kog1p (Loewith et al., 2002) is also necessary for TOR signaling *in vivo* in *C. elegans* and *S. cerevisiae* (Hara et al., 2002; Loewith et al., 2002). GβL, the third component of the mTORC1 complex (Kim et al., 2003; Loewith et al., 2002) binds tightly to the mTOR catalytic domain and enhances association of Raptor with mTOR (Kim et al., 2003). TORC1 functions in coupling transcription, ribosome biogenesis, translation initiation, nutrient uptake and autophagy to the abundance and quality of available nutrients. Thus, TORC1 functions as a temporal regulator of cell growth (Jacinto et al., 2004).

TORC2 contains TOR2, LST8 and the proteins AVO1 (adheres voraciously to TOR2), AVO2 and AVO3 (Jacinto et al., 2004; Loewith et al., 2002; Sarbassov et al., 2004; Wedaman et al., 2003). The mTORC2 contains GβL and rictor (rapamycin insensitive companion of mTOR, AVO3 homologue), but not Raptor (Sarbassov et al., 2004). TORC2 signaling is rapamycin insensitive owing to the inability of FKBP12/rapamycin to bind to TOR2 in yeast TORC2 (Loewith et al., 2002). Recent findings show that mTORC2 phosphorylates Akt/PKB and thereby regulates its function (Sarbassov et al., 2005). Like yeast TORC2, mTORC2 mediates the rapamycin-insensitive component of TOR signaling (Sarbassov et al., 2004) and seems to function upstream of Rho GTPases to regulate the actin cytoskeleton (Jacinto et al., 2004). Thus, the mTORC2 complex mediates spatial control of cell growth by regulating the cell-cycle dependent polarization of the actin cytoskeleton (Loewith et al., 2002; Sarbassov et al., 2004). To summarize both mammalian complexes seem to respond to nutrients (Jacinto et al., 2004), but they are structurally and functionally distinct; TORC2 controlling the polarization of the actin cytoskeleton, whereas TORC1 controls protein synthesis (Jacinto et al., 2004).

2.2.5 TOR action in *C. elegans*

The role of yeast and mammalian TOR homologs in regulation of cell growth and proliferation is also at least partially conserved in other multicellular organisms (Jacinto and Hall, 2003; Long et al., 2002) CeTOR mutants show an overall developmental growth arrest at the L3 larval stage, metabolic changes, increased longevity and altered translational regulation.

Deleting TOR in *C. elegans* leads to a pronounced intestinal phenotype with large, highly refractile and autofluorescent lipofuscin granules (intestinal lysosomes), characterized by an increase in the gut lumen size and a decreased ability of the intestine to digest and absorb nutrients; both effects are apparently due to an inhibition of global protein synthesis (Long et al., 2002). Moreover, *C. elegans* TOR (CeTOR) deficiency results in delayed somatic and gonadal development and eventual developmental arrest at late L3 stage (Long et al., 2002). Moreover, the CeTOR-deficient larvae exhibit an increase in the size and number of lipid-laden hypodermal vesicles (Clokey and Jacobson, 1986; Kostich et al., 2000; Matyash et al., 2001).

While studies in yeast and mammalian cells demonstrate that TOR mediates responses to nutrient deprivation, and that loss of TOR mimics starvation, (Long et al., 2002) the phenotype of CeTOR-deficient animals differs from that of larvae arrested at L3 by starvation. Wild type starved worms do not exhibit the intestinal phenotypes of CeTOR deficiency and resume development even after 10 days of starvation when returned to food, whereas CeTOR worms die after 7-8 days. These findings suggest that CeTOR may have functions in worms other than in regulation of responses to starvations.

The *C. elegans* genome contains a single homologue of the scaffolding protein eIF-4G, which functions to assemble the 43S ribosomal pre-initiation complex. F1s raised on CeeIF-4G RNAi closely resemble the severe intestinal atrophy of CeTOR-deficient animals (Long et al., 2002). Moreover, disruption of the *C. elegans* homologues of the general translation initiation factors eIF-2α and eIF-2β produces phenotypes identical to those produced by CeeIF-4G RNAi (Long et al., 2002). Therefore, it is inferred that the major changes resulting from eIF-4G deficiency reflected a defect in overall mRNA translation rather than a selective deficiency in the expression of mRNAs with complex structures in their 5` untranslated segment. Moreover, the F1 generation of worms fed on RNAi of the *C. elegans* S6K homologue (*cep70*) did not exhibit any of the phenotypes caused by CeTOR deficiency, but rather a distinct set of phenotypes, including a slight developmental delay, a slightly reduced final body size, and larger nonrefractile intestinal vesicles in adults. Thus, the major phenotypes of CeTOR deficiency are not due to a deficiency of S6K function, suggesting that this signal transduction pathway functions differently in worms than it does in flies and mammals (Figure A). These data suggest that

CeTOR is an upstream regulator of global mRNA translation, in contrast to its more specific role in regulating translation in mammals.

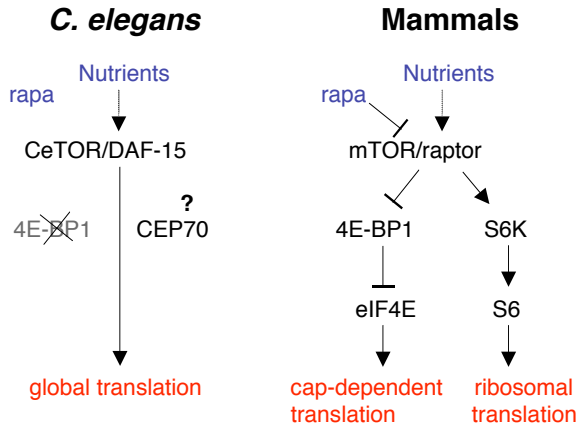

Figure A. Model of TOR signaling network in *C. elegans* and mammalian cells. Indicated are the key elements of the pathway that have been identified to date. The mammalian TOR signallng pathway mediates the regulation of cell growth and cell proliferation via its two main targets 4E-BP1 and S6K. Although homologs of mTOR, raptor and S6K exist in the worm (CeTOR, DAF-15, CEP70, respectively) the signalling downstream of CeTOR seems less conserved than in *Drosophila.* Apparently, CeTOR does not signal nutritional cues through CEP70 and seems to have a more global role in regulating protein synthesis than in mammals. Moreover, no *C. elegans* homolog of 4E-BP1 has been identified and the animal has a natural resistance against rapamycin (rapa).

2.3 Insulin/IGF-I-pathway

Cell growth and cell proliferation are also promoted by the evolutionarily conserved PI3K (phosphatidylinositol 3-kinase) pathway (Conlon and Raff, 1999; Duncan and Hershey, 1985; Potter and Xu, 2001; Weinkove et al., 1999). Insulin and its signaling systems are implicated in both central and peripheral mechanisms governing the ingestion, distribution, metabolism, storage of nutrients and life span regulation in organisms from worms to humans (for review see (Porte et al., 2005)). In mammals, insulin plays a role in metabolism by regulating glucose homeostasis through the promotion of cellularglucose uptake and conversion of glucose to lipid. (Leibiger et al., 1998; Takahashi et al., 1997). Insulin regulates embryonic growth, whereas the insulin-like growth factor I (IGF-I) regulates embryonic and postembryonic growth (Baker et al., 1993). Thus, both insulin and IGF-I regulate food utilization pathways, metabolism and promote growth in mammals (Clemmons, 2001). IGF-I is mainly produced by the liver and increases in concentration systemically in parallel to growth hormone-mediated postnatal and adolescent growth, before declining with elderly age (for review see (Foulstone et al., 2005)). In *C. elegans* the insulin-like molecule *daf-2* controls organismal growth in response to poor nutrient conditions (Kimura et al., 1997) and in *Drosophila,* the insulin/IGF receptor homolog

Drosophila insulin receptor also controls organismal growth directly by regulating cell size and cell number (Brogiolo et al., 2001).

Insulin, or an insulin-like ligand, binds to and activates its cognate receptor, a receptor tyrosine kinase (RTK) on the surface of responsive cells (Figure B). Once activated, RTKs autophosphorylate and thereby create phospho-tyrosine binding sites for the insulin receptor substrate (IRS) family of scaffolding proteins. IRS proteins become phosphorylated on several tyrosine residues by the RTK and these residues act as a binding site for PI3K. The recruitment and activation of PI3K to the plasma membrane generates the lipid second messenger 3-phosphoinositide (phosphatidylinositol-3.4.5-triphosphates, PIP_3) by phosphorylation of the lipid phophatidylinositol-4.5-biphosphate (PIP_2) (for review see (Saltiel and Kahn, 2001)). The increased PIP_3 level recruits the serine/threonine protein kinase Akt/PKB to the plasma membrane by binding to its N-terminal pleckstrin homology domain and leading to the phosphorylation and activation of Akt/PKB by PDK1 (phosphoinositide-dependent protein kinase 1) (Alessi et al., 1996; Scheid et al., 2002). This process is antagonized by the lipid phosphatase encoded by the tumor suppressor gene PTEN (phosphatase and tensin homolog deleted on chromosome 10), which limits Akt/PKB activation by decreasing PIP_3 levels (Ogg and Ruvkun, 1998). Activated Akt/PKB in turn inhibits the activity of a family of forkhead transcription factors (FOXO1 (FKHR), FOXO3a (FKHRL1) and FOXO4 (AFX) through direct phosphorylation (Biggs et al., 1999; Kops and Burgering, 1999; Nakae et al., 2000; Nakae et al., 1999; Rena et al., 1999). The phosphorylation of FOXO (forkhead box 'other') proteins on two or three serine or threonine residues by Akt/PKB, in parallel or complemetary to serum- and glucocorticoid-regulated protein kinase (SGK) (Kobayashi and Cohen, 1999), creates binding sites for 14-3-3 proteins. Cytoplasmic sequestration of FOXO proteins by 14-3-3 promotes their ubiquitination and degradation (Matsuzaki et al., 2003), which combined with nuclear exclusion (Brunet et al., 1999; Brunet et al., 2001; Kops and Burgering, 2000), results in an insulin-induced transcriptional repression of FOXO target genes, which are involved in apoptosis, cell cycle entry control, stimulate glucose production and the response to DNA damage and oxidative stress (Brunet et al., 1999; Furukawa-Hibi et al., 2002; Henderson and Johnson, 2001; Kops et al., 2002; Medema et al., 2000; Schmoll et al., 2000; Tran et al., 2002). In addition to their transcriptional activation capabilities, FOXO proteins have been shown to induce cell cycle arrest by repressing transcription of genes encoding D-type cyclins (Ramaswamy et al., 2002; Schmidt et al., 2002). Thus,

multiple FOXO transcriptional targets are thought to mediate the diverse functions of the insulin-signaling pathway.

2.3.1 Insulin/IGF-I-like signaling in *C. elegans*

Components of the insulin-like signaling pathway have been highly conserved during evolution and identification of a homologous pathway in *C. elegans* has provided insights into mechanisms governing insulin action in mammals (Tissenbaum and Ruvkun, 1998). The insulin-like signaling pathway begins with the genes *unc-64* and *unc-31*. *unc-64* encodes a syntaxin homolog (Ogawa et al., 1998), which is involved in synaptic transmission, while *unc- 31* encodes a CAPS homolog (calcium-dependent activated protein for secretion). Mammalian CAPS appears to be involved in calcium-stimulated peptide secretion (Ann et al., 1997). It is thought that these two proteins affect insulin processing and/or release in producing cells (Ailion et al., 1999). A total of 38 insulin family members have been identified in the *C. elegans* genome (Gregoire et al., 1998; Li et al., 2003; Pierce et al., 2001), but there appears to be only a single insulin/IGF-I receptor, *daf-2* (dauer larva formation) in worms, whereas in mammals there are several homologous receptors, including the insulin receptor and IGF-1 receptor (for review see (Gems and Partridge, 2001)). The gene *daf-2* may be the common ancestor of human insulin receptor, human IGF-I receptor, and the human insulin-related receptor, because its sequence is equally distant from all of them (Tissenbaum and Ruvkun, 1998; Vanfleteren and De Vreese, 1995). Activation of *daf-2* by its ligand(s) leads to PI3K activation (Figure B), which results in generation of PIP_3 (Alessi and Downes, 1998). PI3K contains two subunits, a regulatory subunit (for review see (Cantrell, 2001)), and the catalytic subunit p110, encoded in *C. elegans* by the gene *age-1* (Morris et al., 1996). Downstream of *age-1* are the kinases PDK-1, AKT-1 and AKT-2 (Paradis et al., 1999; Paradis and Ruvkun, 1998). DAF-18 encodes a homolog of the mammalian tumor suppressor PTEN phosphoinositide phosphatase (Gil et al., 1999; Liaw et al., 1997; Ogg and Ruvkun, 1998; Rouault et al., 1999), which regulates the levels of PIP_3 by dephosphorylating the inositol ring in the third position (Maehama and Dixon, 1998). Activation of *daf-2* signaling is thought to lead to phosphorylation and thereby inactivation of the forkhead transcription factor DAF-16 (Lin et al., 1997a). DAF-16 most closely related human homologs are AFX, FKHR, and AF6/FKHRL1 (Galili et al., 1993; Hillion et al., 1997; Ogg et al., 1997; Parry et al., 1994). The subcellular localization of DAF-16 is regulated by AKT and SGK-1 phosphorylation (Hertweck et al., 2004; Ogg et al., 1997). SGK-1 acts in parallel to the

AKT, with which it forms a multimeric protein complex (Hertweck et al., 2004). All three kinases (AKT-1, AKT-2, SGK-1) in the complex are able to suppress DAF-16 function by direct phosphorylation. Several genes have been identified downstream of *daf-16* including the heat shock proteins HSP70 and HSP90 (Cherkasova et al., 2000; Yu and Larsen, 2001) possibly explaining the thermotolerance of *daf-2* mutants. Another transcriptional target of DAF-16 is *scl-1* (SCP-like extra-cellular protein), a putative secretory protein with homology to the mammalian cystein-rich secretory protein family (CRISP). SCL-1 is required for the stress resistance and life span extension of *daf-2* mutants (Ookuma et al., 2003).

In addition to the relatively well-defined branch of the insulin pathway that proceeds linearly from *daf-2* through *age-1, pdk-1, sgk-1* and *akt,* there appears to be a less defined branch downstream of *daf-2* in parallel to *age-1*. Existence of this branch is inferred from the lack of suppression of *daf-2* mutants by the *pdk-1* and *akt-1* gain-of-function mutations that completely suppress *age-1* (Paradis et al., 1999; Paradis and Ruvkun, 1998) and supported by the finding that *daf-18* rescues the dauer phenotype due to *daf-2* mutations with less efficiency than *daf-16* (Ogg et al., 1997). These observations suggest that in *C. elegans* PI3K is but one of the mediators of insulin/IGF-I signals and that these signals converge on *daf-16*. It is interesting to notice that the AKT proteins are more important for regulating dauer formation, SGK-1 is crucial for the control of the postembryonic development, stress response and life span (Hertweck et al., 2004). It is believed that at least one additional, still unknown branch of the DAF-2 pathway exists that is independent of AKT and SGK-1 (Hertweck et al., 2004). In *C. elegans* a block in the *daf-2* signaling pathway, induced by scarce nutrients, high temperature or mutations in signaling components results in retarded postembryonic development, constitutive dauer formation (Daf-c), increase in fat storage, defective egg-laying, extended life span and increased stress tolerance for a variety of stress treatments, including heat shock, UV radiation, heavy metals, and oxidative damage induced by paraquat (Honda and Honda, 1999; Johnson et al., 2000; Kimura et al., 1997; Larsen, 1993; Lithgow et al., 1994; Murakami and Johnson, 1996; Paradis et al., 1999). Moreover, mutations in this pathway also affect fertility and embryonic development. Mutations of *daf-16* suppress all of the *daf-2* phenotypes, including dauer arrest, life span extension, reduced fertility and viability defects (dead eggs and L1/L2 larval arrest) (Kimura et al., 1997) demonstrating that the diverse effects of insulin-like signaling on metabolism, development, reproduction and

lifespan are mediated transcriptionlly by *daf-16* (Garofalo, 2002; Tatar et al., 2001; Tissenbaum and Ruvkun, 1998; Vanfleteren and De Vreese, 1995).

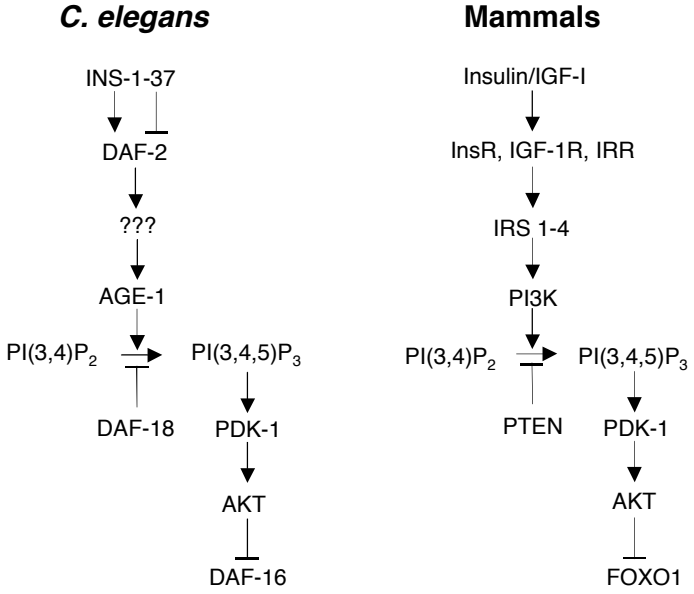

Figure B. Comparative diagram of the evolutionarily conserved insulin/IGF-I signalling and *daf-2* pathways in *C. elegans* and mammals. Indicated are the key elements of the pathways. Activation of downstream components through multiple phosphorylation events controls metabolism, development and lifespan by restricting the activity of the forkhead transcription factors DAF-16 or FOXO1 and subsequent inhibition of their target genes.

2.3.1.1 Lifespan

Reduction in the activity of the *daf-2* pathway doubles normal lifespan and functions exclusively during adulthood to influence lifespan in *C. elegans* (Dillin et al., 2002a; Kenyon et al., 1993; Kimura et al., 1997; Morris et al., 1996). The lifespan increase associated with lower *daf-2* signaling is completely abrogated by loss-of-function mutation in *daf-16*, indicating that *daf-16* is the major downstream effector of *daf-2* signaling and plays an unique role in life span regulation (Lin et al., 1997a; Ogg et al., 1997). The eventual activation of the transcription factor indicates that the insulin/IGF-I receptor-like signal pathway regulates ageing by modulating gene expression (Lin et al., 1997a; Ogg et al., 1997). It appears that the increased longevity resulting from DAF-16 activation is due to the additive effect of many genes, which individually exert a small effect on lifespan (for review see (Gems et al., 2002)). *daf-2* mutants express high levels of antioxidant enzymes such as catalase and mitochondrial superoxide dismutase 3 (*sod-3*) (Honda and Honda, 1999; Honda and Honda, 2002; Murphy et al., 2003; Wolkow et al., 2000), suggesting that the up-regulation of detoxifying enzymes may be involved in the mechanism of *daf-16* mediated lifespan extension. Indeed, the cytosolic catalase *ctl-1* is required for the extension of adult life span by *daf-2* (Taub et al., 1999). As DAF-16 is a

regulator of many genes that respond to and minimize the effects of oxidative stress (Honda and Honda, 1999; Murphy et al., 2003) these findings highlight the central position of oxidative stress in the aging-regulatory machinery, and suggest that the lower level of free radicals in *daf-2* mutants are essential for life span extension. In eukaryotic cells, the mitogen-activated protein kinase (MAPK) signaling cascades transduce signals in response to a variety of stresses. Interestingly, the MAPK protein p38 seems to act upstream of DAF-16 to activate DAF-16 in response to ROS (Kondo et al., 2005) suggesting that DAF-16 is a major mediator of the oxidative stress response controlled by multiple pathways to cope with oxidative stress.

Lifespan can be extended by perturbing sensory neurons or germ cells (Patel et al., 2002; Wolkow et al., 2000). These findings are consistent with the model that sensory neurons influence lifespan by down regulating the *daf-2* pathway (Apfeld and Kenyon, 1999). Studies have demonstrated that restoring *daf-2* signaling only in the nervous system, but not in muscle or intestine, reduced the life span of *daf-2* mutant animals to normal, implying that neuronal *daf-2* signaling is sufficient for longevity regulation (Apfeld and Kenyon, 1998; Wolkow et al., 2000). Conversely, DAF-16 expression in neurons is not sufficient to extended lifespan by more than about 20% and expressing DAF-16 in the intestine increases lifespan-substantially by 50%-60%. It therefore seems that for full lifespan extension DAF-16 function is required in more than one tissue (Libina et al., 2003). Libina and colleges show that different tissues interact, acting as signaling centers to specify the lifespan of the animals (Libina et al., 2003). Taken together, these findings indicate that DAF-16 acts in the intestine and to a lesser extent in neurons to control the expression of genes that regulate lifespan (Libina et al., 2003). The lifespan of *C. elegans* is also regulated by the reproductive system. Killing the germ line precursor cells extends lifespan by approximately 60% (Apfeld and Kenyon, 1999; Hsin and Kenyon, 1999). Performing the same experiment in *daf-2* mutants causes the animals to live approximately four times as long as normal. This synergy raises the possibility that germ line and *daf-2* signaling might act in parallel pathways to regulate lifespan. In both cases, lifespan extension requires DAF-16 and regulates DAF-16 accumulation in nuclei (Hsin and Kenyon, 1999; Lin et al., 2001). However, ablating the germ line of hatching larvae causes DAF-16 to accumulate in nuclei only during adulthood (Lin et al., 2001), whereas, when lifespan is extended by mutations in the *daf-2* pathway, DAF-16 accumulates in nuclei of many cell types throughout development and into adulthood (Lin et al., 2001). Thus, these findings indicate that different spatial and temporal patterns of DAF-16 nuclear

accumulation can be associated with DAF-16 dependent lifespan extension (Lin et al., 2001) and that tissue specificity (Libina et al., 2003) and parallel signaling pathways (Paradis and Ruvkun, 1998) contribute to the complexity of the DAF-2 signaling to influence the localization and function of DAF-16.

As mentioned before, the *daf-2* pathway is thought to shorten lifespan by inhibiting *daf-16* activity via AKT -dependent phosphorylation of DAF-16 on one or more phosphorylation sites. When the consensus AKT phosphorylation sites in DAF-16 are altered, DAF-16 accumulates in the nucleus, demonstrating that nuclear accumulation is inhibited by AKT phosphorylation. Conversely, the *daf-2* pathway still inhibits dauer formation and lifespan extension even when the consensus AKT sites on DAF-16 are mutated (Lin et al., 2001) This suggests that the *daf-2* pathway uses both AKT-dependent and AKT-independent pathways to inhibit DAF-16 activity (Lin et al., 2001).

Moreover, differential splicing of *daf-16* RNA yields to three transcripts. *daf-16a1* and *daf-16a2* encode proteins that differ by two amino acids. The third, *daf-16b*, encodes a protein with a different amino terminus. Many strong *daf-16 (-*) mutations are predicted to affect *daf-16a*, but not *daf-16b* (Lin et al., 2001; Ogg et al., 1997), indicating that DAF-16b cannot substitute for DAF-16a. Lin and colleges show that DAF-16b is required for the pharynx to enter the full dauer state, but not for lifespan extension and most aspects of dauer formation (Lin et al., 2001). These findings highlight the high level of complexity of this pathway.

2.3.1.2 Dauer

The dauer is a developmentally growth arrested alternative third larval (L3) stage with slowed metabolic rates, large amounts of stored fat and increased lifespan (Kimura et al., 1997; Malone et al., 1996). Entry into this state is triggered by harsh environmental conditions, including high temperature, starvation and high concentration of dauer pheromone, a constitutively secreted substance serving as an indicator of population density (Golden and Riddle, 1982; Golden and Riddle, 1984a; Golden and Riddle, 1984b). Dauers can survive in harsh environments because of their distinctive adaptive features in morphology, behaviour, metabolism, and life span. Interestingly, these stress resistant larvae exhibit elevated levels of detoxifying enzymes like catalase *(ctl-1)* and super-oxide dismutase *(sod-3)* (Honda and Honda, 1999) that contribute to the antioxidant defense and

increased resistance to oxidative stress of dauers (Murakami and Johnson, 1998). When environmental conditions improve, dauers undergo a series of developmental changes and re-enter the reproductive cycle by molting into an L4 larvae and subsequently into adult worms. In the L1 and L2 larval stages, environmental cues are sensed in part by chemosensory neurons in the amphid sensory organ in the head (Bargmann and Horvitz, 1991; Schackwitz et al., 1996). These neurons in turn relay the environmental information to a complex regulatory system that makes the critical decision to proceed to the dauer or the L3 stage. Genetically, three parallel pathways have been found to regulate entry into the dauer stage, the *daf-2* pathway, the TGF-β (transforming growth factor β) pathway and a pathway that includes the receptor guanylyl cyclase *daf-11* and the HSP90 homologue encoded by *daf-21* (Inoue and Thomas, 2000). Formation of partial dauers (defined as animals mosaic for dauer and nondauer phenotypes) is a hallmark of mutations in the *daf-2* pathway, as partial dauers are not induced in wild type worms or by mutations in the other two parallel pathways under any conditions (Vowels and Thomas, 1992). Interestingly, DAF-16 neuronal expression is sufficient to cause dauer formation at 25°C, but neither, muscle or intestinal DAF-16 is necessary or sufficient for dauer formation (Libina et al., 2003).

2.3.2 Parallels between human and *C. elegans* insulin/IGF-1-like signaling

There are several intriguing parallels between the *C. elegans daf-2* pathway and the human insulin/IGF-I pathways. In humans, insulin and IGF-I regulate food utilization pathways, metabolism, ageing and promote cell growth and proliferation (Clemmons, 2001). The *daf-2* signaling pathway also regulates metabolism and aging. Consistent with a role of neurons in the mediation of *daf-2* signals in *C. elegans*, IGF-I production by the liver is known to be regulated by growth hormone (GH), the secretion of which by the anterior pituitary is stimulated by hypothalamic neurons. The activity of hypothalamic neurons in turn are regulated by circulating IGF-I levels through a negative feedback loop (Ghigo et al., 1999). Moreover, a decrease in insulin/IGF-I signaling in mice due to brain insulin receptor or IRS 2 deficiencies causes longevity in mice (Brown-Borg et al., 1996; Steger et al., 1993). Since insulin receptor null mice are not viable, but heterozygous females live 33% longer and males 16% longer than wild type mice. These heterozygous mice are not dwarf, their energy metabolism and fertility are normal (Holzenberger et al., 2003). This may be due to the fact that in mammals the insulin family is reported to have eight

members that may regulate different physiological processes through different receptors (Nef and Parada, 2000).

Interestingly, the heterozygous mice show a greater resistance to oxidative stress, analagous to the stress-resistance of *C. elegans daf-2* mutants. One current hypothesis is that insulin sensitivity is a phenotype under strong selective forces during aging that allows some individuals to reach the limits of human life span (for review see (Barbieri et al., 2003)). Results show that reduced IGF-I plasma levels are associated with longevity (for review see (Barbieri et al., 2003)). Furthermore, healthy centenarians have been shown to have a low degree of oxidative stress and high antioxidant defense, which seem to be important in guaranteeing their longevity (Mecocci et al., 2000; Monti et al., 2000; Paolisso et al., 1998) analogous to the situation in *daf-2* mutant worms. These results suggest that the genetic link among insulin-like signaling, oxidative stress, and longevity, originally discovered in *C. elegans*, also exists in humans. It is therefore possible that a moderate pharmacological reduction of insulin signaling might reduce the rate of ageing in mammals.

2.4 Crosstalk between TOR and insulin/IGF-I signaling pathways

The activity of mTOR is not only controlled by the supply of amino acids, but also by cellular energy state and growth factors that activate the protein kinase Akt/PKB (for review see (Harris and Lawrence, 2003)) (Figure C). mTOR has been implicated in the insulin/IGF-I network in mammalian cells based on the fact that activation of Akt/PKB leads to the phosphorylation and activation of mTOR(Alessi and Downes, 1998; Pullen and Thomas, 1997; Scott et al., 1998). The tuberous sclerosis complex (TSC1/TSC2, respectively (hamartin/tuberin) acts as a negative regulator downstream of Akt/PKB and upstream of mTOR and is a major target through which Akt/PKB, AMPK and perhaps amino-acid sufficiency control mTOR activity (Oldham and Hafen, 2003; Shamji et al., 2003). In the proposed mechanism, the 5'AMP-activated protein kinase (AMPK) phosphorylates and activates TCSC2, thereby inhibiting mTOR activation, in response to changes in the intracellular ATP/AMP ratio (Hardie et al., 1998; Inoki et al., 2003). TSC2 encodes a human homologue of the GTPase-activating protein (GAP) Rap1 (Wienecke et al., 1995) whereas TSC1 encodes a novel protein containing two coiled-coil domains. The Tuberous Sclerosis heterodimer functions as a GTPase activator of the Ras-related small GTPase Rheb (Ras homolog enriched in brain) accelerating GTP hydrolysis by Rheb

directly and thereby inhibiting mTOR signaling (Manning and Cantley, 2003; Patel et al., 2003; Stocker et al., 2003; Tee et al., 2003; Wienecke et al., 1995; Zhang et al., 2003). Rheb has been shown to bind to the mTOR complex independently of Rheb's guanyl nucleotide charging and its ability to bind TSC (Long et al., 2005). Rheb is a positive regulator of mTOR kinase activity in a GTP-dependent manner (Long et al., 2005) and is opposed by the TSC complex, by virtue of the ability of the TSC complex to act as a Rheb GTPase activator, directly promoting the conversion of Rheb-GTP to Rheb-GDP. The inhibitory action of the TSC complex on Rheb is attenuated by Akt/PKB-catalyzed TSC2 phosphorylation, whereas the TSC-Rheb-GTPase activator activity is enhanced by AMP-activated protein kinase-catalyzed TSC2 phosphorylation (Findlay et al., 2005; Harris and Lawrence, 2003; Hay and Sonenberg, 2004). Thus, the TSC complex is a major site at which PI3K signaling and energy sufficiency control mTOR signaling. Interestingly, growth factors and amino acids are also known to regulate actin polymerization (Jacinto et al., 2004) raising the possibility that growth factor and nutrient cues may also regulate mTORC2 through TSC and Rheb. Thus, the crosstalk that occurs between the nutrient-regulated TOR pathway and the growth factor-regulated insulin/IGF-I pathway ensures that cell proliferation only occurs when amino acids, energy and growth factors are in sufficient supply.

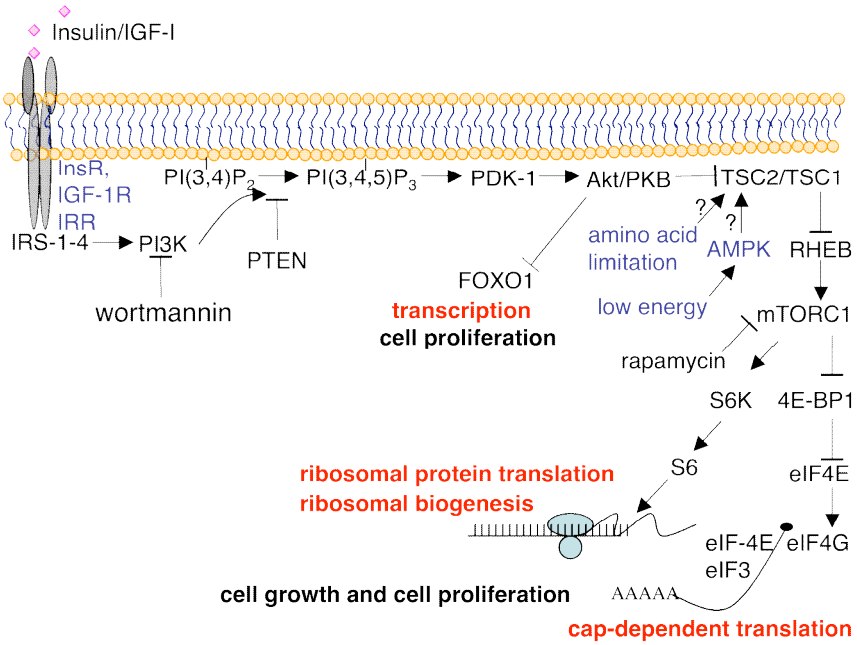

Figure C. A schematic of insulin action on the mTOR signaling pathway. Multiple pathways impinge on the mTORC1 to regulate translational machinery by activating S6K and hence ribosomal biogenesis, and by inactivating 4E-BP1, a repressor of the translation initiation factor eIF4E. The TOR pathway integrates the input of intracellular amino acids, growth factors (insulin/IGF-I) and cellular energy status to control cell growth and cell proliferation. The growth factor signal is transduced to TSC2 via the insulin-signalling pathway. Thus, the crosstalk between the nutrient-regulated TOR pathway and the insulin/IGF-I pathway ensures that cell proliferation only occurs when amino acids, energy and growth factors are in sufficient supply.

2.4.1.1 TOR and *daf-2* signaling in *C. elegans*

mTOR is a downstream component of insulin/IGF-I signaling in mammals(Oldham and Hafen, 2003; Raught et al., 2000; Scott et al., 1998; Zhang et al., 2000), but it is not clear how these two signaling pathways converge in *C. elegans*. Inactivation of *C. elegans* DAF-2 signaling causes dauer-stage arrest (Kimura et al., 1997; Morris et al., 1996; Paradis et al., 1999; Paradis and Ruvkun, 1998). Deficiency of CeTOR in respect to dauer development promotion is complex. Mutants in CeTOR and the *C. elegans* homolog of Raptor *daf-15* arrest as dauer-like L3 larvae with partial dauer morphology and dauer-like movement, but their feeding is not completely suppressed (Jia et al., 2004). Formation of partial dauers (defined as animals mosaic for dauer and nondauer phenotypes) is a hallmark of mutations in the *daf-2* pathway (Vowels and Thomas, 1992). The CeTOR larvae are similar to *daf-15* larvae, consistent with a similarity in gene function (Jia et al., 2004) raising the possibility that features of the TORC1 are conserved in *C. elegans.* Moreover, CeTOR RNAi animals share certain features of the pleiotropic *daf-2* (-) phenotype, such as lipid accumulation mainly in intestinal cells (Ashrafi et al., 2003; Vellai et al., 2003), reduced fertility (Tissenbaum and Ruvkun, 1998; Vellai et al., 2003), reduced viability (Tissenbaum and Ruvkun, 1998; Vellai et al., 2003) and life span extension. *daf-15* and CeTOR mutants shift metabolism to accumulate fat, as do predauer larvae and CeTOR(RNAi) enhanced dauer formation in *daf-2(e1370*) mutants. These genetic interactions between the CeTOR and *daf-2* signaling pathways suggest that they could be related in controlling metabolism, ageing and reproductive growth and that CeTOR at least partially mediates DAF-2 signaling.

Mammalian TOR controls the translation machinery via activation of S6K and via inhibition of the translation inhibitor 4E-BP (Schmelzle and Hall, 2000). However, this mechanism apparently is not used in *C. elegans*, because *cep70* (the homologue of p70 S6K) RNAi did not phenocopy loss of CeTOR function and searches of the *C. elegans* genome failed to detect a 4E-BP ortholog (Long et al., 2002). Thus, the developmental arrest at the L3 stage of CeTOR mutants is likely to result from global inhibition of mRNA translation (Long et al., 2002) suggesting a more global role for the CeTOR/*daf-15* complex in translational control through effectors distinct from S6K and 4E-BP.

Dual regulation of p70 S6K via TOR and PI3K signaling is seen in flies (Zhang et al., 2000). In *Drosophila*, TOR is also required for normal growth as TOR deficiencies lead to developmental arrested larvae (Oldham and Hafen, 2003; Zhang et al., 2000) and vesicle aggregation in the larval fat body (Zhang et al., 2000) (a fat accumulation phenotype), both similar to the phenotypes observed in CeTOR and *daf-15* mutants. Thus, although the molecular mechanisms may differ, the phenotypic outcomes of TOR signaling are analagous between *C. elegans* and Drosophila. The major phenotypic difference between flies and worms with respect to TOR signaling is that TOR-deficient flies are smaller than wild type, whereas CeTOR and *daf-2* mutants are the same size as wild type (Jia et al., 2004; Long et al., 2002) (for review see (Tissenbaum and Guarente, 2002)).

CeTOR and *daf-15* signaling also modulate adult longevity with both mutants exhibiting extended lifespan (Jia et al., 2004; Vellai et al., 2003). *daf-16* activity, which is required for *daf-2* life span extension is also required for increased *daf-15*/+ longevity (Jia et al., 2004), whereas CeTOR influences lifespan in a *daf-16*-independent manner (Vellai et al., 2003). Nevertheless, the extended lifespan of *daf-2 (e1370)* mutants is not increased further by treatment of CeTOR RNAi (Vellai et al., 2003) raising the possibility that TOR and the DAF-2 pathway are related in controlling lifespan. The precise relationships between *daf-2*, CeTOR, *daf-15* and *daf-16* are not yet clear. *daf-15* exhibits *daf-16* effects on longevity, but *daf-16*-independent effects on dauer formation and fat deposition. Further complicating the picture, DAF-16 negatively regulates *daf-15* transcription in a possible feedback loop (Jia et al., 2004). Thus, *daf-15* may be a point of integration of insulin/IGF-I and nutrient signaling pathways to regulate *C. elegans* larval development, metabolism and longevity (Jia et al., 2004). Although the detailed signaling connections between TOR and PI3K signaling cascades require clarification, these findings point to TOR as a possible mediator of insulin signaling and nutrient sensing in C. *elegans*.

2.5 The PI3K-like kinase family members ATM and ATR

The integrity of genomic DNA is constantly under threat, even in perfectly healthy cells. To ensure genome integrity organisms activate evolutionarily conserved cell cycle checkpoints in response to DNA damage to delay cell cycle progression and activate DNA damage repair systems or elicit apoptosis. All eukaryotic cells studied to date employ the PI3K-related kinase family members ATM (ataxia-telangiectasia mutated) and ATR (ataxia-telangiectasia- and Rad3-related) as key components in the cellular response to

damaged DNA (Abraham, 2001; Keith and Schreiber, 1995; Savitsky et al., 1995; Shiloh and Kastan, 2001). These proteins modify several checkpoint and repair proteins post-translationally in response to DNA damage (Furuta et al., 2003; Lee et al., 2003b; Lisby et al., 2003; Oakley et al., 2003; Zou et al., 2002).

Depending on the distinct positions and functions within the DNA damage signaling cascades, proteins involved in the DNA damage response have been classified as sensors, that associate directly or indirectly with damaged DNA and detect the damage, transducers, that transmit the signal of damaged DNA obtained from the sensors, or effectors, that elicit the various specific biological responses (for review see (Stergiou and Hengartner, 2004)). Atop of the presumably non-linear DNA damage pathways are the protein kinases ATM (*S. cerevisiae* and *S. pombe* Tel1) and ATR (*S. cerevisiae* Mec1, *S. pombe* Rad3) that, either directly or in collaboration with other factors, sense DNA damage or stalled replication forks and initiate signaling cascades (Figure D) by phosphorylating several proteins that regulate cell cycle progression, facilitate the repair of the damage or lead to the induction of apoptosis (for review see (Abraham, 2001)).

Damage recognition is usually a mutlistep reaction (for review see (Sancar et al., 2004)). In both yeast and mammalian cells the MRN (Mre11/Rad50/Nbs1) complex appears to be the earliest senor of DNA double-strand breaks (DSBs) by directly binding to DNA ends (for review see (Lisby and Rothstein, 2005; McGowan and Russell, 2004)). This binding reflects the first stage in the assembly of the repair foci and likely facilitates the tethering of the DNA ends together via a zinc-hook in Rad50 (Hopfner et al., 2002). A number of modulators of the MRN complex have been identified, including MDC1 and 53BP1 in human cells (Mochan et al., 2003). The rapid induction of ATM kinase activity following IR suggests that it acts as a sensor at an early stage of signal transduction in mammalian and yeast cells (Banin et al., 1998; Canman and Lim, 1998). The finding that the presence of a few breaks (2-4) activates the majority of ATM suggests that the cellular response to DSBs is either off or on, rather than being a graded response (for review see (McGowan and Russell, 2004)). The rapidity and stoichiometry of the reaction indicates that ATM is not activated only by directly binding to DSBs, ratherit is known that the MRN complex stimulates the protein kinase activity of ATM (for review see (Lisby and Rothstein, 2005)). In the absence of DNA damage, inactive ATM is proposed to exist as homodimer in which the kinase domain of one subunit faces the autophosphorylation site of the other one. ATM binds preferentially to DNA termini, apparently in a monomeric form (Smith et al., 1999).

Upon ATM activation, intermolecular phosphorylation of the subunits promotes dimer dissociation, which in turn allows accessibility of cellular substrates to the ATM kinase domain, setting off the chain of phosphorylation events of many downstream targets that leads to either DNA damage-induced cell cycle arrests in G_1, S and G_2 phases or cell death (for review see (Kurz and Lees-Miller, 2004)).

Multiple substrates of the ATM kinase participate in DNA-induced cell-cycle arrests. These include p53, Mdm2 and Chk2 in the G_1 checkpoint, Nbs1, Brca1, FancD2 and SMC1 in the transient S-phase arrest (Kim et al., 2002b; Lim et al., 2000; Taniguchi et al., 2002; Wu et al., 2000; Xu et al., 2002; Yazdi et al., 2002; Zhou and Elledge, 2000) and the tumor suppressor Brca1 and mammalian Rad17 in the G_2/M checkpoint (Xu et al., 2001a). Some of these proteins, like p53, histone H2AX and Chk2, are direct substrates of ATM (for review see (McGowan and Russell, 2004)). Others may be phosphorylated indirectly through ATM-mediated regulation of other protein kinases, such as Chk1 (for review see (Goodarzi et al., 2003; Shiloh, 2003)). Through the phosphorylation and activation of the checkpoint kinases Chk1 and Chk2 the initiating signal is further diversified and amplified (Motoyama and Naka, 2004).

After the activation of ATM upon DNA damage, stage two in checkpoint activation is dependent on the multi-component RP-A complex (replication protein A) that arrives to the sites of DNA lesions several minutes after MRN and which recognizes and promotes unstable single strand DNA (ssDNA) and thus. The MRN complex has been implicated in the initial nucleolytic resection of DSB to generate single stranded DNA critical for the subsequent protein assemblies (for review see (Lee and Paull, 2004; Lisby and Rothstein, 2005; McGowan and Russell, 2004)). Upon resection of the DNA end in *S. cerevisiae*, Tel1 (ATM) dissociates from the lesion (for review see (Lisby et al., 2004)). After dissociation of Tel1 the checkpoint continues to be activated by Mec1 (ATR), which is recruited to single stranded DNA by RP-A (for review see (Lisby and Rothstein, 2005). Subsequently, single stranded DNA bound RP-A recruits the checkpoint complexes Rad17/Rfc2-5, Rad9/Hus1/Rad1 (9-1-1) and ATR/ATRIP in yeast and mammalian cells (for review see (Lisby and Rothstein, 2005)). In response to genotoxic damage, the checkpoint 9-1-1 complex is loaded around DNA by the pentameric Rad17-RFC2-5 containing clamp loader complex independent of ATM or ATR (for review see (Parrilla-Castellar et al., 2004; Roos-Mattjus et al., 2002). Thus, Rad17-RFC and the 9-1-1 complex cooperate to detect damaged DNA (for review see (Stergiou and Hengartner, 2004)). The

DNA-bound sensor 9-1-1 complex then facilitates ATR-mediated phosphorylation and activation of Chk1, a protein kinase that regulates S-phase progression, G_2/M arrest, replication fork stabilization and coordination of DNA repair (for review see (Parrilla-Castellar et al., 2004)). The exact function of Rad17 and the sliding clamp 9-1-1 complex have not been determined, but they are believed to substitute for the normal replication factors to promote a form of DNA replication that is more appropriate under damage conditions (for review see McGowan, 2004 #775}).

Tel1 and Mec1 have partially redundant and complementary roles in checkpoint activation (Craven et al., 2002; Takata et al., 2004; Usui et al., 2001). This complementarity is likely due to Tel1 and Mec1 being recruited to different DNA structures, namely DNA ends (early) and single-stranded DNA (later) via interactions with the MRN complex and RP-A respectively (for review see (Lisby et al., 2004)). Thus, ATM and ATR become activated in response to DSBs and phosphorylate downstream components like H2AX. Additionally, due to its specificity for single stranded lesions, ATR is activated by a broader range of DNA damage stimuli than ATM, including UV irradiation (for review see (Sancar et al., 2004)). ATM and/or ATR activation allows the recruitment of large DNA repairsome protein complex, which includes Brca1, to the site of DNA damage and subsequent activation of effector proteins (for review see (Ting and Lee, 2004)). .

ATR is constitutively associated with the conserved protein ATRIP (Cortez et al., 2001). Within the ATR/ATRIP complex the function of ATR is to phosphorylate and activate checkpoint kinases, checkpoint transducers and several proteins involved in repair. Both ATR and ATRIP are reported to be DNA binding proteins and ATRIP binding is stimulated by the RP-A complex that coats single stranded DNA in response to spontaneous replication blocks or other forms of DNA damage (Zou and Elledge, 2003).

Spontaneous DNA damage is believed to result from stalled or collapsed replication forks (for review see (Lisby and Rothstein, 2004)). DNA replication stress is sensed primarily by ATR/ATRIP in mammalian cells and its orthologs in yeast, but also ATM plays an active role in repair of collapsed replication forks (for review see (Lisby and Rothstein, 2005)). The presence of foci of DNA repair complexes on DNA in S phase implies that DNA lesions are continuously being recognized and repaired during replication (for review see (Lisby and Rothstein, 2004)).

In mammalian cells, Chk1 transduces UV damage signals sensed by ATR, and Chk2 transduces the DSB signal sensed by ATM (for review see (Sancar et al., 2004)) leading to the activation of specific checkpoints that rapidly inhibit Cdk (cycline-dependent kinases) activity, delaying progression of the cell cycle to provide time to repair DNA or to complete replication (Figure D). DNA damage can cause cell cycle arrest at the G_2/M checkpoint to prevent initiation of mitosis (for review see (Kastan and Bartek, 2004)). Chk1 and Chk2 delay cell cycle transition by controlling the inhibitory phosphorylation of Cdk, largely mediated through inhibitory phosphorylation of the Cdk-activating phosphatases Cdc25A (cell division cycle 25) and Cdc25C (Furnari et al., 1997; Peng et al., 1997; Rhind et al., 1997; Rhind and Russell, 1998; Sanchez et al., 1997). Phosphorylation of Cdc25 phosphatases by Chk1 or Chk2 creates a binding site for 14-3-3 proteins which subsequently sequesters them to the cytoplasm where they are degraded by the ubiquitin proteasome pathway (for review see (Sancar et al., 2004)). This prevents the CDC25 phosphatases from removing an inhibitory phospho-tyrosine on cyclin B/Cdc2 and cyclin A/Cdc2 complexes, blocking Cdk activation and subsequent entry into mitosis. Thus, cytoplasmic delocalization of Cdc25 causes an arrest at the G_2/M border. Initially, Cdc25C was thought to be the effector of the G_2/M checkpoint (Peng et al., 1997), but the current opinion is that phophatase Cdc25A is the main effector of the G_2/M checkpoint in response to ATM-Chk2 or ATR-Chk1 signaling.

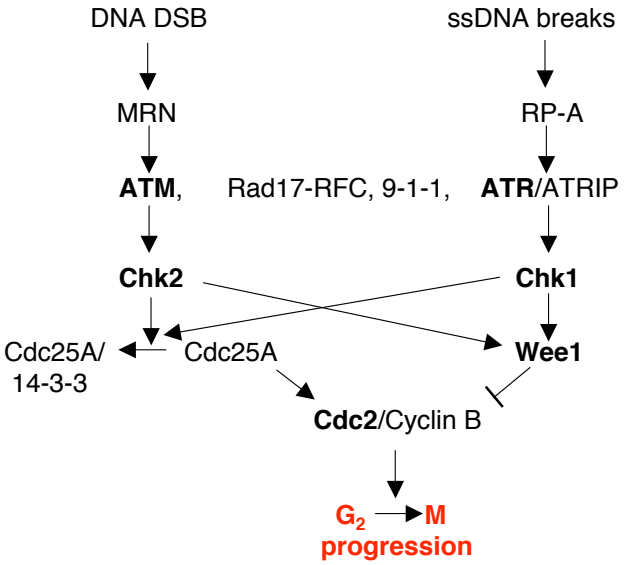

Figure D. Components of the G_2/M checkpoint in human cells. ATR functions both cooperatively and in parallel with ATM as initiator of the DNA damage checkpoint response. Upon DNA damage, sensor proteins ATM, ATR/ATRIP, Rad17-RFC, 9-1-1 are recruited to the site of damage. The sensors communicate the DNA damage signal directly and/or indirectly to the transducers Chk1 and/or Chk2. These kinases are implicated in triggering G_2/M arrest by preventing Cdc25A phosphatase-dependent dephosphorylation of the Cdc2/cyclinB complex. Inhibition of the mitotic inducer Cdc2 is brought about by inactivation of Cdc25 and activation of Wee1. Protein kinases are indicated in bold.

2.6 Dysregulation of PI3K-related family members

Malfunction of physiological pathways underlying nutrient signaling and energy homeostasis can have major consequences for human health, and the modern society. PI3K-related family members are important modifier of cancer cell proliferation, survival, growth and treatment sensitivity (for review see (Foulstone et al., 2005)). In this respect, dysfunction of signaling pathways involving PI3K-related family members have been implicated in a variety of diseases like ataxia-telangiectasia, cancer, type-2 diabetes, tuberous sclerosis and ageing-mediated degeneration. A clearer understanding of the molecular pathways that underlie the pathophysiology of metabolic diseases, tumor syndromes and human cancers will generate new therapies for these threatening diseases and may possibly open avenues for pharmacological manipulation of aging.

2.6.1 Ataxia-telangiectasia (AT) and Seckel syndrome

The gene ATM is mutated in the human disease AT and cells from AT patients typically lack detectable ATM protein. These patients exhibit abnormalities in telomere morphology and have abnormal responses to IR, including increased cell death, increased chromosomal breakage and cell cycle checkpoint defects. In addition, AT patients exhibit progressive cerebellar ataxia, immune deficiencies, gonadal atrophy, oculocutaneous telangiectasias, radiation sensitivity, premature ageing and an increased risk of cancer, particularly for lymphomas. ATR mutations causing partial loss of ATR activity in humans have been associated with the human autosomal recessive disorder Seckel syndrome, which shares features with AT (O'Driscoll et al., 2003).

Based on the central function of ATM and ATR in the DNA damage response network that controls cell cycle progression, these PI3K-related kinases have the potential to delay or prevent cancer. Upon activation, ATM and ATR phosphorylate several important tumor suppressors, including p53, BRCA1, and CHK1. Mutations compromising these checkpoints might allow cell proliferation, survival, increased genomic instability and tumor progression (Bartkova et al., 2005). The transcription factor and tumor suppressor p53 is the single most commonly mutated tumor suppressor gene in human cancers (Hussain et al., 2000) and is considered to be the guardian of the genome (Lane, 1992). Interestingly, mutations in BRCA1, BRCA2, ATM, p53, CHK2 and PTEN account for 20-30% of the familial aggregation of breast cancer (Heikkinen et al., 2005a; Heikkinen et al., 2005b).

2.6.2 Role of the TOR and insulin/IGF signalling pathways in cancer

The development of a tumor requires a series of genetic mutations in key processes, commonly referred to as the hallmarks of cancer. These key features are mutations leading to selective growth and proliferation of tumor cells, recruitment of blood vessels and stromal cell populations, and cellular invasion and metastasis. The potential role of PI3Kinase in signaling to cell growth and proliferation has sparked interest in its role in cell transformation. Thus, dysregulation of pathways upstream and downstream of mTOR are implicated in the pathogenesis of cancer. Several members of the insulin/mTOR-signaling network are tumor suppressor genes (PTEN, TSC1, TSC2, LKB1) or proto-oncogenes (PI3K, Akt), and the network may thus play a crucial role in carcinogenesis. Inhibition of mTOR and PI3K by rapamycin can modify tumor cell survival, growth and chemotherapy sensitivity *in vivo* for certain cell types (Wendel et al., 2004). The role of insulin/mTOR signaling in tumorigenesis is believed to be mediated partly through the regulation of the level of the eIF4E protein, which is upregulated by mTOR signaling. Moderate overexpression of the potent oncogene eIF4E can cause deregulated cell proliferation and malignant transformation (De Benedetti and Rhoads, 1990; Lazaris-Karatzas et al., 1992) and eIF4E levels in the tumor margins strongly correlate with the recurrence of head and neck carcinomas after surgery (De Benedetti and Harris, 1999; Nathan et al., 1997). Deregulated mTOR signaling is also seen in Cowden's disease (patients suffer from harmatomas with tendency of malignant transformation), where loss of the tumor suppressor PTEN activates Akt/PKB independently of growth factor signaling (for review see (Cantley and Neel, 1999)). In fact high levels of deregulated mTOR activity are associated with several hamartoma syndromes, including tuberous sclerosis, Cowden's disease and Peutz-Jeghers syndrome. These disorders are all caused by mutations in tumor-suppressor genes that negatively regulate mTOR/PI3K signaling system. Moreover, the reduced expression of PTEN protein correlated with lymph node metastases and worse prognosis in the patients with breast cancer (Tsutsui et al., 2005).

The TSC syndrome (tuberous sclerosis) is a human autosomal dominant disorder, characterized by mutations in either the TSC1 (van Slegtenhorst et al., 1997) or the TSC2 (Krymskaya, 2003) gene and estimated to affect 1 in 6000 individuals most commonly infants and young children (Gomez, 1991). Mutations in TSC1 or TSC2 lead to upregulated mTOR signaling. A hallmark of tuberous sclerosis is the widespread

development of harmatomas (benign growth in multiple organs), often containing abnormally large cells, which affect a variety of tissues (Gomez, 1991; Sparagana and Roach, 2000). Although these tumors rarely become malignant, their presence in various tissues gives rise to several clinical manifestations, including neurological disorders (e. g. epilepsy and autism), skin lesions, cardiac dysfunction, and kidney and lung failure (for review see (Manning and Cantley, 2003)).

As proper regulation of the PI3K-Akt pathway is critical for the prevention of tumorigenesis (Manning and Cantley, 2003) mTOR is a prime strategic target for anti-cancer therapeutic research and development. Rapamycin is clinically used to inhibit host rejection of transplanted organs, growth of tumor cells and the occlusion of coronary arteries after angioplasty (Garza et al., 2002; Huang and Houghton, 2003; Odorico and Sollinger, 2002). The importance of understanding the molecular mechanisms that control mTOR function is underscored by recent clinical trials showing that rapamycin or its derivates are efficacious in the treatment of solid tumors in patients with metastatic renal cell carcinoma and non-small cell lung, prostate, and breast cancer (Hidalgo et al., 2000).

2.6.3 Type-2 diabetes mellitus and obesity

Development of insulin resistance or unresponsiveness to insulin, reflecting impairment of insulin action at the cellular level, plays an important role in the etiology of common metabolic disorders, including type-2 diabetes and obesity, but is also associated with a wide variety of human disorders, including cardiovascular disease (for review see (Manning and Cantley, 2003; Porte et al., 2005)). Given the critical role of PI3K in regulating glucose metabolism, it is reasonable to suspect that alterations in expression or regulation of this enzyme may contribute to the development of insulin resistance. Indeed such alterations have been observed in an insulin-resistant animal model, providing experimental evidence for a role of deregulation of the PI3K pathway in the development of metabolic diseases. Interestingly, FOXO1 +/- mice are protected against diet-induced diabetes, consistent with the theory that FOXO proteins function as insulin antagonists with pro-diabetic function. Type-2 diabetes mellitus is a polygenic, multifunctorial disease with a pathology that includes defects in insulin-stimulated glucose disposal in peripheral tissues, insulin suppression of hepatic glucose production, and glucose-mediated insulin secretion by pancreatic β-cells (Kahn and Rossetti, 1998). Decreased insulin secretion and reduced β-cell mass usually contribute to the development of the disease at a later stage (DeFronzo, 1997). Long-term complications of diabetes particularly affect the blood

vessels by increasing the risk of the patient to develop macroangiopathies such as coronary heart diseases and microroangiopathies such as kidney failures and blindness. Obesity, on the other hand, is known to enhance the incidence of coronary heart diseases, hypertension, type-2 diabetes mellitus, and cancer, all of which are known to shorten lifespan (Manning and Cantley, 2003). Studies helping elucidate the multiple actions of insulin would help to explain the close association between these two metabolic disorders.

2.7 C. elegans

The evolutionary conservation of the biochemical and genetic regulation of fundamental processes has allowed the discovery and dissection of signal transduction pathways in lower species, such as the nematode *C. elegans* (Figure E), to act as models to delineate the genetics and regulation of these processes in mammalian cells. The origin of the name Caenorhabditis elegans is a blend of Greek and Latin (*Caeno*, recent; *rhabditis*, rod; *eleans*, nice). The power of this model organism is evidenced by fact that fundamental cellular processes such as RNA mediated interference (RNAi), programmed cell death, *trans*-splicing of mRNA and the genetic link among insulin-like signaling, oxidative stress, and longevity were all originally discovered in *C. elegans*. The appreciation and the impact of findings in *C. elegans* for the human society is last but not least evident by the awarding of the Nobel Prize for Medicine in 2002 to Sydney Brenner, H. Robert Horvitz and John Sulston for their work on the genetics of development and programmed cell death in *C. elegans.*

Figure E. Nomarski picture of an adult *C. elegans* hermaphrodite. The head is oriented to the left and the vulva to the bottom.

The soil nematode *C. elegans* as a model organism offers great potential for genetic analysis, partly because of its rapid life cycle, large brood size and its sequenced genome. *C. elegans* can grow productively at any temperature between 12°C and 25,6°C. A single hermaphrodite produces on average 300-350 progeny and has the potential to produce more than 1000 progeny when mated. The large brood size favors the application of

forward and backward genetic screens. Importantly, researchers agreed to use the same genetic background (Bristol strain) to generate their mutants in, making all *C. elegans* stocks around the world isogenic, permitting direct comparisons between different mutants.

In *C. elegans* there exist two sexes, the hermaphrodite and the male. The XO males arise spontaneously in XX hermaphrodite populations by means of X chromosomal nondisjunction at a frequency of about 0.1%. The male can inseminate the hermaphrodite, which will use male sperm preferentially (Ward and Carrel, 1979). Thus, the natural *C. elegans* mode of inbreeding by the self-fertilizing hermaphrodite combined with the ability to cross hermaphrodites with males offers conveniences for genetic based research. The *C. elegans* genome, roughly about the size of a single human chromosome (100 million base pairs), contains more than 19000 genes. In 1998 the *C. elegans* genome was sequenced (with the exception of a few gaps that were completed in 2002), making it the first multicellular organism for which we obtained the complete genetic information. In 2003 the genome sequence of the related nematode *C. briggsae* was also determined, allowing researchers to study the comparative genomics of these two organisms. As exons are around 80% and introns only 30% conserved between these species, conserved elements in non-coding regions are likely to represent functional control elements, facilitating the analysis of promoter regions. The *C. elegans* life cycle from embryogenesis and postembryonic development through four larval stages (L1 –L4) to the adult takes around 2 days at 25°C. Moreover, the existence of temperature-sensitive mutants provide a useful means of propagating and analysing mutations in genes that are essential for fertility or viablility.

Perhaps the most unique advantages offered by this organism for the study of development are the constancy of somatic cell number and the constancy of somatic cell position from individual to individual. A newly hatched *C. elegans* hermaphrodite contains 558 nuclei and an adult 959 nuclei (Sulston and Horvitz, 1977). Moreover, virtually every cell in the body is accessible to laser microsurgery. Thus, *C. elegans* has been especially useful for studying cellular differentiation. Additionally, the useful features of this organism are the transparency of the body, its short life span (around 2 weeks at 25,5°C), the anatomical simplicity, small size (1-1.5 mm-long adult), and its cheap and easy maintenance. Nomarski DIC microscopy combined with fluorescent protein reporters can be used for analysis of the timing and tissue specificity of transcription as well as expression pattern of

individual proteins in living transgenic animals under different stimuli. The short life span of *C. elegans* and the availability of mutants with greatly increased longevity have stimulated its use as a model for research on aging. *C. elegans* is also one of the simplest organisms with a nervous system. It comprises 302 neurons which have been completely mapped (Riddle et al., 1999). Conveniently, the worms feed on microorganisms such as *E. coli* bacteria and survive storage at –80°C.

2.7.1 Germ line

The germ line is one of the best-characterized and most extensively studied cellular compartments in *C. elegans* (Kimble et al., 1984; Machaca and L'Hernault, 1997; McCarter et al., 1997). During early embryogenesis, the germ line is set apart from the soma via a series of four unequal divisions of the germ line blastomeres (P0, P1, P2, P3) (Figure F). The cytoplasmic germ line granules, which are believed to play a role in the determination of germ fate specification (Illmensee and Mahowald, 1974), are asymmetrically segregated in the P-cell lineage to the germ line founder cell P4 (thus termed P-granules) and are present in all progeny germ cells except for mature sperm. The germ line precursor cell P4, which is formed at the 16-24 cell stage, is exceptional among the embryonic founder cells in that it divides only once during embryogenesis at approximately the 100-cell stage. In newly hatched larvae of both sexes the gonad consists of a four-cell gonad primordium of the two somatic precursor cells, Z1 and Z4, which proliferate and differentiate into the somatic structures of the gonads including the distal tip cells (DTC). The daughters of the P4 cell, the two germ line precursor cells, Z2 and Z3 generate the entire germ line by extensive proliferation at variable rates throughtout larval and adult stages giving rise to about 1000 germ cells per gonad arm in the adult hermaphrodite.

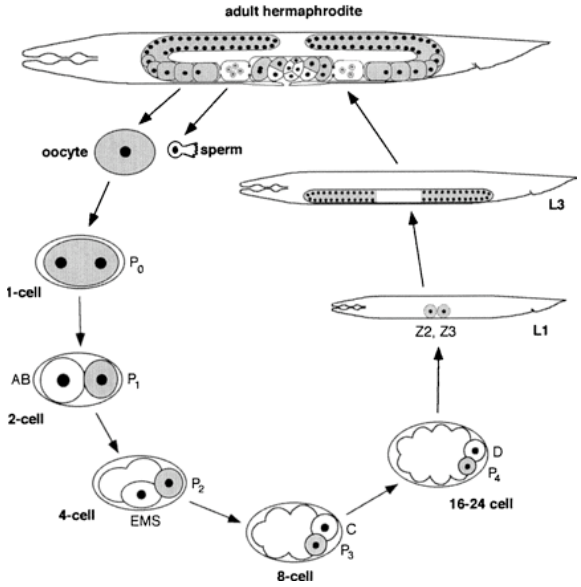

Figure F. The *C. elegans* germ line cycle. During early embryogenesis, the germ line is set apart from the soma via a series of four unequal divisions of the germ line blastomeres P0 to P4. The cytoplasmic germ line granules, which are believed to play a role in the determination of germ fate specification, are asymmetrically segregated in the P-cell linage to the germ line founder cell P4 (thus termed P-granules) and are present in all progeny germ cells except for mature sperm (Illmensee and Mahowald, 1974). The germ line precursor cell P4, which is formed at the 16-24 cell stage, is exceptional among the embryonic founder cells in that it divides only once during embryogenesis, at approximately the 100-cell stage. The two daughters of P4, Z2 and Z3, generate the entire adult germ line by extensive proliferation during larval development including sperm and oocytes. All germ line cells except mature sperm contain P granules (shaded). From (Xu et al., 2001b).

Adult hermaphrodite worms possess two equivalent reflexed gonad arms with partially cellularized germ nuclei (further referred to as germ cell) at different stages of proliferation and differentiation. Cytoplasmic bridges to the rachis, a core of cytoplasm that runs the length of the distal arm, connect germ cells in this specialized syncytium. Primary spermatocytes are cellular, while oocytes remain connected to each other and the rachis by a thin bridge. Each gonad arm displays a distal-to-proximal polarity in its pattern of mitosis, meiosis and gametogeneis (McCarter et al., 1997). The mitotically active germ cells at the distal end of each gonad arm (Figure G) serve as a self-renewing population of stem cells for the germ line throughout adulthood (Hirsh et al., 1976).

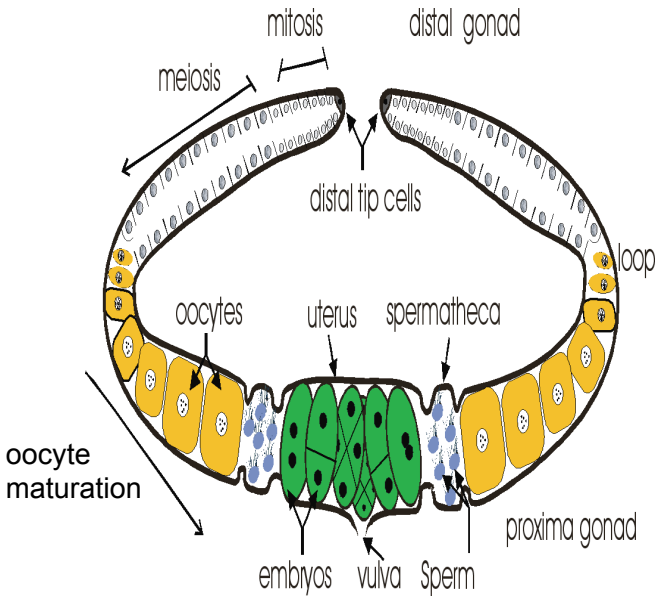

Figure G. Schematic diagram of the *C. elegans* germ line. The adult hermaphrodite has a two-armed gonad in which germ nuclei are in a syncytium. Germ cells divide mitotically at the distal end of each germ line arm, enter meiosis and differentiate into oocytes as they move more proximally. Oocytes are fertilized as they pass through the spermatheca and encounter sperm. Embryogenesis starts in the worm and continues after the eggs have been laid through the vulva.

Germ line proliferation is controlled by an inductive interaction between the somatic distal tip cells and the germ line, balancing mitosis and differentiation (Kimble and Hirsh, 1979) (Figure H). Although the DTC is absolutely necessary for the maintenance of a distal mitotic population of germ cells, its influence is not fully sufficient; the proximal sheath and/or spermathecal cells are also required for efficient distal proliferation (McCarter et al., 1997). Nevertheless, the GLP-1 (germ line proliferation defective) signaling pathway is a major controller of this decision (Seydoux and Schedl, 2001).

The *C. elegans* genome encodes two putative Notch-like transmembrane receptors, LIN-12 (lineage abnormal) and GLP-1, which function with common components, designated LAG (LIN-12 and GLP-1). Spatially controlled activation of the GLP-1 pathway occurs when membrane-bound LAG-2 ligand, expressed in the somatic DTC, binds to the GLP-1 receptor, possibly restricting GLP-1 signaling to the distal end of the germ line (Austin and Kimble, 1987; Crittenden et al., 1994; Henderson et al., 1994; Lambie and Kimble, 1991, Fitzgerald, 1995 #551; Tax et al., 1994; Yochem and Greenwald, 1989). Ligand binding is thought to cause the cleaved intracellular portion of GLP-1 (GLP-1(INTRA)) to translocate to the nucleus of the germ cells and bind the LAG-1 transcription factor, thereby causing the transcription of target genes that promote proliferation and/or inhibit entry into meiosis (Mumm and Kopan, 2000). The somatic signal is continuously required in the germ line to

transduce the proliferative signal. If the GLP-1 signaling pathway is rendered inactive, all germ cells enter meiosis, depleting the stem cell population (Austin and Kimble, 1987; Lambie and Kimble, 1991). Although the exact mechanism is unclear (Crittenden et al., 1994; Fitzgerald and Greenwald, 1995), it appears that at increasing distance from the DTC, the level of ligand falls, GLP-1 signaling decreases and germ cells exit the mitotic cycle and enter meiosis. Berry and colleagues proposed that the proliferative region is maintained by a positive feedback of GLP-1 signaling on *glp-1* expression (Berry et al., 1997). Initially, ligand binding activates GLP-1 signaling, leading to proliferation and increased *glp-1* mRNA translation. Increased *glp-1* mRNA translation provides more receptor, which can respond to the ligand. As germ cells move proximally, the localized source of ligand decreases, leading to reduced receptor production. When signaling by GLP-1 falls below a certain threshold, germ cells exit the mitotic cell cycle to enter meiotic prophases and *glp-1* mRNA translation ceases. Consistent with this model, the switch from proliferation to meiotic entry occurs between on average 19 and 26 cell diameters for the distal end (Hansen et al., 2004). In the late L3 larval stage the germ cells most distant from the DTC enter meiosis. The first germ cells to enter meiosis start gametogenesis at the L4 larval stage, undergo spermatogenesis by completing meiosis I and II and become localized to the spermatheca. Hermaphrodite worms are basically female animals that produce sperm for a brief period of time during the L4 stage of larval development. After the L4 to adult molt a switch in the germ line sex determination pathway occurs, with the consequence that gametogenesis converts to oocyte production for the duration of adulthood. Thus, in the adult hermaphrodite the more proximal germ cells initiate prophase of meiosis I, and progress through the leptotene and zygotene stages in the transition zone (Crittenden et al., 1994, Dernburg, 1998 #555). Near the loop in the gonad, the female germ cells exit pachytene (for review see (Hubbard and Greenstein, 2000; Seydoux and Schedl, 2001) progress into the diplotene stage of meiosis I and eventually pause in diakinesis of meiosis I, where six individual bivalent chromosomes can be identified (McCarter et al., 1997). The presence of sperm triggers the oocytes to complete meiosis and stimulates ovulation (McCarter et al., 1999).

Post-transcriptional regulation plays a major role within the *C. elegans* germ line. The spatial restriction of GLP-1 accumulation appears to result from a translational control mechanism. The GLP-1 signaling pathway regulates the proliferative versus meiotic entry decision, at least in part, by spatially inhibiting *gld-1* and *gld-2* (defective in germ line development) which function parallel in redundant pathways downstream of GLP-1

signaling to promote meiotic development and/or inhibit proliferation of germ cells (Francis et al., 1995b; Kadyk and Kimble, 1998) (Figure H). GLP-1 inhibits the accumulation of the KH domain-containing RNA binding protein GLD-1, a conserved translational repressor of the STAR/Quaking family (Jan et al., 1999; Jones and Schedl, 1995; Lee and Schedl, 2001). GLD-2 belongs to the DNA-β nucleotidyl transferase super family and encodes the catalytic subunit of a poly(A) polymerase (Wang et al., 2002). Interestingly, GLD-2 lacks an RNA binding domain. GLD-2 and GLD-3 seem to act together as cytoplasmic heterodimeric poly(A) polymerase by the KH RNA binding domain of GLD-3 recruiting GDL-2 to specific mRNAs, (Eckmann et al., 2002; Wang et al., 2002). Thus, all three evolutionarily conserved GLD proteins have roles in regulating mRNAs. The gene for either *gld-1* or *gld-2* is sufficient to promote meiotic entry since in either of their single null mutant animals, germ cells enter meiosis normally, but show defects in their meiotic progression (Francis et al., 1995a; Hansen et al., 2004; Kadyk and Kimble, 1998). However, in animals that lack both *gld-1* and *gld-2* activity, a synthetic overproliferative germ line is formed, believed to derive from a defect in meiotic entry, rather than meiotic progression (Hansen et al., 2004; Kadyk and Kimble, 1998). This phenotype is epistatic to *glp-1* null indicating that *gld-1* and *gld-2* function downstream of GLP-1 signaling (Kadyk and Kimble, 1998). Therefore, GLP-1 signaling promotes proliferation, at least in part by turning off the activities of *gld-1* and *gld-2*.

A major mechanism by which GLP-1 signaling maintains the stem cell population is by inhibiting GLD-1 protein accumulation in the distal end of the germ line, thereby restricting its activity to more proximal regions (Hansen et al., 2004). The exact mechanism by which alteration of GLP-1 signaling in the distal germ line change *gld-1* and *gld-2* activities is not determined yet, but it is interesting to note that FBF (*fem-3* binding factor) has been shown to inhibit GLD-1 accumulation in the distal end of the germ line (Crittenden et al., 2002; Zhang et al., 1997). GLD-1 levels are low in the distal end, then increase until reaching a high level app. 20 cells diameters from the distal end (Hansen et al., 2004; Jones et al., 1996). FBF is a collective term for the products of two almost identical genes, *fbf-1* and *fbf-2*, which appear to be redundant (Zhang et al., 1997). FBF belongs to the PUF (Pumilio and FBF) family of RNA-binding proteins and was originally identified for its role in germ line sex determination (Zhang et al., 1997). Loss of FBF activity results in premature entry into meiotic prophase and depletion of the stem cell population in the late fourth larval stage (Crittenden et al., 2002). FBF acts, at least in part, by repressing the activity of *gld-1* mRNA via two FBF binding sites in the *gld-1* 3`UTR

(untranslated region) (Crittenden et al., 2002). Thus, FBF is a post-transcriptional negative regulator of GLD-1 accumulation (Crittenden et al., 2002). Strikingly, low GLD-1 levels allow proliferation whereas high GLD-1 levels promote meiosis (Hansen et al., 2004). Therefore, FBF promotes mitosis and maintains germ line stem cells most likely by keeping GLD-1 levels low in the distal region of germ line (Crittenden et al., 2002). GLD-1 accumulation by FBF acts through the translational regulator *nos-3* (*Drosophila* nanos) while regulation of *gld-2* in this processes is likely to be mediated by something other than, or in addition to FBF (Hansen et al., 2004). Hansen and colleagues suggest a model in which GLP-1 signaling regulates the size of the stem cell population by regulating GLD-1 levels, at least in part, through antagonism between the repressive activity of FBF and the positive activates of NOS-3 and GLD-2 (Hansen et al., 2004). Thus, FBF and NOS-3 function in opposite directions to regulate meiotic entry. Whereas FBF promotes proliferation and and/or inhibits meiotic entry (Crittenden et al., 2002) NOS-3 inhibits proliferation and/or promotes meiotic entry, both accomplishing these functions, at least in part by regulating GLD-1 accumulation. The GLD-1 accumulation pattern is important in controlling the proliferation versus meiotic development decision, with low GLD-1 levels allowing proliferation and increased levels promoting meiotic entry (Hansen et al., 2004). Thus, the proposed GLP-1 positive feedback mechanism could be accomplished through *gld-1* (Marin and Evans, 2003). GLD-1 binds the GLP-1 3'UTR and represses its translation. In the part of the germ line closest to the DTC, GLP-1 signaling is high and represses GLD-1 accumulation (Hansen et al., 2004). More proximally, further away from the DTC-bound LAG-2 ligand GLP-1 signaling is reduced, allowing for increased expression of GLD-1, which then can bind to the 3'UTR of GLP-1 inhibit its translation.

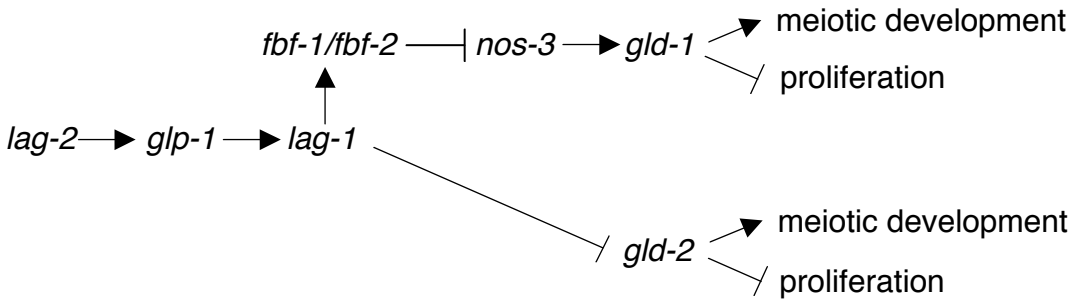

Figure H. Genetic model of the regulation of proliferation versus meiotic entry. GLP-1 signaling inhibits the redundant *gld-1* and *gld-2* pathways in the distal end of the gonad. For *gld-1*, this inhibition involves *fbf*-1 and *fbf-2* inhibiting the promotion of *gld-1* activity by *nos-3*. As cells move proximally, the *gld-1* and *gld-2* pathways become active, causing meiotic entry to occur. Upon inhibition of both pathways, germ cells are defective in entering meiotic prophase, forming an overproliferative germ line. Modified from (Hansen et al., 2004).

In *C. elegans*, regulation of mRNA also plays a major role in the decision between spermatogenesis and oogenesis (Puoti et al., 1997). A mode to control mRNAs during animal development relies on RNA binding proteins that bind specific mRNAs, often through elements in their 3'UTRs and thereby regulate their translation, stability, or localization (Thompson et al., 2000). This mechanism is particularly conspicuous in the germ line. The specification of a germ cell as sperm or oocytes relies on essentially the same sex determination pathway that governs male or female development in somatic tissues (Nicoll et al., 1997). In the germ line, however, the somatic pathway is modified by germ line-specific regulators that control mRNA activities (Puoti et al., 1997). Normally XX animals are hermaphrodite, making sperm first and then oocytes, and XO males making sperm continuously. In hermaphrodites, a cascade of 3' UTR controls modulating the activity of sex determination genes regulates the transient generation of sperm. Thus, the *fem* genes, *fog-1* and *fog-3* must be active early to allow a brief period of spermatogenesis in the L4, but must be inactive later to allow the switch to continuous oogenesis in the adult (Riddle et al., 1997). GLD-3 negatively regulates FBF, which derepresses the male-promoting *fem-3* mRNA and thereby promotes spermatogenesis (Eckmann et al., 2002). After the L4 to adult mold, FBF binds the distinct regulatory element PME in the *fem-3* 3'UTR, the *fem-3* male-promoting activity is repressed, and as a result the germ line switches from spermatogenesis to oogenesis (Zhang et al., 1997). FBF and NOS-3 physically interact (Kraemer et al., 1999) and are thought to function together in repressing *fem-3* translation relating to germ line sex determination (Ahringer and Kimble, 1991).

2.7.2 Programmed cell death

Three different, genetically separable pathways leading to apoptosis in *C. elegans* have so far been described; somatic cell death, physiological germ line cell death and DNA damage-mediated germ cell death. *C. elegans* undergoes a highly reproducible and regulated cell autonomous somatic cell death, which allows every cell to be followed during development (Ellis and Horvitz, 1986; Liu and Hengartner, 1999). Physiological germ cell death is thought to maintain tissue homeostasis, whereas DNA damage-mediated germ cell death involves a conserved set of upstream checkpoint proteins needed to eliminate cells with damaged DNA to maintain genomic stability (Gartner et al., 2000; Gumienny et al., 1999).

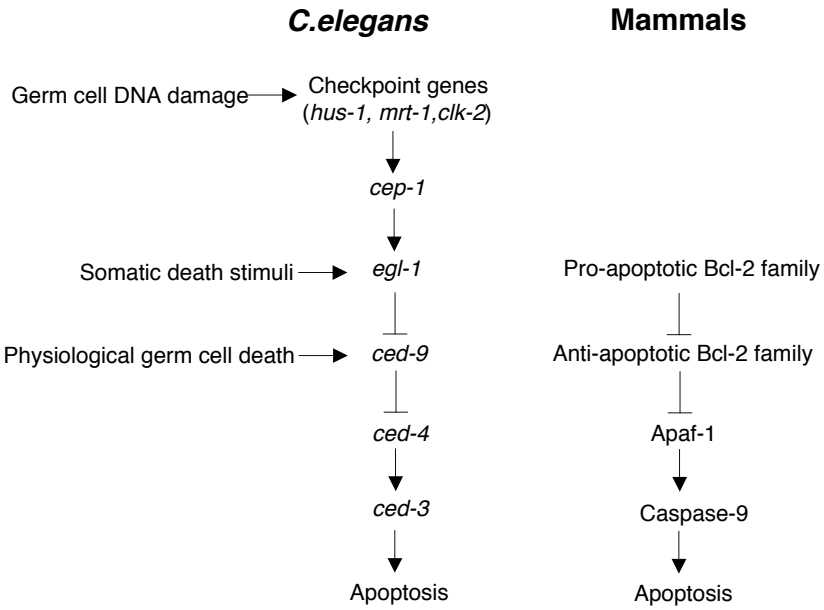

Figure I. Comparative diagram of the evolutionarily conserved apoptosis pathways in *C. elegans* and mammals. Functional homologues of caspases and their regulators across species are indicated by the same position. In *C. elegans* three genetically distinct cell death programs represent different death signals, which use distinct upstream mechanisms to engage the core apoptosis machinery. The DNA damage mediated germ cell death requires the action of *cep-1* and the cell cycle checkpoint genes *hus-1*, *mrt-1*, *clk-2*. Upon DNA damage human p53 is known to activate the transcription of several genes including members of the pro-apoptotic Bcl-2 family (Miyashita and Reed, 1995; Nakano and Vousden, 2001). Modified from (Deng et al., 2004).

2.7.2.1 Somatic cell death

In the *C. elegans* hermaphrodite 131 out of the 1090 somatic cells undergo programmed cell death during embryogenesis and larval development (Sulston and Horvitz, 1977, Sulston, 1983 #612). The death of these cells is due to the activities of four genes (Figure I), namely the pro-apoptotic BH3-only protein *egl-1* (egg-laying defective), the anti-apoptotic Bcl-2-like protein *ced-9* (cell-death defective), the Apaf-1-like adaptor protein (*ced-4*) and the pro-caspase (*ced-3*) (Horvitz, 1999). In cells destined to survive, CED-9 binds to CED-4 and thereby blocks CED-4s ability to activate the caspase CED-3 (Hengartner et al., 1992, Horvitz, 1999 #572, Chen, 2000 #613). Thus, the pro-apoptotic activity of CED-3 and CED-4 is antagonized by CED-9 (for review see (Hengartner and Horvitz, 1994)). In cells that are destined to die, *egl-1* transcription is activated (Conradt and Horvitz, 1999). Binding of the CED-9 inhibitor EGL-1 to the mitochondrial protein CED-9 causes the mitochondrial protein CED-4 to relocalize to perinuclear membranes resulting in the binding and activation of CED-3 and subsequent CED-3-dependent killing (for review see (Hengartner, 1999)).

2.7.2.2 Germ line cell death

In *C. elegans* the DNA damage-mediated germ cell death, as well as the physiological germ cell death pathway, can lead to germ cell apoptosis during meiotic development (Hofmann et al., 2000). Both of these germ cell apoptosis pathways (Figure I) use the same apoptotic core machinery as somatic cell death (*ced-9*, *ced-4* and *ced-3*), but appear to be regulated by distinct signaling pathways upstream of the core apoptotic machinery (Gumienny et al., 1999). Whereas somatic cell death is regulated by a combined action of *egl-1, ced-9, ced-4* and *ced-3,* physiological germ cell death only depends on *ced-9, ced-4* and *ced-3* and DNA damage-induced germ line apoptosis requires the combined action of *egl-1, ced-9, ced-4* and *ced-3* and the cell cycle regulators *clk-2* (also called *rad-5*), *hus-1*, *mrt-2* and *cep-1* (Deng et al., 2004; Gartner et al., 2000; Gumienny et al., 1999; Lettre et al., 2004; Schumacher et al., 2001). Thus, DNA damage-activated germ cell apoptosis acts through a conserved checkpoint pathway that includes *clk*-2 (clock abnormality), *mrt-2* (mortal germ line), *hus-1* (human HUS1 related) and *cep-1* (*C. elegans* p53-like protein). Interestingly, none of these genes is required for physiological germ cell death (for review see (Derry et al., 2001)).

2.7.2.3 DNA damage-mediated germ cell death

DNA damage activates a conserved DNA damage response pathway that induces both a transient cell cycle arrest of mitotic germ cells and apoptosis of meiotic pachytene cells in the *C. elegans* germ line to prevent the propagation of gametes with damaged genomes (Ahmed et al., 2001; Gartner et al., 2000). Mitotic cells in the distal arm of the germ line transiently halt cell proliferation after irradiation but continue to grow, as indicated by a decrease in cell number and an enlargement of cellular and nuclear size compared to untreated worms (Gartner et al., 2000). The intranuclear mechanisms that signal apoptosis after DNA damage overlap with those that initiate cell cycle arrest. Cell cycle arrest and apoptosis are two responses to DNA damage that are spatially separated and under developmental control (Figure J).

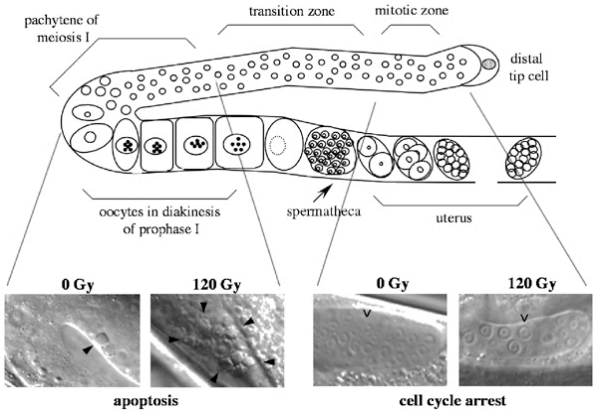

Figure J. Cellular DNA damage responses in the adult hermaphrodite germ line. Distal-to-proximal polarity of mitotic and meiotic germ cell nuclei. Following DNA damage, germ cells in the mitotic region undergo proliferation arrest (right, open arrowheads), whereas meiotic germ cell nuclei undergo programmed cell death (left, filled arrowheads). From (Stergiou and Hengartner, 2004).

As mentioned before, the three checkpoint genes *clk-2*, *hus-1* and *mrt-2* are required for DNA damage-induced germ cell apoptosis, but also for germ cell proliferation arrest (Gartner et al., 2000). The *C. elegans* homologue of the mammalian tumor suppressor protein p53 *cep-1* is also required for DNA damage-induced apoptosis in the *C. elegans* germ line, but is dispensable for DNA damage-induced cell cycle arrest, somatic cell death and physiological germ cell death (Derry et al., 2001; Schumacher et al., 2001). Interestingly, *Drosophil*a p53 is also required for DNA damaged induced apoptosis, but not for cell cycle checkpoint activation (Sogame et al., 2003), contrasting to the situation in mammalian cells where p53 can mediate both cell cycle arrest and apoptosis, depending on cell type and stimulus. The fact that the *C. elegans* p53 homolog participates in a conserved signaling pathway in response to DNA damage suggests that p53-dependent gla (germ line apoptosis) genes will be involved in the maintenance of genome stability (Hofmann et al., 2002). Consistent with this hypothesis, this p53-dependent class contains genes such as *rad-50* and *rad-51*, which are required for DNA repair and meiotic recombination (Lettre et al., 2004). Moreover, GLD-1 has been identified as a negative regulator of CEP-1, mediating its repressive effect by directly binding to the 3'UTR of *cep-1* mRNA and subsequent repression of its translation (Schumacher et al., 2005). As GLD-1 is present distally from late pachytene cells, these early meiotic pachytene germ cells are likely to be protected by GLD-1 from p53 mediated germ cells death, providing a molecular mechanism to explain the link between DNA damage signaling and germ line cell fate determinants (Schumacher et al., 2005).

2.7.2.4 Physiological germ cell death

Physiological germ cell death is believed to be part of a developmental program used to eliminate excess germ cells in order to control germ cell number homeostasis (Gumienny et al., 1999). In the adult hermaphrodite, approximately half of the female germ cells undergo physiological germ cell death that manifests itself by the presence of 0-4 corpses per germ line bend at any given time (Gumienny et al., 1999). As in mammalian tissues, populations of germ cells respond to growth factor regulation and are subjected to stochastic events, like the elimination of many cells by programmed cell death to maintain tissue homeostasis.

Recent data suggest that stress-induced germ cell death, through starvation, oxidative, osmotic and heat stresses, are independent of *egl-1* and *cep-1* and therefore believed to be mediated via the physiological germ cell apoptosis pathway (Navarro, R., Poster 1218 15th International *C. elegans* Meetin). Moreover, the MAPKKs (mitogen-activated protein kinase kinase) *mek-1* (MAP kinase or ERK kinase) and *sek-1* (SAPK/ERK kinase) together are required for stress-induced germ cell apoptosis by heat shock, osmotic and oxidative stress. Interestingly, under normal conditions, activation of the Ras/MAPK pathway in the germ line promotes progression of meiotic germ cells from an apoptosis-resistant pachytene stage to a transient selection stage, where cells are highly sensitive to apoptosis (for review see (Gumienny et al., 1999)). Thus, the Ras/MAPK pathway seems to promote apotosis by implementing developmental factors as well as stress stimuli. However, these MAPKKs are not necessary to induce apoptosis by starvation, suggesting that this kind of stress is induced by another, yet unknown pathway.

2.8 The prefoldin URI

The evolutionarily conserved *URI* gene (unconventional prefoldin RPB5 interactor, also called *NNX3, FLJ10575*), originally identified as *RMP* (RPB5-mediating protein) is located on human chromosome 19 (Dorjsuren et al., 1998). Expression of human *URI* mRNA was detected ubiquitously in various tissues, but enriched in the testis and prostate, pancreas and skeletal muscle (Dorjsuren et al., 1998). Two alternatively spliced transcriptional variants encoding different isoforms have been described for the gene. The shorter isoform lacks 35 nt in the coding region, resulting in a frame shift at the 5'end, and subsequently has a different N-terminus than the larger one (Dorjsuren et al., 1998).

Human URI protein consists of 494 amino acids, but runs at an apparent molecular weight of 90 kDa in SDS phage. It possesses a nuclear (NLS) and cytoplasmic localization signal (CLS), both of which are important for its subcellular localization (Delgermaa et al., 2004). The CLS acts dominantly, since URI was mostly localized in the cytoplasm with weak and diffuse signals in the nucleus, and the NLS was indispensable for the nuclear localization of URI only in the absence of the CLS (Delgermaa et al., 2004). Consistent with this, the nonessential yeast URI homolog (Bud27p) has also been documented to be a cytoplasmic protein (Saccharomyces Genome Database http://yeastgenome.org).

URI is an unconventional large member of ATP independent prefoldin (PFD) chaperone family (Gstaiger et al., 2003). In contrast to other known PFD family proteins, URI contains additional highly conserved protein domains (Cowan and Lewis, 1999; Geissler et al., 1998; Vainberg et al., 1998) implying that URI has multiple functions. The URI protein comprises a prefoldin domain, an RPB5 interaction region and an URI box, all of which are evolutionarily conserved among eukaryotes (Gstaiger et al., 2003).

2.8.1 Prefoldins

Like other molecular chaperones, archaeal PFD can selectively interact with and stabilize nonnative (unfolded) hydrophobic peptide sequences that are ultimately buried in the folded protein but which become exposed transiently during protein synthesis or upon denaturation in conditions of cellular stress. PFDs thereby promote the correct folding of substrate proteins (Leroux et al., 1999; Okochi et al., 2002; Siegert et al., 2000). The crystal structure of the archaeal PFD derived from *Methanobacterium thermoautotrophicum* has been obtained at atomic resolution, showing a jellyfish-like appearance in which the individual tentacles are formed by canonical antiparallel coiled-coils with considerable flexibility and which are likely to be independently mobile in solution (Siegert et al., 2000). The six tentacle-like coiled-coils of archaeal PFD whose N- and C-terminal helices project outward from a double β-barrel oligomerization domain enclose a substrate-binding cavity and act in concert to bind unstabilized nonnative proteins near the opening of the cavity (for review see (Martin et al., 2004)). The tentacles can also undergo an *en bloc* movement to accommodate an unfolded substrate (Lundin et al., 2004). The distal regions of the coiled-coils expose hydrophobic patches that are required for multivalent binding of nonnative protein substrate (for review see (Martin et al., 2004)). This unique structure of the archaeal PFD is conserved in eukaryotes (Martin-Benito et al., 2002) (Figure K). Yeast and bovine PFD complexes, originally termed GimC

(genes involved in microtubule biogenesis complex) and prefoldin, respectively, each comprise six distinct but structurally related small molecular weight-proteins of 14-23 kDa (Geissler et al., 1998; Leroux et al., 1999; Vainberg et al., 1998) whereas their archaeal counterpart contains only two types of different subunits present in two and four copies, respectively. There are two related classes of PFD subunits, namely α and β, both of which are composed of N- and C-terminal α-helical coiled-coil structures connected by either one (β-class PFDs) or two (α-class PFD) β-hairpins. Each of the two eukaryotic α-class subunits (PFD3/Gim2 and PFD5/Gim5) and the 4 β-class subunits (PFD6/Gim1, PFD4/Gim3, PFD2/Gim4, and PFD1/Gim6) assemble independently from each other into the $\alpha_2\beta_4$ hetero-hexameric PFD chaperone complex (Leroux et al., 1999; Siegert et al., 2000)(personal communication Victor Lundin).

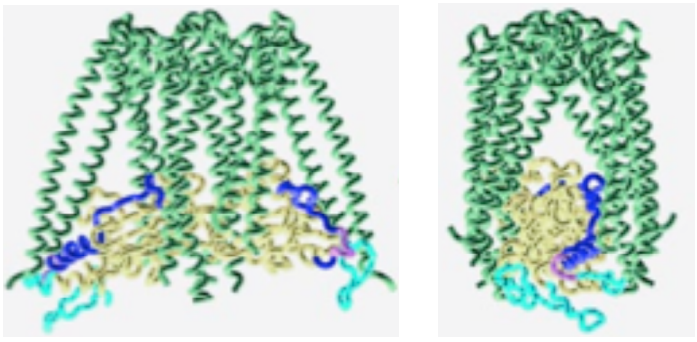

Figure K. Three-dimensional reconstitution by electron microscopy of the eukaryotic PFD complex. Individual PFD subunits assemble over their β-hairpins(s) into a hexameric, jellyfish-like architecture of which the individual tentacles (blue) are formed by canonical antiparallel coiled coils with considerable flexibility. Actin (violet, blue, ochre) appears to interact with PFD in a region that is consistent with the distal regions of the coiled-coils. From (Martin-Benito et al., 2002).

PFDs have been proposed to play a general role in *de novo* protein folding in archaea and are known to assist in the biogenesis of actin, tubulins and potentially other proteins in eukaryotes. They cooperate with the cytosolic group II chaperonin CCT/TRiC in folding (Figure L). Chaperonins are seven- to nine-membered double ring complexes that assist in the folding of nascent or denatured proteins by capturing them in their central cavity and promoting correct folding in an ATP dependent manner (for review see (Bukau and Horwich, 1998; Ellis and Hartl, 1999; Fink, 1999; Hartl, 1996; Sigler et al., 1998). The PFD complex binds a protein folding intermediate in the cavity and transfers them after completion of synthesis to the chaperonin CCT for post-translational folding (Hansen et al., 1999; Martin-Benito et al., 2002; Vainberg et al., 1998). Both, PFD and CCT are known to associate with translating ribosomes (Siegers et al., 2003). Yeast and mammalian prefoldin have been suggested to interact directly with CCT (chaperonin-containing TCP-1) (Leroux et al., 1999; Vainberg et al., 1998). It seems that both N- and C-terminal

regions of the prefoldin β-subunit are important for molecular chaperone activity and for the interaction with the chaperonin (Okochi et al., 2004). The two nonhomologous cytoskeletal proteins actin and tubulin interact with PFD, presumably via the two PFD interaction sites present in each of the substrates (Rommelaere et al., 2001). The substrate and chaperonin binding sites on prefoldin are in close proximity, which suggests a possible handover mechanism of PFD substrates to the chaperonin, facilitating the delivery of actin and tubulins in a defined orientation relative to the subunit topology of the chaperonin ring and preventing aggregation (Llorca et al., 1999; Okochi et al., 2004). PFD interacts with two specific subunits in each of the CCT ring (Martin-Benito et al., 2002). As CCT is involved in folding of many proteins, PFDs seem to function as CCT adaptors, recruiting CCT for folding of a specific subset of substrates.

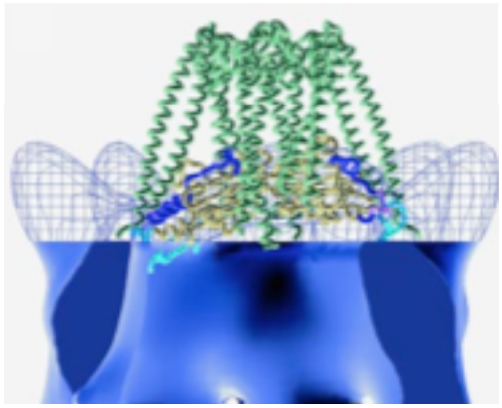

Figure L. Model of PFD-CCT cooperation in protein folding. The PFD complex binds a protein folding intermediate in its cavity and transfers it after completion of protein synthesis to the chaperonin CCT for post-translational folding. From (Martin-Benito et al., 2002).

In *C. elegans*, it has been shown that depletion of PFD genes by RNA-mediated interference (RNAi) results in embryonic lethality, suggesting PFDs have essential functions in multicellular organisms. CePFD (*C. elegans* PFD) are expressed from embryo to adulthood with overlapping expression patterns and are enriched in muscle cells similar to the expression pattern of CeCCT (*C. elegans)*, consistent with its known function in actin folding. Examination of one-cell embryos shows that depletion of PFD subunits by RNAi causes severe cytoskeletal defects including problems with meiosis, pronuclear migration, pronuclear rotation, spindle assembly, structure and position, as well as cytokinesis. This leads to abnormal chromosome segregation and disruption of cell polarity resulting in a variable stage of embryonic arrest and phenocopies the lack of tubulin in the embryo suggesting that tubulin folding is an essential and evolutionary conserved *in vivo* function of the PFD complex (personal communication Victor Lundin).

2.8.2 The URI complex

Human URI is part of an approximately 1 MDa multiprotein complex (Figure M) containing, amongst other proteins, a core subunit of RNA polymerase II RPB5 (Dorjsuren et al., 1998; Woychik et al., 1990), the ATPases TIP48 and TIP49 (Kanemaki et al., 1997; Wood et al., 2000), two β-class PFDs (PFD2 and PFD4-related) and the α-class PFD STAP1 (SKP2-associated alpha-PFD 1). STAP1 interacts with the F-box protein SKP2 (S-phase kinase-associated protein 2) (Gstaiger et al., 2003), a substrate recognition component of the cell cycle-regulatory SCF^{SKP2} ubiquitin ligase complex (Lisztwan et al., 1998; Sutterluty et al., 1999). As neither of the α-class PFDs STAP1 or URI are part of the described PFD/GimC complex, the URI complex likely represents a novel PFD-like complex (Gstaiger et al., 2003). The binding partners of URI within the URI complex implicate it in transcription, folding, ubiquitin-mediated protein degradation and recombination-mediated processes. Yeast Urip has been reported as an interaction partner for scRpb5p and scPFD6p (Ito et al., 2001a; Ito et al., 2001b), providing further evidence that the URI complex is conserved throughout species and putatively identifying an additional β-class PFD (PFD6) as part of the URI PFD-complex.

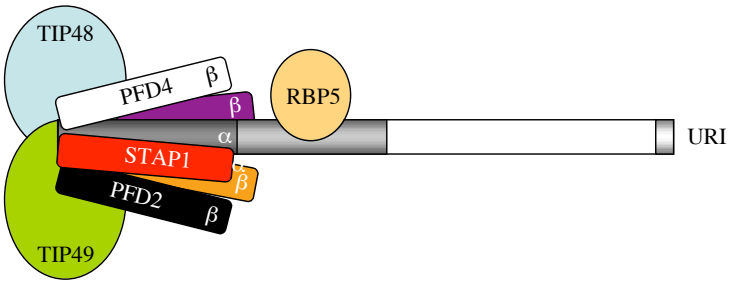

Figure M. Schematic representation of known components of the mammalin URI complex. The N-terminal α–class prefoldin domain of URI is believed to assemble in a hexamic PFD-like complex along with the α-class prefoldin STAP1, the β-class prefoldins PFD2 and PFD4rel and two unidentified β-class prefoldins. RBP5 binds to a discrete domain of URI directly. The binding sites of TIP48 and TIP49 have not been mapped.

2.8.3 Functions of the URI complex

Genetic and biochemical studies in yeast and human cells revealed that URI is a target of nutrient signaling and participates in the regulation of nutrient-sensitive, TOR-dependent transcription programs (Gstaiger et al., 2003). ScUrip is downregulated in response to amino acid starvation in yeast and loss of scUrip resulted in viable cells exhibiting phenotypes like cell elongation and agar penetration, hallmarks of invasive growth that are induced by nutrient limitation (Gimeno et al., 1992; Gstaiger et al., 2003). URI deletion also results in the downregulation of different tRNA species and upregulation of genes

encoding for proteins that primarily function in amino acid metabolism (Gstaiger et al., 2003). Thus, part of the normal function of scUrip is to contribute directly or indirectly to the expression of both RNA polymerase $_{II}$ and $_{III}$ transcripts. A large fraction of genes activated in *URI* deletion cells exhibit a consensus-binding site for the Gcn4p transcription factor in their 5' promoter regions (Gstaiger et al., 2003) and require GCN4 for their induction. Consistent with this, Gcn4p levels were up regulated under conditions of amino acid sufficiency in URI-deleted cells (Gstaiger et al., 2003). This upregulation of Gcn4p was at least in part Gcn2p-independent (Gstaiger et al., 2003). As scUrip represses GCN4-dependent transcription it may contribute to ternary (eIF2-GTP-Met-tRNA$_i^{Met}$) complex formation and consequently to the suppression of GCN4 protein translation, and subsequent GCN4 dependent transcription programs under nutrient-rich conditions. However, not all scUrip dependent genes, including certain tRNA genes, are GCN4-dependent (Gstaiger et al., 2003). Interestingly, the majority of those Gcn4p genes whose expression is induced in URI depleted cells overlap with those genes that have been previously identified to be also affected by amino acid starvation or repression by the TOR pathway (Gstaiger et al., 2003). TOR coordinates nutrient availability with cell growth and cell proliferation at least in part by controlling the transcription of distinct sets of nutrient metabolism genes.

TOR is known to repress the translation of GCN4 and activate the GATA transcription factors Gln3p and Gat1p. Because Gcn4p can facilitate the induction of certain Gln3p target genes, this negative effect of TOR on GCN4 translation is critical to prevent the expression of genes under the dual control of GLN3 or GAT1 and Gcn4p in rich media (Chen et al., 1995; Cherkasova and Hinnebusch, 2003). GLN3 and GAT1 are indeed induced in URI-depleted cells in a Gcn4p-dependent manner, providing a potential explanation for the activation of TOR-controlled genes in URI-depleted cells. Consistent with this, Gcn4p is expressed in URI-depleted cells at levels similar to those of rapamycin-treated wild type cells. Moreover, rapamycin did not affect Gcn4p levels in URI-depleted cells. Under amino acid starvation however, Gcn4p can be induced in URI depleted cells as in wild type cells. These results suggest a model in which loss of scUrip triggers the activation of genes under dual control of Gcn4p and Gln3p at least in part through the translational derepression of Gcn4p. scUrip protein levels are downregulated in response to various nutritional signals known to inhibit TOR activity, such as nitrogen starvation or rapamycin. Thus, scUrip is a competent of a TOR-controlled downstream effector pathway that modulates nutrient-sensitive gene expression.

The role of URI in nutritional pathways is conserved in mammals, as human URI also participates in mTOR signaling. Human URI is phosphorylated in response to insulin in a rapamycin- and wortmannin (PI3K inhibitor)-sensitive manner, implicating URI as a downstream component of the rapamycin-sensitive TOR signaling cascade and suggests that TOR regulates nutrient-dependent transcription at least partially through URI phosphorylation (Gstaiger et al., 2003). Thus, URI is an evolutionary conserved component of a signaling pathway that coordinates nutrient availability with gene expression to coordinate cell growth and cell proliferation.

2.8.4 Additional binding partners of URI

2.8.4.1 RNA polymerase II subunit 5 (RPB5)

Eukaryotes evolved three different RNA polymerases (RNA pol $_{I}$, $_{II}$ and $_{III}$), each consisting of 12-18 different subunits that carry out type-specific transcription programs in conjunction with a number of biochemically distinct accessory factors (Werner et al., 1992). RNA pol $_{I}$ transcribes the 5.8S-18S-28S ribosomal RNA precursor, RNA pol $_{II}$ transcribes all pre-mRNAs, and RNA pol$_{III}$ is involved in the production of tRNAs and a variety of other small RNAs. Thus, RNA polymerases are key enzymes responsible for the regulated expression of all genes within the eukaryotic nucleus.

The evolutionarily highly conserved RNA pol subunit RPB5 is a key structural and functional component that is shared by all three RNA polymerases. Moreover, RPB5 is in close contact to promoter DNA when RNA pol$_{II}$ is recruited into the preinitiation complex (Kim et al., 1997). The intricate regulation of pol $_{II}$ transcription underlies cell growth and cell proliferation. To modulate transcription, regulatory factors communicate with basal transcription factors and/or RNA polymerases in a variety of ways. It has been reported that RPB5 interacts with the general transcription factor IIB (TFIIB), one of the components of the RNA pol $_{II}$ basal transcriptional machinery, implying that RPB5 is one of the communicating subunits of RNA pol $_{II}$ involved in transcriptional regulation. Moreover, RPB5 has been also implicated in direct protein-protein interactions with gene-specific activator proteins, such as the transactivator hepatitis B virus protein X (HBx) (Cheong et al., 1995; Lin et al., 1997b; Todone et al., 2000; Woychik, 1998; Woychik et al., 1990). Thus, RPB5 plays a role in facilitating communication between the RNA pol core and a variety of basal and gene-specific transcription factors (Dorjsuren et al., 1998).

The putative transcriptional corepressor URI was reported to regulate transcription by competing with the transcriptional coactivator HBx for binding to RPB5. The specific binding of URI and RPB5 requires the RPB5 binding region of URI and a central part of the RPB5 protein, which overlaps with the HBx-binding region. Thus, URI negatively modulates RNA pol $_{II}$ function by competitively binding to RPB5 and thereby antagonizing the coactivator function of HBx (Dorjsuren et al., 1998; Lin et al., 1997b). In addition, URI binds TFIIB and interacts with the central part of RPB5 as a co-repressor of transcription (Cheong et al., 1995; Lin et al., 1998). URI also regulates transcription through interaction with the general transcription factor II F (TFIIF), which assembles in the preinitiation complex and functions in both transcriptional initiation and elongation (Wei et al., 2003). Although URI has inhibitory effects on various types of activated transcription it is not likely to have a global effect (Dorjsuren et al., 1998). Thus, URI may function via several proteins/pathways to regulate transcription of a certain subset of genes (Wei et al., 2003).

2.8.4.2 TBP interacting protein TIP48 (TIP48) and TIP49

DNA helicases play important roles in all aspects of DNA metabolism such as transcription, DNA replication, recombination and repair, performing a variety of tasks ranging from unwinding a simple DNA duplex at the replication fork to more elaborate actions such as migration of Holliday junctions (Lohman and Bjornson, 1996; Matson and Kaiser-Rogers, 1990). In general, helicases use energy derived from the hydrolysis of nucleoside triphosphates to catalyze the breakage of hydrogen bonds that hold DNA strands together. Many also use this energy to fuel their processive translocation along DNA, which often occurs with a unique directionality (Lohman and Bjornson, 1996). Both TIP48 (also called TIP49b) and TIP49 (also called TIP49a or RUVBL1) structurally resemble the prokaryotic DNA helicase RuvB of *Escherichia coli*. RuvB is targeted to Holliday junctions, which arise during genetic recombination and DNA repair, by the DNA-binding protein RuvA. Together they function to promote branch migration of these DNA structures (Parsons et al., 1995; Rafferty et al., 1996; Shinagawa and Iwasaki, 1996; West, 1996; West, 1997). RuvB assembles around the DNA as hexameric rings, which are thought to move along the DNA using energy-derived from the hydrolysis of ATP (Adams and West, 1995; Bujalowski et al., 1994; Tsaneva et al., 1993; Tsaneva and West, 1994). *E. coli ruvB* mutants exhibit an increased sensitivity to UV light, ionizing irradiation and mitomycin C. Moreover, RuvB protein is DNA damage-inducible as part of the SOS response to DNA damage suggesting a function in recombinational repair (Benson et al., 1988; Shinagawa et al., 1988).

TIP48 and TIP49 are thought to interact directly and do not complement each others function (Wood et al., 2000). Their interaction and activity requires their Walker A and Walker B boxes, motifs characteristic of nucleoside-5'-triphosphate binding sites of DNA/RNA helicases that are involved in ATP binding and ATP hydrolysis and that mediate processes like transcription, DNA repair, and chromatin remodeling (Schmid and Linder, 1992, Gorbalenya, 1989 #588; Walker et al., 1982 Wood, 2000 #579).

The intranuclear localization of TIP49 is regulated in a cell cycle-dependent manner, exhibiting a typical dot-shaped nuclear staining pattern, suggesting that TIP49 is included in macromolecular structures in the nucleus, but diffusely present during mitosis (Makino et al., 1998). TIP49 (Holzmann et al., 1998; Kanemaki et al., 1997; Qiu et al., 1998) and TIP48 have been reported to bind to several transcription factors, amongst others the central component of transcriptional regulation TBP (TATA-box binding protein) and the transcriptional corepressor URI (Bauer et al., 1998; Gstaiger et al., 2003). TIP49 also binds to the transactivation domain of the transcription factor E2F1 and modulates both its transformation and apoptotic activities (Dugan et al., 2002). Moreover, TIP49 associates with the nuclear matrix, β-catenin and LEF-1/TCF and the replication protein 3 (Bauer et al., 1998; Holzmann et al., 1998; Kanemaki et al., 1997). Thus, TIP48 and TIP49 represent a novel class of co-factors that are recruited by different transcriptional activation domains and thus might function in diverse pathways (Wood et al., 2000). Interestingly, TIP48 and TIP49 are also known to bind the amino-terminus of c-Myc and act as essential cofactors for c-Myc-mediated oncogenic transformation (Wood et al., 2000). This is of special interest as *c-Myc* is one of the mostly frequently mutated genes in human cancer (Cole, 1986). Moreover, TIP49 regulates β-catenin-mediated neoplastic transformation, likely via effects on chromatin remodeling (Feng et al., 2003). TIP49 was found in complexes with chromatin remodeling and histone-modifying factors and cofactors, including the TIP60 histone acetylase and TIP60-associated proteins BAF53 and TRRAP (transactivation/transformation-domain associated protein) and is therefore also likely to function in chromatin remodeling (Feng et al., 2003; Ikura et al., 2000). Also, the yeast homologs of TIP49 and TIP48, called Rvb1p and Rvb2p respectively, were found in a chromatin remodeling complex containing the Swi2/Snf2-related Ino80p, and loss of Ino80 causes sensitivity to DNA damaging agents (Ebbert et al., 1999; Shen et al., 2000). Although their functional roles need clarification, one explanation for these diverse findings is that the TIP48 and TIP49 ATPases function in several different complexes that

are respectively involved in transcriptional activation, chromatin remodeling and DNA repair and/or genomic integrity.

2.8.4.3 DNA methyltransferase 1-associating protein

The DNA methyltransferase DNMT1 is involved in DNA methylation and gene silencing (Bestor, 2000; Robert et al., 2003; Robertson et al., 2000; Rountree et al., 2000). DNMT1 has a preference for hemi-methylated DNA and is therefore thought to be involved in maintenance methylation or copying methyl-CpG patterns following DNA replication (Pradhan et al., 1999). The cellular localization pattern of DNMT1 is cell cycle dependent, localising diffusely in the nucleoplasm during G_1 and G_2 phases, but associating with replication foci during S phase suggesting that DNMT1-mediated methylation is coupled to DNA replication. Regions in the amino-terminus of DNMT1 are believed to be responsible for targeting the enzyme to replication foci and maintaining methylation of the daughter strand (Chuang et al., 1997). Thus, PCNA (proliferating cell nuclear antigen) is thought to bring DNMT1 to the replication foci (Chuang et al., 1997). The amino-terminus of DNMT1 also associates with the putative transcriptional co-repressor DNA methyltransferase 1-associating protein (DMAP1) (Robert et al., 2003; Robertson et al., 2000; Rountree et al., 2000). DMAP1 associates with DNMT1 during S phase of the cell cycle at replication foci (Rountree et al., 2000). The physical interaction of URI with DMAP1 changes the subcellular localization of URI from the cytoplasm to the nucleus (Delgermaa et al., 2004) and thereby facilitates the co-repressor activity of URI in a dose-dependent manner (Delgermaa et al., 2004). Thus, it is possible that a complex involving DMAP1, URI and DNMT1 functions to modify chromatin structure at specific promoter regions, leading to transcriptional repression. Experimental evidence from DNMT1-deficient ES cells suggests that DNA methylation protects against spurious mitotic recombination and chromosomal instability, providing evidence that DNA methylation is liked to DNA stability (Chen et al., 1998). In this thesis evidence is presented that URI is also important for maintenance of DNA stability.

2.8.4.4 Paf1 complex

The yeast Paf1 complex was originally identified as an RNA pol $_{II}$ associated complex that minimally contains the proteins Paf1, Cdc73, Rtf1, Leo1 and Ctr9 (Mueller and Jaehning, 2002; Shi et al., 1997; Squazzo et al., 2002). Genetic and biochemical evidence in yeast demonstrate that the Paf1 complex components affect gene expression by playing a role in various processes including the coupling of transcriptional (transcription initiation,

elongation, and RNA processing) and posttranscriptional events such as histone H2B mono-ubiquitination and subsequent histone H3 methylation (Krogan et al., 2003; Mueller et al., 2004; Ng et al., 2003; Palancade and Bensaude, 2003; Pokholok et al., 2002; Rondon et al., 2004; Squazzo et al., 2002; Stolinski et al., 1997). The Paf1 complex has been shown to be required for the recruitment of the methyltransferase COMPASS (SPP1, SDC1, SWD3, and BRE2) to chromatin (Hampsey and Reinberg, 2003; Krogan et al., 2003; Ng et al., 2003). Moreover, it has been implicated in the regulation of genes whose products function in metabolism (lipid and nucleic acid) and cell cycle control (Betz et al., 2002; Porter et al., 2002). In addition to its connection to cell cycle, the Paf1 complex appears to function downstream of the PKC1-MAP kinase pathway (Chang et al., 1999; Porter et al., 2002). These effects of the Paf1 complex can be explained, at least in part, though its ability to associate with forms of RNA pol $_{II}$. Consistent with this, Paf1p was found to be associated with the transcribed regions as well as promoters of several yeast genes *in vivo* (Pokholok et al., 2002). Furthermore, the Paf1 complex interacts with Hpr1P, a stoichiometric component of the THO/TREX complex that was implicated in transcriptional elongation and transcription-induced recombination (Chavez et al., 2000; Strasser et al., 2002).

The Paf1 complex is evolutionarily conserved from yeast to humans and, like its yeast counterpart, mammalian Paf1 associates with modified forms of the large subunit of RNA pol $_{II}$, in particular those phosphorylated on serine^5 or serine^2 within the carboxyl-terminal domain, that are known to be important for transcription elongation and RNA 3'end processing (Rozenblatt-Rosen et al., 2005; Shi et al., 1997; Shi et al., 1996; Stolinski et al., 1997; Yart et al., 2005). Moreover, the human tumor suppressor protein parafibromin (human ortholog of scCdc73) physically interacts with the human orthologues of yeast Paf1 complex components. Parafibromin is believed to function as a negative regulator of the cell cycle as depletion of human parafibromin by RNAi promotes entry into S phase. Additionally, parafibromin, together with components of the human Paf1 complex, associates with human URI (Yart et al., 2005). Interestingly, inactivation of the HRPT2 tumor suppressor gene (encodes Parafibromin) is associated with the pathogenesis of the hereditary hyper-parathyroidism-jaw tumor syndrome and malignancy in sporadic parathyroid tumors. Hyper-parathyroidism-jaw tumor syndrome is characterized by parathyroid tumors, as well as ossifying fibromas of the mandible and maxilla, bilateral renal cysts, hamartomas, and Wilm's tumor (Carpten et al., 2002; Jackson et al., 1990; Szabo et al., 1995).

3 Aim of the project

The overall focus of work described in this thesis was to characterize the *C. elegans* URI homologue, with the goal to obtain insights into the *in vivo* function of URI in a multicellular organism. Model organisms have been vital tools in dissecting the signaling pathways that are deregulated in human diseases like cancer and diabetes. Our laboratory is particularly interested in metabolic control mediated by the TOR and insulin/IGF-I-like pathways. The extensive conservation of the insulin signaling pathway across divergent multicellular species such as mammals, *D. melanogaster* and *C. elegans* opens this pathway up to genetic dissection in model organisms. *C. elegans* provided the first indication that lifespan is regulated hormonally by the insulin/IGF-I-like signaling pathway and subsequent work added to our current knowlege of the regulation of ageing and longevity. Our initial analysis indicated that mammalian URI is regulated by the insulin signaling pathway. Thus, the experimentally tractable model organism *C. elegans* was choosen to test the putative role of *C. elegans* URI (URI-1) in the insulin/IGF-like signaling pathway with a special focus on regulation of longevity and ageing by taking advantage of its short generation time and the facile genetic and molecular tools developed for this metazoan organism. These results would therefore allow us to build a broader model of URI function, with the final goal to provide novel insights relevant to insulin action in mammals.

Another goal was to use an unbiased genetic approach to identify processes that are affected by loss of URI-1 function. This has involved the analysis of *uri-1* depleted animals by mutation and RNAi and characterization of the resulting morphological phenotypes. *C. elegans* has been employed to address the physiological relevance of previous finding concerning the function of URI that are based on cell culture experiments and yeast genetics in a multicellular organism. This work has identified a novel and unexpected role for URI-1 in ensuring DNA stability that opens new avenues of research into the function of the URI protein family, with particular implications for human cancer. We specifically selected the *C. elegans* hermaphrodite germ line to explore the function of URI-1 since its formation and function require many fundamental biological processes, such as DNA replication, mitosis, meiosis, apoptosis and DNA repair.

4 Results

4.1 Molecular identification of a C. elegans URI homologue

The putative *C. elegans* URI homologue C55B7.5 was identified by BLAST search of the *C. elegans* genomic sequence, exhibiting 21% identity and 45% similarity to human URI based on the protein sequence (Gstaiger et al., 2003). The corresponding gene, which we termed *uri-1,* encodes a protein with signature sequences common to URI proteins of *Homo sapiens*, *Drosophila melanogaster*, *Caenorhabditis elegans*, *Saccharomyces cerevisiae* and *Arabidopsis thaliana*, including the conserved α-class PFD domain, the RPB5 binding domain and the URI box (Figure 1). The essential gene *uri-1*, also known as 1H71, maps to a gene-rich region on chromosome I; +1.15. It comprises four exons, three introns and generates an unspliced transcript of 1739 bp (www.wormbase.org). The only existing *uri-1(tm939)* deletion allele, generated by the NBP-Japan, is a sequenced 646 bp deletion mutant which lacks the second α-helix of the PFD domain and the entire RPB5 binding domain, placing the 3`coding region out of frame, likely representing a molecular null (Figure 1). URI-1 appears to be the only URI homolog encoded by the *C. elegans* genome. Analysis of the genetic environment suggests that *uri-1* is unlikely to be part of an operon, as the gene flanking its 5`region is transcribed in the opposite direction and the 3`flanking gene is several hundret base pairs away from the *uri-1* gene. In most operons, the individual genes are about 100 bp apart (Riddle et al., 1997). Sequence homology comparison of the 5` and 3`UTR of *uri-1* between *C. elegans* and *C. briggsae* reveal a conserved region flanking the 5`region of *uri-1* close to its transcription start most likely representing conserved elements of the *uri-1* promoter. Moreover, this analysis reveals that the gene situated 3' of *uri-1* also has a conserved structure in front of its ATG region likely to represent a promoter region. Thus, it appears that *uri-1* does not belong to the about 25% of all *C. elegans* genes arranged in operons for regulated co-expression (Timmons and Fire, 1998).

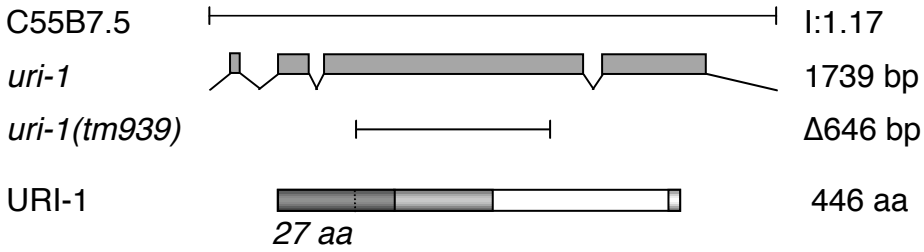

Figure1. Characterization of *uri-1* in *C. elegans*. Genomic structure of *C. elegans uri-1* (C55B7.5) and *uri-1* deletion mutant *(tm939)*. URI-1 encodes a 446 amino acid protein with a putative prefoldin domain (dark), a direct binding side for the common subunit of all three RNA polymerases RPB5 (grey) and the URI-1 box (light) depicted below.

Given that PFD proteins assemble in hexameric complexes we wondered if the worm ortholgues of the mammalian URI complex are conserved in the worm and function together in a conserved *C. elegans URI-1* complex homolog. Northern blot analyses of total RNA from wild-type mixed stage *C. elegans* using full length *uri-1* cDNA as probe detected a single band of approximately 1500 bp, most likely representing *uri-1* RNA. The developmental profile of *uri-1* RNA shows that *uri-1* expression is developmentally regulated, being weakly expressed during the L1-L4 larval stages (including the dauer larval stage) and highly abundant in the 1-day old adult, suggesting a function for *uri-1* in the adult worm (Figure 2A). Database searches to identify additional *C. elegans* homologues of the mammalian URI complex led to the identification of the *C. elegans* gene homologues of RPB5 (H27M09.2, *rpb-5*), STAP1 (F35H10.6, *stap-1*), PFD2 (H20J04.5, *pfd-2*) and TIP48 (T22D1.10, *ruvb-2*). As in the case of *uri-1* the other components of the putative URI-1 complex are upregulated in adult worms, suggesting a functional role for the *C. elegans* URI-1 complex in the adult worm (Figure 2A,B). To determine if the increased expression of *uri-1* at the adult stage is due to specific structures that are only present in the adult worm or to increased ubiquitous expression, northern blot analysis using developmentally synchronized populations of animals were performed, revealing that *uri-1* mRNA is expressed in the adult worm (Figure 2C). *uri-1* message is detected in worms with masculinised (*fem-3*) (Barton et al., 1987) as well as femininised (*fem-1*) (Nelson et al., 1978) germ lines, but not in *glp-4* mutant worms lacking nearly the entire germ line (Beanan and Strome, 1992). Therefore, consistent with a function in germ line development this comparative analysis demonstrated that *uri-1* is a germ line enriched gene, expressed in both types of gametes (Figure 2C). Moreover, based on assembled data from *553 C. elegans* DNA microarray experiments, including 179 experiments involving many growth conditions, developmental stages and varieties of mutants, co-regulated

genes were grouped together and visualized in a three-dimensional expression map that displays correlations of gene expression profiles as distances in two dimensions and gene density in the third dimension in terrain map mountains (Kim et al., 2001). Due to this clustering *uri-1* belongs to the functional group of the microarray topology map mountain 7 enriched for genes involved in specific functions in the germ line, oocytes, meiosis, and mitosis. *pfd*-2 and *stap*-1 belong to mountain 2, which is enriched for germ line and oocyte genes (Kim et al., 2001). Collectively, these results point to a role for *uri-1* directly or indirectly in mitotic and/or meiotic cell divisions of the germ line (Kim et al., 2001).

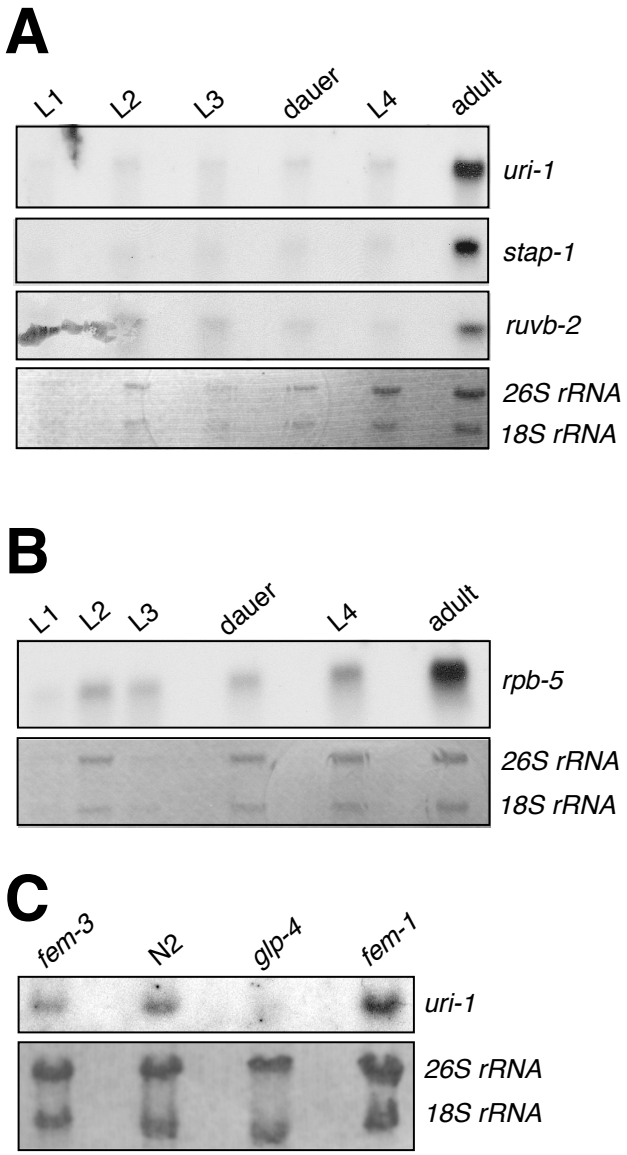

Figure 2. Northern blot analysis of *uri-1* expression. (A) Developmental northern blot demonstrating that uri-1, stap-1 and ruvb-2 are slightly expressed during larval development and upregulated in the adult worm. (B) Developmental northern blot showing that rpb-5 is also upregulated in the adult worm. (C) Northern blot of total RNA of 1 day old adult N2, *fem-1(hc17), fem-3(q20)* and *glp-4(bn2)* worms raised at 25°C demonstrating that *uri-1* is a germ line-enriched gene expressed in both types of gametes. Ribosomal RNA was used as loading control.

4.2 Characterization of URI-1 at the protein level

In order to determine if the human URI complex is conserved in *C. elegans*, the identified *C. elegans* homologues of the human URI complex were cloned and binding assays were performed. *In vitro* pull down experiments with GST-tagged *C. elegans* RPB5 (CeRPB5) and *in vitro* translated ^{35}S-labeled URI-1 showed that CeRPB5 binds URI-1 (Figure 3A). This result suggests that the identified *C. elegans* URI-1 is an ortholog of human URI and points to the possibility that *C. elegans* URI-1 also assembles in a PFD-like complex in the worm (Figure 3A). The observed three bands in the *in vitro* translated (IVT) URI-1 line are like to result from alternative ATG usage or proteolytic cleavage. Additional support for the possibility that URI-1 forms a PFD-like complex in *C. elegans* is provided by *in vitro* GST pull downs of GST-tagged *C. elegans* TIP48 and *C. elegans* PFD-2 with *in vitro* translated, radioactive labeled URI-1, demonstrating that the interactions of URI with TIP48 as well as the β-class PFD member PFD2 are conserved in the worm (Figure 3B). Strikingly, the GST-tagged CeRPB5 also binds *in vitro* translated human URI (Figure 3C) and GST-tagged *C. elegans* URI-1 binds *in vitro* translated human TIP48 and human TIP49 (Figure 3D,E). Figure 3 D and E demonstrate that the interactions between components of the human URI complex are conserved in *C. elegans* and support the existence of a *C. elegans* URI-1 complex resembling the human URI complex. These findings indicate that structural features of the URI complex have been remarkably high conserved throughout evolution.

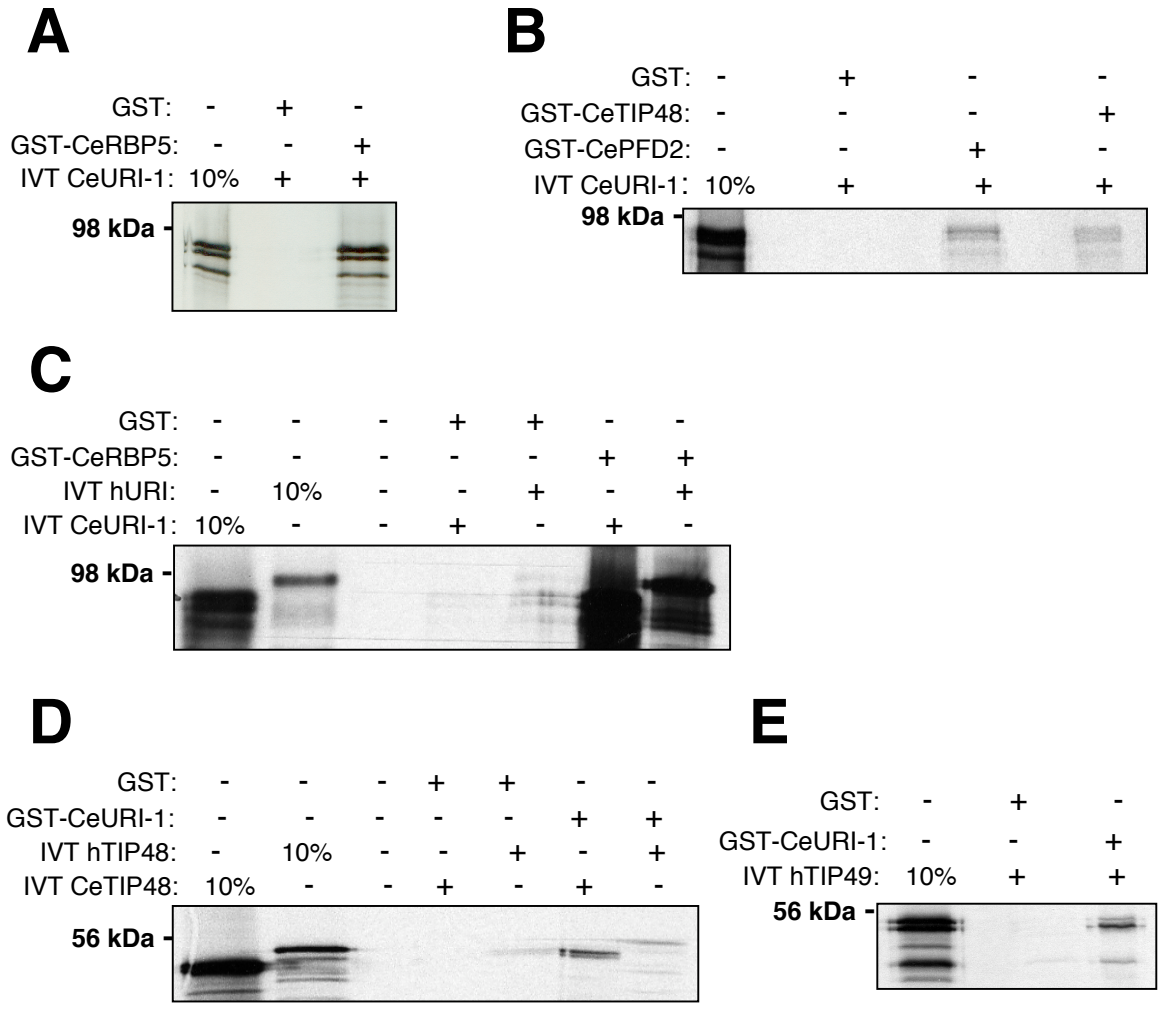

Figure 3. *In vitro* binding assays of URI-1 and other components of the URI-1 complex. (A) The GST-tagged *C. elegans* RPB5 homolog binds specifically *in vitro* translated (IVT) *C. elegans* URI-1. (B) GST-tagged *C. elegans* TIP48 and PFD-2 homologues bind specifically IVT *C. elegans* URI-1. (C) The GST-tagged *C. elegans* RBP5 homologue binds specifically the IVT *C. elegans* as well as the human URI homologues. The faint band in the fifth lane represents spill over from IVT *C. elegans* URI-1 and not human URI bound to the negative control, judged by the size of the band. (D) The GST-tagged *C. elegans* URI-1 is able to specifically bind IVT *C. elegans*, as well as human, TIP48. The fifth band represents spill over from IVT *C. elegans* TIP48 homolog and does not represent human TIP48 judged by the size of the band. (E) The GST-tagged *C. elegans* URI-1 is able to specifically bind human TIP49.

To examine the tissue distribution and sub-cellular localization of endogenous URI-1 protein, we generated two polyclonal peptide antibodies. Two rabbits (#11 and #12) were injected with a 25 amino acid peptide of the N-terminal PFD domain of URI-1 protein and additional two rabbits (#17 and #18) were injected with the C-terminal 25 amino acids of the URI-1 sequence (URI box) (Figure 4A). All four affinity purified α-URI-1 antibodies recognized GST-URI but not GST in western blotting using 50 ng of recombinant protein, albeit to different extents (Figure 4B). Both C-terminal antibodies give a strong signal with antibody #18 being more potent than #17 at the used concentration (Figure 4B). Using BSA as a standard for protein concentration revealed that antibody #18 was able to detect a

band of only 10 ng GST-tagged bacterial URI-1 in a 20s exposure and that #17 detected in that time recombinant URI-1 at a concentration of 1ng per lane (data not shown). Although both of the N-terminal antibodies recognize bacterially expressed GST-tagged URI-1 at the same size as the C-terminal antibodies do, they give a much weaker signal, #11 being stronger than #12 (Figure 4B). Thus, all four antibodies are able to detect a band at 120 kDa of recombinant *C. elegans* URI-1 protein, which does not appear in the GST control, most likely representing full length GST-tagged URI-1. Moreover, all antibodies detect lower molecular weight bands in the GST-URI-1 lane, likely reflecting specific recognition of proteolytic fragments of URI-1.

While all four antibodies failed to detect endogenous URI-1 in SDS-boiled whole worm protein extracts (data not shown) enrichment of endogenous URI-1 by immuno precipitation (IP) and western blotting with the C-terminal #18 antibody led to the detection of a single band, which is not present in the IgG control, most likely representing endogenous URI-1 (Figure 4C). Additionally, IPs using antibody #18 were blotted with all four α-URI-1 antibodies revealing that antibody #17 recognizes a band at the same size as antibody #18, but neither of the N-terminal antibodies recognize URI-1 immunoprecipitated by antibody #18 (Figure 4D). Neither of the N-terminal antibodies was able to immunoprecipitate URI-1 (data not shown).

The cDNA sequence of the *uri-1* gene predicts a protein of 446 amino acids with an estimated molecular weight of 52 kDa, whereas endogenous URI-1 runs around 90 kDa on SDS-PAGE. This up-shift is a feature shared with human and yeast URI-1 homologues, suggesting post-translational modification that alter its mobility in SDS-PAGE. Consistent with this idea, URI-1 protein contains 28 serine, 22 threonine, 11 tyrosine (potential sites of phosphorylation) and 40 lysine (potential sites of ubiquitination) residues (www.wormbase.org). Importantly, the molecular weight of the protein detected by these purified antibodies correlates in size with the *in vitro* translated protein band (Figure 3A). We conclude that the band at approximately 90 kDa represents endogenous URI-1 protein. To confirm that this 90 kDa band represents URI-1 protein, lysate derived from *uri-1*(RNAi) depleted worms and untreated wild type worms were immunoprecipitated with antibody #17 and immunoblotted with antibody #18 demonstrating that this band at around 90 kDa indeed represents URI-1 and that antibodies #17 and #18 are specific for URI-1 (Figure 4E). In summary, all antibodies recognize recombinant URI-1 with high detection sensitivity (between 5-50 ng in 20 second exposure) and both C-terminal antibodies

recognize endogenous URI-1 in immunoprecipitation and western blotting, whereas the N-terminals do not recognize endogenous URI-1 at the tested concentrations.

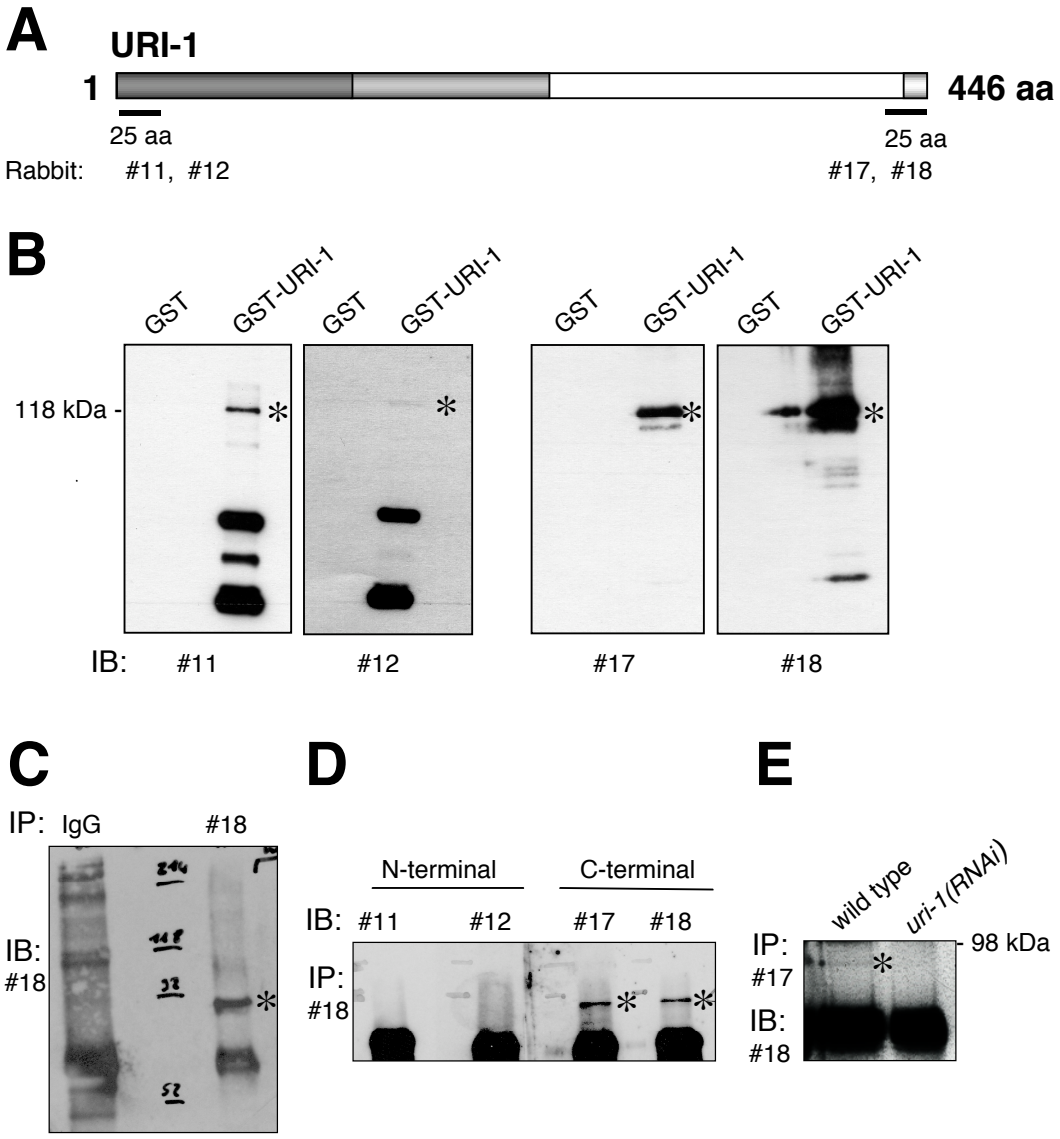

Figure 4. Characterization of α-URI-1 antibodies. (A) Schematic diagram of the domain structure of URI-1 protein. The epitopes for the individual antibodies are indicated. (B) All four antibodies recognize recombinant GST-URI-1 but not GST (50 ng/lane), but to a different extent. Affinity purified antibodies were diluted 1:500 (0.2 mg/mL stock) for western blotting. As the lane between GST control and GST-tagged URI-1 was left empty, the band seen in the #18 blot in this lane represents spill over during loading. (C) Immunoprecipitated endogenous URI-1 is recognized by the C-terminal antibody #18 as a band of 90 kDa which is absent in the control lane. (D) Endogenous URI-1 immunoprecipitated by antibody #18 is detected by #17 and #18 by western blotting, but not by the N-terminal antibodies. (E) Depletion of URI-1 by RNAi eliminates the 90 kDa band immunoprecipitated by antibody #17 and detected by antibody #18 demonstrating that these antibodies are specific for URI-1.

The cellular distribution of URI-1 was investigated by immunostaining of formaldehyde fixed whole worm samples using the C-terminal α-URI-1 antibody #18. This staining revealed that URI-1 localizes in punctate cytoplasmic structures in hermaphrodite spermatozoa (Figure 5A,B) suggesting that URI is included in cytoplasmic macromolecular structures. To determine if URI-1 is expressed throughout the entire process of spermatogenesis, *spe-27* and *spe-6* mutant animals, in which sperm is arrested at the haploid spermatid or primary spermatocytes stage respectively, were stained for URI-1 (Figure 5C and data not shown). This analysis demonstrated that URI-1 is expressed in the hermaphrodite germ line in all sperm stages from primary spermatids to activated spermatozoa in a punctuated cytoplasmic manner. To test if the sperm staining of antibody #18 is specific we performed peptide competition (50 times excess), which diminished the staining completely, suggesting that the sperm localization pattern is specific for URI-1 (data not shown). Moreover, sperm free (*glp-4*) animals are negative for this staining pattern, demonstrating that the observed staining is sperm-specific (Figure 5D). Staining of the male-enriched strain *him-8* with antibody #18 confirmed that URI-1 is expressed during the whole process of spermatogenesis in male animals and revealed that the sperm staining is sex independent (Figure 5E). Thus, URI-1 localizes in male gametes during the entire process of spermatogenesis in hermaphrodites and males.

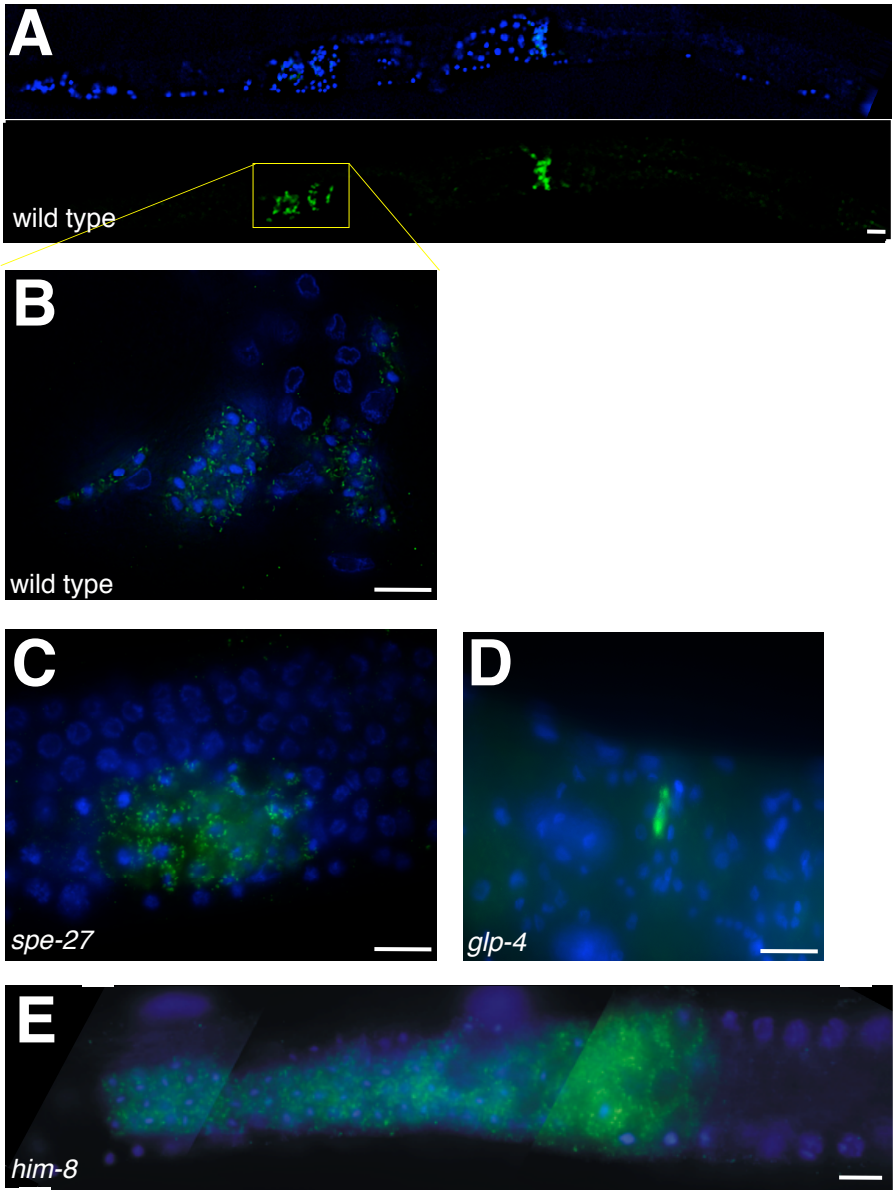

Figure 5. URI-1 is expressed in male and hermaphrodite sperm. (A) Overview of URI-1 recognition by the antibody #18 (green) in an adult hermaphrodite stained with the nuclear dye DAPI (blue). (B) Zoom into the spermathecal region of an adult hermaphrodite showing that URI-1 recognized by the antibody #18 (green) localized in punctuated structures in the cytoplasm of activated spermatozoa. (C) URI-1 is also expressed in haploid spermatids in the *spe-27* adult hermaphrodite. (D) URI-1 staining is diminished in the germ line deficient *glp-4* strain grown at the restrictive temperature. (E) URI-1 localizes during the whole spermatogenesis in the sperm cytoplasm in the adult male germ line of male-enriched *him-8* animals.

As only the antibody #18 recognizes URI-1 with this formaldehyde-based staining procedure, we wondered if changing the fixation conditions would yield a larger spectrum of URI-1 recognition by all four antibodies. Application of a methanol-based staining procedure revealed that URI-1 is present in the mitotic as well as meiotic part of the germ line, including both types of gametes, and in embryos from the P0 cell stage until after the 200-cell stage of embryogenesis (Figure 6-10). URI-1 was detectable more faintly in the distal mitotic region and became abundant in the transition zone up to oocytes, where germ cells start to enter meiotic prophase (Figure 6,7). Both C-terminal antibodies detect mainly

cytoplasmic URI-1 in mitotic germ cells as well as meiotic germ cells (Figure 6) including oocytes (Figure 7). Occasionally nuclear (data not shown) and membranous (Figure 7E) staining patterns of URI-1 are detected in these tissues using the C-terminal antibodies. To determine if this staining is specific, young wild type worms were injected with dsRNA *uri-1* and the germ line of these worms was extracted 48 hrs afterwards and immunostained with the antibody #18. The resulting reduction of signal confirmed that the staining is specific for URI-1 (Figure 6 E,F and 7 E,F). The cytoplasmic localization of URI-1 detected by the C-terminal antibodies always appears in a punctate staining pattern, suggesting that URI is included in macromolecular structures in the cytoplasm.

Interestingly, while both N-terminal antibodies detect URI-1 cytoplasmically in the same tissues as the C-terminal antibodies, they additionally detect URI-1 staining at the membrane and in the nucleus (Figure 7 C,D). This additional staining likely represents a fraction of URI-1 that is often not detectable by the C-terminal antibodies due to the C-terminal epitope being masked either by protein interaction partners or by interactions of URI-1 with subcellular structures. The nuclear localization of URI-1 appears in a dot-like staining pattern, suggesting that URI-1 is included in macromolecular structures in the nucleus. Consistent with its nuclear localization pattern, the URI-1 sequence possesses a putative nuclear localization sequence (PTDKKLR). Rarely, the N-terminal antibodies failed to detect nuclear URI-1 in the mitotic part of the germ line (Figure 6 C,D). One interpretation of this may be that slight variations in fixation conditions alter the accessibility of the epitope.

To attempt to confirm these stainings using an independent technique that avoids the possible complications of epitope masking, we generated a GFP-tagged URI-1 *unc-119*-rescuing construct, bombarded this construct into *unc-119* mutant worms and scored for restoration of wild type movement. We obtained 3 independent, apparently rescued lines (wild type movement), which exhibited germ line GFP fluorescence similar to the staining pattern of the C-terminal antibodies in oocytes (Figure 7 H). Unfortunately none of these lines stability integrated and expressed the construct. Thus, attempts to generate a GFP-tagged URI-1 expressing transgenic strain to verify the obtained antibody staining were unsuccessful.

The four α-URI-1 antibodies also detect URI-1 in embryos in a comparable sub-cellular localization pattern as in the mitotic and meiotic germ line, with the N-terminal antibodies detecting nuclear, cytoplasmic and membranous URI-1 (Figure 8A-D) and the C- terminal antibodies detecting predominantly cytoplasmic (Figure 8E-H), but occasionally also membranous, URI-1 staining (Figure 8G,H). Immunostaining of embryos derived from dsRNA *uri-1*-injected wild type demonstrated the specificity of the embryonic staining pattern of antibody #18 (Figure 10H,I). That URI-1 can be detected in early cell stages strongly suggests that URI-1 is expressed from maternal RNA, since zygotic transcription is not thought to begin in the germ line until the 100-cell stage (Seydoux and Dunn, 1997).

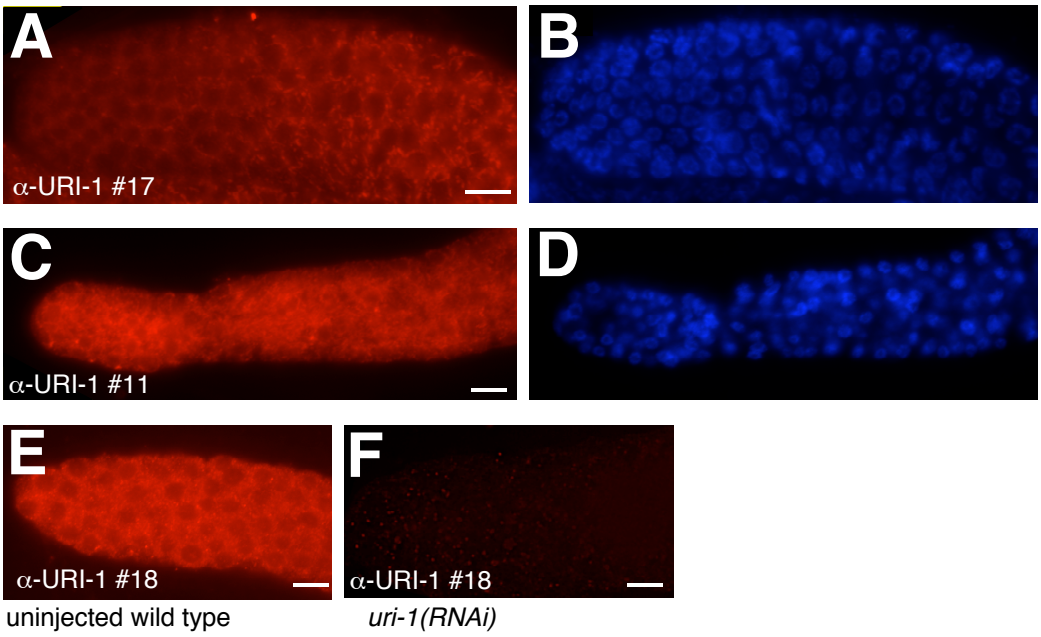

Figure 6. URI-1 localization in the mitotic part of the germ line. (A-B) The C-terminal α-URI-1 antibody #17 (red) produces a cytoplasmic, punctuate staining pattern of URI-1 in the distal region of the *C. elegans* germ line. DAPI (blue) is used as nuclear dye (C-D) The N-terminal α-URI-1 antibody #11 replicates the staining pattern of the C-terminal α-URI-1 antibody #17 in the mitotic part of the germ line. (E-F) The C-terminal α-URI-1 antibody #18 also produces a similar cytoplasmic staining pattern, which is diminished by depletion of URI-1 by injection of dsRNA, comfirming that this staining pattern is specific for URI-1. Scale bar represents10 μm.

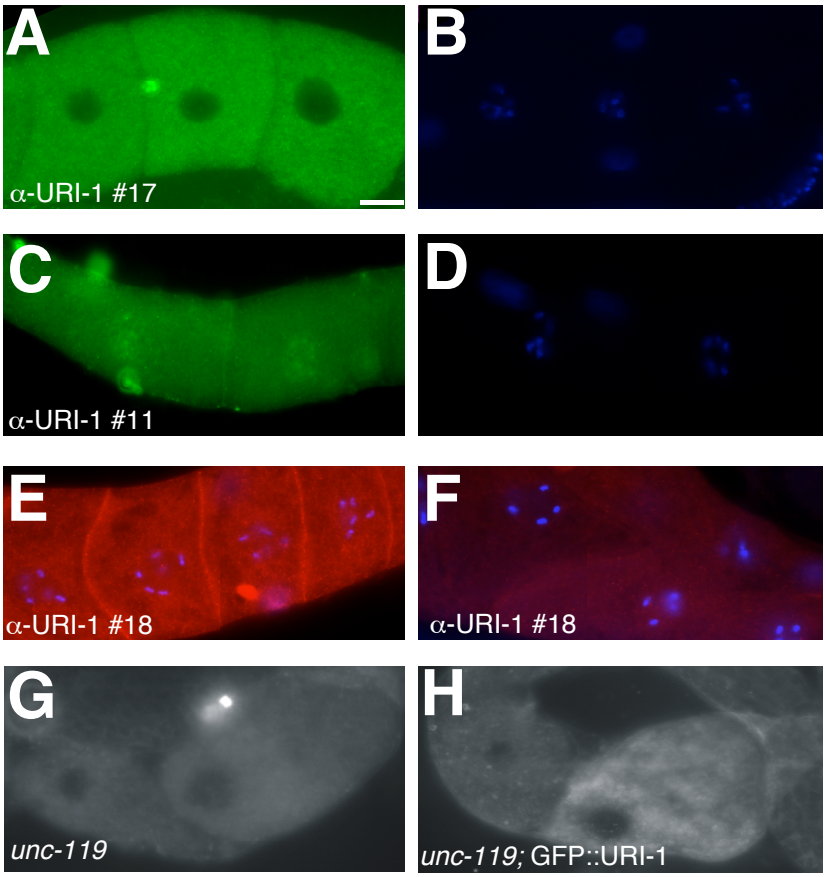

Figure 7. URI-1 localization in oocytes. (A-B) The C-terminal α-URI-1 #17 (green) detects cytoplasmic URI-1 during the whole process of oogenesis. DAPI (blue) is used as nuclear dye (C-D) The N-terminal α-URI-1 #11 (green) detects cytoplasmic, membranous and nuclear URI-1 in oocytes. (E) The C-terminal α-URI-1 antibody #18 (red) detects cytoplasmic and membranous URI-1. This staining pattern is diminished 48 hrs post-injection of *uri-1* dsRNA demonstrating the specificity of the staining for URI-1 (F). Note that depletion of *uri-1* by RNAi disrupts oocyte morphology. (G-H) GFP-tagged URI-1 also expresses in oocytes in a cytoplasmic manner. Scale bar represents 10 μm.

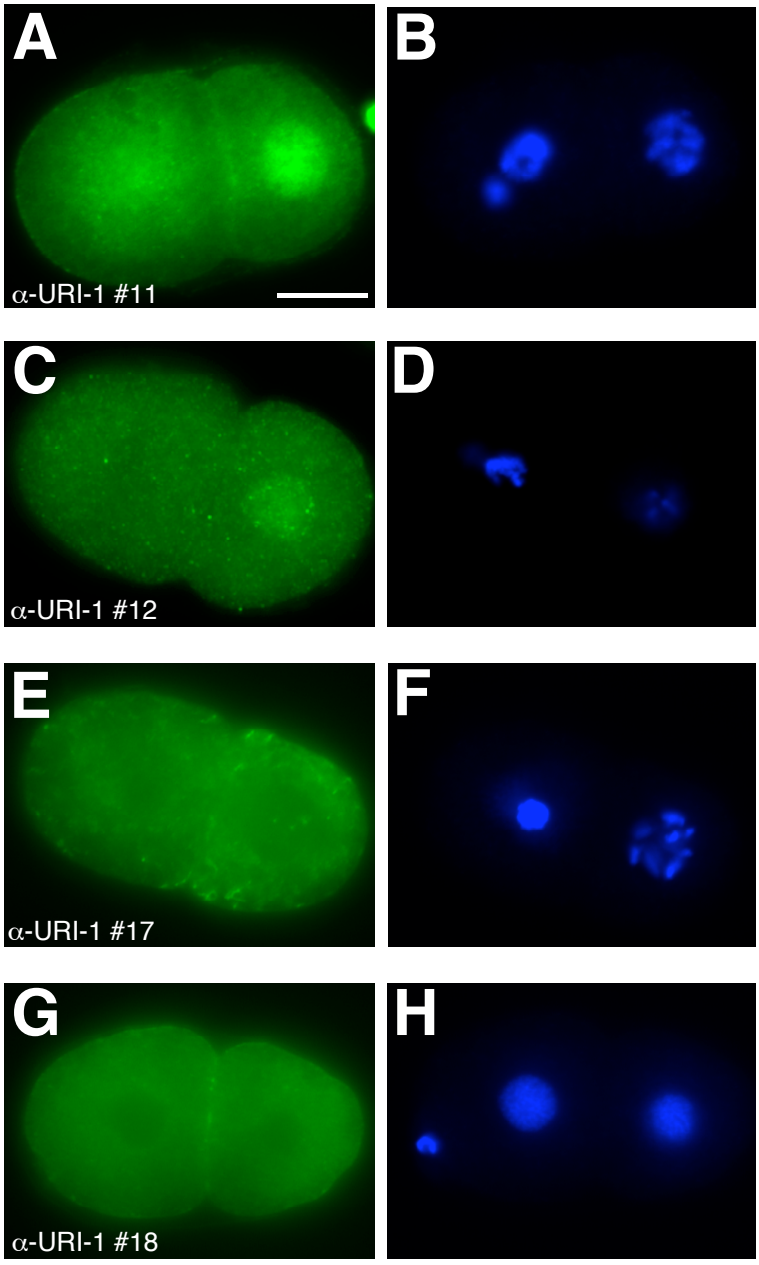

Figure 8. URI-1 expression pattern in embryos. (A-B) The N-terminal α-URI-1 antibody #11 detects cytoplasmic, membranous and nuclear URI-1 in the *C. elegans* embryo (green). DAPI (blue) is used as nuclear dye. (C-D) The N-terminal α-URI-1 antibody #12 detects cytoplasmic and nuclear URI-1 in the *C. elegans* embryo (green). (E-F) The C-terminal α-URI-1 antibody #17 detects only cytoplasmic URI-1 in the *C. elegans* embryo (green). (G-H) The C-terminal α-URI-1 antibody #18 detects cytoplasmic and membranous in the *C. elegans* embryo (green). Scale bar represents10 μm.

Interestingly, the nuclear staining patterns of URI-1 using antibodies #11 and #12 are cell cycle-dependent. URI-1 detected by the antibody #12 accumulates in the nucleus during G_1, S, and G_2 phases of the cell cycle but is absent from late prophase until anaphase in a cell lineage-independent way from P0 until at least the 12-cell stage (see Figure 9).

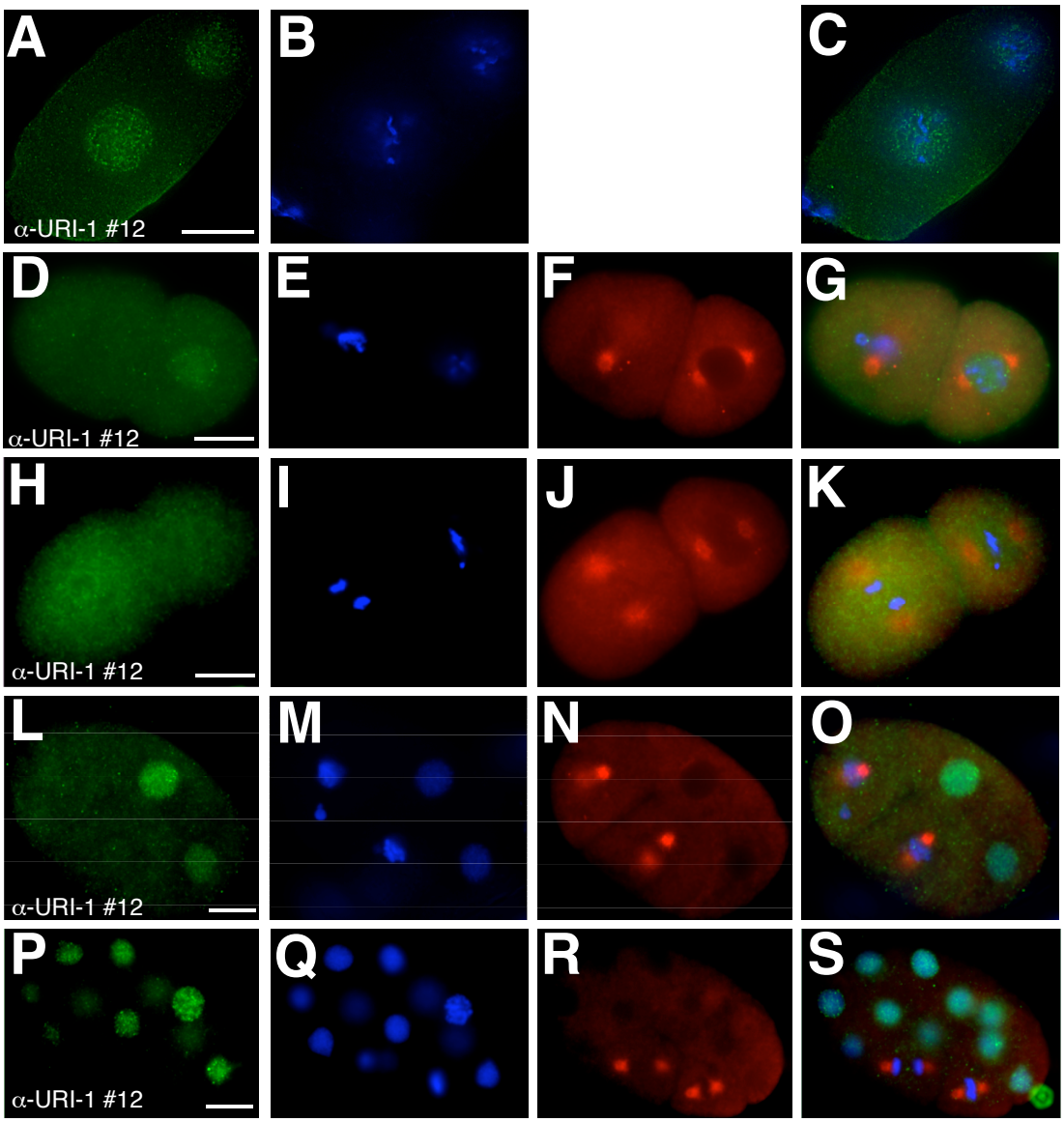

Figure 9. URI-1 exhibits a cell cycle-dependent nuclear localization pattern. Immunostaining using antibody #12 (green) reveals that URI-1 (A,D,H,L,P) is nuclear during the G_1, S and G_2 phases of the cell cycle but is absent from the DNA from late prophase until anaphase in a lineage-independent manner as URI-1 is nuclear in the P1 cell during prophase (D-G) but is absent in the P1 cell during metaphase (H-K). The nuclear dye DAPI (blue, B,E,I,M,Q) and tubulin (red, F,J,N,R) mark the individual cell cycle phases in (A-C) 1-cell, (D-K) 2-cell, (L-O) 4-cell and (P-S) 12-cell embryos. Scale bar represents10 μm.

The antibodies #18 (Figure 10A) and #12 (Figure 10D) strongly recognize P-granules, as evidenced by colocalization with GFP-PGL-1, a tagged protein that is a constitutive component of P-granules PGL-1 (Kawasaki et al., 1998). URI-1 co-localized with P-granules from the 1-cell stage until beyond the 100-cell stage of embryogenesis, as well as in the germ line at the nuclear pores (Figure 10 and data not shown). RNAi diminishes, but not eliminate, the P-granule staining of antibody #18 (Figure 10 H,I) probably reflecting an inability of the RNAi to completely remove the high amount of URI-1 present in P-

granules. P-granules are large non-membranous ribonucleo-protein particles of diverse and dynamic composition that contain determinants of germ cell fates and are exclusively found in the cytoplasm of all *C. elegans* germ cells and germ cell precursors (Schisa et al., 2001). P-granules are uniformly distributed in the cytoplasm of oocytes and are maternally contributed to the embryo. After fertilization, P-granules move in the cytoplasm to the posterior pole of the embryo, and at the first cell division are segregated into the cytoplasm of the P1 cell. Although P-granules are cytoplasmic in younger embryos they are associated closely with germ cell nuclei in older embryos, larvae and adult germ lines. P-granules intimately associate with the nuclear pore complex at the outer nuclear envelope in both mitotic and meiotic nuclei at nearly all stages of development (Pitt et al., 2000). Thus, P-granules are nucleus-associated perinuclear structures of adult germ cells and older embryos as well as cytoplasmic structures of oocytes and early embryos. Homozygous *uri-1* mutant embryos derived from URI-1 heterozygous animals as well as embryos derived from the P0 generation under the influence of *uri-1(RNAi)* (referred to as *uri-1(RNAi)*P0) display apparently normal P-granule localization and segregation to a single blastomere during early embryogenesis, suggesting that URI is not required for the localization of P-granules (data not shown). However, it is difficult to draw a definitive conclusion from this experiment as maternally provided URI-1 may be sufficient for P-granule localisation. Experiments with F1 generation animals subjected to *uri-1(RNAi)* (referred to as *uri-1(RNAi)*F1) exhibit frequent embryonic lethality and embryonic disorganisation, precluding analysis of P-granule localisation in these embryos. Interestingly however, inhibition of transcription or mRNA export in the adult gonad rapidly disrupts the integrity of perinuclear P-granules, pointing to the possibility that URI-1 localization at P-granules could potentially be linked to translational control and/or RNA transport (Amiri et al., 2001).

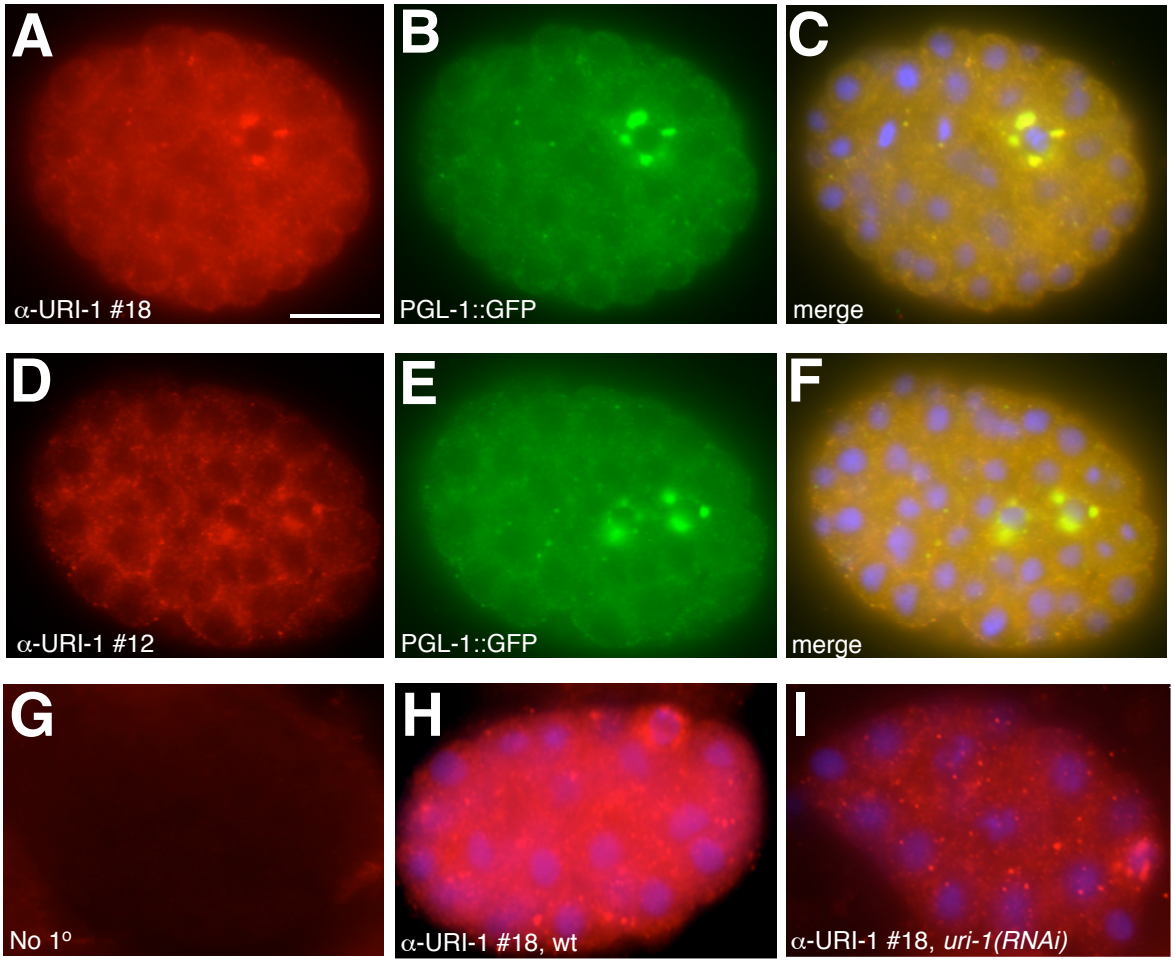

Figure 10. Co-localization of URI-1 with P-granules by N- and C-terminal α-URI antibodies. (A-C) URI-1 (red) detected by the C-terminal α-URI-1 #18 co-localizes during early embryogenesis with the P-granule marker GFP::PGL-1 (green). DAPI (blue) is used as nuclear dye. (D-F) URI-1 (red) detected by the N-terminal α-URI-1 #12 also co-localizes after the 100-cell stage with the P-granules component PGL-1 (green) in the *C. elegans* embryos. (G) Staining pattern observed in the absence of a primary antibody. Comparison of staining by α-URI-1 #18 in wild type embryos (H) or embryos collected 28 hrs after injection with *uri-1* dsRNA (I). (G-I) were photographed with the same exposure time and intensity. Depletion of URI-1 by RNAi diminishes, but does not eliminate this URI-1 staining pattern. Scale bars represent 10 μm.

In summary, URI-1 is detected in the same tissues of the embryo and germ line by all four antibodies. The fact that the sub-cellular staining patterns of all four α-URI-1 antibodies inconsistently overlap (detection of cytoplasmic, membranous and nuclear URI-1) is possibly accounted for by small differences in fixation conditions revealing or not revealing different epitopes of URI-1. Consistently with the obtained antibody stainings, the mammalian URI-1 homolog also localises to the nucleus, membrane and cytoplasm (personal communication Nabil Djouder and Matthias Gstaiger). Taken together URI-1 is specifically expressed in embryos, sperm, ooctyes and mitotic germ cells in the cytoplasm, membrane and nuclei dependent on the antibody, suggesting multiple functions for URI-1

in the individual cellular compartments. Most importantly, URI-1 protein and mRNA expression are both enriched in the germ line, suggesting a functional role for URI-1 in this compartment.

4.3 Functional analysis of URI-1

To assess the *in vivo* function of *uri-1* we analyzed the phenotypes of *uri-1* mutants and of *uri-1* depletion by RNAi. Both methods of inhibition of *uri-1* function resulted almost without exception in the same phenotypes. We noticed that starting the RNAi feeding at the L1 larval stage affects the P0 generation stronger than feeding at the L4 larval stage, whereas the next generation is more affected by a feeding started at the L4 larval stage of the P0 generation than at the L1 larval stage. These analyses revealed pleiotropic morphology defects demonstrating that the gene product is required for embryogenesis, larval development, fertility, vulval morphology, overall stability (sensitivity to applied pressure) and multiple aspects of germ line development (Table 1 and Figure 11). The frequency of these phenotypes were enhanced at higher temperatures (data not shown).

Phenotype	**wild type**	***uri-1* -/-**	***uri-1(RNAi)*F1**
emb	0-1	6-10	2-70$^{\infty,\#}$
pvl	0	6-10*	16-24*
rup	0	8-38$^{*,\bullet}$	23-30*
L3 arrest	0	42-50	n.d.
fertile	100	0	3-13
molt	0	5-10	n.d.
adults	99-100	14-43°	28-55°

Table 1. Depletion of *uri-1* leads to pleiotropic defects at 25°C. Data represents the percentage of each genotype displaying the indicated phenotypes. **o***all protruding vulaa (pvl) and rupture (rup) are sterile. $^{\infty}$ embryonic lethality (emb) occurs around the 200-cell stage, $^{\#}$value depending if RNAi is applied by feeding or injecting, $^{\bullet}$ rup occurs after the final molt, $^{\circ}$portion which reached the adult stage, n=100 per genotype, moting problems (molt).

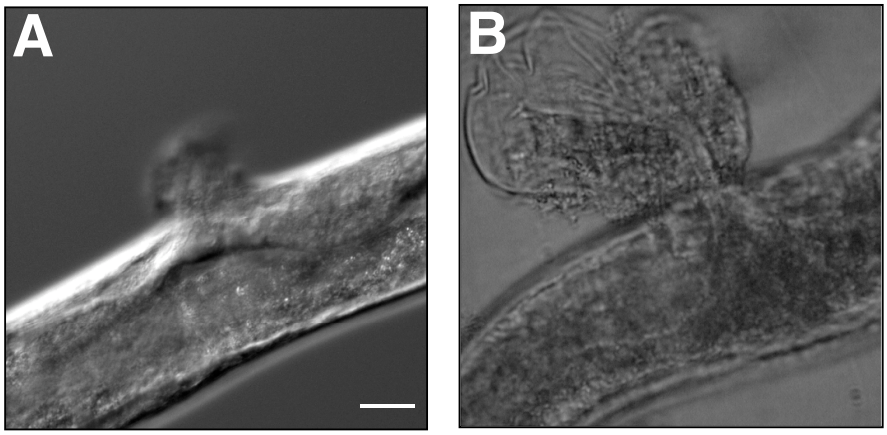

Figure 11. Selected morphologic abnormalities of *uri-1* depleted worms. (A) Example of a protruding vulva (pvl) of an adult *uri-1(RNAi)*F1 hermaphrodite. (B) Example of an exploded adult *uri-1(RNAi)*F1 hermaphrodite. These animals explode through the vulva after the last molt. Scale bar represents 30 μm.

4.4 URI-1 in respect to C. elegans TOR and daf-2 signaling pathways

Given that human URI is a positive downstream effector of the insulin-sensitive TOR signaling pathway we wondered if URI-1 could play a conserved role in the insulin/IGF-I-like and/or the TOR signaling pathways in *C. elegans*. To investigate if URI-1 is a component of either of these pathways in *C. elegans,* URI-1 mutants and worms depleted by RNAi were tested for characteristic phenotypes that arise from mutations of components of these pathways.

4.4.1 Is URI-1 a component of the CeTOR signaling cascade?

We have noted the *let-363* (CeTOR) mutant animals share certain features with *uri-1* mutants, such as a developmental arrest at the L3 larval stage (Long et al., 2002), reduced fertility (Vellai et al., 2003), reduced viability (Vellai et al., 2003) and sensitivity to applied pressure (Long et al., 2002). As the L3 larval arrest observed in *let-363* mutant animals has been characterized as dauer-like arrest (Jia et al., 2004) and *let-363(RNAi)* enhanced dauer formation in the temperature sensitive *daf-2(1370)* strain at 20°C we wondered if *uri-1* also genetically interacts with *daf-2* in the process of dauer formation. Depleting *uri-1* by RNAi in the P0 and F1 generation of the temperature sensitive *daf-2(e1370)* mutant does not enhance dauer formation (Figure 12) indicating that, in contrast to *let-363*, *uri-1* does not interact genetically with *daf-2(1370)* in the dauer formation pathway.

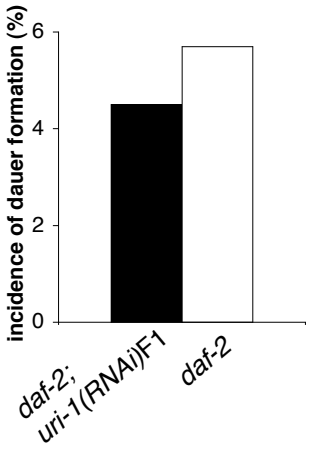

Figure 12. The effect of URI-1 depletion on dauer formation. Comparative analysis of dauer formation incidence of the thermo sensitive *daf-2(e1370ts)* mutant and *daf-2(e1370ts); uri-1(RNAi)*F1 at 20°C demonstrating no synthetic interaction between *uri-1* and *daf-2* on the dauer formation process. A parallel-performed wild type control was used to determine the functionality of *uri-1(RNAi)*.

Another characteristic of *C. elegans* TOR is its influence on lifespan, as depletion of CeTOR extens lifespan (Vellai et al., 2003). Thus, we performed lifespan assays with heterozygous and homozygous *uri-1* mutants at 25°C (Figure 13A,B). These analyses revealed that *uri-1* has no influence on adult lifespan.

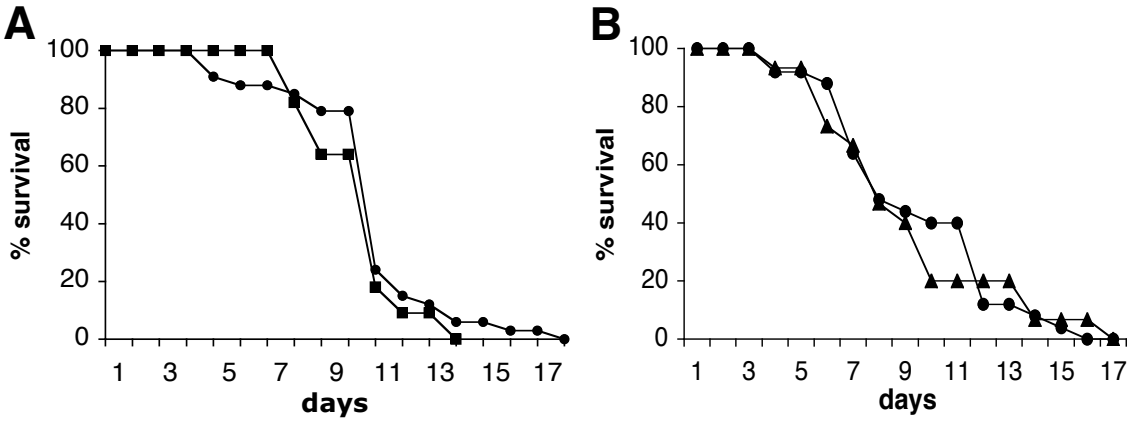

Figure 13. The effect of URI-1 on lifespan. Lifespan from hatching of heterozygous (■) (A) and homozygous (▲) (B) *uri-1* mutants compared with the wild type (●) (A,B) at 25°C, demonstrating that *uri-1* depleted worms live as long as wild type worms (n= 30). Note that xploded animals were excluded from the assay.

Another characteristic phenotype of CeTOR-deficient worms is the size increase of refractile and autofluorescent intestinal vesicles (lysosomes) and a decrease in the number and size of non-refractile intestinal vesicles (Long et al., 2002). Thus, we investigated these morphological features of *uri-1*-depleted L3 larvae of the F1 generation under the influence of *uri-1(RNAi)* (referred to as *uri-1(RNAi)*F1) compared with wild type L3 larvae (Figure 14) demonstrating that *uri-1* deficient worms do not phenocopy the intestinal phenotype of CeTOR mutant animals.

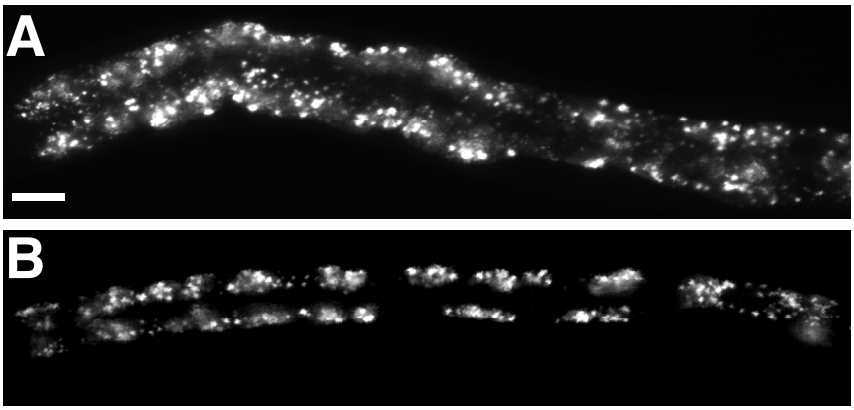

Figure 14. Comparative analysis of lipofusin accumulation. DAPI channel autofluorescence images of a mid-L3 stage wild type animal raised on control RNAi (A) or *uri-1(RNAi)*F1 (B). Anterior is oriented towards the left. No difference in size of refractile (autofluorescent) intestinal vesicles is observed between the two different samples. Images were obtained with the same exposure time and intensity. Scale bar 20 μm.

4.4.2 Is URI-1 a component of the *daf-2* signaling pathway?

In *C. elegans* many mutations in the insulin/IGF-I-like signaling pathway show pleiotropic phenotypes, including adult life span extension, dauer formation, increased resistance to thermal and oxidative stress, reduced brood size and reduced viability (Ailion et al., 1999; Friedman and Johnson, 1988; Honda and Honda, 1999; Tissenbaum and Ruvkun, 1998). We noted that *uri-1* depleted animals share certain features of the pleiotropic *daf-2* phenotype, such as reduced fertility and reduced viability, but do not regulate adult life span (Figure 13). Mutation in genes in the *daf-2* pathway can increase, decrease, or have no effect on life span (for review see (Tissenbaum and Guarente, 2002)). Therefore, we tested additional characteristics of the insulin/IGF-I-like signaling pathway. Under conditions of stress and nutritional deprivation, usually crowding, worms can exit reproductive development and enter an alternative larval stage called dauer larva (Cassada and Russell, 1975). The dauer stage is apparently non-aging and worms can remain as dauer larvae for months (Klass and Hirsh, 1976). Until now only two components of the insulin/IGF-I-like signaling pathway form dauers inappropriately under non-inducing

conditions (Daf-c) at 25°C and screens for simple loss-of-function mutants with a strong Daf-c phenotype at 25°C have probably been saturated (e.g. (Malone and Thomas, 1994)). Therefore, it is not surprising that *uri-1* mutant do not form dauers at 25°C. The existence of more Daf-c genes is supported by the discovery of synthetic Daf-c mutants, in which the single mutants are not Daf-c at 20°C, but the double mutant is Daf-c leading to the finding of additional components of the *daf-2* signaling pathway (Ailion and Thomas, 2000; Avery et al., 1993; Daniels et al., 2000). As mentioned above, *uri-1* does not belong to this class of Daf-c genes (Figure 12). The process of dauer formation is also facilitated by high temperature (27°C), called the Hid phenotype (high-temperature-induced dauer formation) which has the potential to identifiy new genes of the insulin signaling pathway (Ailion and Thomas, 2003). Dauer formation at temperatures above 25°C is very sensitive to small temperature differences and requires special care (Ailion and Thomas, 2000). Using this method with some slight modifications (SDS treatment to identify the dauers) we obtained inconsistent results. In some experiments in which the behaviour of positive (*daf-2*) and negative (*ppn-1*, *tag-22*) controls were as expected we saw no increase in dauer formation induced by *uri-1* depletion (Figure 15A). However, in other experiments *uri-1* depletion did suggest a trend towards an increase in dauer formation (Figure 15B), albeit without reaching statistical significance. Thus, our best efforts to control incubator temperature were insufficient to prevent significant variability in dauer counts and did not allow us to conclude whether *uri-1* depletion affects the Hid phenotype.

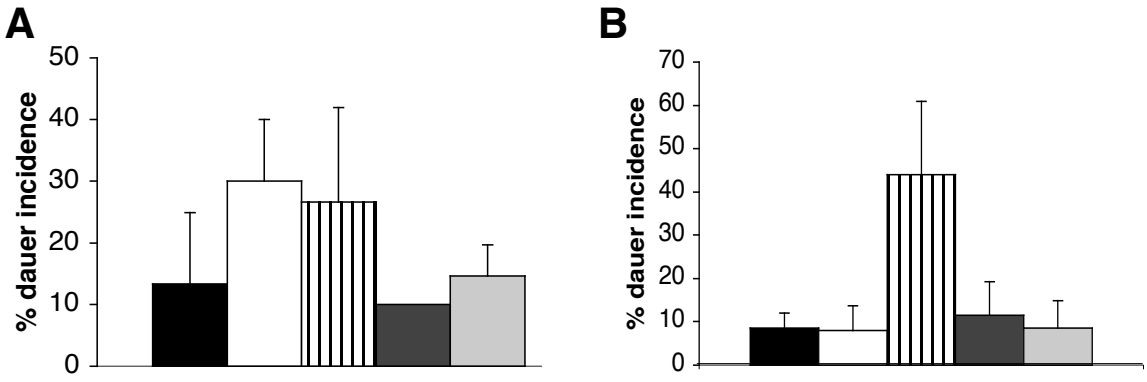

Figure 15. Analysis of dauer incidence in *uri-1(RNAi)*F1 animals. (A and B) Two representative experiments depicting mean + std. dev. percentage of animals exhibiting the Hid phenotype at 27°C. Wild type (black bars), *uri-1(RNAi)*F1 (white bars), *daf-2(e1370)* (positive control, vertical striped bars), *ppn-1* (C37C3.6) (negative control, dark grey bars) *tag-22* (C45G3.1) (negative control, light grey bars) are plotted. *ppn-1* (C37C3.6) and *tag-22* (C45G3.1) have been selected as negative controls as, like *uri-1*, they show emb, pvl, rup, stp and unc phenotypes, but are not linked to *daf-2* or CeTOR signaling.

Another characteristic of mutation of the *daf-2* signaling pathway (e.g. *age-1*, *daf-2*) is the increased intrinsic thermo-tolerance and resistance to oxidative stress of larva and adult mutant animals (Lithgow et al., 1995; Wolkow et al., 2002). Therefore, we assessed if *uri-1*-depleted worms are more resistant to heat stress or oxidative damage. As in the case of longevity, *uri-1(RNAi)*F1 exhibit wild type sensitivity to thermal stress (37°C) (Figure 16) and to the oxidative damage-inducing compound paraquat (see Figure 29 and description in section 4.5.1.1).

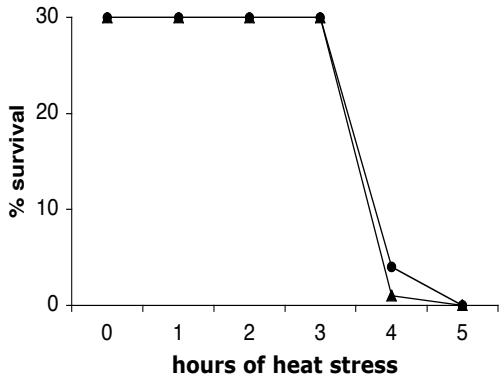

Figure 16. Thermo tolerance of *uri-1(RNAi)*F1 and wild type animals. Survival of *uri-1(RNAi)*F1 and wild type young adults at 37°C showed no increased resistance of *uri-1* depleted animals to termal stress.

In conclusion, apart from L3 larval arrest, *uri-1* depletion causes none of the phenotypes that are characteristic of mutants of genes that function in the TOR and/or *daf-2* signaling pathways. Unlike in yeast and mammalian cells where loss of URI mimics inhibition of TOR signaling, loss of *uri-1* function in *C. elegans* does not phenocopy loss of CeTOR or *daf-2* signaling.

4.5 Functional analysis of URI-1 in the germ line

In addition to somatic defects such as protruding vulva, rupture, embryonic lethality, uncoordination, molting problems and L3 larval arrest, depletion of *uri-1* also results in multiple germ line defects. The germ line of fertile heterozygous *uri-1* (data not shown) and *uri-1(RNAi)*P0 (Figure 17B) adult animals show pathfinding and oocyte defects. The homozygous *uri-1*, as well as *uri-1(RNAi)*F1 (Figure 17 C,D) animals show more severe germ line defects and develop into sterile animals, suggesting that URI-1 is essential for fertility. These animals completely lack oocytes and exhibit bubbles in their body cavity, which are not present in the wild type animal (Figure 17D).

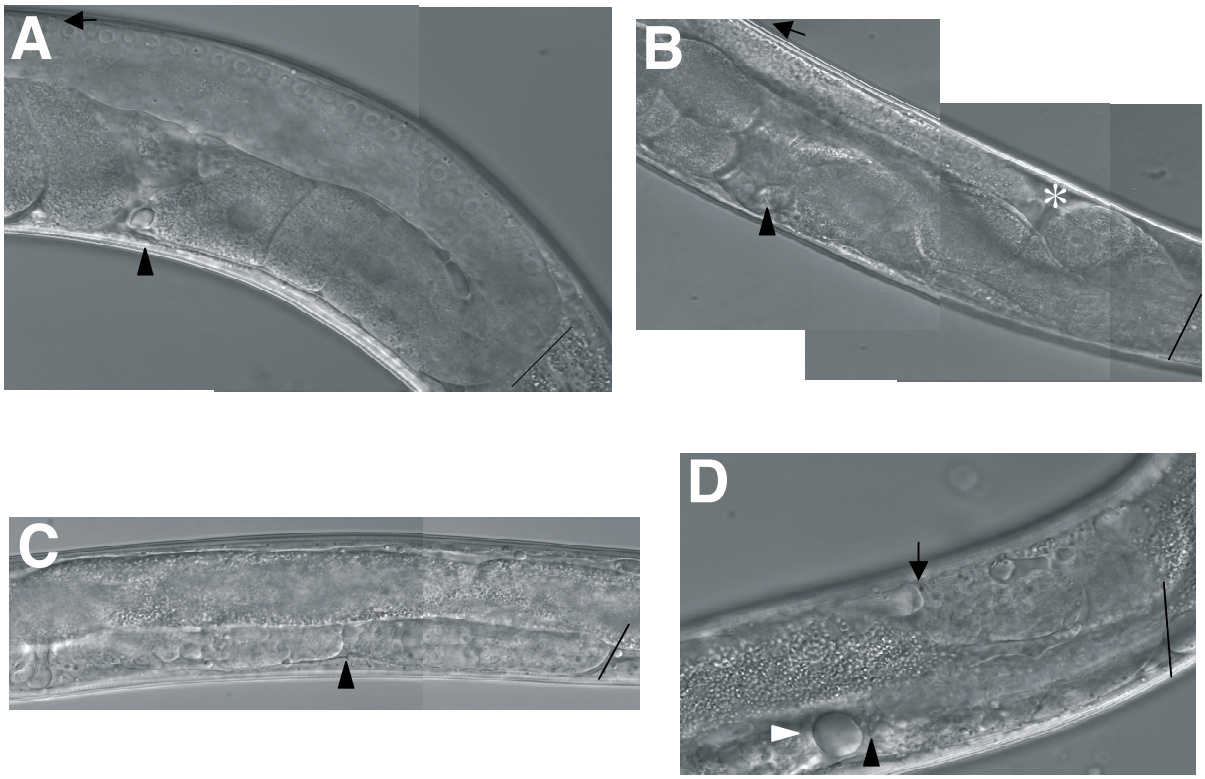

Figure 17. Differential interference contrast (DIC) pictures of adult *C. elegans* germ lines. (A) wild type loop area, (B) *uri-1(RNAi)*P0 loop area and (C,D) *uri-1(RNAi)*F1 loop areas of animals grown at 25°C. Arrows indicate the distal tip cell, Black arrowheads indicate either spermathecal region or alternatively the proximal end of the germ line. The white * in (B) indicates a pathfinding defect and the white arrowhead in (D) indicates a bubble. Black lines indicate the loop.

We reasoned that the bubbles observed in the *uri-1* depleted animals likely represent yolk accumulations in the pseudo-coelomocytic space. In wild type animals, yolk is synthesized in the body wall muscle and secreted into the body cavity, where it is endocytosed, primarily by coelomocytes (Grant and Hirsh, 1999). Thus, yolk is stored in oocytes with the highest level in the most full-grown oocyte (Grant and Hirsh, 1999). Yolk accumulation in the body cavity is a sign of age or an endocytosis defect (Grant and Hirsh, 1999). To test if the bubbles in *uri-1* depleted animals represent yolk accumulations in the body cavity we performed *uri-1(RNAi)*F1 and control RNAi in the transgenic strain carrying YP170::GFP, which expresses a GFP-tagged egg yolk protein (vitellogenin 2). This assay shows that indeed the bubbles seen in the *uri-1* depleted animals represent yolk (Figure 18). The most likely cause of these yolk accumulations are that *uri-1* depleted animals lack oocytes and subsequently lack the ability to endocytose and store yolk.

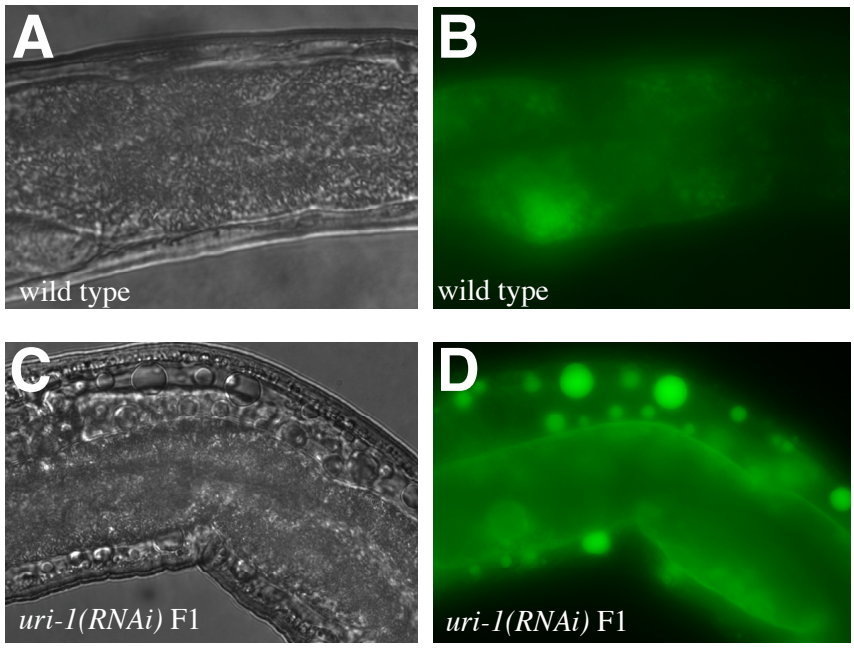

Figure 18. Yolk accumulation in *uri-1* depleted animals. Imunofluorescence and DIC pictures of yolk granules in *uri-1(RNAi)*F1 and control animals of the transgenic strain carrying the yolk protein YP170::GFP reporter (Grant and Hirsh, 1999). In wild type control RNAi animals the body cavity is dark and void of GFP accumulations. In *uri-1(RNAi)*F1 animals uptake of YP170::GFP is deficient, resulting in accumulation of yolk bubbles in the pseudo-coelomocytic space. Scale bar 10 μm.

The sterile *uri-1* homozygous mutants, as well as *uri-1(RNAi)*F1, exhibit a small germ line phenotype due to a severe reduction in germ cell number (Figure 19 and Table 2). Male *uri-1(RNAi)*F1 animals also suffer from a reduction of germ cells (data not shown) indicating that the function of URI-1 is sex-independent. In wild type hermaphrodites the first germ cells that enter the meiotic cycle in each gonad arm (approximately 40) differentiate as primary spermatocytes, then secondary spermatocytes, spermatids and finally form activated spermatozoa (approximately 160). Thereafter, a switch in sexual fate occurs so that all germ cells, which differentiate afterwards, develop as oocytes (Riddle et al., 1997). In homozygous *uri-1* mutants we observe a complete lack of oocytes. About 35% (n=30) of *uri-1* depleted germ lines do not show any sign of gametogenesis. If gametogenesis occurs, it leads to the presence of sperm in the corresponding gonads. However, the spermatocytes do not always complete the meiotic divisions, since both spermatocytes (Figure 19, arrow heads) and mature sperm (Figure 19, arrows) were observed in these adult hermaphrodites. Accordingly, the amount of sperm in the adult small germ lines of homozygous *uri-1* mutant is reduced (13±10, n=10) compared to wild type (approximately 160).

As shown in Table 2, heterozygous *uri-1* hermaphrodites were sub-fertile at 25ºC with significantly decreased brood size. Consistent with this reduction of brood size in response to the loss of URI-1 function, L1 fed *uri-1(RNAi)* animals of the P0 generation (*uri-1(RNAi)*P0) also display a reduced brood size compared to wild type. Moreover, the germ cell number of these animals is reduced to 73% of the wild type number (Table 2). This shows that URI-1 is haplo-insufficient in ensuring normal germ cell number and brood size. Interestingly, genotypic wild type animals arising from an *uri-1* +/- heterozygous mother give rise to approximately half of the brood size of wild type worms with a wild type mother. This shows that zygotically provided URI-1 is insufficient for its role in germ line cells and *uri-1* has to be maternally supplied to ensure normal brood size. The fact that homozygous *uri-1* mutants display defects in oogenesis and spermatogenesis, but the heterozygous do not, suggests that these processes are less sensitive to the loss of *uri-1* levels than brood size and overall germ cell number. *uri-1(RNAi)*F1 animals contain an average of 89 germ cells (Table 2), however the most severely affected animals of the *uri-1(RNAi)*F1 contain only a few germ cells (around 18) without any visible gametes, most probably reflecting a stronger loss of URI-1 function. Taken together, these findings demonstrate that the effect of *uri-1* on germ cell number and fertility is dose dependent and provide the first evidence of a functional role of URI-1 in oogenesis, spermatogenesis, regulation of germ cell number, fertility and germ line viability.

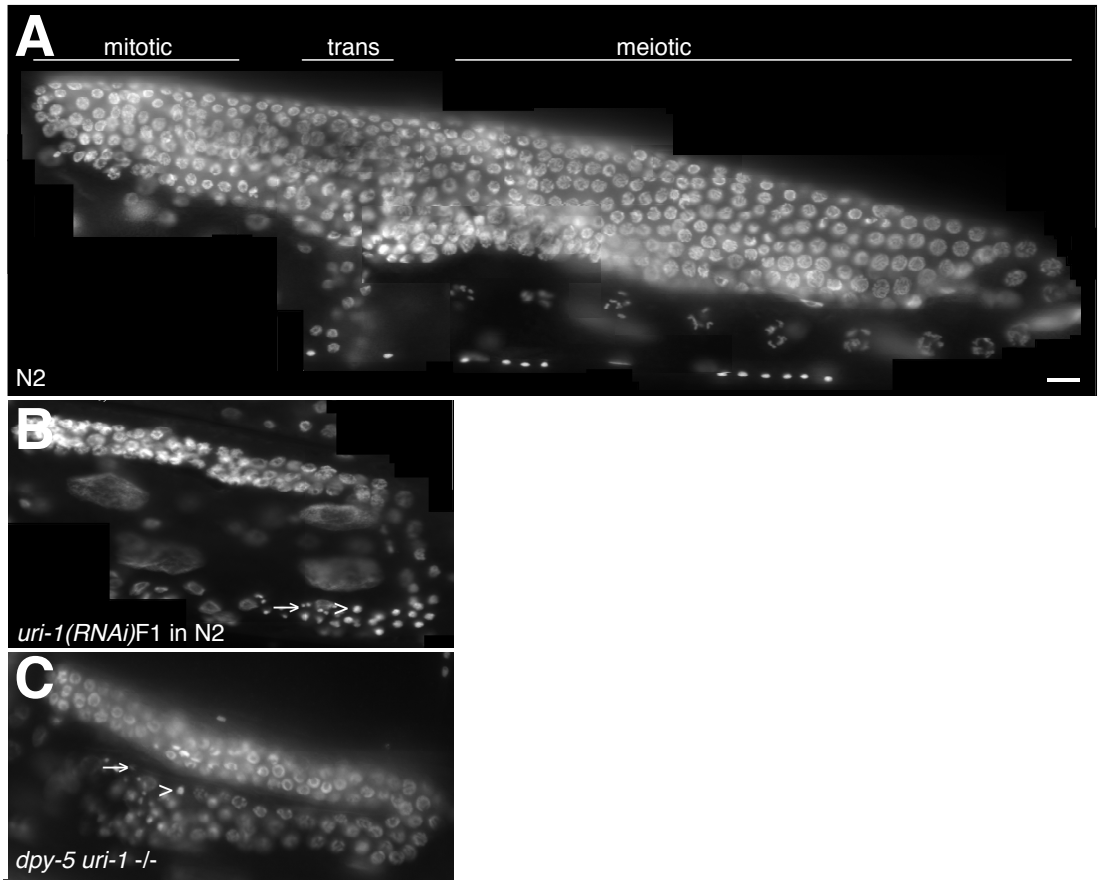

Figure 19. Morphological defects of *uri-1* depleted germ lines. Germ nuclei stained with the nuclear dye DAPI in wild-type (A), *uri-1(RNAi)*F1 (B) and homozygous *dpy-5 uri-1(tm939)* (C) adult hermaphrodites raised at 25°C. As the homozygous *uri-1* mutant is embryonic lethal or sterile, the *uri-1* mutation was marked with the close *dpy-5* mutation and cultured as a heterozygous stock to facilitate this and subsequent analysis. Arrows indicated haploid sperm and arrowheads spermatids. The vulva in each animal is down and oriented to the left. Scale bar 10 μm.

Genotype	Brood size	% sterility	Germ nuclei /gonad arm
N2	213 ± 39 (n=20)	0 (n=20)	325 ± 31 (n=10)
uri-1 +/-	74 ± 32 (n=20)	0 (n=20)	n.d
uri-1 -/-	0 ± 0 (n=20)	100 (n=20)	85 ± 24 (n=20)
N2 (mother *uri-1* +/-)	92 ± 25 (n=20)	0 (n=20)	n.d.
uri-1dpy-5/dpy-5unc-14	55 ± 27 (n=30)	0 (n=30)	238 ± 32 (n=10)
uri-1dpy-5 -/-	0 ± 0 (n=30)	100 (n=30)	67 ± 14 (n=20)
uri-1(RNAi) P0	40 ± 23 (n=20)	0 (n=20)	278 ± 31 (n=10)
uri-1(RNAi) F1	3 ± 9 (n=30)	87 (n=30)	89 ± 63 (n=110)

Table 2. Quantification of the germ line defects due to *uri-1* depletion. Analysis of brood size, fertility and germ cell number of *uri-1(RNAi)* and *uri-1(tm939)* mutant hermaphrodites at 25°C. "±" indicates std. dev. and "n" number of analyzed animals.

Since the germ lines of *uri-1* mutants are smaller and have a reduced cell number, we wondered whether URI-1 plays a role in germ cell proliferation. As a hermaphrodite develops from L1 larvae to adulthood, the number of somatic cell nuclei roughly doubles (556 to 1090) and the number of germ cells increases from 2 to up to 2000 germ cells per gonad (Riddle et al., 1997). Therefore, germ line development requires extensive proliferation of cells. The role of URI-1 in germ line development may result from a requirement of URI-1 in proliferation. Germ line cells located at the distal end of the gonad arm constitute a proliferating stem cell population. During the larval development of *C. elegans*, the number of germ cells gradually increases up to the L3 larval stage, when a transition occurs to a period of rapid proliferation (Capowski et al., 1991). A time course analysis of germ line development in wild type compared with *uri-1(RNAi)*F1 worms revealed that the rapid increase in germ cell number at the end of L3 does not occur in the *uri-1(RNAi)*F1 animals. The germ cell number stagnates or increases without significance during the L4 larval and adult stage (Figure 20A) leading to a significant difference in germ cell number between *uri-1* depleted and wild type worms at 25^{o}C. To confirm that *uri-1* is required for germ cell proliferation, we performed *uri-1(RNAi)* in the *gld-2 gld-1* double mutant which has an over-proliferative germ line containing mainly mitotic cells due to meiotic entry defects (Hansen et al., 2004; Kadyk and Kimble, 1998). Loss of *uri-1* in this background suppresses the over-proliferation defect, resulting in small germ lines with a dramatically reduced cell number (Figure 20B). We therefore conclude that *uri-1* is required for proliferation of mitotic germ cells.

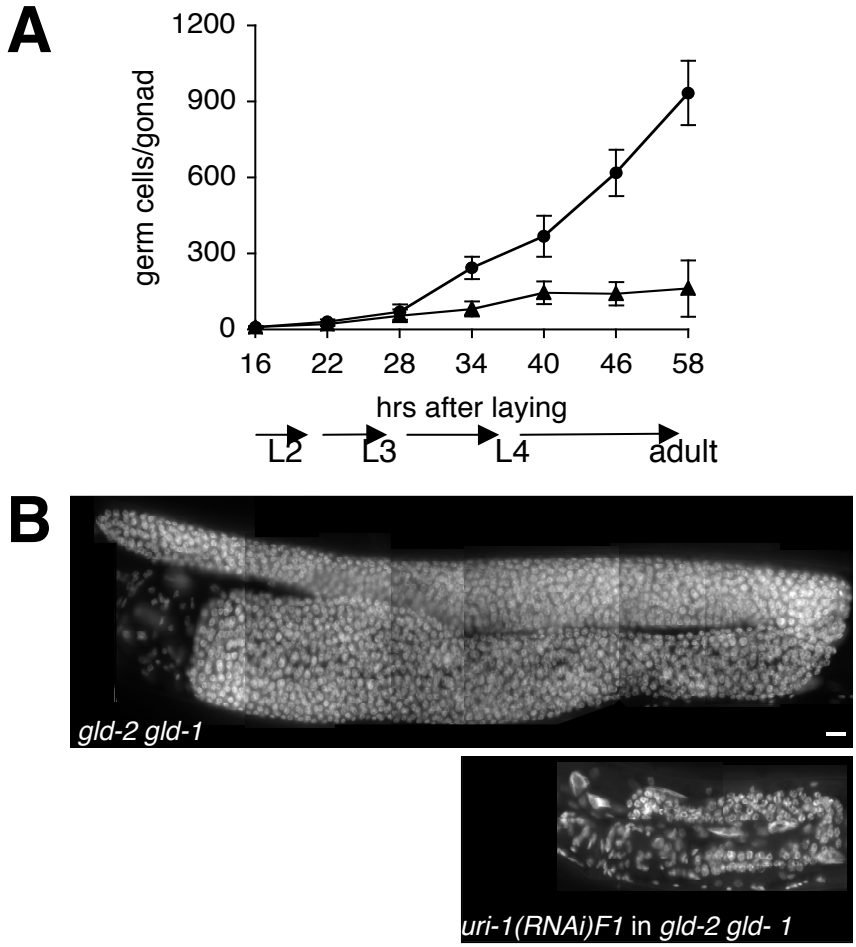

Figure 20. Effects of URI-1 on germ cell proliferation in *uri-1(RNAi)*F1 and wild type animals raised at 25°C. (A) Defects of germ line development. Number of germ nuclei per gonad arm in *uri-1(RNAi)*F1 (n=19-25, ▲) and wild type (n=9-25, ●) worms. Progeny of staged animals was synchronized by letting the P0 generation lay eggs for 2 hrs, fixed according the indicated time points and stained with the nuclear dye DAPI. Germ cells identified by their DNA morphology where counted. Error bars indicate std. dev. (B) Effect of URI-1 reduction on mitotic germ cells. The cell fate defective *gld-2(q497) gld-1(q485); unc-32(e189)* mutant does not suppress the *uri-1* small germ line phenotype. The vulva in each animal is down and oriented to the left. Scale bar 10 μm.

To determine if the cell proliferation defect of germ cells is due to induction of a cell division block, gonads of *uri-1(RNAi)*F1 and homozygous *uri-1* mutant animals were stained with the M-phase marker anti-phospho-histone H3 antibody (PH3). Histone H3 is specifically phosphorylated on Ser^{10} or on both Ser^{10} and Ser^{28} in M phase and this modification is essential for chromosome condensation and segregation (Goto et al., 1999; Hendzel et al., 1997). The germ lines of homozygous *uri-1* and *uri-1(RNAi)*F1 gonads display a significantly increased number of PH3-positive nuclei in the mitotic region

compared to wild type gonads (Figure 21A). Elevated PH3 staining is seen either in over-proliferative gonads (Kadyk and Kimble, 1998) or gonads that suffer from a mitotic cell cycle block (Kim et al., 2002c). Since cell proliferation is reduced in *uri-1* mutants, as shown above, the increased number of cells positive to PH3 suggests that an enhanced fraction of the few germ cells present in sterile *uri-1* as well as *uri-1(RNAi)F1* animals are transiently or permanently blocked between late prophase and telophase of the mitotic cell cycle. As mentioned above, some germ lines are less affected than others by reduction of URI-1 function. In germ lines containing gametes, we observe spermatids that are also stained with the PH3 antibody indicating an additional cell cycle block at M-phase of spermatocyte meiosis (Figure 21B) (Golden et al., 2000). Arrest at the primary spermatocyte stage was not absolute (23-72%), however, some mature sperm were seen in most animals. We conclude that URI-1 promotes maturation of primary spermatocytes to mature sperm. This phenotype does not reflect a role for URI-1 in spermatogenesis, since loss of *uri-1* by RNAi in the *glp-1* mutant, in which germ cells enter meiosis early and consequently proliferate far less than in wild type worms, suppresses the URI-1 phenotype leading to the *glp-1* phenotype without any visible defect in spermatogenesis (Figure 21C). We propose the defect in spermatogenesis in the URI-1 deficient germ lines is a consequence of the cell division defect of *uri-1* mutants rather than a direct effect of URI-1 on spermatogenesis. To summarize, our data show that loss of URI-1 activity leads to a cell cycle block that occurs in both mitotic and meiotic cells. The suppression of the *uri-1(RNAi)*F1sperm phenotype by *glp-1* and the proliferation defect of *uri-1(RNAi)*F1 germ lines in the *gld-2 gld-1* double mutants indicates that the main function of URI-1 is in mitotic cells.

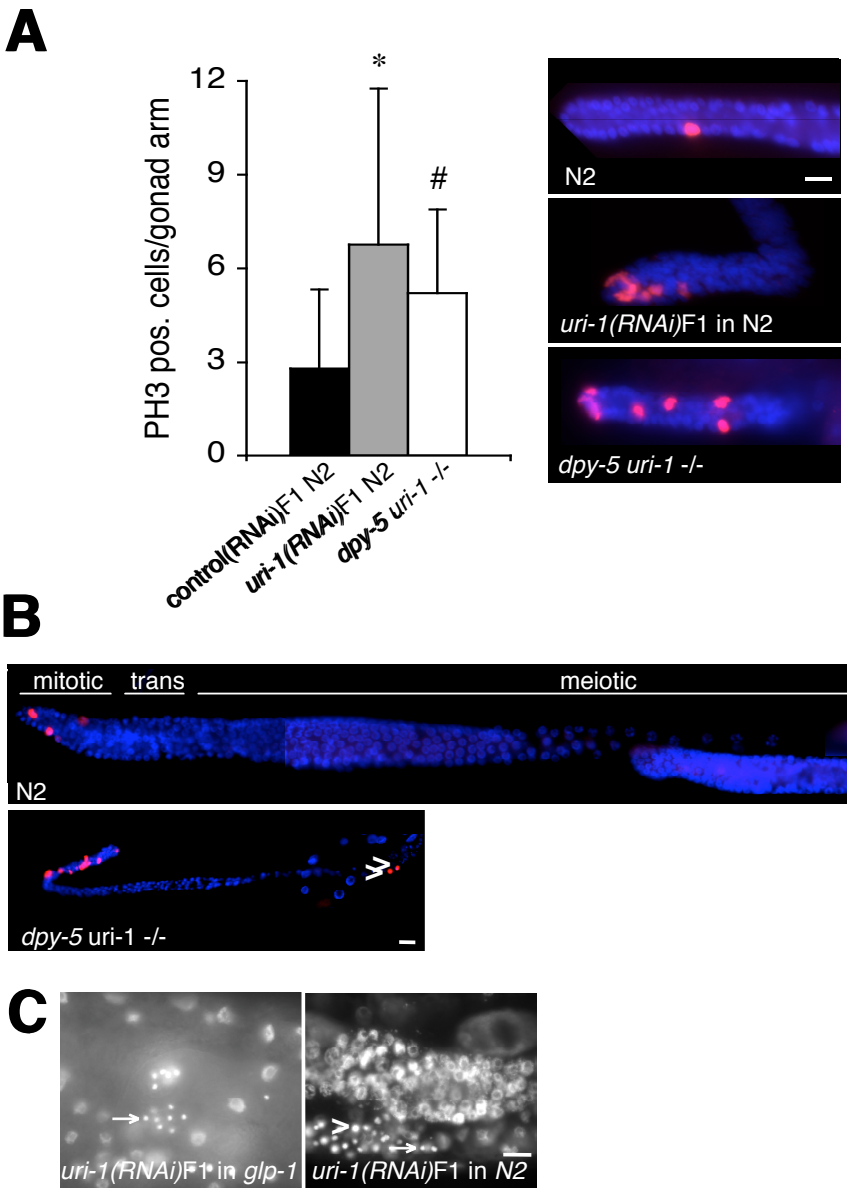

Figure 21. Loss of URI-1 blocks cell cycle progression in the germ line. (A) Staining and quantification of phospho histone 3 (PH3)-positive (Cy3) germ nuclei (visualized with DAPI) per gonad arm in the distal region of staged homozygous *uri-1(tm939)* (n=24, light), *uri-1(RNAi)*F1 (n=65, grew) compared to wild type (n=65, dark) adult hermaphrodites (Student test p-values: ∗ = $7.9 \bullet 10^{-8}$, # = $1{,}0 \bullet 10^{-4}$). The vulva in each animal is down and oriented to the right Scale bar 10 μm. Error bars indicate std. dev. (B) PH3 staining (Cy3) of homozygous *uri-1* mutant and wild type germ line nuclei (visualized with DAPI). The sperm in each animal is oriented to the right. Arrowheads indicate sperm. Scale bar 10 μm. (C) Proliferation is required for the defect caused by loss of *uri-1*. DAPI staining of *uri-1(RNAi)*F1 and *glp-1; uri-1(RNAi)*F1 sperm. Loss of *uri-1* by RNAi in the *glp-1* mutant suppresses the URI-1 phenotype leading to the *glp-1* phenotype (premature meiotic entry), without any visible defect in spermatogenesis, suggesting that the process of spermatogenesis per se is not affected through the loss of URI-1 function. As URI-1 leads to proliferation defects and the number of cell cycles performed prior to differentiation seems to have an impact on spermatogenesis in the URI-1 depleted animal as shown above we conclude that *uri-1* is indirectly required for sperm differentiation and meiotic cell cycle due to its function in proliferation. Arrows indicate haploid sperm and arrowheads spermatids. The vulva in each animal is down and oriented to the left. Scale bar 10 μm.

To further investigate the potential effect of loss of *uri-1* function on cell cycle progression we stained the *uri-1(RNAi)*F1 and control animals with the nuclear dye DAPI. This staining revealed the enrichment of a naturally occurring mitotic cell figure with condensed chromosomes that are not yet aligned to the metaphase plate and most likely represent prometaphases (Figure 22). The frequency of this enriched cell cycle phase correlates with the frequency of PH3 positive cells per gonad arm. The DNA morphology of the *uri-1* deficient worms is similar to that in cell cycle arrested cells seen in the *gld-3(q145)* mutant, apart from the fact that the nuclei are uniform in size in *gld-3* mutants (Kadyk et al., 1997). In addition, the size of the germ nuclei in *uri-1* animals is enlarged (see arrowheads in Figure 22), a phenomenon that is also observed during radiation-induced cell proliferation arrest and which results from growth without proliferation (Gartner et al., 2000). However, unlike the effects of a single γ-irradiation dose, which induces homogeneous increase in size of nuclei, loss of URI-1 function induces heterogeneous enlargement. The different extent of enlargement could suggest that individual cells receive proliferation-blocking stimuli at different times, or that DNA damage is uniform and the responses are variable representing a transient rather than a permanent block in cell cycle progression.

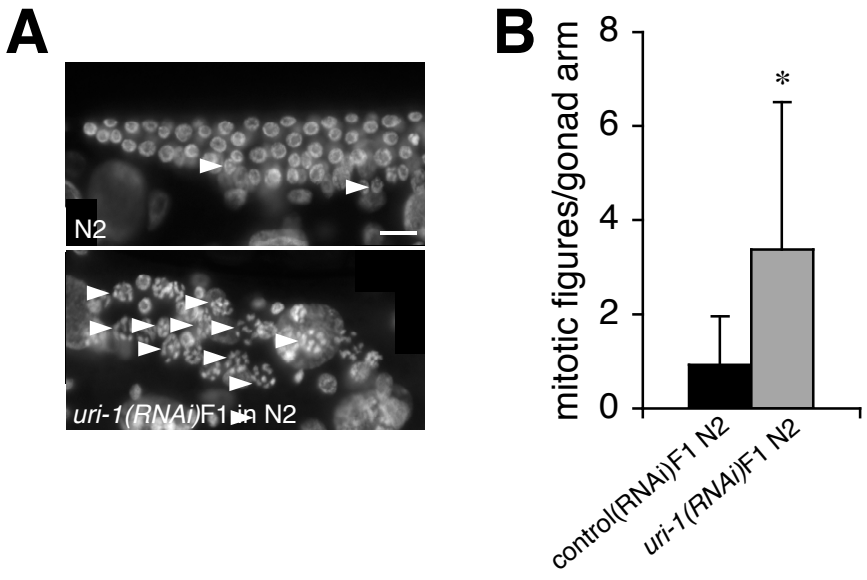

Figure 22. Loss of URI-1 blocks cell cycle progression in the germ line. DAPI staining and prometaphase quantification of untreated wild type (n=35, dark) and *uri-1(RNAi)*F1 (n=35, grey) staged adult hermaphrodites. Prometaphase counts indicating a mitotic block (p-value: $* = 5.2 \bullet 10^{-5}$). Error bars indicate std. dev. The DAPI picture of the distal part of the gonad of a good example of *uri-1(RNAi)F1* and control worms. The arrowheads point to a mitotic figure of a germ line cell with apparently condensed chromosomes and different extent of enlargement. This kind of DNA morphology is similar to a wild type cell cycle phase and accumulates in germ lines in the loss of *uri-1* functions suggesting these nuclei represent a block at a naturally occurring stage of the cell cycle probably representing prometaphase. The vulva in each animal is down and oriented to the left. Scale bar 10 μm.

Mutation in genes that appear to be involved in regulating cell cycle progression, like *emb-29* and *glp-3*, cause an arrest of the cell cycle at the G_2/M transition (Riddle et al., 1997). Block at G_2/M border is often due to activation of the DNA checkpoint machinery by damaged or incompletely replicated DNA (for review see (Hartwell and Weinert, 1989)). Since we observe a mitotic cell cycle block in the germ line of the homozygous *uri-1* mutant, we wondered whether this block could be triggered by damaged DNA. To test this, we performed TUNEL staining, which labels DNA strand breaks and DNA fragmentation. In the small germ line of the homozygous *uri-1* mutant, as well as *uri-1(RNAi)*F1 animals, a significantly increased TUNEL staining was observed in the germ line compared to wild type animals (Figure 23A,B). This dramatically increased TUNEL staining is not due to apoptosis since *uri-1(RNAi)*F1 in the apoptosis-defective *ced-3(lf) or ced/9(gf)* mutant does not rescue the small germ line phenotype (Figure 23C and Table 3). Thus loss of URI-1 results in extensive DNA breaks in the adult germ line of *C. elegans*.

In *C. elegans, hus-1* is required for DNA damage-induced cell cycle arrest and apoptosis. HUS-1::GFP localizes diffusely in proliferating germ nuclei under normal conditions. In response to DNA damage, HUS-1::GFP re-localizes in the nucleus and concentrates at distinct nuclear foci that overlap with chromatin, believed to be sites of DNA breaks (Hofmann et al., 2002). To confirm that loss of URI-1 leads to DNA damage in the germline and to check if the DNA damage sensing mechanisms are functional in the absence of URI-1, we performed *uri-1(RNAi)*F1 in the HUS-1::GFP strain. *uri-1(RNAi)*F1 in this strain resulted in the formation of nuclear HUS-1::GFP foci in the germline (Figure 23 D,E), consistent with the results obtained with the TUNEL assay. Thus, in the absence of exogenous DNA damage stimuli, loss of URI-1 function results in increased DNA damage that activates the cellular DNA damage sensing machinery in the germline.

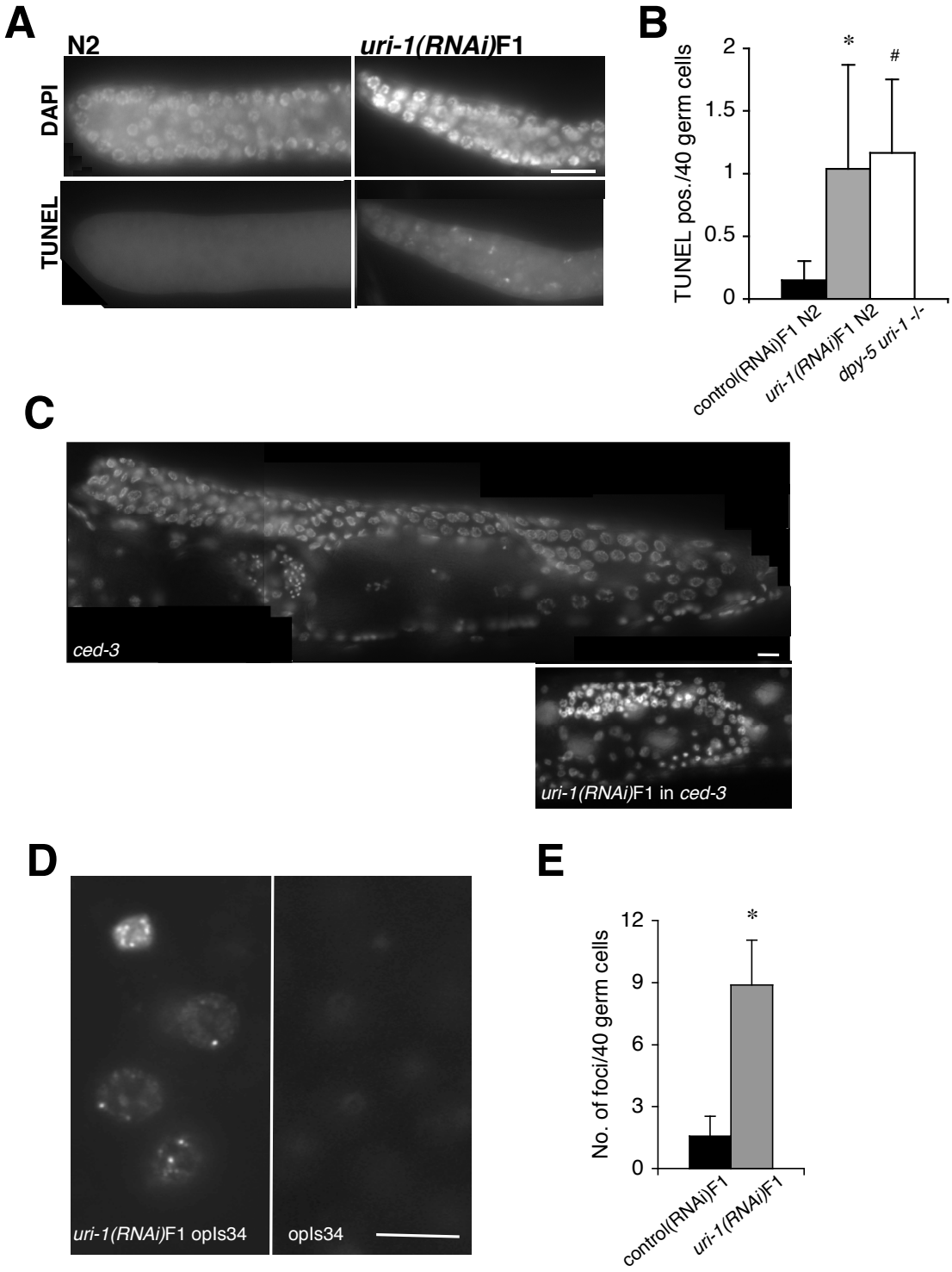

Figure 23. Accumulation of DNA breaks in the adult hermaphrodite germ line in response to the loss of *uri-1* function. (A) DAPI (top panels) and TUNEL (lower panels) staining of wild type (N2) and *uri-1(RNAi)*F1 worms. (B) Quantification of TUNEL (TdT-mediated dUTP nick end labeling) staining in the homozygous *uri-1(tm939) (n=9,* white*), uri-1(RNAi)*F1 (n=25, grey) and N2 (n=25, dark) gonads (p-values: ∗ = 2,3•10^{-6}, # = 3,6•10^{-9}). Error bars indicate std. dev. The vulva in each animal is down and oriented to the left. Scale bar 10 µm. (C) The severe reduction in germ cell number is not caused by apoptosis. DAPI staining of methanol fixed *ced-3*; *uri-1(RNAi)*F1 and *ced-3* mutant adult hermaphrodites. The small germ line phenotype due to the loss of URI-1 is not suppressed in the *ced-3* mutant background. The vulva in each animal is down and oriented to the left. Scale bar 10 µm. (D) GFP fluorescence showing nuclear HUS-1::GFP foci in the presence of *uri-1(RNAi)*F1 in the *hus-1(op241);unc-119(ed3);opIs34* strain. Scale bar 5 µm. (E) Quantification of *uri-1(RNAi)*F1 (grey) and control (dark) RNAi in the *hus-1(op241);unc-119(ed3);opIs34* (n=*55* for each), which is thought to re-localize in the nucleus upon DNA damage to places DNA breaks (p-values: ∗ = 3,4 •10^{-43}). Error bars indicate std. dev.

Genotype	Germ nuclei per gonad arm	
	vector control	*uri-1(RNAi)*F1
ced-3	338 ± 56 (n=5)	77 ± 36 (n=15)
ced-9	352 ± 29 (n=5)	90 ± 58 (n=15)

Table 3. The small germ line phenotype of homozygous *uri-1* mutants is not due to apoptosis. Quantification of germ cell number in the indicated genetic background with control and *uri-1(RNAi)* F1 at 25°C . "±" indicates std. dev. and "n" number of analyzed animals. Note that the *ced-9* mutant is a gain-of-function mutation.

To support the hypothesis that *uri-1* depleted mitotic germ cells suffer from damaged DNA (Figure 23 and 24) and exhibit a G_2/M like arrest (Figure 21) due to checkpoint activation, we reasoned that it may be possible to suppress the cell cycle arrest by inactivating checkpoint genes that become activated following DNA damage that arises due to URI-1 depletion. To this end we generated an *atm-1; uri-1* double mutant and performed *uri-1(RNAi)*F1 in several checkpoint mutants such as *mre-11* (meiotic recombination), *mrt-2* (mortal germ line), *hus-1* (hydroxyurea-sensitive), *rad-51* (radiation sensitivity abnormal), *wee-1 (wee-1 like)*, *cep-1* (*C. elegans* p53) and *chk-2* (checkpoint kinase). However, inactivation of these checkpoint genes failed to rescue the small germ line phenotype of *uri-1*(RNAi)F1 animals (for example see Figure 25). It is possible that URI-1 depletion causes multiple types of DNA lesions, and that cell cycle arrest is induced by the concerted action of multiple pathways.

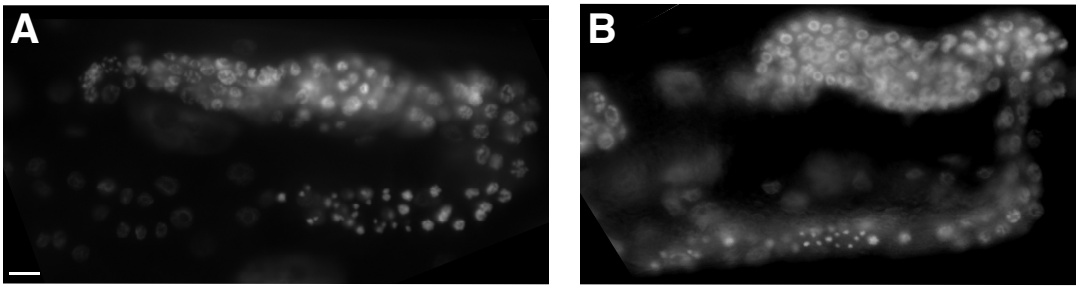

Figure 25. Generation of an *atm-1; uri-1* double mutant. DAPI stained germlines of (A) *uri-1* mutant and (B) *atm-1;uri-1*double mutant animals. Inactivation of the DNA damage sensor *atm-1* by mutation does not rescue the small germ line phenotype of homozygous *uri-1* mutant animals. Scale bar 10 μm.

As URI-1 depletion results in a G_2/M-like mitotic germ cell arrest, we wondered if the S phase checkpoint is functional in URI-1 depleted worms. If URI-1 would be necessary to arrest cells in S phase in response to DNA damage, in the absence of URI-1, cells with damaged genomes could escape S phase and would instead be sensed by the G_2/M checkpoint, leading to the observed phenotype. In order to probe the role of *uri-1* in the DNA replication checkpoint, *uri-1* depleted and wild type worms were treated with hydroxyurea (HU) to interrupt DNA replication by depleting deoxynucleotides. As shown by fluorescence microscopy, mitotic nuclei in the wild type germ line were enlarged and reduced in number because of cell cycle arrest combined with continued growth in response to HU treatment (Figure 26). Mitotic germ cells of *uri-1* depleted worms responded normally to S phase checkpoint activation upon HU treatment, demonstrating that *uri-1* is not required for the sensing or implementation of the S phase checkpoint (Figure 26).

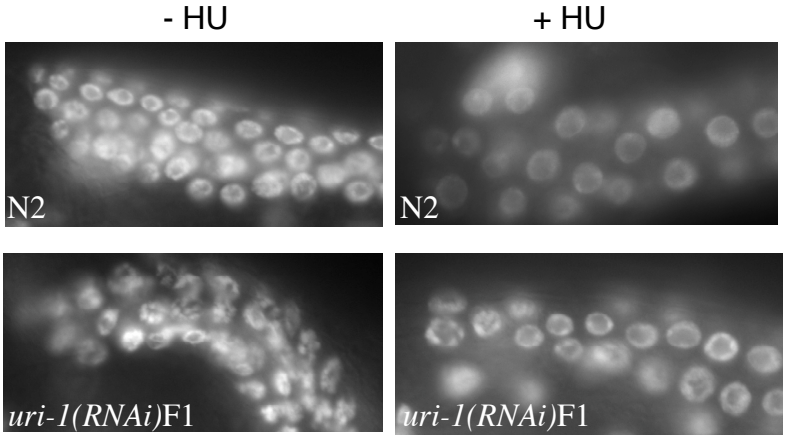

Figure 26. Morphological changes of mitotic germ cell nuclei induced by hydroxyurea (HU). Fluorescence images of DAPI-stained nuclei of untreated (-HU) and hydroxyurea treated (+HU) germ lines. Upon HU treatment, mitotic nuclei in the wild-type germ line were substantially enlarged and reduced in number. Mitotic germ cells of *uri-1* worms responded by S phase checkpoint activation upon HU treatment suggesting that *uri-1* is not required for S phase checkpoint activation. Scale bar 10 μm.

To prove generally that DNA damage during larval development can lead to a small germ line phenotype, we showed that the *rad-51* mutant worms (Alpi et al., 2003), which cannot repair γ-radiation induced DNA damage, develop into sterile adults with small germ lines when γ-irradiated at the L2/L3 larval stage, phenocopying *uri-1* depleted animals (Figure 27).

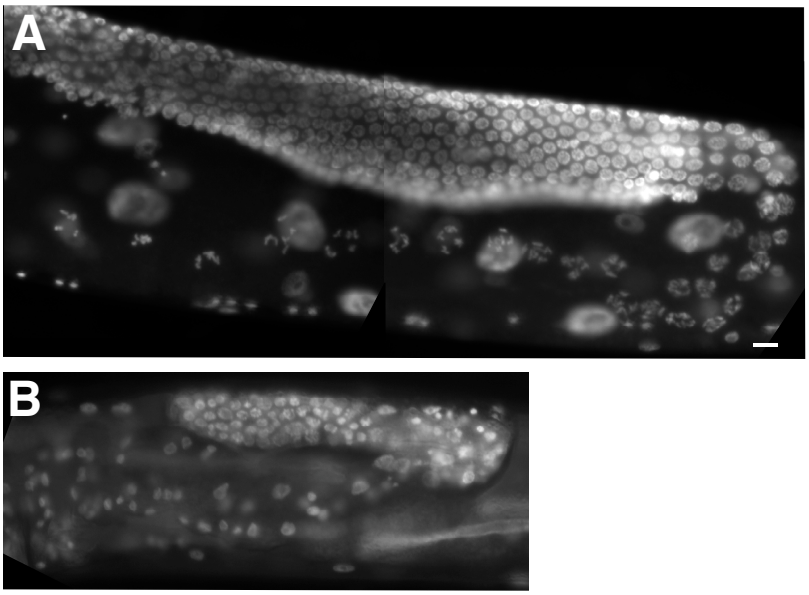

Figure 27. DNA damage during larval development reduces germ cell number. (A) Fluorescence images of DAPI stained untreated *rad-51* and (B) L4 γ-irradiated *rad-51* (120 gray) adult animals. In each animal the vulva is oriented to the bottom and the distal tip cell to the left. Scale bar represents 10 μm.

To confirm genetically that depletion of *uri-1* leads to DNA damage we analyzed another germ line phenotype of *uri-1* depleted animals. The heterozygous *uri-1* mutant as well as *uri-1(RNAi)*P0 animals, show an approximately 3-fold higher Acridine Orange (AO) staining (Figure 28 A,C) and 3-fold higher number of apoptotic corpses in their meiotic region (*gla* phenotype) compared to wild type (Figure 28B). The higher AO staining and apoptotic corpses indicate that apoptosis is increased in the germ line of these animals. This *gla* effect of *uri-1(RNAi)*P0 is completely suppressed in *ced-9(gf)* and *ced-3(lf)* mutant backgrounds, confirming that the increased rate of cell death in the heterozygous *uri-1* mutant and *uri-1(RNAi)*P0 animals is caused by apoptosis (Figure 28B,C). To investigate whether the increased apoptosis results from damaged DNA, we depleted *uri-1* in *cep-1* mutant worms. CEP-1 is the homologue of the tumor suppressor protein p53 and is known to be required for DNA damage-induced germ cell apoptosis (Schumacher et al., 2001), but dispensable for physiological germ cell death or programmed cell death (Schumacher et al., 2001). The *gla* phenotype of *uri-1(RNAi)*P0 is suppressed in the *cep-1* null background (Figure 28D). This indicates that the *gla* phenotype in *uri-1* animals is due to DNA damage-induced activation of p53 and subsequent apoptosis induction. To summarize, reduction of half the *uri-1* gene dose sensitizes meiotic germ cells to p53-mediated DNA damage-induced germ cell apoptosis in absence of exogenous DNA damage.

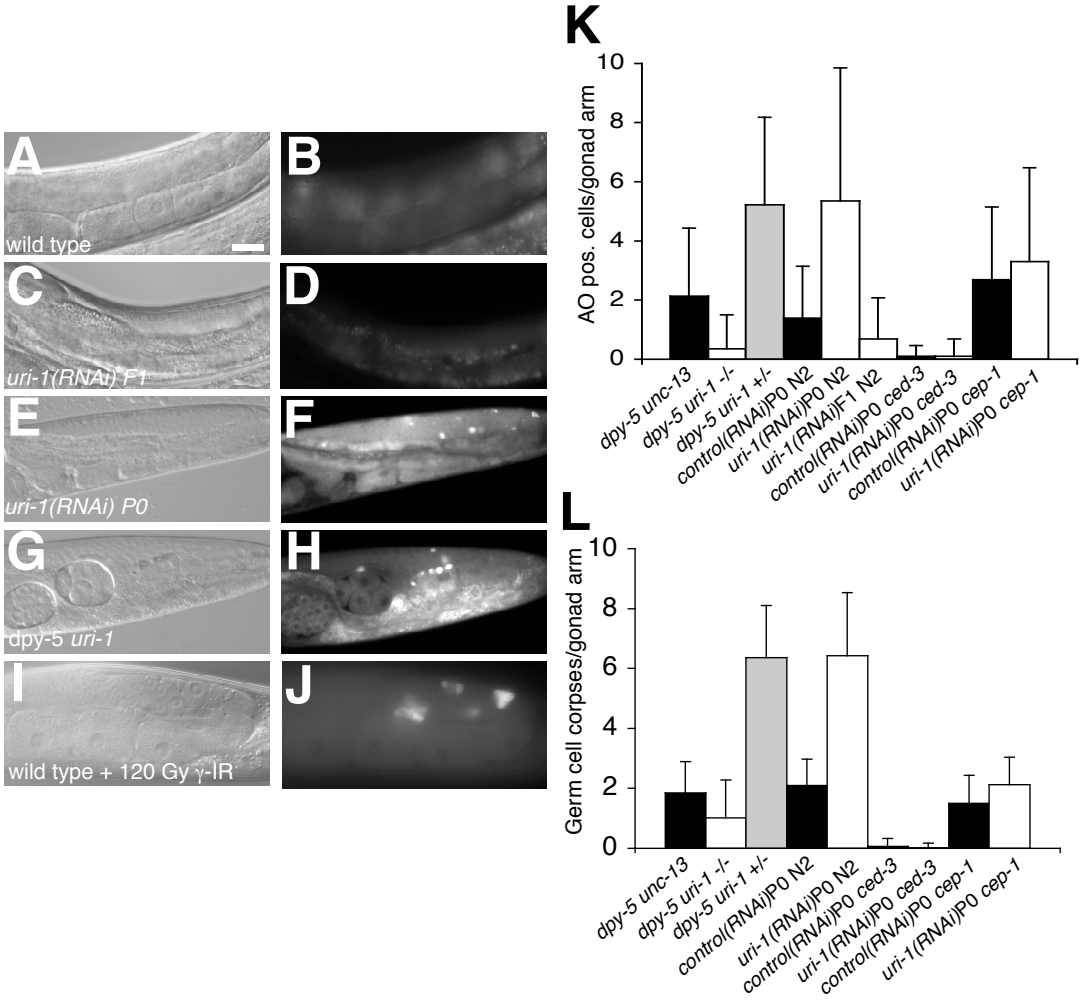

Figure 28. Effect of *uri-1* depletion on meiotic cells. Loss of *uri-1* sensitizes meiotic germ cell to apoptosis. (A) AO staining of the indicated genotypes reveals a gla phenotype of *uri-1* depleted animals. Scale bar 10μm. Apoptotic corpse (B) and AO positive cell counts (C) in the heterozygous *uri-1* mutant and *uri-1(RNAi)P0* animals confirm the *gla* phenotype, which is completely suppressed by mutations of the apoptotic pathway components *ced-3(lf)* and *ced-9*(gf) (p-values: ∗ = $3{,}0 \bullet 10^{-20}$, # = $2{,}3 \bullet 10^{-19}$). Error bars indicate std. dev. (D) Apoptotic corpse counts in N2 and *cep-1* germ lines of *uri-1(RNAi)P0* and control animals reveal that the *gla* phenotype of URI-1 is completely suppressed by mutations of the DNA damage sensor *p53* (*C. elegans cep-1*). Error bars indicate std. dev.

4.5.1 How does URI-1 ensure DNA stability?

DNA breaks can be caused endogenously due to recombination intermeditates, replication defects, repair defects, abnormal chromatin structure, spontaneous depurinisation and reactive oxygen species (for review see (Sancar et al., 2004)). As depletion of URI-1 leads to DNA damage in the germ line we wondered if this damage could reflect a function of URI-1 in or more of these processes to ensure DNA stability. As different DNA damaging stimuli generate different types of DNA lesions, which in turn trigger different kinds of DNA repair pathways, the sensitivity of *uri-1* mutants to different exogenous DNA damaging stimuli was examined in experiments described in the following sections in an attempt to identify the process through which URI-1 ensures DNA stability.

4.5.1.1 Does URI-1 reduction cause increased sensitivity to oxidative stress?

It is interesting to note that genome-wide gene interaction approaches in *Saccharomyces cerevisiae* revealed a synthetic lethality interaction of the viable single mutant of the yeast homolog of *uri-1* (BUD27) in combination with the viable single mutant of the endonuclease RAD27, a homologue of mammalian FEN-1, indicating that one or more essential functions of the URI are genetically redundant with FEN-1. As FEN-1 is implicated in base excision repair (BER) (Kim et al., 1998; Wu et al., 1999a) and processing of Okazaki fragments during DNA replication (Bambara et al., 1997; Ishimi et al., 1988; Murante et al., 1998; Waga et al., 1994) we wondered if URI-1 functionally complements the *C. elegans* FEN-1 homologue (*crn-1*), or acts in a parallel pathway in BER and replication to *crn-1*. Reactive oxygen species (ROS) and methyl methanesulfonate (MMS) are known to stimulate (for review see (Barzilai and Yamamoto, 2004)). BER is a major repair mechanism for endogenous DNA damage such as uracil residues in DNA, apurinic/apyrimidinic AP sites and oxidative damage (for review see (Barzilai and Yamamoto, 2004)).

ROS such as O_2^-, H_2O_2 and OH^-, are generated during cellular metabolism, especially during mitochondrial energy production (Fridovich, 1995). These ROS in turn cause oxidative damage to DNA (Beckman and Ames, 1997) and therefore represent a source of endogenous DNA damage. Oxidative damage in DNA is repaired primarily via the BER pathways, which appears to be the simplest of the three excision repair pathways (for review see (Barzilai and Yamamoto, 2004)). Thus, mutants suffering from an increase of endogenous ROS production or of components of the BER pathway would be expected to have a natural sensitivity to ROS inducing agents. The herbicide paraquat (methyl viologen) is commonly used to generate oxidative stress *in vivo*. It is metabolically reduced to a stable paraquat radical (PQ^+) in a NAD(P)H-dependent reaction catalyzed by NADPH-cytochrome P-450 reductase. The paraquat radical in turn reduces molecular oxygen, producing the superoxide radical (O_2^-), which inflicts cellular injury by damaging biological macromolecules (Bagley et al., 1986; Bus et al., 1976; Chan and Weiss, 1987; Shull et al., 1991). Therefore, the response of URI-1 deficient worms to oxidative stress was tested by treating *uri-1(RNAi)*P0; *uri-1* mutants and control RNAi treated wild type worms with several doses of paraquat. As the development of *C. elegans* is inhibited by paraquat (Hartman et al., 1995), growth delay was monitored in two genotypes. These

assays revealed that *uri-1(RNAi)*P0 *uri-1* mutants do not show a statistically significant difference to wild type in sensitivity to ROS (Figure 29), suggesting that URI-1 deficiency does not cause defects in the pathways that detoxify ROS or that mediate repair of ROS-induced DNA lesions.

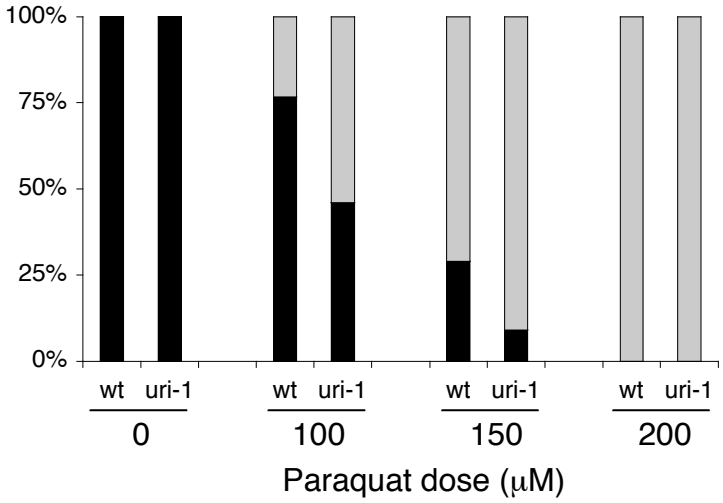

Figure 29. Comparative analysis of paraquat sensitivity.; *uri-1* mutants treated with *uri-1(RNAi)*P0 (uri-1) and wild type (wt) L1 larvae were cultured on NGM agar containing 0.2 mM paraquat. The survival and growth delay of the indicated genotypes was scored by counting the frequency of adult (black bars) and L4 (grey bars) worms after 4 days at 20°C. Approximately 40 animals were scored for each strain. No lethality was observed for any strain. The slight growth delay observed for *uri-1,uri-1(RNAi)*P0 mutants was not statistically significant.

The major endogenous source of ROS is oxidative metabolism in the mitochondria (for review see (Barzilai and Yamamoto, 2004)). Mutant worms with mitochondrial defects have altered mitochondrial morphology, consistent with defective mitochondrial function (Lee and Ruvkun, 2002). As defective mitochondrial function has the potential to endogenously damage DNA and human URI co-localizes with mitochondria (personal communication Nabil Djouder) we wondered if URI-1 plays a functional role at mitochondria. Therefore, we investigate the effect of URI-1 on mitochondrial morphology (as a readout of mitochondrial function) by performing *uri-1(RNAi)*F1 and control RNAi in transgenic animals carrying a *myo-3* promoter driven mito::GFP construct (Labrousse et al., 1999). The body wall muscle of wild type adult worms show tubular mitochondrial matrix that often runs parallel to the myofibrils (Labrousse et al., 1999). Wild type and *uri-1(RNAi)*F1 animals displayed similar mitochondrial patterns suggests that URI-1 does not affect mitochondria morphology and likely does not interfere with mitochondrial function in adult *C. elegans* muscle cells. From these data, and the fact that URI-1 reduction leads to the activation of the DNA damage-mediated germ line cell death pathway and oxidative damage is believed to be transmitted via the physiological germ cell death pathway

(Navarro, R., Poster 1218 15th International *C. elegans* Meeting), we conclude that DNA damage induced by URI-1 depletion is unlikely to result from increased endogenous ROS production or from a requirement for URI-1 in the BER pathway.

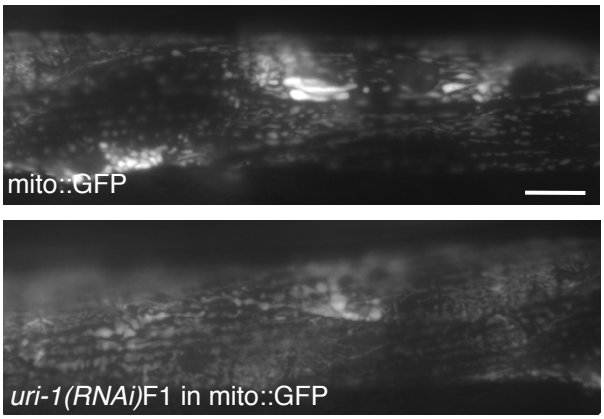

Figures 30. Mitochondrial morphology in *C. elegans* muscle cells. The effect of *uri-1* depletion was detected in transgenic animals expressing mito::GFP with the *myo-3* promoter (Labrousse et al., 1999). Muscle cells usually have tubular mitochondria that run parallel with the body axis (wild type). Depletion of *uri-1* by RNAi does not disrupt mitochondrial morphology. Scale bar 10 μm.

4.5.1.2 Does depletion of URI-1 cause sensitivity to methyl methanesulfonate (MMS)?

Consistent with a role for RAD27 in BER, inactivation of RAD27 results in a severe sensitivity to MMS (Johnson et al., 1995; Reagan et al., 1995; Sommers et al., 1995).
MMS is a SN2 methylating DNA-damaging agent that leads to DNA strand breaks arising from collision of replication forks with MMS-induced alkylation (for review see (Nyberg et al., 2002)). The cytotoxic effect of MMS on wild type animals was compared to heterozygous *uri-1; uri-1(RNAi)*P0 animals. Both strains exhibited a similar growth arrest response to MMS, indicating that the persistence of cytotoxic repair intermediates that are formed during the processing of methylated DNA bases or abasic site can be equally repaired in both strains. That results argue against a role of URI-1 in mismatch repair (MMR) and BER, which are the two main pathways that repair the kind of damage generated by MMS (for review see (Nyberg et al., 2002)).

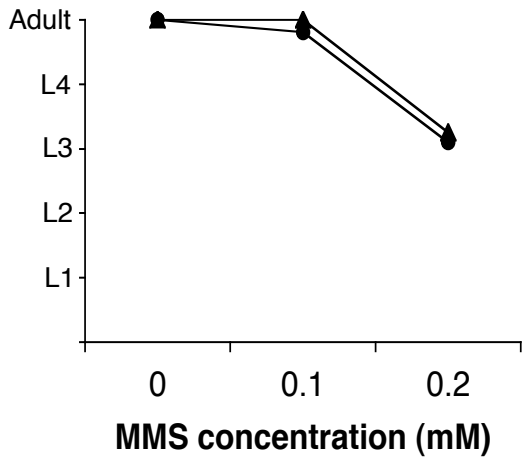

Figure 31. Effect of *uri-1* depletion on MMS induced cytotoxicity. Wild type and *uri-1; uri-1(RNAi)*P0 L4 larvae (n=20) were exposed to chronic increased concentrations of MMS and their progeny were subsequently scored for stage of arrest 5 days after treatment at 20°. The terminal developmental stage attained by wild type (●) and *uri-1 uri-1(RNAi)*P0 (▲) animals is shown.

4.5.1.3 Does depletion of URI-1 cause sensitivity to γ-irradiation?

Double strand breaks occur normally during meiotic prophase to initiate meiotic recombination events (Roeder, 1997). In eukaryotes, DNA double-strand breaks, which are also induced by γ-irradiation, are repaired by the concerted action of two mechanisms, error-prone non-homologous end joining (NHEJ) and homologous recombination repair (HHR), based on homologous recombination between sister DNA molecules (for review see (Khanna and Jackson, 2001)). Comparison of the γ-irradiation sensitivity of *uri-1* depleted and control animals reveals that *uri-1* depleted animals exhibit wild type behavior in terms of hatching efficiency and mitotic cell cycle arrest induction (Figure 32), suggesting that URI-1 is not a component of HRR or NHEJ.

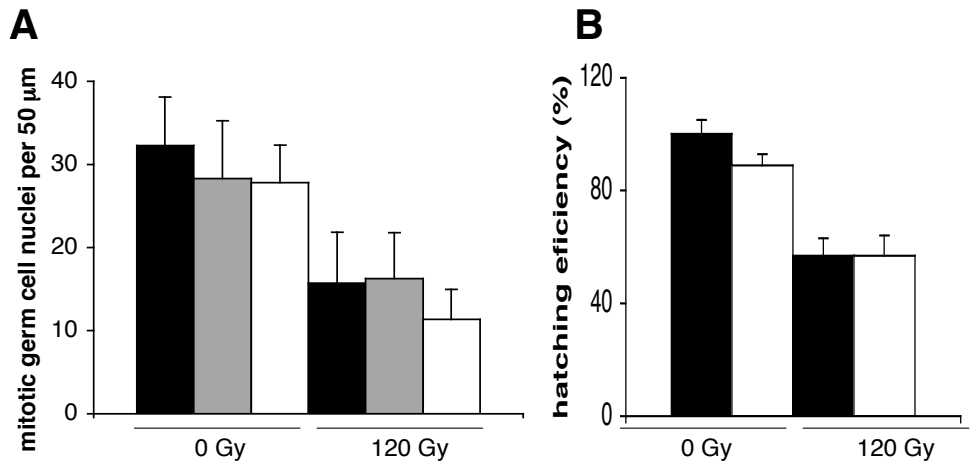

Figure 32. Response of wild type and *uri-1* depleted animals to γ-irradiation. (A) Radiation-induced cell cycle arrest of mitotic germ cells was scored as mitotic germ cell enlargement 8 after γ-irradiation (120 Gray) in wild type (black bars), *uri-1* mutant (grey bars) and *uri-1, uri-1(RNAi)*P0 (white bars) as L4 larvae. Error bars indicate std. dev. (B) Hatching efficiency was scored as the percentage of surviving embryos laid after irradiation of the mothers with the indicated dose of gamma irradiation. Error bars indicate std. dev.

4.5.1.4 Does depletion of URI-1 cause sensitivity to UV irradiation?

Depending on whether the modified base is removed as a free base or as an oligonucleotide, excision repair is divided into two major mechanisms, BER and nucleotide excision repair (NER), respectively. The highly conserved NER eliminates many bulky DNA lesions including 6-4 photoproducts and cyclobutane pyrimidine dimers, generated by UV light by two related sub-pathways (for review see (Lindahl and Wood, 1999)). While general global genome repair (GGR) removes DNA damage from the entire genome, cells also have a more specialized transcription-coupled repair (TCR) pathway that corrects DNA lesions located on the actively transcribed strand (Mullenders and Berneburg, 2001). NER pathways can be conceptually divided into five biochemical steps: damage recognition, incision, excision, repair synthesis and DNA ligation. The biological consequences of NER defects are apparent from the inherited multi-system disorders xeroderma pigmentosum (XP), trichothiodystrophy and Cockayne syndrome that are characterized by hyper-photosensitivity and a wide spectrum of neuro-developmental abnormalities. XP patients show in addition a high incidence of UV-related skin cancers (for review see (Berneburg and Lehmann, 2001)). Comparison of the UV sensitivity of *uri-1* depleted and control animals reveal that *uri-1* depleted animals show a modest sensitivity to high UV dose (Figure 33). The modest hypersensitivity indicated a role for URI-1 in repair, replication and/or chromatin remodeling (for review see (Lindahl and Wood,

1999)). This result is consistent with the genetic interaction of the *S. cerevisiae* URI-1 homolog with RAD27, as inactivation of RAD27 also results in a modest sensitivity to UV in yeast. However, *S. cerevisiae* RAD27 is not a member of the NER epistasis group, but rather falls into the epistasis group of genes that are involved in DNA damage tolerance and mutagenesis (RAD6) (Reagan et al., 1995). Thus, URI-1 may be involved in DNA damage tolerance.

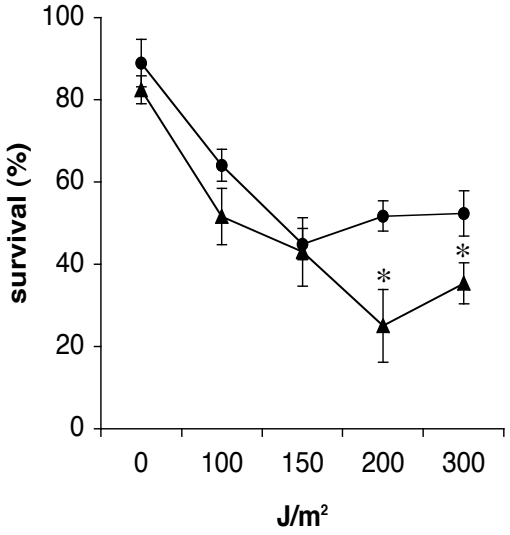

Figure 33. Hypersensitivity of *uri-1* depleted animals to UV irradiation. Heterozygous *uri-1* mutant animals fed on *uri-1(RNAi)* (▲) and control animals (●) were UV irradiated at the L4 larval stage with the indicated dose. F1 embryos laid during the time period of 24-36 hrs after the UV irradiation were scored for hatching efficiency revealing that *uri-1* depleted animals are hypersensitive to high dose of UV irradiation. Error bars indicate std. dev. and * represents $p < 0.05$ (Students t-test).

4.5.1.5 Is URI-1 involved in recombination and replication?

The *C. elegans* homologue of the yeast DSB-generating enzyme Spo11p (sporulation 11) is required for meiotic recombination in the nematode (Dernburg et al., 1998). As depletion of *uri-1(RNAi)*F1 in the *spo-11* background at 25°C does not rescue the small germ line phenotype of *uri-1* (data not shown) this phenotype seems not to depend on active recombination. Moreover, a common phenotype for mutation of genes which mediate recombination in *C. elegans* is an increase frequency of spontanous generated males in the population (Dernburg et al., 1998; Takanami et al., 2000), a phenomenon not seen with *uri-1* depleted animals. Thus URI-1 does not appear to play a role in recombination.

To get a first indication if URI-1 functions in replication, the sensitivity to camptothecin was assayed. The genotoxin camptothecin inhibits the release of DNA topoisomerase I

from DNA, leaving a single-strand break. When a DNA replication fork collides with this complex, the single-strand break is converted to a DSB. Thus, active replication is required to generate camptothecin-induced DSBs and results in cytotoxic effects during S phase. This is in contrast to irradiation that induces breaks during all cell cycle phases (for review see (Pizzolato and Saltz, 2003)). Thus, active replication is required for the toxicity of camptothecin. In *C. elegans*, camptothecin induces embryonic lethality and a strong cell cycle arrest (van Haaften et al., 2004). As heterozygous *uri-1;uri-1(RNAi)* mutants and wild type animals show a comparable sensitivity to camptothecin (Figure 34) we conclude that replication is not blocked in the *uri-1* mutant and that *uri-1* is not involved in the repair of collapsed replication forks.

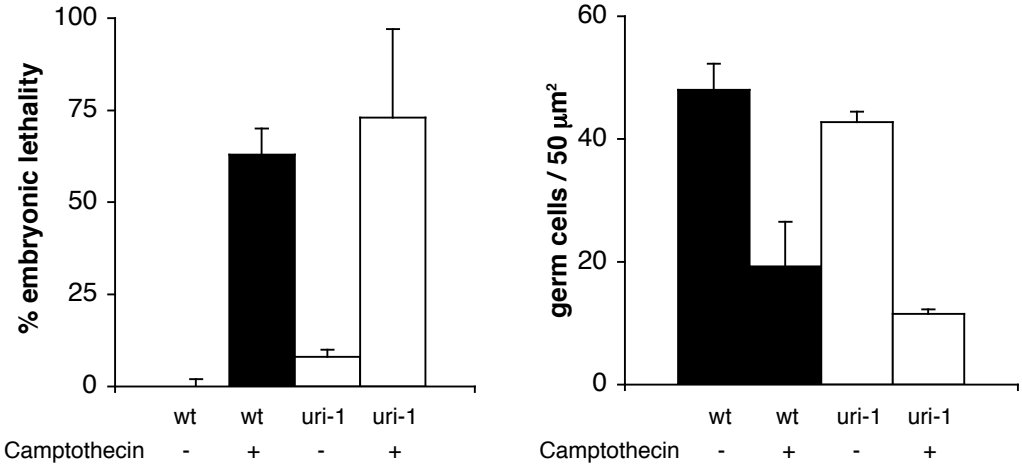

Figure 34 . Sensitivity of *uri-1* mutants to DNA damage generated by camptothecin. (A) Worms were treated with 0.14 mM camptothecin and the percentage of embryonic lethality of the F1 progeny was determined as described above. Error bars indicate std. dev. (B) Camptothecin induces cell-cycle arrest in *C. elegans*. Staged heterozygous *uri-1; uri-1(RNAi)*P0 and wild type animals treated with 0.14 mM camptothecin for 2 hrs show fewer germ cell nuclei and the size of their nuclei and cytoplasm becomes greatly enlarged. Error bars indicate std. dev.

4.5.1.6 Is URI-1 involved in chromatin remodelling?

Given that URI has been implicated in chromatin remodeling in human cells and shown to regulate the activity of the transcription factor E2F in *Drosophila* (personal communication Yandong Shi) we decided to test whether the germ line phenotype observed in *uri-1* depleted animals might reflect a role of URI-1 in chromatin remodeling. Interestingly, the *C. elegans* E2F homolog *efl-1* (E2F-like), together with several chromatin-remodeling factors, have been implicated in the repression of ectopic vulval cell fate induction (Boxem and van den Heuvel, 2002; Ferguson and Horvitz, 1985; Ferguson et al., 1987). In *C. elegans* the vulva is derived from the descendants of three out of six equivalent vulva

precursors cells (VPCs), P5.p, P6.p and P7.p (Fay and Han, 2000). The activity of the EGF receptor-Ras-MAP kinase signaling pathway is responsible for inducing the P(5-7).p cells to adopt a vulval fate by overcoming inhibitory signals from synthetic multivulva genes (synMuv). On the basis of genetic interactions, the synMuv genes have been grouped into two functionally redundant classes, A and B. Animals with loss-of-function mutations in both a class A and class B gene show multivulvae (Muv) because P3.p, P4.p and P8.p adopt induced vulval fates, while mutants in a single gene or genes of a single class are non-Muv (for review see (Ferguson and Horvitz, 1989)). The class B synMuv genes have been shown to encode orthologues of proteins that interact physically or functionally with Rb, including E2F, histone deacetylases, as well as components of the NuRD (nucleosome-remodeling and histone deacetylase) and other chromatin remodeling complexes and have been proposed to remodel chromatin and repress transcription of genes important for vulval cell fate specification and during cell cycle progression (Ahringer, 2000; Ceol and Horvitz, 2001; Harbour and Dean, 2000; Lu and Horvitz, 1998; Solari and Ahringer, 2000). Recently, a class C synMuv gene class has been found, formed among others by the putative *C. elegans* TIP60 histone acetyltransferase and the homologue of the mammalian SWI/SNF family of ATPase p400 (Ceol and Horvitz, 2004). Given that URI-1 interacts genetically with the Drosophila E2F homolog (|personal communication Yandong Shi) we decided to test genetically if *uri-1* is a synthetic multivulva (synMuv) gene. However, *uri-1(RNAi)*F1 in neither the synMuv class A, B nor C backgrounds produced a synMuv phenotype at 25°C (Table 4). Consistent with this result, the *C. elegans* homologue RUVBL-1, which is found in mammalian TIP60 histone acetylase complexes and the URI complex (Feng et al., 2003; Gstaiger et al., 2003; Ikura et al., 2000) does not show a synthetic interaction with class B mutations (Ceol and Horvitz, 2004).

Genotype	Penetrance of Muv phenotype (%)
lin-15A(n767)	0 (n=30)
lin-15A(n767); uri-1(RNAi)	1 (n=30)
lin-15B(n744)	0 (n=30)
lin-15B(n744); uri-1(RNAi)	0 (n=30)
trr-1C(n3630)	0 (n=30)
trr-1C(n3630); uri-1(RNAi)	0 (n=30)

Table 4. Analysis of genetic interactions between *uri-1* and synMuv class A, B and C genes. The penetrance of the Muv phenotype of each strain was determined at 25°C after growth for two generations. The efficiency of *uri-1(RNAi)*F1was tested on a parallel wild type plate. To analyze the Muv phenotype, L4 larvae and adults worms of the indicated genotypes were scored for the presence of pseudovulval invaginations. Note that strain n767 exhibit a slow growth phenotype.

5 Discussion

The data presented here using *C. elegans* as a model provide the first functional characterization of a URI homologue in a multicellular organism. The *C. elegans* genome contains a single homologue of mammalian URI, which has been previously implicated in nutrient signaling via the insulin-sensitive branch of the TOR signaling pathway and shown to assemble in a ~ 1 MD multiprotein complex termed the URI complex (Gstaiger et al., 2003). We provide biochemical evidence that an URI-like complex exists in *C. elegans*, comprising the *C. elegans* homologues of the mammalian URI complex, namely URI-1, PFD-2, RPB-5, STAP-1, RUVB-1 and RUVB-2. Strikingly, the mammalian and *C. elegans* components of the URI complex are able to bind one another, demonstrating the extremely high degree of evolutionary conservation of this complex. Consistent with the idea that the identified members of the *C. elegans* URI-1 complex may function together, northern blot analysis revealed that their expression profiles are developmentally co-regulated, with a striking upregulation at the adult stage, suggesting a functional role for the URI-1 complex in the adult worm.

In this respect, *uri-1* encodes a germ line-enriched transcript both at the RNA and the protein level. The generation of polyclonal antibodies to URI-1 revealed that URI-1 is expressed in the mitotic as well as in the meiotic part of the germ line, including sperm and oocytes, as well as in the embryo in a cytoplasmic, membranous and nuclear manner depending on the antibody and fixation condition used. Thus, only one of the C-terminal antibodies (#18) recognizes URI-1 in formaldehyde–based whole worm preparations sex-independently during the whole process of spermatogenesis in a punctuated cyptoplasmic manner. The labeled structures in the sperm are likely to represent structural proteins like myosin, spectrin, and/or actin or maybe mitochondria. Interestingly, mammalian URI-1 colocalizes with mitochondria (personal communication Nabil Djouder) and binds myosin and actin (personal communication Matthias Gstaiger) providing good candidates for co-localization attempts. As URI-1 belongs to the PFD family of molecular chaperones which have been implicated in the *de novo* folding of actin and tubulin (for review see (Hartl, 1996)) it is possible that URI-1 detected by the C-terminal α-URI-1 antibody #18 represents the portion of URI-1 involved in folding or protein stabilization.

Using a methanol-based staining procedure, all four α-URI-1 antibodies recognize the same tissues, namely the mitotic and meiotic part of the germ line, including both kinds of gametes, as well as embryos, but with variations in their sub-cellular staining pattern. The C-terminal α-URI-1 antibodies recognize mainly the cytoplasmic portion of URI-1 with occasional recognition of membranous and nuclear URI-1, whereas the N-terminal α-URI-1 antibodies recognize mainly the nuclear portion with fainter cytoplasmic staining and occasional detection of membranous URI-1. These variations could be due to small alterations in the fixation procedure like strength of squeezing. Alternatively, the variations may be accounted for by masking of the antibody epitope or for other reasons of inaccessibility of the antibody to the antigen. As URI-1 is believed to assemble in a multiprotein complex via its N-terminal domain it is tempting to speculate that URI-1 functions as a prefoldin in the cytoplasm, in particular because the tips of the individual α-helices of PFDs are known to be involved in protein-protein interactions with their substrate and the N-terminal α-URI-1 antibodies are raised exactly against the N-terminal tip of the α-helix of URI-1. Thus, the faint detection of URI-1 by the N-terminal α-URI-1 antibodies in the cytoplasm could be due to the fact that only the substrate-unloaded portion of URI-1 can be recognized by the N-terminal antibodies as the interaction of the substrate with the N-terminal epitope may prevent antibody binding. Respectively, the C-terminal antibodies may mainly recognize cytoplasmic URI-1 because of the involvement of the C-terminus of URI-1 in nuclear processes that exclude the α-URI-1 antibodies from the URI-1 epitope. Generation of a GFP-tagged URI-1 expressing transgenic strain would help to resolve this issue. Mapping of the URI-1 binding sites of known URI-1 binding partners would allow the dissection of URI-1 functions via its protein domains. As the specificity of the C-terminal α-URI-1 antibody #17 has been proven on western blot as well as the specificity of the C-terminal α-URI-1 antibody #18 in immunofluorescence, and since all four α-URI-1 antibodies recognize the same structures and the same sub-cellular localization of URI-1, even if to a different extent, these α-URI-1 antibodies are very likely to be specific for URI-1.

Interestingly, the N-terminal α-URI-1 antibodies show a cell cycle dependent nuclear localization pattern in *C. elegans* embryos, being excluded from the DNA when the nucleus disassembles during late prophase until anaphase. URI-1 could bind structures in the nucleus, which disassemble during late prophase and telophase, explaining the diminishing of the staining during these cell phases. In this respect it is interesting that a

prometaphase block is seen in *uri-1* depleted mitotic germ cells. The failure of URI-1 detection during this cell cycle phase could alternatively be accounted for by inaccessibility of URI-1 at that time to the α-URI-1 antibody because of the high condensation state of the DNA or masking of the N-terminus of URI-1 by a bound protein or proteins. The data in this thesis also shows that URI-1 is expressed ubiquitously during embryogenesis and throughout the germ line. This may reflect a general role for URI-1 in proliferation, as the embryo and the germ line are the structures with the highest proliferation dynamics in the worm.

C. elegans URI-1 colocalizes with germ line-specific P-granules in the embryo and the germ line and therefore may represent a constitutive component of these structures. Previous results functionally linked the mammalian and yeast URI homologue to nutrient signaling via the TOR cascade. In this respect it is interesting to note that the *C. elegans* homologue of mammalian eIF5A and the mRNA cap-binding protein and regulator of translational initiation eIF4E are also components of P-granules (Amiri et al., 2001; Hanazawa et al., 2004). The *C. elegans* homolog of eIF4E (IFE-1) is also germ line-enriched and required for spermatogenesis, in both hermaphrodites and males. eIF-5A has been proposed to regulate steps subsequent to translation initiation, or to participate in mRNA degradation (Ganoza et al., 2002; Zuk and Jacobson, 1998). The *C. elegans* homologue of eIF-5A (IFF-1) is sterile, exhibiting an underproliferative germ line resulting from impaired mitotic proliferation in both sexes. Several genes have been identified to encode protein components of P-granules, such as *pgl-1*, *glh-1*, *glh-2*, *glh-3* and *glh-4* that are found on P-granules at all stages of the *C. elegans* life cycle and are required for postembryonic development of the germ line similarly to eIF4E, eIF5A and URI-1 (Gruidl et al., 1996; Kuznicki et al., 2000). Inhibition of transcription or mRNA export in the adult germ line rapidly disrupts the integrity of perinuclear P-granules suggesting functions for these granules related to translational regulation, RNA delivery and/or stability (Amiri et al., 2001). Consistent with a function in translational regulation, analyses of the *in vivo* function of URI-1 revealed that depletion of *uri-1* also leads to multiple germ line defects, in particular impaired spermatogenesis and mitotic proliferation, pointing to the possibility that URI-1 could play role in translational control and/or RNA transport in *C. elegans*. An attractive scenario is that URI-1 regulates multiple aspects of germ line development by controlling the translation of multiple germ line RNAs. This is particularly interesting because the activity of eIF4E is regulated via its association with 4E-BPs, which when bound to eIF4E prevent its binding to eIF4G, thereby inhibiting translation initiation.

Given that 4E-BPs and URI are regulated by the insulin-sensitive TOR signaling pathway, we wondered if URI-1 would be a conserved component of this pathway. Therefore, we tested if depletion of *uri-1* would phenocopy the depletion of known players of the CeTOR and/or insulin/IGF-I-like (*daf-2*) signaling pathway. We discovered that URI-1 is not involved in regulation of longevity, heat tolerance, stress tolerance, nor does it phenocopy the intestinal phenotype of CeTOR depletion, all established functions of the *daf-2* and/or CeTOR signaling pathways (Lithgow et al., 1995; Long et al., 2002; Vellai et al., 2003; Wolkow et al., 2000). Nevertheless, we noted that *uri-1* mutant animals share certain features with the CeTOR and *daf-2* mutants, such as reduced fertility and viability. Moreover, *uri-1* and CeTOR depleted animals are sensitive to applied pressure and show an L3 larval arrest. Strong inhibition of mitochondrial respiration and inhibition of mitochondrial DNA replication also leads to a development arrest at the L3 larval stage suggesting that the L3 to L4 is likely to represent a large energy-demanding step in development and may involve an energy-sensing regulatory mechanism (Dillin et al., 2002b, Tsang, 2002 #911).

At 25°C homozygous *uri-1* animals exhibit a L3 larval arrest, but no formation of dauer larvae. Depletion of *uri-1* in the temperature sensitive *daf-2* mutant background failed to increase the incidence of dauer formation, in contrast to depletion of CeTOR (Jia et al., 2004). Moreover, in the case for CeTOR and *C. elegans* raptor (*daf-15*) the L3 larval arrest has been characterized as dauer-like arrest (Jia et al., 2004). Formation of partial dauers (defined as animals mosaic for dauer and nondauer phenotypes) is a hallmark of mutations in the *daf-2* pathway (Vowels and Thomas, 1992). Electron microscopic observation of *daf-15* demonstrates that head shape, cuticle and intestinal ultrastructure are non-dauer whereas sensory structure and excretory gland morphology are intermediate between that of dauer and nondauer stages and feeding is not completely suppressed (Jia et al., 2004). As inhibition of TOR activity induces autophagy in yeast and mammalian cells (for review see (Schmelzle and Hall, 2000)), this function could be conserved in *C. elegans*. Recently, autophagy has been shown to be required for dauer morphogenesis as RNAi directed against autophagy genes renders constitutively formed *daf-2* dauer larvae incapable of completing morphogenesis (Melendez et al., 2003). This suggests that autophagy may be induced in *daf-15* and CeTOR mutants, maybe preventing activation of essential dauer functions, and thus inducing the partial dauer phenotypes of these mutants (Jia et al., 2004). It would be interesting to perform electron microscopic analysis of the L3 larval

arrest phenotype of *uri-1* depleted worms to determine if they also display partial dauer phenotypes.

It became evident during this study that URI-1 is not likely to be a component of the insulin/IGF-I like signaling pathway in *C. elegans*. This is perhaps not surprising as the activities of TOR do not seem to be as highly conserved in *C. elegans* as they are between yeast, flies and mammals. For example, depletion of the *C. elegans* S6K homologue does not exhibit any of the phenotypes caused by CeTOR deficiency, no homologue of 4E-BP1 has been identified in the *C. elegans* genome and *C. elegans* has a natural resistance against rapamycin (Long et al., 2002). Thus, while *C. elegans* may not be the best model system to map the position of *uri-1* in the TOR signaling pathway it provides the opportunity to uncover new functions of URI-1, and possibly of TOR, that may also be conserved in other organisms.

Here we have investigated the *in vivo* function of URI-1 in *C. elegans*. Depletion of *uri-1* by mutation or RNAi causes somatic defects including protruding vulva, rupture, molting defects, embryonic lethality and a L3 larval arrest. The pvl phenotype, a characteristic for cell division defects, is believed to reflect aberrant proliferation kinetics as depletion of the homolog of the cyclin-dependent kinase inhibitor p27 (*chi-1)* and several null mutants of other cell cycle genes including cyclin D, cyclin E, cdk-1 and cdk-4 exhibit a pvl phenotype (Boxem and van den Heuvel, 2001; Fay and Han, 2000; Kostic et al., 2003; Sasagawa et al., 2003). The rupture phenotype seen in *uri-1* depleted animals may reflect the terminal phenotype of the pvl-causing defect and is consistent with the idea that URI-1 is necessary for cell proliferation.

Mutations in *uri-1* are pleiotropic in nature, likely reflecting that it is a multifunctional gene. Depletion of *uri-1* also causes multiple germ line defects e.g. path finding defect. Specifically, we found that *uri-1* homozygous animal develops into sterile adults with a small germ line. This phenotype is due to a severe defect in cell proliferation. Consistent with the effect on cell proliferation we observe a cell cycle block, which appears to be due to DNA damage. In addition, the meiotic arrest observed in developing sperm could also be the result of DNA damage, representing an alternative readout of DNA damage signaling pathways. Finally, DNA damage-induced p53-mediated apoptosis is enhanced in the heterozygous mutant. Taken together these results point to a participation of URI-1 in one or more cellular processes, which when deregulated lead, directly or indirectly, to

DNA breaks, which in turn, cause an arrest of cell cycle progression. This would account for the decreased cell proliferation and small germ line in the homozygous *uri-1* mutant and the observed apoptosis in the heterozygous *uri-1* mutant (see model in Figure 35). The fact that the *C. elegans* p53 homologue participates in a conserved signaling pathway in response to DNA damage suggests that p53-dependent gla genes such as *uri-1* will be involved in the maintenance of genome stability (Hofmann et al., 2002).

Consistent with the model that DNA damage is the causative factor of the *uri-1* loss-of-function phenotype, the combined mutation of the *C. elegans* RecQ homolog *him-6* with *top3*α (Kim et al., 2002c) also shows DNA breaks and a small germ line phenotype similar to *uri-1* mutants. In addition, we find that γ-irradiation at the L2/L3 larval stage in the *rad-51* mutant, which cannot repair γ-irradiation-induced DNA damage, results in development of sterile adults with small germ lines. Inactivation of checkpoint genes such as *mre-11, mrt-2, hus-1, atm-1, rad-51, wee-1, cep-1* or *chk-2* failed to rescue the small germ line phenotype of *uri-1* mutants. Thus, it is possible that loss of URI-1 causes multiple types of DNA lesions, requiring the concerted action of multiple pathways. Given that an efficient rescue of the mitotic germ cell block in *uri-1* deficient germ lines may not result in increased proliferation or appearance of oocytes, but rather in increased apoptosis, as the damaged cells may progress mitosis but then undergo apoptosis, further rescue attempts should be performed in an apoptosis-resistant strain. It is also possible that, in addition to a role in the generation or repair of damaged DNA, URI-1 is involved in the recovery from DNA damage, which involves disassembly of the cell cycle checkpoint and recombination apparatus (Lisby et al., 2003). A role of URI-1 in this process would provide an alternative explanation for the failure of *uri-1* depleted animals to recover from checkpoint-mediated arrest by eliminating checkpoint genes.

How could URI-1 ensure DNA stability? The amount of DNA breaks present in the *uri-1(RNAi)*F1 germ cells (detected with HUS-1::GFP) is comparable to wild type worms treated with low dose (5-10 gray) of γ-irradiation (Hofmann et al., 2002) highlighting the severity of the endogenous damage caused by the loss of URI-1. Induction of HUS-1::GFP foci formation suggests that sensing of DNA damage is still functional in URI-1 deficient animals (Bermudez et al., 2003; Hofmann et al., 2002). Corroborating this is the fact that the DNA damage-induced cellular responses, including inhibition of mitotic cell cycle progression and p53-dependent apoptosis are functional in *uri-1* mutants. Therefore sensing, transduction and execution of DNA damage signals are functional in URI-1

depleted worms. Thus, it is more than likely that URI-1 is involved in preventing and/or repairing endogenous, genotoxic DNA damage to maintain genome integrity. The 9-1-1 complex is loaded onto chromatin in response to many different genotoxic stresses, including UV and stalled replication forks, suggesting that the complex plays a role in the cellular responses activated by many types of DNA damage (for review see (Parrilla-Castellar et al., 2004)). Interestingly, *uri-1* depleted animals are hypersensitive to high doses of UV irradiation, suggesting that UV-mediated damage triggers the defect that is caused by loss of *uri-1* function. This would be consistent with a role for URI-1 in a recombination-dependent process like replication and repair (review see (Friedberg et al., 1995)).

Endogenous DNA breaks can arise for example from replication errors, repair intermediates, and alterations in chromatin remodeling, generating fork structures, bubbles, Holliday structures, and other nonduplex DNA forms, possibly providing high affinity binding sites for repair and/or checkpoint proteins (for review (Abraham, 2001; Koundrioukoff et al., 2004; Lindahl and Wood, 1999; Osborn et al., 2002; Sancar et al., 2004)). Thus, the low mutation rate observed in wild type organisms is not a consequence of intrinsically accurate DNA replication but instead reflects the existence of mechanisms that are capable of removing DNA polymerase errors (for review see (Umar and Kunkel, 1996)). More DNA breaks arise in rapidly proliferating cells than in slowly proliferating or resting cells, potentially explaining why the two most rapidly dividing cellular compartments in *C. elegans* (embryo and germ line) are affected by loss of URI-1. Interestingly, *S. cerevisiae rad27* (Tong et al., 2001) is synthetically lethal with the *S. cerevisiae* orthologue of *uri-1* (*bud27*) (Reagan et al., 1995). The human orthologue of *rad27*, the potential cancer susceptibility gene human flap endonuclease 1 (FEN1) (Harrington and Lieber, 1994; Lieber, 1997; Stillman, 1989), is known to play a role in maintaining genetic stability in eukaryotic genomes (for review see (Henneke et al., 2003; Kucherlapati et al., 2002)). It is also known to function in DNA repair (BER, NIR, HR and NHEJ) (Ishchenko et al., 2003; Klungland and Lindahl, 1997; Lieber, 1997; Tishkoff et al., 1997; Wu et al., 1999b) and DNA replication, two processes essential for proper proliferation.

Several links between DNA repair, replication and chromatin remodeling have been established (Morrison and Shen, 2005; Shen et al., 2000). Chromatin is intimately involved in many DNA transactions, including transcription, replication, repair and recombination,

and any event impairing the stability of chromatin structure is likely to compromise DNA metabolism and genome integrity (for review see (Koundrioukoff et al., 2004)). For example PCNA has been shown to be involved in chromatin remodeling, replication and repair (for review see (Majka and Burgers, 2004)). Interestingly, human and *C. elegans* URI are part of a multi-protein complex that contains, among other proteins, the ATPases TIP48 and TIP49 (Gstaiger et al., 2003) which are established components of several chromatin remodeling complexes including the human hTIP60 HAT complex (Frank et al., 2003). Moreover, our lab recently showed that URI-1 binds a component of the Paf1 complex in human cells, which is important for histone modification and cell cycle control (Yart et al., 2005). The co-activator Paf1 complex is recruited, among others, by Gcn4p *in vivo* (Swanson et al., 2003), and Gcn4p requires the Paf1 complex for full activation (Swanson et al., 2003). The chromatin remodeling complex SWR-C, which is involved in chromatin modification and transcriptional elongation by Paf1 complex components, displays genetic interactions with genes encoding prefoldin subunits (Krogan et al., 2003). Hence, it is tempting to speculate that URI serves a chaperone function within the Paf1-linked multiprotein complex. That URI is also a target of regulation by the TOR and PI3K pathways raises the intriguing possibility that URI- Paf1 complexes may be transcriptional endpoints of nutritional and growth factor cues. Consistently, mutations of the human Paf1 complex component Parafibromin is associated with the pathogenesis of hereditary hyper-parathyroidism-jaw tumor syndrome characterized among others by hamartomas (Carpten et al., 2002, Jackson, 1990 #717, Szabo, 1995 #718) and deregulated mTOR activity is associated with several hamartoma syndromes (Tsutsui et al., 2005).

Interestingly, URI-1 is required for germ line silencing (Kim et al., 2005). Many mutations that prevent silencing in the germ line also cause genome instability (Ketting et al., 1999). For example, depletion of the *C. elegans* orthologues of the Polycomb group (PcG) chromatin repressors MES-2, MES-3 and MES-6 lead to germ line degeneration and sterility (Capowski et al., 1991; Holdeman et al., 1998; Korf et al., 1998; Xu et al., 2001a). The MES complex is responsible for di- and trimethylation of histone H3 Lys27 in the adult germ line and in early embryos, which is believed to mark silenced chromatin in germ cells, providing a link between the sterility phenotype, genomic stability and germ line silencing (Bender et al., 2004; Plath et al., 2003). Transcriptional silencing, the regional inactivation of transcription, involves a specialized chromatin structure, termed silent chromatin, that impedes transcription, as well as other physiological DNA transaction, including initiation of DNA replication (Stevenson and Gottschling, 1999).

Considering that the yeast transcriptional activator Gcn4 recruits the Gcn5 histone acetylase complexes to specific promoters and thereby creates local domains of histone H3 hyperacetylation that subsequent facilitate transcriptional activation (Kuo et al., 2000), one could speculate that URI-1 participates in a similar mechanism to regulate Gcn4p target gene expression. Consistently, Gcn5p controls expression of many inducible genes, including those involved in amino acid biosynthesis (e.g. (Georgakopoulos and Thireos, 1992)). With this in mind, we hypothesize that URI-1 is either involved in modulation of chromatin and thereby regulates transcription or that URI-1 modulates transcription, which in turn regulates chromatin by upregulation of chromatin remodelers. Given these links, it is tempting to speculate that at least one function of URI-1 is dedicated to chromatin remodelling and/or replication and repair, potentially explaining the endogenous DNA damage seen in animals depleted of *uri-1* activity (see model Figure 35).

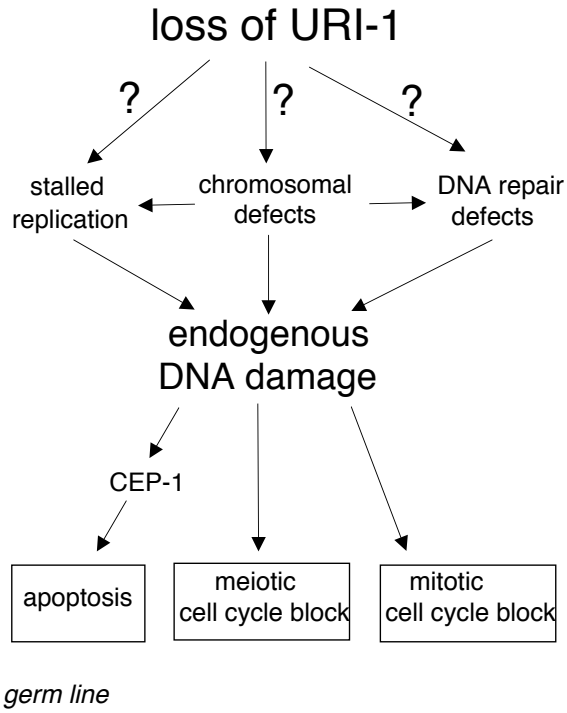

Figure 35. A simplified model of URI-1 function. DNA damage caused by deficiency of URI-1 affects germ cells by leading to proliferation arrest in the mitotic region and p53-dependent apoptosis in the meiotic part of the germ line. This phenotypes are consistent with reported read outs of the DNA-damage response (Stergiou and Hengartner, 2004, Deng, 2004 #76). Genetic and cell biological analysis show that URI-1 prevents DNA damage and the subsequent activation of the DNA damage signaling pathway by functioning directly or indirectly either in DNA damaging processes and/or their repair.

In mammalian and yeast cells, URI has been shown to play a central role in regulation of nutrient-sensitive, TOR-dependent gene expression programs. Interestingly a link between genomic stability and nutrient status has been suggested (Brunn et al., 1997; Chial et al.,

2000; Fiorentino and Crabtree, 1997; Gingras et al., 1999a; Kurz and Lees-Miller, 2004; Suzuki et al., 2003a; Suzuki et al., 2003b; Yang and Kastan, 2000). One of these reports shows that the yeast dna2 mutant, which shows all of the characteristics of cells blocked at the G_2/M border, can be rescued by the over-expression of the nutrient sensor Tor1p (Fiorentino and Crabtree, 1997). Also, *dna-2* is a player in cellular processes like germ line development and DNA repair in *C. elegans* (Lee et al., 2003a) and has been shown in yeast to play a role in DNA replication (Kao et al., 2004). Moreover, the *dna-2 mre-11* double mutant exhibits a small germ line phenotype similar to URI-1 (Lee et al., 2003a). Like TOR, mammalian ATM has been shown to be sensitive to the PI3K inhibitor wortmannin and to phosphorylate 4E-BP1 *in vivo* ((Brunn et al., 1997; Gingras et al., 1999a; Yang and Kastan, 2000) and for review see (Abraham, 2004)). Yeast Eap1p was reported to have a separate function from its eIF4E-binding in the maintenance of genetic stability (Chial et al., 2000). Glucose starvation and insulin treatment have the potential to induce DNA damage (Suzuki et al., 2003a; Suzuki et al., 2003b; Yang and Kastan, 2000). Moreover, stress responses like starvation cause mutations in *C. elegans* (for review see (Rosenberg and Hastings, 2004)). Finally, mutants of genes implicated in nutrient sensing, starvation and mitochondrial respiratory chain-deficiency in general display a L3 larval arrest (Long et al., 2002; Tsang et al., 2001), similar to the arrest observed in *uri-1* mutants, pointing to the possibility that the function of URI as a mediator of nutrient signals is conserved is *C. elegans.* The transition from L3 to L4, which entails an increase in mtDNA copy number, has been speculated to involve an energy-sensing checkpoint (Tsang et al., 2001) and is around the developmental time point at which the proliferation defect of URI-1 emerges. All these data suggest a possible link between nutrient status, DNA metabolism and DNA damage. In summary, our findings identify a novel role of URI-1 in the maintenance of DNA integrity by affecting directly or indirectly DNA metabolism. As DNA breaks are threatening for cells and bear a mutagenic potential, it will be interesting to test if this novel function of the evolutionarily conserved protein URI-1 is conserved in higher organisms. As the mammalian URI-1 orthologue co-exists in a biochemical complex with human PAF-1 complex, it will be interesting to test if URI-1 maintains DNA stability by affecting the state of chromatin. URI-1 may be a novel link between the epigenetic regulation of chromatin structure and genomic integrity.

6 Future prospects

An interesting linkage between DNA damage and TOR mediated nutrient signaling now becomes apparent (for review see (Proud, 2004) and (Fiorentino and Crabtree, 1997; Kumar et al., 2000; Natarajan et al., 2001; Suzuki et al., 2003a; Yang and Kastan, 2000)). Characterization of individual players of the DNA damage and TOR signaling pathways would lead to a better understanding of the connection between these two fundamental pathways. We contributed to the understanding of this link by establishing a role for *C. elegans* URI-1, whose homologues in *S. cerevisiae*, *Drosophila melanogaster* and mammalian cells have been clearly implicated in nutrient signaling via the TOR pathway, in the maintenance of DNA stability. It will be important to determine in future work whether this function of URI-1 represents a completely independent function of URI-1, or whether it suggests that the TOR pathway is linked to DNA stability.

From the data presented in this thesis it appears that the most likely scenarios of *C. elegans* URI-1 function in ensuring DNA stability are that URI-1 is an active component or modulator of the replication and/or repair machinery. This is best supported by the findings that *uri-1* depleted cells are hypersensitive to UV irradiation in *C. elegans*. Consistent with this, there is genetic evidence that the *uri-1* yeast homologue interacts with the endonuclease RAD27, homologue of the tumor suppressor gene encoding the flap endonuclease FEN-1 (Henneke et al., 2003). To further investigate whether *C. elegans* URI-1 functions in combination with *C. elegans* FEN-1 to mediate DNA repair, it would be interesting to test if URI-1 relocalizes upon DNA damage to sites of repair foci. Another possible mode of URI-1 action is suggested by the findings that *uri-1* has been implicated in the transcriptional regulation of GCN4 target gene expression in *S. cerevisiae*. It would therefore be interesting to test if this function is conserved in *C. elegans* particularly because GCN4 is known to regulate purine biosynthesis (Natarajan et al., 2001) and subsequently has the potential to interfere with replication. Thus, inhibition of GCN4 function due to URI-1 depletion may cause replication defects, potentially resulting in the observed DNA damage phenotype of *uri-1* deficient worms.

Recent work in our laboratory suggests that the *Drosophila* URI-1 homologue regulates the activity of the E2F transcription factor. E2F has been implicated in the DNA damage response, as well as in chromatin remodelling (Magnaghi-Jaulin et al., 1998; Stevens and

La Thangue, 2004). Interestingly, other proteins that physically interact with mammalian URI, such as TIP49 (Feng et al., 2003), DMAP1 (Robert et al., 2003; Robertson et al., 2000; Rountree et al., 2000) and the PAF1 complex (Krogan et al., 2003), have also been shown to affect chromatin remodeling. Since alteration in chromatin structure can lead to defects in DNA repair, replication, transcription and recombination (for review see (Bassal and El-Osta, 2005)) it is possible that URI-1 is required for correct chromatin remodelling, possibly through its function as a chaperone. Aberrent chromatin remodelling in the absence of URI-1 may therefore account for the DNA damage observed in *uri-1* mutants. Supporting the idea of a function of URI-1 in chromatin remodelling, a recent study demonstrated that *uri-1* and two additional genes that encode components of the URI-1 complex (*ruvb-1* and *ruvb-2*) are necessary for post-transcriptional gene silencing, through mechanisms such as heterochromatin formation and RNAi (Kim et al., 2005). Thus, it would be interesting to test whether *uri-1* depleted worms show abnormal sensitivity to chromatin remodeling agents (for review see (Kurz and Lees-Miller, 2004)). Additionally, the condensation state of chromatin in *uri-1* depleted worms could be directly monitored using antibodies that detect covalent modifications of histone that correlate with transcriptionally active chromatin (histone H4 acetylation at lysine^{5}) or as a marker for transcriptional elongation (histone H3 lysine^{4} and lysine^{79} methylation) (Reddy and Villeneuve, 2004). A role of URI-1 in chromatin remodeling has the potential to explain not only the role of URI-1 in DNA stability but also may provide the mechanism through which URI regulates the expression of GCN4 target genes in yeast. Consistent with this idea, in *S. cerevisiae*, GCN4 has been shown to modulate the promoter regions of its target genes by directing the coactivator complex SAGA to their promoter regions, which modulates chromatin structure via histone acetylation (Brown et al., 2001). We are just at the beginning of understanding the *in vivo* function of URI-1. Ongoing genetic, biochemical and cell biological studies in *S. cerevisiae*, *C. elegans*, *D. melanogaster*, mice and mammalian tissue culture will undoubtedly uncover more regulatory pathways in which URI functions. The unexpected findings of this study that URI-1 maintains genomic stability in *C. elegans* should be used to direct future research to investigate if this function is conserved in mammals, in particular with respect to the generation of cancer. Since the TOR signaling pathway and pathways that regulate DNA stability are strongly linked to human cancers and/or metabolic diseases, a better understanding of the key molecular players of these fundamental processes has the potential to identify novel drug targets for the treatment of a variety of widespread diseases.

7 Materials and Methods

Strains

Standard methods were used for the maintenance and manipulation of *C. elegans* (Brenner, 1974). Bristol strain N2 was used in this study as the standard wild type strain. The following additional strains were used: *uri-1(tm939), uri-1(tm939) dpy-5(e61)/dpy-5(e61) unc-14(e57)*, *dpy-5(e61) unc-14(e57)*, *atm-1*(gk186)*; uri-1*(tm939); *dyp-5(e61)/atm-1 (gk186*), *ced-3(n1286)*, *ced-4(n2273), ced-9(n1950)*, *gld-2(q497) gld-1(q485); unc-32(e189)*, *hus-1(op241); unc-119(ed3); opIs34, unc-119(ed3), glp-4(bn2)*, *fem-1(hc17)*, *fem-3(q20), glp-1(q231), mre-11(ok179/nT1[unc-?(n754) let-?], daf-2(e1370), mrt-2(e2663), hus-1(op241), rad-51(tg9), wee-1(ok418), cep-1((gk138)*, *chk-2(gk212)*, *spo-11(ok79)/nT1[unc-?(n754) let-?],), trr-1(n3630)/mIn1[dpy-10(e128) mIs14], lin-15(n767) and lin-15(n744)*. The *uri-1(tm939)* mutant allele was isolated and kindly provided by the NBP-Japan. Primers used for PCR screening of the *tm939* allele were 5'-CGCGGATCCATCATGAGCGAACTCTACGTTGC-3' and 5'-CCGCTCGAGCGGTCA ATTTCTATGCCTGGAAGC-3'. Since the homozygous mutant exhibits a sterile or embryonic lethality phenotype, it was marked with the recessive *dpy-5* mutation and cultivated as heterozygous *uri-1(tm939) dpy-5(e61)/dpy-5(e61) unc-14(e57)*. The *gld-2(q497) gld-1(q485); unc-32(e189)* strain (Kadyk and Kimble, 1998) was kindly provided by J. Kimble (University of Wisconsin, Madison, Wisconsin). The *vit-2* strain (YP170::GFP) (Grant and Hirsh, 1999)was kindly provided by B. Grant (State University of New Jersey, NJ). The mito:GFP with a *myo-3* promoter expressing strain (Labrousse et al., 1999) was kindly provided by A.M. van der Bliek (University of California, LA). All other strains used in this paper were provided by the *Caenorhabditis* Genetics Center, which is funded by the NIH National Center for Research Resources (NCRR).

Northern blot analysis

To prepare RNA, the *fem-1*, *fem-3*, *glp-4* and N2 strains were grown at 15°C for 5 days then bleached. Worms were synchronized at the L1 stage and raised at 25°C, the restrictive temperature for the used temperature-sensitive mutants. Under these conditions *glp-4* (Beanan and Strome, 1992) obtains nearly no germ cells (approximately 12) and is treated as germ line free animal, *fem-3* animals produce sperm but no oocytes (Barton et al., 1987) and *fem-1* animals generate oocytes but no sperm (Nelson et al., 1978). For the developmental profile worms were frozen at the indicated larval stage and for the germ

line expression analysis 1-day old adult worms were frozen and total mRNA was prepared by using the TRIZOL (GIBCO) method (Hope., 1999). Total RNA was fractionated in formaldehyde-agarose gels by electrophoresis transferred to a Hybond-N^+ membrane and hybridized in ExpressHyb™ Hybridization Solution (BD Biosiences) according manufactures protocol with a full length ^{32}P-labeled *uri-1* cDNA probe (using the Prime-It II Random Primer Labeling Kit; Stratagene). The amount of total mRNA was normalized using rRNA as standard.

GST-tagged proteins

In vitro translates were made using the TNT reticulocyte translation system (Promega) with the addition of ^{35}S-L-methionine according to the manufacturers protocol (25 µl TNT rabbit reticulocyte lysate, 2 µl TNT reaction buffer, 1 µl amino acid mix minus methionine, 1 µl RNase inhibitor (40 U/µl), 1.5 µg DNA as indicated, 1 µl TNT T7 RNA polymerase, 4 µl ^{35}S-methionine (1 µCi), ddH_2O to 50 µl). For the preparation of GST-fusion proteins and incubation with *in vitro* translates bacteria were inoculated overnight in LB-media and added the next morning in a 1:10 ratio to fresh LB-media and incubated until the culture reached OD 0.4. Protein expression was induced by addition of IPTG to a final concentration of 100 µM for 4 hrs. Bacteria were pelleted and lysed in NETN buffer (20 mM Tris-HCl pH 8.0, 100 mM NaCl, 1 mM EDTA, 0.5% NP-40, 1 mM DTT, 1µg/ml aprotinin, 1 µM PMSF), sonicated and centrifuged. The supernatant was incubated with GSH-sepharose 4B beads (Amersham) for up to two hrs at 4°C, washed 4 times and then processed. 5 µ IVT was incubated with the beads for 1 hr in TNN buffer, washed and sample was loaded on a SDS-PAGE. Following separation on SDS-PAGE, gels were incubated 2 hrs in Destain solution (25% MeOH, 14% acetate), 45 min in EN^{3}HANCE solution (DuPont) and 20 min in tap water. The gel was dried and exposed to film.

Immunmoprecipitation and western blotting

Immunoprecipitation were performed from worms (0.5-3.5 ml) were frozen at -80°C for 10 min and lysed at 4°C in TNN buffer (50 mM Tris-HCl pH 7.5, 10 mM NaCl, 5 mM EDTA, 0,5% NP-40, 50 mM NaF, 0,2 mM Na_3VO_4, 1µM DTT, 1 µM PMSF, 1 mg/ml aprotinin) by using the One-shot machine following sonification on ice. Proteins were equalized with the Bradford method (Biorad) and taken up in additional TNN buffer for the immunoprecipitation. Lysates were cleared by centrifugation (15 min, 12000 rpm, 4°C), the lysate pre-cleared with protein A sepharose beads (Amersham) and the respective

primary antibody added (2.5 μg/ml) for 2 hrs followed by incubation with protein A beads for 1 hr (40 μl). Beads were washed 3x in TNN buffer, boiled in Laemmli buffer and loaded on a SDS-PAGE gel. Immunoblotting of the SDS-PAGE gel was performed onto nitrocellulose membrane (Schleicher & Schuell) in between Whatmann paper at 400 mA for 1 hr. Blots were incubated with primary antibody overnight in 5% skim milk in TBST (α-URI-1 1:500), washed with TBST, 2 hr incubation with secondary rabbit or mouse HRP-linked antibody (Amersham) respectively in 5% skim milk (1:5000) and processed for western blotting by enhanced chemiluminescence ECL (Amersham) according to the manufacturers instructions.

Antibody generation

α-URI-1 peptide antibodies were raised against the synthetic peptide 25 amino acid sequence STSRDPAPVITEKKVSKFRASRHRN, corresponding to the carboyxl-terminal region and the synthetic peptide MSELYVAECNAAKARLEVETECRRI, corresponding to the amino-terminal region of *C. elegans* URI-1. The peptide was coupled to keyhole limpet hemocyanin KLH (Calbiochem), by incubation of 10 mg of peptide with 10 mg of KLH for 1 hr in 4 ml PBS and 1 ml 0.4% glutaraldehyde in ddH_20. Then, 5 ml PBS were added, dialyzed overnight in PBS and sent for injection into two rabbits each peptide. α-peptide antibodies were affinity-purified using peptide columns prepared with 10 mg peptide and 0.5 g CH-Sepharose 4B (Pharmacia). The beads were washed 15 min over gravity with 1 mM HCl, and mixed with peptide in coupling buffer (0.1 M $NaHCO_3$, 0.5 M NaCl, pH 8.0) in a 1:2 ratio, 4 hrs at 4°C. The column was washed with coupling buffer and active groups blocked with 0.1 M Tris-HCl pH 8.0 for 1 hr at room temperature (no rotation). Beads were finally washed with 4 cycles of buffer A (0.1 M Na-acetate, 0.5 NaCl, pH 4.0) and buffer B (0.1 M Tris-HCl pH 8.0, 0.5 M NaCl). Note that columns were subjected to one round of purification followed by PBS washes prior to use. For the coupling 4 ml of antibody serum was added to the column, the column was washed extensively with PBS, and the antibody was eluted with 0.2 M glycine (pH 2.2) and fractions were neutralized with 1M K_2HPO_4 (3:1 ratio). The column was regenerated by addition of 1M K_2HPO_4 followed by PBS wash. Fractions with significant protein amounts were pooled and dialyzed overnight in 35% glycerol/PBS and stored at -80°C.

Immunostaining

For the PH3 staining 1-day post-L4 adult gonads were dissected in PBST (0.3% Triton-X), transferred to a 96-well plate, washed once in ice cold PBS for 5 min and fixed in 4%

formaldeyde in PBS on ice for 30 min. Thereafter, the gonads were washed in PBST 3 times each for 5 min and fixed in methanol on ice for 2 minutes. Then, they were washed in PBST 4 times quickly and incubated at 4 degrees overnight with the rabbit polyclonal anti-phospho-histone 3 antibody (1:500 in PBST, Upstate). The next day the gonads were washed twice briefly in PBST and then 3 times in PBST each for 10 min at RT and incubated for 2 hrs with the secondary antibody (anti-rabbit cy3, 1:200) in PBST at RT. Then gonads where washed 3 times in PBST each for 10 min (1 μg/ml DAPI was added in the first wash) and mounted with 3 μl Vectashield per sample on the cover slide for further analysis.

For the formaldehyd-based whole-mount fixation worms were cleaned by sucrose floatation, washed in PBS for 1.5 hrs with several media changes to allow gut excretion. 2 x Ruvkun fixation buffer was added to a final concentration of 1 x at 4°C, 20% formaldeyde was added to a final concentration of 4%, mixed and frozen in dry ice/ethanol. The worm containing tubes were melt under a stream of tap water and the freezing procedure was repeated 3 additional time. Afterward the tubes were incubated on ice with occasional agitation for 30 min and washed twice in Tris-Triton buffer. Then worms were resuspended in Tris-Triton buffer and 1% β-mercaptoethanol was added, incubated with mild agitation at RT for 4 hrs for reduction of disulfid linkages. Worms were washed with 15x of 1xBO_3, 0.01 % Triton for 15 min at RT with gentle agitation. Then worms were incubated in 1xBO_3 buffer, 0.3% H_2O_2, 0.01% Triton for 15 min at RT with gently agitation. Worms were washed with 1xBO_3 buffer, 0.01% Triton and incubated overnight in AbA (1x PBS, 1% BSA, 0.5% Triton, 0.05% Sodiumazid, 1mM EDTA). For the staining the first antibody was diluted in fresh AbA buffer and incubated overnight at 4ºC with gentle agitation (1:250) in a total volume of 400 μl. The next morning the worms were washed for 20 min with AbB (1x PBS, 0.1% BSA, 0.5% Triton, 0.05% Sodiumazid, 1mM EDTA) with several changes at RT, resuspended with AbB and gently agitated for 3 hrs, rinses once with AbA and the secondary antibody was added in fresh AbA (1:250) for 3-4 hrs. Worms were washed with AbB as above, DAPI was added to the second last wash and the worms were mounted.

For the methanol-based staining procedure young adults were cut open on a slide in PBS, squeezed-cracked, fixed 30 min in -20°C methanol, washed 10 min at RT in PBS and the first antibody was added overnight in PBS, 0.2% Tween, 1% BSA at RT (1:250). The next morning the slides were washed 3 x in PBS, 0.2% Tween each for 10 in and incubated for

1 hrs with the secondary antibody (1:100) in the dark at 37°C, washed 3x in PBS each for 10 and mounted. For the specificity control worms were progressed through that staining procedure 48 or 72 hrs after injection.

Dauer assays

Growth at 27°C requires special care and was performed as described (Ailion and Thomas, 2000). To evaluate the Hid phenotype semi synchronous F1 broods of *uri-1* depleted and RNAi control treated wild type worms were screened for dauers incidence at appropriate times after growth form the L1 stage on at 27°C. To exclude false positive counts 2 ml 1% SDS solution was added to the plates (middle size) 15 min before counting. Data present in each bar are from a single set of assays that were conducted at the same time on the same incubator shelf.

To test a synthetic interaction with the *daf-2* pathway thermo-sensitive *daf-2(e1370)* mutant animals were fed on *uri-1(RNAi)* and control RNAi and the F1 generation was scored for dauer incidences at 20°C.

Life span assay. Life span assays were done at 25°C of animals that had not starved out or gone through dauer before. From plates containing staged wild type or *uri-1* mutants, individual larva were picked to plates at 25 degree. Hatching accounted for day 1 of the life span assay. Animals were transferred to new plates every 1-2 days while producing progeny. After egg production ceased, animals were transferred to new plates every 4-7 days. Animals were tapped with a pick every day and were scored as dead when they did not move after 3 times tap with the pick. Animals that explode or had crawled off the plate, were not included in the study.

Thermo tolerance

To analyze the tolerance to heat stress *uri-1(RNAi)*F1 and control RNAi fed animals were placed as staged young adults on several plates at 37°C. Every hour a plate of the indicated genotype was removed from the incubator and tested for survivals. Animals were tapped with a pick and were scored as dead when they did not move after 3 times tap with the pick.

Characterization of brood size and embryonic lethality

L4 hermaphrodites of the desired genotype were individually cloned onto agar plates and cultured at 25°C. The hermaphrodites were transferred to fresh plats every 24 hr. The brood size of each animal is the sum of non-hatched and hatched progeny. For the determination of the embryonic lethality L4 animals were transferred to a nematode growth-medium plate containing the corresponding RNAi food. These animals were allowed to lay eggs for 1-2 days. We remove the P0 animals and counted the eggs after 24 hrs to calculate the percentage of lethality.

RNAi analysis

Double stranded RNA was applied to worms by feeding (Timmons et al., 2001). A L4440 plasmid containing a fragment of the C55B7.5 was used (Fraser et al., 2000). The bacteria were seeded on NGM agar plates containing 6 mM IPTG and 50 µl 100 mg/ml carbencillin per liter. Worms were added as L1s on the following day and raised at 25°C. Temperature sensitive strains are raised at 15 degrees in their P0 generation and shifted as L1 larvae to 25°C. Control animals were fed with bacteria carrying an empty L4440 construct. Phenotypes were observed in the P0 and F1 progeny of worms that were fed with the respective dsRNA at the indicated time points.

Germ cell counts

Synchronized wild type L1 larvae were fed on *uri-1(RNAi)* and the vector control L4440(RNAi) plates at 25°C until adulthood. The worms where then transferred every 2 hrs to new plates and the F1 generation (also fed on RNAi) was collected and methanol fixed (-20°C for at least 10 min) at the indicated time points. After washing them twice in PBS, the worms were suspended in PBS including DAPI at 0.1 µg/ml for 30 min at RT. After washing them twice with PBS 3 µl Vectashield was added to the worms and they were mounted on slides. Germ cells identified by their nuclear morphology according to DAPI staining were counted. Stages of the animals were determined by vulval morphology and differentiation of somatic gonads.

Cell death assay

For the apoptotic corpse counts 1-day post-L4 adult worms synchronized worms in the L1 stage were mounted in a drop of M9 buffer containing 2.5 mM levamisole and observed using Nomarski optics. Only germ cells in the pachytene region before the gonad bends (distal region) of one gonad arm were scored for cell corpses.

For the AO staining 1-day post-L4 adult worms were incubated in 200 µl of 100 mM Acridine Orange solution in an OP50 solution on NGM plates for 2 hrs in the dark. To decrease background gut fluorescence the worms were fed on normal plates for 1 hr and observed in 5 µl sodium azide (0.1 µg/ml in PBS) under a fluorescence microscope.

DNA breakage detection methods

For the TUNEL (terminal deoxynucleotidyl transferase-mediated dUTP nick end-labeling) which detects DNA strand breaks (nicks) and DNA fragmentation (staggered DNA ends), one day post-L4 gonads were dissected in PBS, transferred to a 96-well plate and fixed in 4% formaldehyde in PBS at RT for 20 min. Then discs were rinsed in PTX (PBS, 0.4% Triton X-100) 3 times and incubated in 100 mM sodium-citrate, 0.1% Triton X-100 at 65°C for 20 min, followed by rinsing twice in PTX. Gonads are then incubated for 30 min at RT in 0.1 M Tris/HCL (pH 7.5) containing 3% BSA and 20% normal bovine serum. The gonads were rinsed twice with PBS at RT and excess fluid were let drain off. Gonads were afterwards incubated in TUNEL reaction mixture (Roche) at 37°C for 1.5 hrs. The reaction was stopped by washing the gonads three times in PTX. DAPI (1 µm/ml) was added into each well for 5 min within the second washing step. 3 µl Vectashield was added to each sample and gonads were mounted on to a cover slip for further analyses.
The HUS-1::GFP nuclear re-localization following DNA damage assay is described elsewhere (Hofmann et al., 2002).

HU

Worms at the L2 stage were plated on NGM plates containing 25 mM HU and pictures of the mitotic part of the germ line were taken 14 hrs after incubation on HU plates at 25°C.

Oxidative stress resistance assay

Homogenous staged L1 larval populations of worms (*uri-1(RNAi)*P0; *uri-1* and control (RNAi) wild type worms) were grown plates containing different amounts of paraquat (0-200 µm) to test their response to oxidative stress. Growth arrest was scored after 4 days and significance has been determined by student′s t-test.

Mitochondrial morphology

The mitochondrial matrix marker contains the *myo-3* promoter from pPD96.52 ligated to the mitochondrial leader and GFP in pPD96.32 (GFP was derived form pPD95.67) in wild type *C. elegans* (Labrousse et al., 1999). Control and *uri-1(RNAi)*F1 at 25°C has been

performed and animal were mounted as young adults in PBS buffer containing 2.5 mM levamisole

Chronic MMS treatment

MMS was dissolved in DMSO (dimethyl sulfoxide) shortly before use and quickly diluted in the agar to the required concentrations. Control RNAi treated wild type worms and *uri-1(RNAi)*P0; *uri-1* mutant animals were examined by placing L4 larvae on plates containing various concentrations of MMS (0-0.2 mM) and scoring their progeny for predominant stage of developmental arrest. Terminal developmental stages were determined by size estimates using a dissecting microscope at 20x magnification.

Irradiation experiments

For the γ-irradiation experiment control RNAi fed and *uri-1(RNAi)*P0; *uri-1* mutant animals were irradiated at the L4 larval stage (120 gray). Mitotic germ cell arrest was scored 8 hrs post irradiation. The hatching efficiency was scored as the percentage of surviving embryos laid 16-26 hrs post irradiation 24 hrs after removal of the mother. Significance has been determined by student′s t-test.

For the UV irradiation experiment control RNAi fed and *uri-1(RNAi)*P0; *uri-1* mutant animals were irradiated at the L4 larval stage at the indicated dose (0-300 J/m^2). The hatching efficiency was scored as the percentage of surviving embryos laid 24-36 hrs post irradiation 24 hrs after removal of the mother. Significance has been determined by student′s t-test.

Camptothecin sensitivity assay

Control RNAi fed and *uri-1(RNAi)*P0; *uri-1* mutant animals at the L4 larval were exposed to 0.14 mM camptothecin in PBS containing 0.5% DMSO for 2 hrs at RT on the plate. Control animals were treated with 0.5% DMSO in PBS. Pictures were taken for determination of the mitotic cell cycle arrest frequency and AO staining was performed 24 hrs after exposure to camptothecin at 25°C.

synMuv phenotype

Control RNAi treated and *uri-1(RNAi)*P0 and *uri-1(RNAi)*F1 of the indicated genotypes were analyzed for their penetrance of the Muv phenotype at 25°C under the dissecting microscope.

8 References

Abastado, J. P., Miller, P. F., Jackson, B. M., and Hinnebusch, A. G. (1991). Suppression of ribosomal reinitiation at upstream open reading frames in amino acid-starved cells forms the basis for GCN4 translational control. Mol Cell Biol *11*, 486-496.

Abraham, R. T. (2001). Cell cycle checkpoint signaling through the ATM and ATR kinases. Genes Dev *15*, 2177-2196.

Abraham, R. T. (2004). The ATM-related kinase, hSMG-1, bridges genome and RNA surveillance pathways. DNA Repair (Amst) *3*, 919-925.

Abraham, R. T., and Wiederrecht, G. J. (1996). Immunopharmacology of rapamycin. Annu Rev Immunol *14*, 483-510.

Adams, D. E., and West, S. C. (1995). Unwinding of closed circular DNA by the Escherichia coli RuvA and RuvB recombination/repair proteins. J Mol Biol *247*, 404-417.

Ahmed, S., Alpi, A., Hengartner, M. O., and Gartner, A. (2001). C. elegans RAD-5/CLK-2 defines a new DNA damage checkpoint protein. Curr Biol *11*, 1934-1944.

Ahringer, J. (2000). NuRD and SIN3 histone deacetylase complexes in development. Trends Genet *16*, 351-356.

Ahringer, J., and Kimble, J. (1991). Control of the sperm-oocyte switch in Caenorhabditis elegans hermaphrodites by the fem-3 3' untranslated region. Nature *349*, 346-348.

Ailion, M., Inoue, T., Weaver, C. I., Holdcraft, R. W., and Thomas, J. H. (1999). Neurosecretory control of aging in Caenorhabditis elegans. Proc Natl Acad Sci U S A *96*, 7394-7397.

Ailion, M., and Thomas, J. H. (2000). Dauer formation induced by high temperatures in Caenorhabditis elegans. Genetics *156*, 1047-1067.

Ailion, M., and Thomas, J. H. (2003). Isolation and characterization of high-temperature-induced Dauer formation mutants in Caenorhabditis elegans. Genetics *165*, 127-144.

Alessi, D. R., Andjelkovic, M., Caudwell, B., Cron, P., Morrice, N., Cohen, P., and Hemmings, B. A. (1996). Mechanism of activation of protein kinase B by insulin and IGF-1. Embo J *15*, 6541-6551.

Alessi, D. R., and Downes, C. P. (1998). The role of PI 3-kinase in insulin action. Biochim Biophys Acta *1436*, 151-164.

Alpi, A., Pasierbek, P., Gartner, A., and Loidl, J. (2003). Genetic and cytological characterization of the recombination protein RAD-51 in Caenorhabditis elegans. Chromosoma *112*, 6-16.

Amiri, A., Keiper, B. D., Kawasaki, I., Fan, Y., Kohara, Y., Rhoads, R. E., and Strome, S. (2001). An isoform of eIF4E is a component of germ granules and is required for spermatogenesis in C. elegans. Development *128*, 3899-3912.

Ann, K., Kowalchyk, J. A., Loyet, K. M., and Martin, T. F. (1997). Novel Ca2+-binding protein (CAPS) related to UNC-31 required for Ca2+-activated exocytosis. J Biol Chem *272*, 19637-19640.

Apfeld, J., and Kenyon, C. (1998). Cell nonautonomy of C. elegans daf-2 function in the regulation of diapause and life span. Cell *95*, 199-210.

Apfeld, J., and Kenyon, C. (1999). Regulation of lifespan by sensory perception in Caenorhabditis elegans. Nature *402*, 804-809.

Ashrafi, K., Chang, F. Y., Watts, J. L., Fraser, A. G., Kamath, R. S., Ahringer, J., and Ruvkun, G. (2003). Genome-wide RNAi analysis of Caenorhabditis elegans fat regulatory genes. Nature *421*, 268-272.

Austin, J., and Kimble, J. (1987). glp-1 is required in the germ line for regulation of the decision between mitosis and meiosis in C. elegans. Cell *51*, 589-599.

Avery, L., Bargmann, C. I., and Horvitz, H. R. (1993). The Caenorhabditis elegans unc-31 gene affects multiple nervous system-controlled functions. Genetics *134*, 455-464.

Avruch, J., Belham, C., Weng, Q., Hara, K., and Yonezawa, K. (2001). The p70 S6 kinase integrates nutrient and growth signals to control translational capacity. Prog Mol Subcell Biol *26*, 115-154.

Backman, S., Stambolic, V., and Mak, T. (2002). PTEN function in mammalian cell size regulation. Curr Opin Neurobiol *12*, 516-522.

Bagley, A. C., Krall, J., and Lynch, R. E. (1986). Superoxide mediates the toxicity of paraquat for Chinese hamster ovary cells. Proc Natl Acad Sci U S A *83*, 3189-3193.

Baker, J., Liu, J. P., Robertson, E. J., and Efstratiadis, A. (1993). Role of insulin-like growth factors in embryonic and postnatal growth. Cell *75*, 73-82.

Bambara, R. A., Murante, R. S., and Henricksen, L. A. (1997). Enzymes and reactions at the eukaryotic DNA replication fork. J Biol Chem *272*, 4647-4650.

Banin, S., Moyal, L., Shieh, S., Taya, Y., Anderson, C. W., Chessa, L., Smorodinsky, N. I., Prives, C., Reiss, Y., Shiloh, Y., and Ziv, Y. (1998). Enhanced phosphorylation of p53 by ATM in response to DNA damage. Science *281*, 1674-1677.

Barbet, N. C., Schneider, U., Helliwell, S. B., Stansfield, I., Tuite, M. F., and Hall, M. N. (1996). TOR controls translation initiation and early G1 progression in yeast. Mol Biol Cell *7*, 25-42.

Barbieri, M., Bonafe, M., Franceschi, C., and Paolisso, G. (2003). Insulin/IGF-I-signaling pathway: an evolutionarily conserved mechanism of longevity from yeast to humans. Am J Physiol Endocrinol Metab *285*, E1064-1071.

Bargmann, C. I., and Horvitz, H. R. (1991). Control of larval development by chemosensory neurons in Caenorhabditis elegans. Science *251*, 1243-1246.

Bartkova, J., Horejsi, Z., Koed, K., Kramer, A., Tort, F., Zieger, K., Guldberg, P., Sehested, M., Nesland, J. M., Lukas, C.*, et al.* (2005). DNA damage response as a candidate anti-cancer barrier in early human tumorigenesis. Nature *434*, 864-870.

Barton, M. K., Schedl, T. B., and Kimble, J. (1987). Gain-of-function mutations of fem-3, a sex-determination gene in Caenorhabditis elegans. Genetics *115*, 107-119.

Barzilai, A., and Yamamoto, K. (2004). DNA damage responses to oxidative stress. DNA Repair (Amst) *3*, 1109-1115.

Bassal, S., and El-Osta, A. (2005). DNA damage detection and repair, and the involvement of epigenetic states. Hum Mutat *25*, 101-109.

Bauer, A., Lickert, H., Kemler, R., and Stappert, J. (1998). Modification of the E-cadherin-catenin complex in mitotic Madin-Darby canine kidney epithelial cells. J Biol Chem *273*, 28314-28321.

Beanan, M. J., and Strome, S. (1992). Characterization of a germ-line proliferation mutation in C. elegans. Development *116*, 755-766.

Beck, T., and Hall, M. N. (1999). The TOR signalling pathway controls nuclear localization of nutrient-regulated transcription factors. Nature *402*, 689-692.

Beckman, K. B., and Ames, B. N. (1997). Oxidative decay of DNA. J Biol Chem *272*, 19633-19636.

Bender, L. B., Cao, R., Zhang, Y., and Strome, S. (2004). The MES-2/MES-3/MES-6 complex and regulation of histone H3 methylation in C. elegans. Curr Biol *14*, 1639-1643.

Benson, F. E., Illing, G. T., Sharples, G. J., and Lloyd, R. G. (1988). Nucleotide sequencing of the ruv region of Escherichia coli K-12 reveals a LexA regulated operon encoding two genes. Nucleic Acids Res *16*, 1541-1549.

Bermudez, V. P., Lindsey-Boltz, L. A., Cesare, A. J., Maniwa, Y., Griffith, J. D., Hurwitz, J., and Sancar, A. (2003). Loading of the human 9-1-1 checkpoint complex onto DNA by the checkpoint clamp loader hRad17-replication factor C complex in vitro. Proc Natl Acad Sci U S A *100*, 1633-1638.

Bernal, A., and Kimbrell, D. A. (2000). Drosophila Thor participates in host immune defense and connects a translational regulator with innate immunity. Proc Natl Acad Sci U S A *97*, 6019-6024.

Berneburg, M., and Lehmann, A. R. (2001). Xeroderma pigmentosum and related disorders: defects in DNA repair and transcription. Adv Genet *43*, 71-102.

Berry, L. W., Westlund, B., and Schedl, T. (1997). Germ-line tumor formation caused by activation of glp-1, a Caenorhabditis elegans member of the Notch family of receptors. Development *124*, 925-936.

Bertram, P. G., Choi, J. H., Carvalho, J., Ai, W., Zeng, C., Chan, T. F., and Zheng, X. F. (2000). Tripartite regulation of Gln3p by TOR, Ure2p, and phosphatases. J Biol Chem *275*, 35727-35733.

Bestor, T. H. (2000). The DNA methyltransferases of mammals. Hum Mol Genet *9*, 2395-2402.

Betz, J. L., Chang, M., Washburn, T. M., Porter, S. E., Mueller, C. L., and Jaehning, J. A. (2002). Phenotypic analysis of Paf1/RNA polymerase II complex mutations reveals connections to cell cycle regulation, protein synthesis, and lipid and nucleic acid metabolism. Mol Genet Genomics *268*, 272-285.

Biggs, W. H., 3rd, Meisenhelder, J., Hunter, T., Cavenee, W. K., and Arden, K. C. (1999). Protein kinase B/Akt-mediated phosphorylation promotes nuclear exclusion of the winged helix transcription factor FKHR1. Proc Natl Acad Sci U S A *96*, 7421-7426.

Boxem, M., and van den Heuvel, S. (2001). lin-35 Rb and cki-1 Cip/Kip cooperate in developmental regulation of G1 progression in C. elegans. Development *128*, 4349-4359.

Boxem, M., and van den Heuvel, S. (2002). C. elegans class B synthetic multivulva genes act in G(1) regulation. Curr Biol *12*, 906-911.

Brenner, S. (1974). The genetics of Caenorhabditis elegans. Genetics *77*, 71-94.

Brogiolo, W., Stocker, H., Ikeya, T., Rintelen, F., Fernandez, R., and Hafen, E. (2001). An evolutionarily conserved function of the Drosophila insulin receptor and insulin-like peptides in growth control. Curr Biol *11*, 213-221.

Brown, C. E., Howe, L., Sousa, K., Alley, S. C., Carrozza, M. J., Tan, S., and Workman, J. L. (2001). Recruitment of HAT complexes by direct activator interactions with the ATM-related Tra1 subunit. Science *292*, 2333-2337.

Brown-Borg, H. M., Borg, K. E., Meliska, C. J., and Bartke, A. (1996). Dwarf mice and the ageing process. Nature *384*, 33.

Brunet, A., Bonni, A., Zigmond, M. J., Lin, M. Z., Juo, P., Hu, L. S., Anderson, M. J., Arden, K. C., Blenis, J., and Greenberg, M. E. (1999). Akt promotes cell survival by phosphorylating and inhibiting a Forkhead transcription factor. Cell *96*, 857-868.

Brunet, A., Park, J., Tran, H., Hu, L. S., Hemmings, B. A., and Greenberg, M. E. (2001). Protein kinase SGK mediates survival signals by phosphorylating the forkhead transcription factor FKHRL1 (FOXO3a). Mol Cell Biol *21*, 952-965.

Brunn, G. J., Fadden, P., Haystead, T. A., and Lawrence, J. C., Jr. (1997). The mammalian target of rapamycin phosphorylates sites having a (Ser/Thr)-Pro motif and is activated by antibodies to a region near its COOH terminus. J Biol Chem *272*, 32547-32550.

Bujalowski, W., Klonowska, M. M., and Jezewska, M. J. (1994). Oligomeric structure of Escherichia coli primary replicative helicase DnaB protein. J Biol Chem *269*, 31350-31358.

Bukau, B., and Horwich, A. L. (1998). The Hsp70 and Hsp60 chaperone machines. Cell *92*, 351-366.

Bus, J. S., Aust, S. D., and Gibson, J. E. (1976). Paraquat toxicity: proposed mechanism of action involving lipid peroxidation. Environ Health Perspect *16*, 139-146.

Canman, C. E., and Lim, D. S. (1998). The role of ATM in DNA damage responses and cancer. Oncogene *17*, 3301-3308.

Cantley, L. C., and Neel, B. G. (1999). New insights into tumor suppression: PTEN suppresses tumor formation by restraining the phosphoinositide 3-kinase/AKT pathway. Proc Natl Acad Sci U S A *96*, 4240-4245.

Cantrell, D. A. (2001). Phosphoinositide 3-kinase signalling pathways. J Cell Sci *114*, 1439-1445.

Capowski, E. E., Martin, P., Garvin, C., and Strome, S. (1991). Identification of grandchildless loci whose products are required for normal germ-line development in the nematode Caenorhabditis elegans. Genetics *129*, 1061-1072.

Cardenas, M. E., Cutler, N. S., Lorenz, M. C., Di Como, C. J., and Heitman, J. (1999). The TOR signaling cascade regulates gene expression in response to nutrients. Genes Dev *13*, 3271-3279.

Carpten, J. D., Robbins, C. M., Villablanca, A., Forsberg, L., Presciuttini, S., Bailey-Wilson, J., Simonds, W. F., Gillanders, E. M., Kennedy, A. M., Chen, J. D.*, et al.* (2002). HRPT2, encoding parafibromin, is mutated in hyperparathyroidism-jaw tumor syndrome. Nat Genet *32*, 676-680.

Cassada, R. C., and Russell, R. L. (1975). The dauerlarva, a post-embryonic developmental variant of the nematode Caenorhabditis elegans. Dev Biol *46*, 326-342.

Ceol, C. J., and Horvitz, H. R. (2001). dpl-1 DP and efl-1 E2F act with lin-35 Rb to antagonize Ras signaling in C. elegans vulval development. Mol Cell *7*, 461-473.

Ceol, C. J., and Horvitz, H. R. (2004). A new class of C. elegans synMuv genes implicates a Tip60/NuA4-like HAT complex as a negative regulator of Ras signaling. Dev Cell *6*, 563-576.

Chan, E., and Weiss, B. (1987). Endonuclease IV of Escherichia coli is induced by paraquat. Proc Natl Acad Sci U S A *84*, 3189-3193.

Chang, M., French-Cornay, D., Fan, H. Y., Klein, H., Denis, C. L., and Jaehning, J. A. (1999). A complex containing RNA polymerase II, Paf1p, Cdc73p, Hpr1p, and Ccr4p plays a role in protein kinase C signaling. Mol Cell Biol *19*, 1056-1067.

Chavez, S., Beilharz, T., Rondon, A. G., Erdjument-Bromage, H., Tempst, P., Svejstrup, J. Q., Lithgow, T., and Aguilera, A. (2000). A protein complex containing Tho2, Hpr1, Mft1 and a novel protein, Thp2, connects transcription elongation with mitotic recombination in Saccharomyces cerevisiae. Embo J *19*, 5824-5834.

Chen, J., Zheng, X. F., Brown, E. J., and Schreiber, S. L. (1995). Identification of an 11-kDa FKBP12-rapamycin-binding domain within the 289-kDa FKBP12-rapamycin-associated protein and characterization of a critical serine residue. Proc Natl Acad Sci U S A *92*, 4947-4951.

Chen, R. Z., Pettersson, U., Beard, C., Jackson-Grusby, L., and Jaenisch, R. (1998). DNA hypomethylation leads to elevated mutation rates. Nature *395*, 89-93.

Cheong, J. H., Yi, M., Lin, Y., and Murakami, S. (1995). Human RPB5, a subunit shared by eukaryotic nuclear RNA polymerases, binds human hepatitis B virus X protein and may play a role in X transactivation. Embo J *14*, 143-150.

Cherkasova, V., Ayyadevara, S., Egilmez, N., and Shmookler Reis, R. (2000). Diverse Caenorhabditis elegans genes that are upregulated in dauer larvae also show elevated transcript levels in long-lived, aged, or starved adults. J Mol Biol *300*, 433-448.

Cherkasova, V. A., and Hinnebusch, A. G. (2003). Translational control by TOR and TAP42 through dephosphorylation of eIF2alpha kinase GCN2. Genes Dev *17*, 859-872.

Chial, H. J., Stemm-Wolf, A. J., McBratney, S., and Winey, M. (2000). Yeast Eap1p, an eIF4E-associated protein, has a separate function involving genetic stability. Curr Biol *10*, 1519-1522.

Choi, K. M., McMahon, L. P., and Lawrence, J. C., Jr. (2003). Two motifs in the translational repressor PHAS-I required for efficient phosphorylation by mammalian target of rapamycin and for recognition by raptor. J Biol Chem *278*, 19667-19673.

Chuang, L. S., Ian, H. I., Koh, T. W., Ng, H. H., Xu, G., and Li, B. F. (1997). Human DNA-(cytosine-5) methyltransferase-PCNA complex as a target for p21WAF1. Science *277*, 1996-2000.

Clemmons, D. R. (2001). Use of mutagenesis to probe IGF-binding protein structure/function relationships. Endocr Rev *22*, 800-817.

Clokey, G. V., and Jacobson, L. A. (1986). The autofluorescent "lipofuscin granules" in the intestinal cells of Caenorhabditis elegans are secondary lysosomes. Mech Ageing Dev *35*, 79-94.

Cole, M. D. (1986). The myc oncogene: its role in transformation and differentiation. Annu Rev Genet *20*, 361-384.

Conlon, I., and Raff, M. (1999). Size control in animal development. Cell *96*, 235-244.
Conlon, I. J., Dunn, G. A., Mudge, A. W., and Raff, M. C. (2001). Extracellular control of cell size. Nat Cell Biol *3*, 918-921.

Conradt, B., and Horvitz, H. R. (1999). The TRA-1A sex determination protein of C. elegans regulates sexually dimorphic cell deaths by repressing the egl-1 cell death activator gene. Cell *98*, 317-327.

Cortez, D., Guntuku, S., Qin, J., and Elledge, S. J. (2001). ATR and ATRIP: partners in checkpoint signaling. Science *294*, 1713-1716.

Cowan, N. J., and Lewis, S. A. (1999). A chaperone with a hydrophilic surface. Nat Struct Biol *6*, 990-991.

Craven, R. J., Greenwell, P. W., Dominska, M., and Petes, T. D. (2002). Regulation of genome stability by TEL1 and MEC1, yeast homologs of the mammalian ATM and ATR genes. Genetics *161*, 493-507.

Crittenden, S. L., Bernstein, D. S., Bachorik, J. L., Thompson, B. E., Gallegos, M., Petcherski, A. G., Moulder, G., Barstead, R., Wickens, M., and Kimble, J. (2002). A conserved RNA-binding protein controls germline stem cells in Caenorhabditis elegans. Nature *417*, 660-663.

Crittenden, S. L., Troemel, E. R., Evans, T. C., and Kimble, J. (1994). GLP-1 is localized to the mitotic region of the C. elegans germ line. Development *120*, 2901-2911.

Cutler, N. S., Heitman, J., and Cardenas, M. E. (1999). TOR kinase homologs function in a signal transduction pathway that is conserved from yeast to mammals. Mol Cell Endocrinol *155*, 135-142.

Cutler, N. S., Pan, X., Heitman, J., and Cardenas, M. E. (2001). The TOR signal transduction cascade controls cellular differentiation in response to nutrients. Mol Biol Cell *12*, 4103-4113.

Daniels, S. A., Ailion, M., Thomas, J. H., and Sengupta, P. (2000). egl-4 acts through a transforming growth factor-beta/SMAD pathway in Caenorhabditis elegans to regulate multiple neuronal circuits in response to sensory cues. Genetics *156*, 123-141.

De Benedetti, A., and Harris, A. L. (1999). eIF4E expression in tumors: its possible role in progression of malignancies. Int J Biochem Cell Biol *31*, 59-72.

De Benedetti, A., and Rhoads, R. E. (1990). Overexpression of eukaryotic protein synthesis initiation factor 4E in HeLa cells results in aberrant growth and morphology. Proc Natl Acad Sci U S A *87*, 8212-8216.

DeFronzo, R. A. (1997). Insulin resistance: a multifaceted syndrome responsible for NIDDM, obesity, hypertension, dyslipidaemia and atherosclerosis. Neth J Med *50*, 191-197.

Delgermaa, L., Hayashi, N., Dorjsuren, D., Nomura, T., Thuy le, T. T., and Murakami, S. (2004). Subcellular localization of RPB5-mediating protein and its putative functional partner. Mol Cell Biol *24*, 8556-8566.

Deng, X., Hofmann, E. R., Villanueva, A., Hobert, O., Capodieci, P., Veach, D. R., Yin, X., Campodonico, L., Glekas, A., Cordon-Cardo, C.*, et al.* (2004). Caenorhabditis elegans ABL-1 antagonizes p53-mediated germline apoptosis after ionizing irradiation. Nat Genet *36*, 906-912.

Dennis, P. B., Fumagalli, S., and Thomas, G. (1999). Target of rapamycin (TOR): balancing the opposing forces of protein synthesis and degradation. Curr Opin Genet Dev *9*, 49-54.

Dernburg, A. F., McDonald, K., Moulder, G., Barstead, R., Dresser, M., and Villeneuve, A. M. (1998). Meiotic recombination in C. elegans initiates by a conserved mechanism and is dispensable for homologous chromosome synapsis. Cell *94*, 387-398.

Derry, W. B., Putzke, A. P., and Rothman, J. H. (2001). Caenorhabditis elegans p53: role in apoptosis, meiosis, and stress resistance. Science *294*, 591-595.

Dever, T. E., Feng, L., Wek, R. C., Cigan, A. M., Donahue, T. F., and Hinnebusch, A. G. (1992). Phosphorylation of initiation factor 2 alpha by protein kinase GCN2 mediates gene-specific translational control of GCN4 in yeast. Cell *68*, 585-596.

Di Como, C. J., and Arndt, K. T. (1996). Nutrients, via the Tor proteins, stimulate the association of Tap42 with type 2A phosphatases. Genes Dev *10*, 1904-1916.

Dillin, A., Crawford, D. K., and Kenyon, C. (2002a). Timing requirements for insulin/IGF-1 signaling in C. elegans. Science *298*, 830-834.

Dillin, A., Hsu, A. L., Arantes-Oliveira, N., Lehrer-Graiwer, J., Hsin, H., Fraser, A. G., Kamath, R. S., Ahringer, J., and Kenyon, C. (2002b). Rates of behavior and aging specified by mitochondrial function during development. Science *298*, 2398-2401.

Dong, J., Qiu, H., Garcia-Barrio, M., Anderson, J., and Hinnebusch, A. G. (2000). Uncharged tRNA activates GCN2 by displacing the protein kinase moiety from a bipartite tRNA-binding domain. Mol Cell *6*, 269-279.

Dorjsuren, D., Lin, Y., Wei, W., Yamashita, T., Nomura, T., Hayashi, N., and Murakami, S. (1998). RMP, a novel RNA polymerase II subunit 5-interacting protein, counteracts transactivation by hepatitis B virus X protein. Mol Cell Biol *18*, 7546-7555.

Dugan, K. A., Wood, M. A., and Cole, M. D. (2002). TIP49, but not TRRAP, modulates c-Myc and E2F1 dependent apoptosis. Oncogene *21*, 5835-5843.

Duncan, R., and Hershey, J. W. (1985). Regulation of initiation factors during translational repression caused by serum depletion. Abundance, synthesis, and turnover rates. J Biol Chem *260*, 5486-5492.

Duvel, K., Santhanam, A., Garrett, S., Schneper, L., and Broach, J. R. (2003). Multiple roles of Tap42 in mediating rapamycin-induced transcriptional changes in yeast. Mol Cell *11*, 1467-1478.

Ebbert, R., Birkmann, A., and Schuller, H. J. (1999). The product of the SNF2/SWI2 paralogue INO80 of Saccharomyces cerevisiae required for efficient expression of various yeast structural genes is part of a high-molecular-weight protein complex. Mol Microbiol *32*, 741-751.

Eckmann, C. R., Kraemer, B., Wickens, M., and Kimble, J. (2002). GLD-3, a bicaudal-C homolog that inhibits FBF to control germline sex determination in C. elegans. Dev Cell *3*, 697-710.

Ellis, H. M., and Horvitz, H. R. (1986). Genetic control of programmed cell death in the nematode C. elegans. Cell *44*, 817-829.

Ellis, R. J., and Hartl, F. U. (1999). Principles of protein folding in the cellular environment. Curr Opin Struct Biol *9*, 102-110.

Fay, D. S., and Han, M. (2000). The synthetic multivulval genes of C. elegans: functional redundancy, Ras-antagonism, and cell fate determination. Genesis *26*, 279-284
.
Feng, Y., Lee, N., and Fearon, E. R. (2003). TIP49 regulates beta-catenin-mediated neoplastic transformation and T-cell factor target gene induction via effects on chromatin remodeling. Cancer Res *63*, 8726-8734.

Ferguson, E. L., and Horvitz, H. R. (1985). Identification and characterization of 22 genes that affect the vulval cell lineages of the nematode Caenorhabditis elegans. Genetics *110*, 17-72.

Ferguson, E. L., and Horvitz, H. R. (1989). The multivulva phenotype of certain Caenorhabditis elegans mutants results from defects in two functionally redundant pathways. Genetics *123*, 109-121.

Ferguson, E. L., Sternberg, P. W., and Horvitz, H. R. (1987). A genetic pathway for the specification of the vulval cell lineages of Caenorhabditis elegans. Nature *326*, 259-267.

Findlay, G. M., Harrington, L. S., and Lamb, R. F. (2005). TSC1-2 tumour suppressor and regulation of mTOR signalling: linking cell growth and proliferation? Curr Opin Genet Dev *15*, 69-76.

Fingar, D. C., Salama, S., Tsou, C., Harlow, E., and Blenis, J. (2002). Mammalian cell size is controlled by mTOR and its downstream targets S6K1 and 4EBP1/eIF4E. Genes Dev *16*, 1472-1487.

Fink, A. L. (1999). Chaperone-mediated protein folding. Physiol Rev *79*, 425-449.
Fiorentino, D. F., and Crabtree, G. R. (1997). Characterization of Saccharomyces cerevisiae dna2 mutants suggests a role for the helicase late in S phase. Mol Biol Cell *8*, 2519-2537.

Fitzgerald, K., and Greenwald, I. (1995). Interchangeability of Caenorhabditis elegans DSL proteins and intrinsic signalling activity of their extracellular domains in vivo. Development *121*, 4275-4282.

Foulstone, E., Prince, S., Zaccheo, O., Burns, J. L., Harper, J., Jacobs, C., Church, D., and Hassan, A. B. (2005). Insulin-like growth factor ligands, receptors, and binding proteins in cancer. J Pathol *205*, 145-153.

Francis, R., Barton, M. K., Kimble, J., and Schedl, T. (1995a). gld-1, a tumor suppressor gene required for oocyte development in Caenorhabditis elegans. Genetics *139*, 579-606.

Francis, R., Maine, E., and Schedl, T. (1995b). Analysis of the multiple roles of gld-1 in germline development: interactions with the sex determination cascade and the glp-1 signaling pathway. Genetics *139*, 607-630.

Frank, S. R., Parisi, T., Taubert, S., Fernandez, P., Fuchs, M., Chan, H. M., Livingston, D. M., and Amati, B. (2003). MYC recruits the TIP60 histone acetyltransferase complex to chromatin. EMBO Rep *4*, 575-580.

Fraser, A. G., Kamath, R. S., Zipperlen, P., Martinez-Campos, M., Sohrmann, M., and Ahringer, J. (2000). Functional genomic analysis of C. elegans chromosome I by systematic RNA interference. Nature *408*, 325-330.

Fridovich, I. (1995). Superoxide radical and superoxide dismutases. Annu Rev Biochem *64*, 97-112.

Friedberg, E. C., Bardwell, A. J., Bardwell, L., Feaver, W. J., Kornberg, R. D., Svejstrup, J. Q., Tomkinson, A. E., and Wang, Z. (1995). Nucleotide excision repair in the yeast Saccharomyces cerevisiae: its relationship to specialized mitotic recombination and RNA polymerase II basal transcription. Philos Trans R Soc Lond B Biol Sci *347*, 63-68.

Friedman, D. B., and Johnson, T. E. (1988). Three mutants that extend both mean and maximum life span of the nematode, Caenorhabditis elegans, define the age-1 gene. J Gerontol *43*, B102-109.

Furnari, B., Rhind, N., and Russell, P. (1997). Cdc25 mitotic inducer targeted by chk1 DNA damage checkpoint kinase. Science *277*, 1495-1497.

Furukawa-Hibi, Y., Yoshida-Araki, K., Ohta, T., Ikeda, K., and Motoyama, N. (2002). FOXO forkhead transcription factors induce G(2)-M checkpoint in response to oxidative stress. J Biol Chem *277*, 26729-26732.

Furuta, T., Takemura, H., Liao, Z. Y., Aune, G. J., Redon, C., Sedelnikova, O. A., Pilch, D. R., Rogakou, E. P., Celeste, A., Chen, H. T.*, et al.* (2003). Phosphorylation of histone H2AX and activation of Mre11, Rad50, and Nbs1 in response to replication-dependent DNA double-strand breaks induced by mammalian DNA topoisomerase I cleavage complexes. J Biol Chem *278*, 20303-20312.

Galili, N., Davis, R. J., Fredericks, W. J., Mukhopadhyay, S., Rauscher, F. J., 3rd, Emanuel, B. S., Rovera, G., and Barr, F. G. (1993). Fusion of a fork head domain gene to PAX3 in the solid tumour alveolar rhabdomyosarcoma. Nat Genet *5*, 230-235.

Ganoza, M. C., Kiel, M. C., and Aoki, H. (2002). Evolutionary conservation of reactions in translation. Microbiol Mol Biol Rev *66*, 460-485, table of contents.

Garofalo, R. S. (2002). Genetic analysis of insulin signaling in Drosophila. Trends Endocrinol Metab *13*, 156-162.

Gartner, A., Milstein, S., Ahmed, S., Hodgkin, J., and Hengartner, M. O. (2000). A conserved checkpoint pathway mediates DNA damage--induced apoptosis and cell cycle arrest in C. elegans. Mol Cell *5*, 435-443.

Garza, L., Aude, Y. W., and Saucedo, J. F. (2002). Can we prevent in-stent restenosis? Curr Opin Cardiol *17*, 518-525.

Geissler, S., Siegers, K., and Schiebel, E. (1998). A novel protein complex promoting formation of functional alpha- and gamma-tubulin. Embo J *17*, 952-966.

Gems, D., and Partridge, L. (2001). Insulin/IGF signalling and ageing: seeing the bigger picture. Curr Opin Genet Dev *11*, 287-292.

Gems, D., Pletcher, S., and Partridge, L. (2002). Interpreting interactions between treatments that slow aging. Aging Cell *1*, 1-9.

Georgakopoulos, T., and Thireos, G. (1992). Two distinct yeast transcriptional activators require the function of the GCN5 protein to promote normal levels of transcription. Embo J *11*, 4145-4152.

Ghigo, E., Gianotti, L., Arvat, E., Ramunni, J., Valetto, M. R., Broglio, F., Rolla, M., Cavagnini, F., and Muller, E. E. (1999). Effects of recombinant human insulin-like growth factor I administration on growth hormone (GH) secretion, both spontaneous and stimulated by GH-releasing hormone or hexarelin, a peptidyl GH secretagogue, in humans. J Clin Endocrinol Metab *84*, 285-290.

Gil, E. B., Malone Link, E., Liu, L. X., Johnson, C. D., and Lees, J. A. (1999). Regulation of the insulin-like developmental pathway of Caenorhabditis elegans by a homolog of the PTEN tumor suppressor gene. Proc Natl Acad Sci U S A *96*, 2925-2930.

Gimeno, C. J., Ljungdahl, P. O., Styles, C. A., and Fink, G. R. (1992). Unipolar cell divisions in the yeast S. cerevisiae lead to filamentous growth: regulation by starvation and RAS. Cell *68*, 1077-1090.

Gingras, A. C., Gygi, S. P., Raught, B., Polakiewicz, R. D., Abraham, R. T., Hoekstra, M. F., Aebersold, R., and Sonenberg, N. (1999a). Regulation of 4E-BP1 phosphorylation: a novel two-step mechanism. Genes Dev *13*, 1422-1437.

Gingras, A. C., Raught, B., and Sonenberg, N. (1999b). eIF4 initiation factors: effectors of mRNA recruitment to ribosomes and regulators of translation. Annu Rev Biochem *68*, 913-963.

Gingras, A. C., Raught, B., and Sonenberg, N. (2001). Control of translation by the target of rapamycin proteins. Prog Mol Subcell Biol *27*, 143-174.

Golden, A., Sadler, P. L., Wallenfang, M. R., Schumacher, J. M., Hamill, D. R., Bates, G., Bowerman, B., Seydoux, G., and Shakes, D. C. (2000). Metaphase to anaphase (mat) transition-defective mutants in Caenorhabditis elegans. J Cell Biol *151*, 1469-1482.

Golden, J. W., and Riddle, D. L. (1982). A pheromone influences larval development in the nematode Caenorhabditis elegans. Science *218*, 578-580.

Golden, J. W., and Riddle, D. L. (1984a). The Caenorhabditis elegans dauer larva: developmental effects of pheromone, food, and temperature. Dev Biol *102*, 368-378.

Golden, J. W., and Riddle, D. L. (1984b). A pheromone-induced developmental switch in Caenorhabditis elegans: Temperature-sensitive mutants reveal a wild-type temperature-dependent process. Proc Natl Acad Sci U S A *81*, 819-823.

Gomez, M. R. (1991). Phenotypes of the tuberous sclerosis complex with a revision of diagnostic criteria. Ann N Y Acad Sci *615*, 1-7.

Goodarzi, A. A., Block, W. D., and Lees-Miller, S. P. (2003). The role of ATM and ATR in DNA damage-induced cell cycle control. Prog Cell Cycle Res *5*, 393-411.

Goto, H., Tomono, Y., Ajiro, K., Kosako, H., Fujita, M., Sakurai, M., Okawa, K., Iwamatsu, A., Okigaki, T., Takahashi, T., and Inagaki, M. (1999). Identification of a novel phosphorylation site on histone H3 coupled with mitotic chromosome condensation. J Biol Chem *274*, 25543-25549.

Grant, B., and Hirsh, D. (1999). Receptor-mediated endocytosis in the Caenorhabditis elegans oocyte. Mol Biol Cell *10*, 4311-4326.

Gregoire, F. M., Chomiki, N., Kachinskas, D., and Warden, C. H. (1998). Cloning and developmental regulation of a novel member of the insulin-like gene family in Caenorhabditis elegans. Biochem Biophys Res Commun *249*, 385-390.

Gruidl, M. E., Smith, P. A., Kuznicki, K. A., McCrone, J. S., Kirchner, J., Roussell, D. L., Strome, S., and Bennett, K. L. (1996). Multiple potential germ-line helicases are components of the germ-line-specific P granules of Caenorhabditis elegans. Proc Natl Acad Sci U S A *93*, 13837-13842.

Grundmann, O., Mosch, H. U., and Braus, G. H. (2001). Repression of GCN4 mRNA translation by nitrogen starvation in Saccharomyces cerevisiae. J Biol Chem *276*, 25661-25671.

Gstaiger, M., Luke, B., Hess, D., Oakeley, E. J., Wirbelauer, C., Blondel, M., Vigneron, M., Peter, M., and Krek, W. (2003). Control of nutrient-sensitive transcription programs by the unconventional prefoldin URI. Science *302*, 1208-1212.

Gumienny, T. L., Lambie, E., Hartwieg, E., Horvitz, H. R., and Hengartner, M. O. (1999). Genetic control of programmed cell death in the Caenorhabditis elegans hermaphrodite germline. Development *126*, 1011-1022.

Hampsey, M., and Reinberg, D. (2003). Tails of intrigue: phosphorylation of RNA polymerase II mediates histone methylation. Cell *113*, 429-432.

Hanazawa, M., Kawasaki, I., Kunitomo, H., Gengyo-Ando, K., Bennett, K. L., Mitani, S., and Iino, Y. (2004). The Caenorhabditis elegans eukaryotic initiation factor 5A homologue, IFF-1, is required for germ cell proliferation, gametogenesis and localization of the P-granule component PGL-1. Mech Dev *121*, 213-224.

Hansen, D., Hubbard, E. J., and Schedl, T. (2004). Multi-pathway control of the proliferation versus meiotic development decision in the Caenorhabditis elegans germline. Dev Biol *268*, 342-357.

Hansen, W. J., Cowan, N. J., and Welch, W. J. (1999). Prefoldin-nascent chain complexes in the folding of cytoskeletal proteins. J Cell Biol *145*, 265-277.

Hara, K., Maruki, Y., Long, X., Yoshino, K., Oshiro, N., Hidayat, S., Tokunaga, C., Avruch, J., and Yonezawa, K. (2002). Raptor, a binding partner of target of rapamycin (TOR), mediates TOR action. Cell *110*, 177-189.

Harbour, J. W., and Dean, D. C. (2000). The Rb/E2F pathway: expanding roles and emerging paradigms. Genes Dev *14*, 2393-2409.

Hardie, D. G., Carling, D., and Carlson, M. (1998). The AMP-activated/SNF1 protein kinase subfamily: metabolic sensors of the eukaryotic cell? Annu Rev Biochem *67*, 821-855.

Harding, H. P., Novoa, I., Zhang, Y., Zeng, H., Wek, R., Schapira, M., and Ron, D. (2000). Regulated translation initiation controls stress-induced gene expression in mammalian cells. Mol Cell *6*, 1099-1108.

Hardwick, J. S., Kuruvilla, F. G., Tong, J. K., Shamji, A. F., and Schreiber, S. L. (1999). Rapamycin-modulated transcription defines the subset of nutrient-sensitive signaling pathways directly controlled by the Tor proteins. Proc Natl Acad Sci U S A *96*, 14866-14870.

Harrington, J. J., and Lieber, M. R. (1994). The characterization of a mammalian DNA structure-specific endonuclease. Embo J *13*, 1235-1246.

Harris, T. E., and Lawrence, J. C., Jr. (2003). TOR signaling. Sci STKE *2003*, re15.

Hartl, F. U. (1996). Molecular chaperones in cellular protein folding. Nature *381*, 571-579.

Hartman, P., Childress, E., and Beyer, T. (1995). Nematode development is inhibited by methyl viologen and high oxygen concentrations at a rate inversely proportional to life span. J Gerontol A Biol Sci Med Sci *50*, B322-326.

Hartwell, L. H., and Weinert, T. A. (1989). Checkpoints: controls that ensure the order of cell cycle events. Science *246*, 629-634.

Hay, N., and Sonenberg, N. (2004). Upstream and downstream of mTOR. Genes Dev *18*, 1926-1945.

Heikkinen, K., Mansikka, V., Karppinen, S. M., Rapakko, K., and Winqvist, R. (2005a). Mutation analysis of the ATR gene in breast and ovarian cancer families. Breast Cancer Res *7*, R495-501.

Heikkinen, K., Rapakko, K., Karppinen, S. M., Erkko, H., Nieminen, P., and Winqvist, R. (2005b). Association of common ATM polymorphism with bilateral breast cancer. Int J Cancer *116*, 69-72.

Heitman, J., Movva, N. R., Hiestand, P. C., and Hall, M. N. (1991). FK 506-binding protein proline rotamase is a target for the immunosuppressive agent FK 506 in Saccharomyces cerevisiae. Proc Natl Acad Sci U S A *88*, 1948-1952.

Helliwell, S. B., Wagner, P., Kunz, J., Deuter-Reinhard, M., Henriquez, R., and Hall, M. N. (1994). TOR1 and TOR2 are structurally and functionally similar but not identical phosphatidylinositol kinase homologues in yeast. Mol Biol Cell *5*, 105-118.

Hemerly, A., Engler Jde, A., Bergounioux, C., Van Montagu, M., Engler, G., Inze, D., and Ferreira, P. (1995). Dominant negative mutants of the Cdc2 kinase uncouple cell division from iterative plant development. Embo J *14*, 3925-3936.

Henderson, S. T., Gao, D., Lambie, E. J., and Kimble, J. (1994). lag-2 may encode a signaling ligand for the GLP-1 and LIN-12 receptors of C. elegans. Development *120*, 2913-2924.

Henderson, S. T., and Johnson, T. E. (2001). daf-16 integrates developmental and environmental inputs to mediate aging in the nematode Caenorhabditis elegans. Curr Biol *11*, 1975-1980.

Hendzel, M. J., Wei, Y., Mancini, M. A., Van Hooser, A., Ranalli, T., Brinkley, B. R., Bazett-Jones, D. P., and Allis, C. D. (1997). Mitosis-specific phosphorylation of histone H3 initiates primarily within pericentromeric heterochromatin during G2 and spreads in an ordered fashion coincident with mitotic chromosome condensation. Chromosoma *106*, 348-360.

Hengartner, M. O. (1999). Programmed cell death in the nematode C. elegans. Recent Prog Horm Res *54*, 213-222; discussion 222-214.

Hengartner, M. O., Ellis, R. E., and Horvitz, H. R. (1992). Caenorhabditis elegans gene ced-9 protects cells from programmed cell death. Nature *356*, 494-499.

Hengartner, M. O., and Horvitz, H. R. (1994). The ins and outs of programmed cell death during C. elegans development. Philos Trans R Soc Lond B Biol Sci *345*, 243-246.

Henneke, G., Friedrich-Heineken, E., and Hubscher, U. (2003). Flap endonuclease 1: a novel tumour suppresser protein. Trends Biochem Sci *28*, 384-390.

Hertweck, M., Gobel, C., and Baumeister, R. (2004). C. elegans SGK-1 is the critical component in the Akt/PKB kinase complex to control stress response and life span. Dev Cell *6*, 577-588.

Hidalgo, M., Villalona-Calero, M. A., Eckhardt, S. G., Drengler, R. L., Rodriguez, G., Hammond, L. A., Diab, S. G., Weiss, G., Garner, A. M., Campbell, E.*, et al.* (2000). Phase I and pharmacologic study of PN401 and fluorouracil in patients with advanced solid malignancies. J Clin Oncol *18*, 167-177.

Hillion, J., Le Coniat, M., Jonveaux, P., Berger, R., and Bernard, O. A. (1997). AF6q21, a novel partner of the MLL gene in t(6;11)(q21;q23), defines a forkhead transcriptional factor subfamily. Blood *90*, 3714-3719.

Hinnebusch, A. G. (1994). Translational control of GCN4: an in vivo barometer of initiation-factor activity. Trends Biochem Sci *19*, 409-414.

Hinnebusch, A. G. (1997). Translational regulation of yeast GCN4. A window on factors that control initiator-trna binding to the ribosome. J Biol Chem *272*, 21661-21664.

Hinnebusch, A. G., and Natarajan, K. (2002). Gcn4p, a master regulator of gene expression, is controlled at multiple levels by diverse signals of starvation and stress. Eukaryot Cell *1*, 22-32.

Hirsh, D., Oppenheim, D., and Klass, M. (1976). Development of the reproductive system of Caenorhabditis elegans. Dev Biol *49*, 200-219.

Hofmann, E. R., Milstein, S., Boulton, S. J., Ye, M., Hofmann, J. J., Stergiou, L., Gartner, A., Vidal, M., and Hengartner, M. O. (2002). Caenorhabditis elegans HUS-1 is a DNA damage checkpoint protein required for genome stability and EGL-1-mediated apoptosis. Curr Biol *12*, 1908-1918.

Hofmann, E. R., Milstein, S., and Hengartner, M. O. (2000). DNA-damage-induced checkpoint pathways in the nematode Caenorhabditis elegans. Cold Spring Harb Symp Quant Biol *65*, 467-473.

Holdeman, R., Nehrt, S., and Strome, S. (1998). MES-2, a maternal protein essential for viability of the germline in Caenorhabditis elegans, is homologous to a Drosophila Polycomb group protein. Development *125*, 2457-2467.

Holzenberger, M., Dupont, J., Ducos, B., Leneuve, P., Geloen, A., Even, P. C., Cervera, P., and Le Bouc, Y. (2003). IGF-1 receptor regulates lifespan and resistance to oxidative stress in mice. Nature *421*, 182-187.

Holzmann, K., Gerner, C., Korosec, T., Poltl, A., Grimm, R., and Sauermann, G. (1998). Identification and characterization of the ubiquitously occurring nuclear matrix protein NMP 238. Biochem Biophys Res Commun *252*, 39-45.

Honda, Y., and Honda, S. (1999). The daf-2 gene network for longevity regulates oxidative stress resistance and Mn-superoxide dismutase gene expression in Caenorhabditis elegans. Faseb J *13*, 1385-1393.

Honda, Y., and Honda, S. (2002). Oxidative stress and life span determination in the nematode Caenorhabditis elegans. Ann N Y Acad Sci *959*, 466-474.

Hope, I. A. (1999). C. elegans. Oxford UniversityPress

Hopfner, K. P., Craig, L., Moncalian, G., Zinkel, R. A., Usui, T., Owen, B. A., Karcher, A., Henderson, B., Bodmer, J. L., McMurray, C. T.*, et al.* (2002). The Rad50 zinc-hook is a structure joining Mre11 complexes in DNA recombination and repair. Nature *418*, 562-566.

Horvitz, H. R. (1999). Genetic control of programmed cell death in the nematode Caenorhabditis elegans. Cancer Res *59*, 1701s-1706s.

Hsin, H., and Kenyon, C. (1999). Signals from the reproductive system regulate the lifespan of C. elegans. Nature *399*, 362-366.

Huang, S., and Houghton, P. J. (2003). Targeting mTOR signaling for cancer therapy. Curr Opin Pharmacol *3*, 371-377.

Hubbard, E. J., and Greenstein, D. (2000). The Caenorhabditis elegans gonad: a test tube for cell and developmental biology. Dev Dyn *218*, 2-22.

Hussain, S. P., Hollstein, M. H., and Harris, C. C. (2000). p53 tumor suppressor gene: at the crossroads of molecular carcinogenesis, molecular epidemiology, and human risk assessment. Ann N Y Acad Sci *919*, 79-85.

Ikura, T., Ogryzko, V. V., Grigoriev, M., Groisman, R., Wang, J., Horikoshi, M., Scully, R., Qin, J., and Nakatani, Y. (2000). Involvement of the TIP60 histone acetylase complex in DNA repair and apoptosis. Cell *102*, 463-473.

Illmensee, K., and Mahowald, A. P. (1974). Transplantation of posterior polar plasm in Drosophila. Induction of germ cells at the anterior pole of the egg. Proc Natl Acad Sci U S A *71*, 1016-1020.

Inoki, K., Zhu, T., and Guan, K. L. (2003). TSC2 mediates cellular energy response to control cell growth and survival. Cell *115*, 577-590.

Inoue, T., and Thomas, J. H. (2000). Suppressors of transforming growth factor-beta pathway mutants in the Caenorhabditis elegans dauer formation pathway. Genetics *156*, 1035-1046.

Ishchenko, A. A., Sanz, G., Privezentzev, C. V., Maksimenko, A. V., and Saparbaev, M. (2003). Characterisation of new substrate specificities of Escherichia coli and Saccharomyces cerevisiae AP endonucleases. Nucleic Acids Res *31*, 6344-6353.

Ishimi, Y., Claude, A., Bullock, P., and Hurwitz, J. (1988). Complete enzymatic synthesis of DNA containing the SV40 origin of replication. J Biol Chem *263*, 19723-19733.

Ito, T., Chiba, T., Ozawa, R., Yoshida, M., Hattori, M., and Sakaki, Y. (2001a). A comprehensive two-hybrid analysis to explore the yeast protein interactome. Proc Natl Acad Sci U S A *98*, 4569-4574.

Ito, T., Tashiro, K., and Kuhara, T. (2001b). [Systematic analysis of Saccharomyces cerevisiae genome: gene network and protein-protein interaction network]. Tanpakushitsu Kakusan Koso *46*, 2407-2413.

Jacinto, E., and Hall, M. N. (2003). Tor signalling in bugs, brain and brawn. Nat Rev Mol Cell Biol *4*, 117-126.

Jacinto, E., Loewith, R., Schmidt, A., Lin, S., Ruegg, M. A., Hall, A., and Hall, M. N. (2004). Mammalian TOR complex 2 controls the actin cytoskeleton and is rapamycin insensitive. Nat Cell Biol *6*, 1122-1128.

Jackson, C. E., Norum, R. A., Boyd, S. B., Talpos, G. B., Wilson, S. D., Taggart, R. T., and Mallette, L. E. (1990). Hereditary hyperparathyroidism and multiple ossifying jaw fibromas: a clinically and genetically distinct syndrome. Surgery *108*, 1006-1012; discussion 1012-1003.

Jan, E., Motzny, C. K., Graves, L. E., and Goodwin, E. B. (1999). The STAR protein, GLD-1, is a translational regulator of sexual identity in Caenorhabditis elegans. Embo J *18*, 258-269.

Jia, K., Chen, D., and Riddle, D. L. (2004). The TOR pathway interacts with the insulin signaling pathway to regulate C. elegans larval development, metabolism and life span. Development *131*, 3897-3906.

Jiang, H. Y., Wek, S. A., McGrath, B. C., Lu, D., Hai, T., Harding, H. P., Wang, X., Ron, D., Cavener, D. R., and Wek, R. C. (2004). Activating transcription factor 3 is integral to the eukaryotic initiation factor 2 kinase stress response. Mol Cell Biol *24*, 1365-1377.

Jiang, Y., and Broach, J. R. (1999). Tor proteins and protein phosphatase 2A reciprocally regulate Tap42 in controlling cell growth in yeast. Embo J *18*, 2782-2792.

Johnson, R. E., Kovvali, G. K., Prakash, L., and Prakash, S. (1995). Requirement of the yeast RTH1 5' to 3' exonuclease for the stability of simple repetitive DNA. Science *269*, 238-240.

Johnson, T. E., Cypser, J., de Castro, E., de Castro, S., Henderson, S., Murakami, S., Rikke, B., Tedesco, P., and Link, C. (2000). Gerontogenes mediate health and longevity in nematodes through increasing resistance to environmental toxins and stressors. Exp Gerontol *35*, 687-694.

Jones, A. R., Francis, R., and Schedl, T. (1996). GLD-1, a cytoplasmic protein essential for oocyte differentiation, shows stage- and sex-specific expression during Caenorhabditis elegans germline development. Dev Biol *180*, 165-183.

Jones, A. R., and Schedl, T. (1995). Mutations in gld-1, a female germ cell-specific tumor suppressor gene in Caenorhabditis elegans, affect a conserved domain also found in Src-associated protein Sam68. Genes Dev *9*, 1491-1504.

Jorgensen, P., and Tyers, M. (2004). How cells coordinate growth and division. Curr Biol *14*, R1014-1027.

Junger, M. A., Rintelen, F., Stocker, H., Wasserman, J. D., Vegh, M., Radimerski, T., Greenberg, M. E., and Hafen, E. (2003). The Drosophila forkhead transcription factor FOXO mediates the reduction in cell number associated with reduced insulin signaling. J Biol *2*, 20.

Kadyk, L. C., and Kimble, J. (1998). Genetic regulation of entry into meiosis in Caenorhabditis elegans. Development *125*, 1803-1813.

Kadyk, L. C., Lambie, E. J., and Kimble, J. (1997). glp-3 is required for mitosis and meiosis in the Caenorhabditis elegans germ line. Genetics *145*, 111-121.

Kahn, B. B., and Rossetti, L. (1998). Type 2 diabetes--who is conducting the orchestra? Nat Genet *20*, 223-225.

Kanemaki, M., Makino, Y., Yoshida, T., Kishimoto, T., Koga, A., Yamamoto, K., Yamamoto, M., Moncollin, V., Egly, J. M., Muramatsu, M., and Tamura, T. (1997).

Molecular cloning of a rat 49-kDa TBP-interacting protein (TIP49) that is highly homologous to the bacterial RuvB. Biochem Biophys Res Commun *235*, 64-68.

Kao, H. I., Campbell, J. L., and Bambara, R. A. (2004). Dna2p helicase/nuclease is a tracking protein, like FEN1, for flap cleavage during Okazaki fragment maturation. J Biol Chem *279*, 50840-50849.

Kastan, M. B., and Bartek, J. (2004). Cell-cycle checkpoints and cancer. Nature *432*, 316-323.

Kawasaki, I., Shim, Y. H., Kirchner, J., Kaminker, J., Wood, W. B., and Strome, S. (1998). PGL-1, a predicted RNA-binding component of germ granules, is essential for fertility in C. elegans. Cell *94*, 635-645.

Keith, C. T., and Schreiber, S. L. (1995). PIK-related kinases: DNA repair, recombination, and cell cycle checkpoints. Science *270*, 50-51.

Kenyon, C., Chang, J., Gensch, E., Rudner, A., and Tabtiang, R. (1993). A C. elegans mutant that lives twice as long as wild type. Nature *366*, 461-464.

Ketting, R. F., Haverkamp, T. H., van Luenen, H. G., and Plasterk, R. H. (1999). Mut-7 of C. elegans, required for transposon silencing and RNA interference, is a homolog of Werner syndrome helicase and RNaseD. Cell *99*, 133-141.

Khanna, K. K., and Jackson, S. P. (2001). DNA double-strand breaks: signaling, repair and the cancer connection. Nat Genet *27*, 247-254.

Kim, D. H., and Sabatini, D. M. (2004). Raptor and mTOR: subunits of a nutrient-sensitive complex. Curr Top Microbiol Immunol *279*, 259-270.

Kim, D. H., Sarbassov, D. D., Ali, S. M., King, J. E., Latek, R. R., Erdjument-Bromage, H., Tempst, P., and Sabatini, D. M. (2002a). mTOR interacts with raptor to form a nutrient-sensitive complex that signals to the cell growth machinery. Cell *110*, 163-175.

Kim, D. H., Sarbassov, D. D., Ali, S. M., Latek, R. R., Guntur, K. V., Erdjument-Bromage, H., Tempst, P., and Sabatini, D. M. (2003). GbetaL, a positive regulator of the rapamycin-sensitive pathway required for the nutrient-sensitive interaction between raptor and mTOR. Mol Cell *11*, 895-904.

Kim, J. K., Gabel, H. W., Kamath, R. S., Tewari, M., Pasquinelli, A., Rual, J. F., Kennedy, S., Dybbs, M., Bertin, N., Kaplan, J. M.*, et al.* (2005). Functional genomic analysis of RNA interference in C. elegans. Science *308*, 1164-1167.

Kim, K., Biade, S., and Matsumoto, Y. (1998). Involvement of flap endonuclease 1 in base excision DNA repair. J Biol Chem *273*, 8842-8848.

Kim, S. K., Lund, J., Kiraly, M., Duke, K., Jiang, M., Stuart, J. M., Eizinger, A., Wylie, B. N., and Davidson, G. S. (2001). A gene expression map for Caenorhabditis elegans. Science *293*, 2087-2092.

Kim, S. T., Xu, B., and Kastan, M. B. (2002b). Involvement of the cohesin protein, Smc1, in Atm-dependent and independent responses to DNA damage. Genes Dev *16*, 560-570.

Kim, T. K., Lagrange, T., Wang, Y. H., Griffith, J. D., Reinberg, D., and Ebright, R. H. (1997). Trajectory of DNA in the RNA polymerase II transcription preinitiation complex. Proc Natl Acad Sci U S A *94*, 12268-12273.

Kim, Y. C., Lee, M. H., Ryu, S. S., Kim, J. H., and Koo, H. S. (2002c). Coaction of DNA topoisomerase IIIalpha and a RecQ homologue during the germ-line mitosis in Caenorhabditis elegans. Genes Cells *7*, 19-27.

Kimble, J., Edgar, L., and Hirsh, D. (1984). Specification of male development in Caenorhabditis elegans: the fem genes. Dev Biol *105*, 234-239.

Kimble, J., and Hirsh, D. (1979). The postembryonic cell lineages of the hermaphrodite and male gonads in Caenorhabditis elegans. Dev Biol *70*, 396-417.

Kimura, K. D., Tissenbaum, H. A., Liu, Y., and Ruvkun, G. (1997). daf-2, an insulin receptor-like gene that regulates longevity and diapause in Caenorhabditis elegans. Science *277*, 942-946.

Klass, M., and Hirsh, D. (1976). Non-ageing developmental variant of Caenorhabditis elegans. Nature *260*, 523-525.

Klungland, A., and Lindahl, T. (1997). Second pathway for completion of human DNA base excision-repair: reconstitution with purified proteins and requirement for DNase IV (FEN1). Embo J *16*, 3341-3348.

Kobayashi, T., and Cohen, P. (1999). Activation of serum- and glucocorticoid-regulated protein kinase by agonists that activate phosphatidylinositide 3-kinase is mediated by 3-phosphoinositide-dependent protein kinase-1 (PDK1) and PDK2. Biochem J *339 (Pt 2)*, 319-328.

Komeili, A., Wedaman, K. P., O'Shea, E. K., and Powers, T. (2000). Mechanism of metabolic control. Target of rapamycin signaling links nitrogen quality to the activity of the Rtg1 and Rtg3 transcription factors. J Cell Biol *151*, 863-878.

Kondo, M., Yanase, S., Ishii, T., Hartman, P. S., Matsumoto, K., and Ishii, N. (2005). The p38 signal transduction pathway participates in the oxidative stress-mediated translocation of DAF-16 to Caenorhabditis elegans nuclei. Mech Ageing Dev *126*, 642-647.

Kops, G. J., and Burgering, B. M. (1999). Forkhead transcription factors: new insights into protein kinase B (c-akt) signaling. J Mol Med *77*, 656-665.

Kops, G. J., and Burgering, B. M. (2000). Forkhead transcription factors are targets of signalling by the proto-oncogene PKB (C-AKT). J Anat *197 Pt 4*, 571-574.

Kops, G. J., Dansen, T. B., Polderman, P. E., Saarloos, I., Wirtz, K. W., Coffer, P. J., Huang, T. T., Bos, J. L., Medema, R. H., and Burgering, B. M. (2002). Forkhead transcription factor FOXO3a protects quiescent cells from oxidative stress. Nature *419*, 316-321.

Korf, I., Fan, Y., and Strome, S. (1998). The Polycomb group in Caenorhabditis elegans and maternal control of germline development. Development *125*, 2469-2478.
Kostic, I., Li, S., and Roy, R. (2003). cki-1 links cell division and cell fate acquisition in the C. elegans somatic gonad. Dev Biol *263*, 242-252.

Kostich, M., Fire, A., and Fambrough, D. M. (2000). Identification and molecular-genetic characterization of a LAMP/CD68-like protein from Caenorhabditis elegans. J Cell Sci *113 (Pt 14)*, 2595-2606.

Koundrioukoff, S., Polo, S., and Almouzni, G. (2004). Interplay between chromatin and cell cycle checkpoints in the context of ATR/ATM-dependent checkpoints. DNA Repair (Amst) *3*, 969-978.

Kozma, S. C., and Thomas, G. (2002). Regulation of cell size in growth, development and human disease: PI3K, PKB and S6K. Bioessays *24*, 65-71.

Kraemer, B., Crittenden, S., Gallegos, M., Moulder, G., Barstead, R., Kimble, J., and Wickens, M. (1999). NANOS-3 and FBF proteins physically interact to control the sperm-oocyte switch in Caenorhabditis elegans. Curr Biol *9*, 1009-1018.

Krogan, N. J., Dover, J., Wood, A., Schneider, J., Heidt, J., Boateng, M. A., Dean, K., Ryan, O. W., Golshani, A., Johnston, M.*, et al.* (2003). The Paf1 complex is required for histone H3 methylation by COMPASS and Dot1p: linking transcriptional elongation to histone methylation. Mol Cell *11*, 721-729.

Krymskaya, V. P. (2003). Tumour suppressors hamartin and tuberin: intracellular signalling. Cell Signal *15*, 729-739.

Kubota, H., Obata, T., Ota, K., Sasaki, T., and Ito, T. (2003). Rapamycin-induced translational derepression of GCN4 mRNA involves a novel mechanism for activation of the eIF2 alpha kinase GCN2. J Biol Chem *278*, 20457-20460.

Kubota, H., Ota, K., Sakaki, Y., and Ito, T. (2001). Budding yeast GCN1 binds the GI domain to activate the eIF2alpha kinase GCN2. J Biol Chem *276*, 17591-17596.

Kucherlapati, M., Yang, K., Kuraguchi, M., Zhao, J., Lia, M., Heyer, J., Kane, M. F., Fan, K., Russell, R., Brown, A. M.*, et al.* (2002). Haploinsufficiency of Flap endonuclease (Fen1) leads to rapid tumor progression. Proc Natl Acad Sci U S A *99*, 9924-9929.

Kumar, V., Sabatini, D., Pandey, P., Gingras, A. C., Majumder, P. K., Kumar, M., Yuan, Z. M., Carmichael, G., Weichselbaum, R., Sonenberg, N.*, et al.* (2000). Regulation of the rapamycin and FKBP-target 1/mammalian target of rapamycin and cap-dependent initiation of translation by the c-Abl protein-tyrosine kinase. J Biol Chem *275*, 10779-10787.

Kunz, J., Henriquez, R., Schneider, U., Deuter-Reinhard, M., Movva, N. R., and Hall, M. N. (1993). Target of rapamycin in yeast, TOR2, is an essential phosphatidylinositol kinase homolog required for G1 progression. Cell *73*, 585-596.

Kuo, M. H., vom Baur, E., Struhl, K., and Allis, C. D. (2000). Gcn4 activator targets Gcn5 histone acetyltransferase to specific promoters independently of transcription. Mol Cell *6*, 1309-1320.

Kurz, E. U., and Lees-Miller, S. P. (2004). DNA damage-induced activation of ATM and ATM-dependent signaling pathways. DNA Repair (Amst) *3*, 889-900.

Kuznicki, K. A., Smith, P. A., Leung-Chiu, W. M., Estevez, A. O., Scott, H. C., and Bennett, K. L. (2000). Combinatorial RNA interference indicates GLH-4 can compensate for GLH-1; these two P granule components are critical for fertility in C. elegans. Development *127*, 2907-2916.

Labrousse, A. M., Zappaterra, M. D., Rube, D. A., and van der Bliek, A. M. (1999). C. elegans dynamin-related protein DRP-1 controls severing of the mitochondrial outer membrane. Mol Cell *4*, 815-826.

Lambie, E. J., and Kimble, J. (1991). Two homologous regulatory genes, lin-12 and glp-1, have overlapping functions. Development *112*, 231-240.

Lane, D. P. (1992). Worrying about p53. Curr Biol *2*, 581-583.

Larsen, P. L. (1993). Aging and resistance to oxidative damage in Caenorhabditis elegans. Proc Natl Acad Sci U S A *90*, 8905-8909.

Lawrence, J. C., Jr., and Abraham, R. T. (1997). PHAS/4E-BPs as regulators of mRNA translation and cell proliferation. Trends Biochem Sci *22*, 345-349.

Lazaris-Karatzas, A., Smith, M. R., Frederickson, R. M., Jaramillo, M. L., Liu, Y. L., Kung, H. F., and Sonenberg, N. (1992). Ras mediates translation initiation factor 4E-induced malignant transformation. Genes Dev *6*, 1631-1642.

Lee, J. H., and Paull, T. T. (2004). Direct activation of the ATM protein kinase by the Mre11/Rad50/Nbs1 complex. Science *304*, 93-96.

Lee, M. H., Han, S. M., Han, J. W., Kim, Y. M., Ahnn, J., and Koo, H. S. (2003a). Caenorhabditis elegans dna-2 is involved in DNA repair and is essential for germ-line development. FEBS Lett *555*, 250-256.

Lee, M. H., and Schedl, T. (2001). Identification of in vivo mRNA targets of GLD-1, a maxi-KH motif containing protein required for C. elegans germ cell development. Genes Dev *15*, 2408-2420.

Lee, S. J., Schwartz, M. F., Duong, J. K., and Stern, D. F. (2003b). Rad53 phosphorylation site clusters are important for Rad53 regulation and signaling. Mol Cell Biol *23*, 6300-6314.

Lee, S. S., and Ruvkun, G. (2002). Longevity: don't hold your breath. Nature *418*, 287-288.

Leibiger, B., Moede, T., Schwarz, T., Brown, G. R., Kohler, M., Leibiger, I. B., and Berggren, P. O. (1998). Short-term regulation of insulin gene transcription by glucose. Proc Natl Acad Sci U S A *95*, 9307-9312.

Leicht, M., Simm, A., Bertsch, G., and Hoppe, J. (1996). Okadaic acid induces cellular hypertrophy in AKR-2B fibroblasts: involvement of the p70S6 kinase in the onset of protein and rRNA synthesis. Cell Growth Differ *7*, 1199-1209.

Leroux, M. R., Fandrich, M., Klunker, D., Siegers, K., Lupas, A. N., Brown, J. R., Schiebel, E., Dobson, C. M., and Hartl, F. U. (1999). MtGimC, a novel archaeal chaperone related to the eukaryotic chaperonin cofactor GimC/prefoldin. Embo J *18*, 6730-6743.

Lettre, G., Kritikou, E. A., Jaeggi, M., Calixto, A., Fraser, A. G., Kamath, R. S., Ahringer, J., and Hengartner, M. O. (2004). Genome-wide RNAi identifies p53-dependent and -independent regulators of germ cell apoptosis in C. elegans. Cell Death Differ *11*, 1198-1203.

Li, W., Kennedy, S. G., and Ruvkun, G. (2003). daf-28 encodes a C. elegans insulin superfamily member that is regulated by environmental cues and acts in the DAF-2 signaling pathway. Genes Dev *17*, 844-858.

Liaw, D., Marsh, D. J., Li, J., Dahia, P. L., Wang, S. I., Zheng, Z., Bose, S., Call, K. M., Tsou, H. C., Peacocke, M.*, et al.* (1997). Germline mutations of the PTEN gene in Cowden disease, an inherited breast and thyroid cancer syndrome. Nat Genet *16*, 64-67.

Libina, N., Berman, J. R., and Kenyon, C. (2003). Tissue-specific activities of C. elegans DAF-16 in the regulation of lifespan. Cell *115*, 489-502.

Lieber, M. R. (1997). The FEN-1 family of structure-specific nucleases in eukaryotic DNA replication, recombination and repair. Bioessays *19*, 233-240.

Lim, D. S., Vogel, H., Willerford, D. M., Sands, A. T., Platt, K. A., and Hasty, P. (2000). Analysis of ku80-mutant mice and cells with deficient levels of p53. Mol Cell Biol *20*, 3772-3780.

Lin, K., Dorman, J. B., Rodan, A., and Kenyon, C. (1997a). daf-16: An HNF-3/forkhead family member that can function to double the life-span of Caenorhabditis elegans. Science *278*, 1319-1322.

Lin, K., Hsin, H., Libina, N., and Kenyon, C. (2001). Regulation of the Caenorhabditis elegans longevity protein DAF-16 by insulin/IGF-1 and germline signaling. Nat Genet *28*, 139-145.

Lin, T. A., Kong, X., Haystead, T. A., Pause, A., Belsham, G., Sonenberg, N., and Lawrence, J. C., Jr. (1994). PHAS-I as a link between mitogen-activated protein kinase and translation initiation. Science *266*, 653-656.

Lin, Y., Nomura, T., Cheong, J., Dorjsuren, D., Iida, K., and Murakami, S. (1997b). Hepatitis B virus X protein is a transcriptional modulator that communicates with transcription factor IIB and the RNA polymerase II subunit 5. J Biol Chem *272*, 7132-7139.

Lin, Y., Tang, H., Nomura, T., Dorjsuren, D., Hayashi, N., Wei, W., Ohta, T., Roeder, R., and Murakami, S. (1998). The hepatitis B virus X protein is a co-activator of activated transcription that modulates the transcription machinery and distal binding activators. J Biol Chem *273*, 27097-27103.

Lindahl, T., and Wood, R. D. (1999). Quality control by DNA repair. Science *286*, 1897-1905.

Lisby, M., Antunez de Mayolo, A., Mortensen, U. H., and Rothstein, R. (2003). Cell cycle-regulated centers of DNA double-strand break repair. Cell Cycle *2*, 479-483.

Lisby, M., Barlow, J. H., Burgess, R. C., and Rothstein, R. (2004). Choreography of the DNA damage response: spatiotemporal relationships among checkpoint and repair proteins. Cell *118*, 699-713.

Lisby, M., and Rothstein, R. (2004). DNA repair: keeping it together. Curr Biol *14*, R994-996.

Lisby, M., and Rothstein, R. (2005). Localization of checkpoint and repair proteins in eukaryotes. Biochimie *87*, 579-589.

Lisztwan, J., Marti, A., Sutterluty, H., Gstaiger, M., Wirbelauer, C., and Krek, W. (1998). Association of human CUL-1 and ubiquitin-conjugating enzyme CDC34 with the F-box protein p45(SKP2): evidence for evolutionary conservation in the subunit composition of the CDC34-SCF pathway. Embo J *17*, 368-383.

Lithgow, G. J., White, T. M., Hinerfeld, D. A., and Johnson, T. E. (1994). Thermotolerance of a long-lived mutant of Caenorhabditis elegans. J Gerontol *49*, B270-276.

Lithgow, G. J., White, T. M., Melov, S., and Johnson, T. E. (1995). Thermotolerance and extended life-span conferred by single-gene mutations and induced by thermal stress. Proc Natl Acad Sci U S A *92*, 7540-7544.

Liu, Q. A., and Hengartner, M. O. (1999). The molecular mechanism of programmed cell death in C. elegans. Ann N Y Acad Sci *887*, 92-104.

Llorca, O., Smyth, M. G., Carrascosa, J. L., Willison, K. R., Radermacher, M., Steinbacher, S., and Valpuesta, J. M. (1999). 3D reconstruction of the ATP-bound form of CCT reveals the asymmetric folding conformation of a type II chaperonin. Nat Struct Biol *6*, 639-642.

Loewith, R., Jacinto, E., Wullschleger, S., Lorberg, A., Crespo, J. L., Bonenfant, D., Oppliger, W., Jenoe, P., and Hall, M. N. (2002). Two TOR complexes, only one of which is rapamycin sensitive, have distinct roles in cell growth control. Mol Cell *10*, 457-468.
Lohman, T. M., and Bjornson, K. P. (1996). Mechanisms of helicase-catalyzed DNA unwinding. Annu Rev Biochem *65*, 169-214.

Long, X., Lin, Y., Ortiz-Vega, S., Yonezawa, K., and Avruch, J. (2005). Rheb binds and regulates the mTOR kinase. Curr Biol *15*, 702-713.

Long, X., Spycher, C., Han, Z. S., Rose, A. M., Muller, F., and Avruch, J. (2002). TOR deficiency in C. elegans causes developmental arrest and intestinal atrophy by inhibition of mRNA translation. Curr Biol *12*, 1448-1461.

Lu, X., and Horvitz, H. R. (1998). lin-35 and lin-53, two genes that antagonize a C. elegans Ras pathway, encode proteins similar to Rb and its binding protein RbAp48. Cell *95*, 981-991.

Lundin, V. F., Stirling, P. C., Gomez-Reino, J., Mwenifumbo, J. C., Obst, J. M., Valpuesta, J. M., and Leroux, M. R. (2004). Molecular clamp mechanism of substrate binding by hydrophobic coiled-coil residues of the archaeal chaperone prefoldin. Proc Natl Acad Sci U S A *101*, 4367-4372.

Machaca, K., and L'Hernault, S. W. (1997). The Caenorhabditis elegans spe-5 gene is required for morphogenesis of a sperm-specific organelle and is associated with an inherent cold-sensitive phenotype. Genetics *146*, 567-581.

Maehama, T., and Dixon, J. E. (1998). The tumor suppressor, PTEN/MMAC1, dephosphorylates the lipid second messenger, phosphatidylinositol 3,4,5-trisphosphate. J Biol Chem *273*, 13375-13378.

Magnaghi-Jaulin, L., Groisman, R., Naguibneva, I., Robin, P., Lorain, S., Le Villain, J. P., Troalen, F., Trouche, D., and Harel-Bellan, A. (1998). Retinoblastoma protein represses transcription by recruiting a histone deacetylase. Nature *391*, 601-605.

Mahajan, P. B. (1994). Modulation of transcription of rRNA genes by rapamycin. Int J Immunopharmacol *16*, 711-721.

Majka, J., and Burgers, P. M. (2004). The PCNA-RFC families of DNA clamps and clamp loaders. Prog Nucleic Acid Res Mol Biol *78*, 227-260.

Makino, Y., Mimori, T., Koike, C., Kanemaki, M., Kurokawa, Y., Inoue, S., Kishimoto, T., and Tamura, T. (1998). TIP49, homologous to the bacterial DNA helicase RuvB, acts as an autoantigen in human. Biochem Biophys Res Commun *245*, 819-823.

Malone, E. A., Inoue, T., and Thomas, J. H. (1996). Genetic analysis of the roles of daf-28 and age-1 in regulating Caenorhabditis elegans dauer formation. Genetics *143*, 1193-1205.
Malone, E. A., and Thomas, J. H. (1994). A screen for nonconditional dauer-constitutive mutations in Caenorhabditis elegans. Genetics *136*, 879-886.

Manning, B. D., and Cantley, L. C. (2003). Rheb fills a GAP between TSC and TOR. Trends Biochem Sci *28*, 573-576.

Marin, V. A., and Evans, T. C. (2003). Translational repression of a C. elegans Notch mRNA by the STAR/KH domain protein GLD-1. Development *130*, 2623-2632.

Martin, J., Gruber, M., and Lupas, A. N. (2004). Coiled coils meet the chaperone world. Trends Biochem Sci *29*, 455-458.

Martin-Benito, J., Boskovic, J., Gomez-Puertas, P., Carrascosa, J. L., Simons, C. T., Lewis, S. A., Bartolini, F., Cowan, N. J., and Valpuesta, J. M. (2002). Structure of eukaryotic prefoldin and of its complexes with unfolded actin and the cytosolic chaperonin CCT. Embo J *21*, 6377-6386.

Marton, M. J., Vazquez de Aldana, C. R., Qiu, H., Chakraburtty, K., and Hinnebusch, A. G. (1997). Evidence that GCN1 and GCN20, translational regulators of GCN4, function on elongating ribosomes in activation of eIF2alpha kinase GCN2. Mol Cell Biol *17*, 4474-4489.

Matson, S. W., and Kaiser-Rogers, K. A. (1990). DNA helicases. Annu Rev Biochem *59*, 289-329.

Matsuo, R., Kubota, H., Obata, T., Kito, K., Ota, K., Kitazono, T., Ibayashi, S., Sasaki, T., Iida, M., and Ito, T. (2005). The yeast eIF4E-associated protein Eap1p attenuates GCN4 translation upon TOR-inactivation. FEBS Lett *579*, 2433-2438.

Matsuzaki, H., Daitoku, H., Hatta, M., Tanaka, K., and Fukamizu, A. (2003). Insulin-induced phosphorylation of FKHR (Foxo1) targets to proteasomal degradation. Proc Natl Acad Sci U S A *100*, 11285-11290.

Matyash, V., Geier, C., Henske, A., Mukherjee, S., Hirsh, D., Thiele, C., Grant, B., Maxfield, F. R., and Kurzchalia, T. V. (2001). Distribution and transport of cholesterol in Caenorhabditis elegans. Mol Biol Cell *12*, 1725-1736.

McCarter, J., Bartlett, B., Dang, T., and Schedl, T. (1997). Soma-germ cell interactions in Caenorhabditis elegans: multiple events of hermaphrodite germline development require the somatic sheath and spermathecal lineages. Dev Biol *181*, 121-143.

McCarter, J., Bartlett, B., Dang, T., and Schedl, T. (1999). On the control of oocyte meiotic maturation and ovulation in Caenorhabditis elegans. Dev Biol *205*, 111-128.
McGowan, C. H., and Russell, P. (2004). The DNA damage response: sensing and signaling. Curr Opin Cell Biol *16*, 629-633.

Mecocci, P., Polidori, M. C., Troiano, L., Cherubini, A., Cecchetti, R., Pini, G., Straatman, M., Monti, D., Stahl, W., Sies, H.*, et al.* (2000). Plasma antioxidants and longevity: a study on healthy centenarians. Free Radic Biol Med *28*, 1243-1248.

Medema, R. H., Kops, G. J., Bos, J. L., and Burgering, B. M. (2000). AFX-like Forkhead transcription factors mediate cell-cycle regulation by Ras and PKB through p27kip1. Nature *404*, 782-787.

Melendez, A., Talloczy, Z., Seaman, M., Eskelinen, E. L., Hall, D. H., and Levine, B. (2003). Autophagy genes are essential for dauer development and life-span extension in C. elegans. Science *301*, 1387-1391.

Meyuhas, O. (2000). Synthesis of the translational apparatus is regulated at the translational level. Eur J Biochem *267*, 6321-6330.

Miron, M., Verdu, J., Lachance, P. E., Birnbaum, M. J., Lasko, P. F., and Sonenberg, N. (2001). The translational inhibitor 4E-BP is an effector of PI(3)K/Akt signalling and cell growth in Drosophila. Nat Cell Biol *3*, 596-601.

Mitchison, J. M., and Creanor, J. (1971). Induction synchrony in the fission yeast. Schizosaccharomyces pombe. Exp Cell Res *67*, 368-374.

Miyashita, T., and Reed, J. C. (1995). Tumor suppressor p53 is a direct transcriptional activator of the human bax gene. Cell *80*, 293-299.

Mochan, T. A., Venere, M., DiTullio, R. A., Jr., and Halazonetis, T. D. (2003). 53BP1 and NFBD1/MDC1-Nbs1 function in parallel interacting pathways activating ataxia-telangiectasia mutated (ATM) in response to DNA damage. Cancer Res *63*, 8586-8591.

Monti, D., Salvioli, S., Capri, M., Malorni, W., Straface, E., Cossarizza, A., Botti, B., Piacentini, M., Baggio, G., Barbi, C.*, et al.* (2000). Decreased susceptibility to oxidative stress-induced apoptosis of peripheral blood mononuclear cells from healthy elderly and centenarians. Mech Ageing Dev *121*, 239-250.

Morris, J. Z., Tissenbaum, H. A., and Ruvkun, G. (1996). A phosphatidylinositol-3-OH kinase family member regulating longevity and diapause in Caenorhabditis elegans. Nature *382*, 536-539.

Morrison, A. J., and Shen, X. (2005). DNA Repair in the Context of Chromatin. Cell Cycle *4*.

Motoyama, N., and Naka, K. (2004). DNA damage tumor suppressor genes and genomic instability. Curr Opin Genet Dev *14*, 11-16.

Mueller, C. L., and Jaehning, J. A. (2002). Ctr9, Rtf1, and Leo1 are components of the Paf1/RNA polymerase II complex. Mol Cell Biol *22*, 1971-1980.

Mueller, C. L., Porter, S. E., Hoffman, M. G., and Jaehning, J. A. (2004). The Paf1 complex has functions independent of actively transcribing RNA polymerase II. Mol Cell *14*, 447-456.

Mueller, P. P., and Hinnebusch, A. G. (1986). Multiple upstream AUG codons mediate translational control of GCN4. Cell *45*, 201-207.

Mullenders, L. H., and Berneburg, M. (2001). Photoimmunology and nucleotide excision repair: impact of transcription coupled and global genome excision repair. J Photochem Photobiol B *65*, 97-100.

Mumm, J. S., and Kopan, R. (2000). Notch signaling: from the outside in. Dev Biol *228*, 151-165.

Murakami, S., and Johnson, T. E. (1996). A genetic pathway conferring life extension and resistance to UV stress in Caenorhabditis elegans. Genetics *143*, 1207-1218.

Murakami, S., and Johnson, T. E. (1998). Life extension and stress resistance in Caenorhabditis elegans modulated by the tkr-1 gene. Curr Biol *8*, 1091-1094.

Murante, R. S., Henricksen, L. A., and Bambara, R. A. (1998). Junction ribonuclease: an activity in Okazaki fragment processing. Proc Natl Acad Sci U S A *95*, 2244-2249.

Murphy, C. T., McCarroll, S. A., Bargmann, C. I., Fraser, A., Kamath, R. S., Ahringer, J., Li, H., and Kenyon, C. (2003). Genes that act downstream of DAF-16 to influence the lifespan of Caenorhabditis elegans. Nature *424*, 277-283.

Nakae, J., Barr, V., and Accili, D. (2000). Differential regulation of gene expression by insulin and IGF-1 receptors correlates with phosphorylation of a single amino acid residue in the forkhead transcription factor FKHR. Embo J *19*, 989-996.

Nakae, J., Park, B. C., and Accili, D. (1999). Insulin stimulates phosphorylation of the forkhead transcription factor FKHR on serine 253 through a Wortmannin-sensitive pathway. J Biol Chem *274*, 15982-15985.

Nakano, K., and Vousden, K. H. (2001). PUMA, a novel proapoptotic gene, is induced by p53. Mol Cell *7*, 683-694.

Natarajan, K., Meyer, M. R., Jackson, B. M., Slade, D., Roberts, C., Hinnebusch, A. G., and Marton, M. J. (2001). Transcriptional profiling shows that Gcn4p is a master regulator of gene expression during amino acid starvation in yeast. Mol Cell Biol *21*, 4347-4368.

Nathan, C. A., Liu, L., Li, B. D., Abreo, F. W., Nandy, I., and De Benedetti, A. (1997). Detection of the proto-oncogene eIF4E in surgical margins may predict recurrence in head and neck cancer. Oncogene *15*, 579-584.

Nef, S., and Parada, L. F. (2000). Hormones in male sexual development. Genes Dev *14*, 3075-3086.

Nelson, G. A., Lew, K. K., and Ward, S. (1978). Intersex, a temperature-sensitive mutant of the nematode Caenorhabditis elegans. Dev Biol *66*, 386-409.

Neufeld, T. P., de la Cruz, A. F., Johnston, L. A., and Edgar, B. A. (1998). Coordination of growth and cell division in the Drosophila wing. Cell *93*, 1183-1193.

Ng, H. H., Dole, S., and Struhl, K. (2003). The Rtf1 component of the Paf1 transcriptional elongation complex is required for ubiquitination of histone H2B. J Biol Chem *278*, 33625-33628.

Nicoll, M., Akerib, C. C., and Meyer, B. J. (1997). X-chromosome-counting mechanisms that determine nematode sex. Nature *388*, 200-204.

Noda, T., and Ohsumi, Y. (1998). Tor, a phosphatidylinositol kinase homologue, controls autophagy in yeast. J Biol Chem *273*, 3963-3966.

Nojima, H., Tokunaga, C., Eguchi, S., Oshiro, N., Hidayat, S., Yoshino, K., Hara, K., Tanaka, N., Avruch, J., and Yonezawa, K. (2003). The mammalian target of rapamycin (mTOR) partner, raptor, binds the mTOR substrates p70 S6 kinase and 4E-BP1 through their TOR signaling (TOS) motif. J Biol Chem *278*, 15461-15464.

Nyberg, K. A., Michelson, R. J., Putnam, C. W., and Weinert, T. A. (2002). Toward maintaining the genome: DNA damage and replication checkpoints. Annu Rev Genet *36*, 617-656.

Oakley, G. G., Patrick, S. M., Yao, J., Carty, M. P., Turchi, J. J., and Dixon, K. (2003). RPA phosphorylation in mitosis alters DNA binding and protein-protein interactions. Biochemistry *42*, 3255-3264.

Odorico, J. S., and Sollinger, H. W. (2002). Technical and immunosuppressive advances in transplantation for insulin-dependent diabetes mellitus. World J Surg *26*, 194-211.

Ogawa, H., Harada, S., Sassa, T., Yamamoto, H., and Hosono, R. (1998). Functional properties of the unc-64 gene encoding a Caenorhabditis elegans syntaxin. J Biol Chem *273*, 2192-2198.

Ogg, S., Paradis, S., Gottlieb, S., Patterson, G. I., Lee, L., Tissenbaum, H. A., and Ruvkun, G. (1997). The Fork head transcription factor DAF-16 transduces insulin-like metabolic and longevity signals in C. elegans. Nature *389*, 994-999.

Ogg, S., and Ruvkun, G. (1998). The C. elegans PTEN homolog, DAF-18, acts in the insulin receptor-like metabolic signaling pathway. Mol Cell *2*, 887-893.

Okochi, M., Nomura, T., Zako, T., Arakawa, T., Iizuka, R., Ueda, H., Funatsu, T., Leroux, M., and Yohda, M. (2004). Kinetics and binding sites for interaction of the prefoldin with a group II chaperonin: contiguous non-native substrate and chaperonin binding sites in the archaeal prefoldin. J Biol Chem *279*, 31788-31795.

Okochi, M., Yoshida, T., Maruyama, T., Kawarabayasi, Y., Kikuchi, H., and Yohda, M. (2002). Pyrococcus prefoldin stabilizes protein-folding intermediates and transfers them to chaperonins for correct folding. Biochem Biophys Res Commun *291*, 769-774.

Oldham, S., and Hafen, E. (2003). Insulin/IGF and target of rapamycin signaling: a TOR de force in growth control. Trends Cell Biol *13*, 79-85.

Oldham, S., Montagne, J., Radimerski, T., Thomas, G., and Hafen, E. (2000). Genetic and biochemical characterization of dTOR, the Drosophila homolog of the target of rapamycin. Genes Dev *14*, 2689-2694.

Ookuma, S., Fukuda, M., and Nishida, E. (2003). Identification of a DAF-16 transcriptional target gene, scl-1, that regulates longevity and stress resistance in Caenorhabditis elegans. Curr Biol *13*, 427-431.

Osborn, A. J., Elledge, S. J., and Zou, L. (2002). Checking on the fork: the DNA-replication stress-response pathway. Trends Cell Biol *12*, 509-516.

Palancade, B., and Bensaude, O. (2003). Investigating RNA polymerase II carboxyl-terminal domain (CTD) phosphorylation. Eur J Biochem *270*, 3859-3870.

Paolisso, G., Tagliamonte, M. R., Rizzo, M. R., Manzella, D., Gambardella, A., and Varricchio, M. (1998). Oxidative stress and advancing age: results in healthy centenarians. J Am Geriatr Soc *46*, 833-838.

Paradis, S., Ailion, M., Toker, A., Thomas, J. H., and Ruvkun, G. (1999). A PDK1 homolog is necessary and sufficient to transduce AGE-1 PI3 kinase signals that regulate diapause in Caenorhabditis elegans. Genes Dev *13*, 1438-1452.

Paradis, S., and Ruvkun, G. (1998). Caenorhabditis elegans Akt/PKB transduces insulin receptor-like signals from AGE-1 PI3 kinase to the DAF-16 transcription factor. Genes Dev *12*, 2488-2498.

Pardee, A. B. (1974). A restriction point for control of normal animal cell proliferation. Proc Natl Acad Sci U S A *71*, 1286-1290.

Parrilla-Castellar, E. R., Arlander, S. J., and Karnitz, L. (2004). Dial 9-1-1 for DNA damage: the Rad9-Hus1-Rad1 (9-1-1) clamp complex. DNA Repair (Amst) *3*, 1009-1014.
Parry, P., Wei, Y., and Evans, G. (1994). Cloning and characterization of the t(X;11) breakpoint from a leukemic cell line identify a new member of the forkhead gene family. Genes Chromosomes Cancer *11*, 79-84.

Parsons, C. A., Stasiak, A., Bennett, R. J., and West, S. C. (1995). Structure of a multisubunit complex that promotes DNA branch migration. Nature *374*, 375-378.
Patel, M. N., Knight, C. G., Karageorgi, C., and Leroi, A. M. (2002). Evolution of germ-line signals that regulate growth and aging in nematodes. Proc Natl Acad Sci U S A *99*, 769-774.

Patel, P. H., Thapar, N., Guo, L., Martinez, M., Maris, J., Gau, C. L., Lengyel, J. A., and Tamanoi, F. (2003). Drosophila Rheb GTPase is required for cell cycle progression and cell growth. J Cell Sci *116*, 3601-3610.

Pause, A., Belsham, G. J., Gingras, A. C., Donze, O., Lin, T. A., Lawrence, J. C., Jr., and Sonenberg, N. (1994). Insulin-dependent stimulation of protein synthesis by phosphorylation of a regulator of 5'-cap function. Nature *371*, 762-767.

Peng, C. Y., Graves, P. R., Thoma, R. S., Wu, Z., Shaw, A. S., and Piwnica-Worms, H. (1997). Mitotic and G2 checkpoint control: regulation of 14-3-3 protein binding by phosphorylation of Cdc25C on serine-216. Science *277*, 1501-1505.

Pierce, S. B., Costa, M., Wisotzkey, R., Devadhar, S., Homburger, S. A., Buchman, A. R., Ferguson, K. C., Heller, J., Platt, D. M., Pasquinelli, A. A*., et al.* (2001). Regulation of DAF-2 receptor signaling by human insulin and ins-1, a member of the unusually large and diverse C. elegans insulin gene family. Genes Dev *15*, 672-686.

Pitt, J. N., Schisa, J. A., and Priess, J. R. (2000). P granules in the germ cells of Caenorhabditis elegans adults are associated with clusters of nuclear pores and contain RNA. Dev Biol *219*, 315-333.

Pizzolato, J. F., and Saltz, L. B. (2003). The camptothecins. Lancet *361*, 2235-2242.
Plath, K., Fang, J., Mlynarczyk-Evans, S. K., Cao, R., Worringer, K. A., Wang, H., de la Cruz, C. C., Otte, A. P., Panning, B., and Zhang, Y. (2003). Role of histone H3 lysine 27 methylation in X inactivation. Science *300*, 131-135.

Pokholok, D. K., Hannett, N. M., and Young, R. A. (2002). Exchange of RNA polymerase II initiation and elongation factors during gene expression in vivo. Mol Cell *9*, 799-809.

Porte, D., Jr., Baskin, D. G., and Schwartz, M. W. (2005). Insulin signaling in the central nervous system: a critical role in metabolic homeostasis and disease from C. elegans to humans. Diabetes *54*, 1264-1276.

Porter, S. E., Washburn, T. M., Chang, M., and Jaehning, J. A. (2002). The yeast pafl-rNA polymerase II complex is required for full expression of a subset of cell cycle-regulated genes. Eukaryot Cell *1*, 830-842.

Potter, C. J., and Xu, T. (2001). Mechanisms of size control. Curr Opin Genet Dev *11*, 279-286.

Poulin, F., Gingras, A. C., Olsen, H., Chevalier, S., and Sonenberg, N. (1998). 4E-BP3, a new member of the eukaryotic initiation factor 4E-binding protein family. J Biol Chem *273*, 14002-14007.

Powers, T., and Walter, P. (1999). Regulation of ribosome biogenesis by the rapamycin-sensitive TOR-signaling pathway in Saccharomyces cerevisiae. Mol Biol Cell *10*, 987-1000.

Pradhan, S., Bacolla, A., Wells, R. D., and Roberts, R. J. (1999). Recombinant human DNA (cytosine-5) methyltransferase. I. Expression, purification, and comparison of de novo and maintenance methylation. J Biol Chem *274*, 33002-33010.

Prescott, D. M. (1976). The cell cycle and the control of cellular reproduction. Adv Genet *18*, 99-177.

Proud, C. G. (2004). The multifaceted role of mTOR in cellular stress responses. DNA Repair (Amst) *3*, 927-934.

Puig, O., Marr, M. T., Ruhf, M. L., and Tjian, R. (2003). Control of cell number by Drosophila FOXO: downstream and feedback regulation of the insulin receptor pathway. Genes Dev *17*, 2006-2020.

Pullen, N., and Thomas, G. (1997). The modular phosphorylation and activation of p70s6k. FEBS Lett *410*, 78-82.

Puoti, A., Gallegos, M., Zhang, B., Wickens, M. P., and Kimble, J. (1997). Controls of cell fate and pattern by 3' untranslated regions: the Caenorhabditis elegans sperm/oocyte decision. Cold Spring Harb Symp Quant Biol *62*, 19-24.

Qiu, H., Dong, J., Hu, C., Francklyn, C. S., and Hinnebusch, A. G. (2001). The tRNA-binding moiety in GCN2 contains a dimerization domain that interacts with the kinase domain and is required for tRNA binding and kinase activation. Embo J *20*, 1425-1438.

Qiu, H., Hu, C., Dong, J., and Hinnebusch, A. G. (2002). Mutations that bypass tRNA binding activate the intrinsically defective kinase domain in GCN2. Genes Dev *16*, 1271-1280.

Qiu, X. B., Lin, Y. L., Thome, K. C., Pian, P., Schlegel, B. P., Weremowicz, S., Parvin, J. D., and Dutta, A. (1998). An eukaryotic RuvB-like protein (RUVBL1) essential for growth. J Biol Chem *273*, 27786-27793.

Rafferty, J. B., Sedelnikova, S. E., Hargreaves, D., Artymiuk, P. J., Baker, P. J., Sharples, G. J., Mahdi, A. A., Lloyd, R. G., and Rice, D. W. (1996). Crystal structure of DNA recombination protein RuvA and a model for its binding to the Holliday junction. Science *274*, 415-421.

Ramaswamy, S., Nakamura, N., Sansal, I., Bergeron, L., and Sellers, W. R. (2002). A novel mechanism of gene regulation and tumor suppression by the transcription factor FKHR. Cancer Cell *2*, 81-91.

Raught, B., Gingras, A. C., Gygi, S. P., Imataka, H., Morino, S., Gradi, A., Aebersold, R., and Sonenberg, N. (2000). Serum-stimulated, rapamycin-sensitive phosphorylation sites in the eukaryotic translation initiation factor 4GI. Embo J *19*, 434-444.

Raught, B., Gingras, A. C., and Sonenberg, N. (2001). The target of rapamycin (TOR) proteins. Proc Natl Acad Sci U S A *98*, 7037-7044.

Reagan, M. S., Pittenger, C., Siede, W., and Friedberg, E. C. (1995). Characterization of a mutant strain of Saccharomyces cerevisiae with a deletion of the RAD27 gene, a structural homolog of the RAD2 nucleotide excision repair gene. J Bacteriol *177*, 364-371.

Reddy, K. C., and Villeneuve, A. M. (2004). C. elegans HIM-17 links chromatin modification and competence for initiation of meiotic recombination. Cell *118*, 439-452.

Rena, G., Guo, S., Cichy, S. C., Unterman, T. G., and Cohen, P. (1999). Phosphorylation of the transcription factor forkhead family member FKHR by protein kinase B. J Biol Chem *274*, 17179-17183.

Rhind, N., Furnari, B., and Russell, P. (1997). Cdc2 tyrosine phosphorylation is required for the DNA damage checkpoint in fission yeast. Genes Dev *11*, 504-511.

Rhind, N., and Russell, P. (1998). Mitotic DNA damage and replication checkpoints in yeast. Curr Opin Cell Biol *10*, 749-758.

Riddle, D. L., Blumenthal, T., Meyer, B. J., Pries, J. R. (1997). *C. ELEGANS II*. Cold Spring Harbor Laboratrory Press

Robert, M. F., Morin, S., Beaulieu, N., Gauthier, F., Chute, I. C., Barsalou, A., and MacLeod, A. R. (2003). DNMT1 is required to maintain CpG methylation and aberrant gene silencing in human cancer cells. Nat Genet *33*, 61-65.

Robertson, K. D., Ait-Si-Ali, S., Yokochi, T., Wade, P. A., Jones, P. L., and Wolffe, A. P. (2000). DNMT1 forms a complex with Rb, E2F1 and HDAC1 and represses transcription from E2F-responsive promoters. Nat Genet *25*, 338-342.

Roeder, G. S. (1997). Meiotic chromosomes: it takes two to tango. Genes Dev *11*, 2600-2621.

Rommelaere, H., De Neve, M., Neirynck, K., Peelaers, D., Waterschoot, D., Goethals, M., Fraeyman, N., Vandekerckhove, J., and Ampe, C. (2001). Prefoldin recognition motifs in the nonhomologous proteins of the actin and tubulin families. J Biol Chem *276*, 41023-41028.

Rondon, A. G., Gallardo, M., Garcia-Rubio, M., and Aguilera, A. (2004). Molecular evidence indicating that the yeast PAF complex is required for transcription elongation. EMBO Rep *5*, 47-53.

Roos-Mattjus, P., Vroman, B. T., Burtelow, M. A., Rauen, M., Eapen, A. K., and Karnitz, L. M. (2002). Genotoxin-induced Rad9-Hus1-Rad1 (9-1-1) chromatin association is an early checkpoint signaling event. J Biol Chem *277*, 43809-43812.

Rosenberg, S. M., and Hastings, P. J. (2004). Genomes: worming into genetic instability. Nature *430*, 625-626.

Rouault, J. P., Kuwabara, P. E., Sinilnikova, O. M., Duret, L., Thierry-Mieg, D., and Billaud, M. (1999). Regulation of dauer larva development in Caenorhabditis elegans by daf-18, a homologue of the tumour suppressor PTEN. Curr Biol *9*, 329-332.

Rountree, M. R., Bachman, K. E., and Baylin, S. B. (2000). DNMT1 binds HDAC2 and a new co-repressor, DMAP1, to form a complex at replication foci. Nat Genet *25*, 269-277.

Rozenblatt-Rosen, O., Hughes, C. M., Nannepaga, S. J., Shanmugam, K. S., Copeland, T. D., Guszczynski, T., Resau, J. H., and Meyerson, M. (2005). The parafibromin tumor suppressor protein is part of a human Paf1 complex. Mol Cell Biol *25*, 612-620.
Rupes, I. (2002). Checking cell size in yeast. Trends Genet *18*, 479-485.

Saltiel, A. R., and Kahn, C. R. (2001). Insulin signalling and the regulation of glucose and lipid metabolism. Nature *414*, 799-806.

Sancar, A., Lindsey-Boltz, L. A., Unsal-Kacmaz, K., and Linn, S. (2004). Molecular mechanisms of mammalian DNA repair and the DNA damage checkpoints. Annu Rev Biochem *73*, 39-85.

Sanchez, Y., Wong, C., Thoma, R. S., Richman, R., Wu, Z., Piwnica-Worms, H., and Elledge, S. J. (1997). Conservation of the Chk1 checkpoint pathway in mammals: linkage of DNA damage to Cdk regulation through Cdc25. Science *277*, 1497-1501.

Sarbassov, D. D., Ali, S. M., Kim, D. H., Guertin, D. A., Latek, R. R., Erdjument-Bromage, H., Tempst, P., and Sabatini, D. M. (2004). Rictor, a novel binding partner of mTOR, defines a rapamycin-insensitive and raptor-independent pathway that regulates the cytoskeleton. Curr Biol *14*, 1296-1302.

Sarbassov, D. D., Guertin, D. A., Ali, S. M., and Sabatini, D. M. (2005). Phosphorylation and regulation of Akt/PKB by the rictor-mTOR complex. Science *307*, 1098-1101.

Sasagawa, Y., Urano, T., Kohara, Y., Takahashi, H., and Higashitani, A. (2003). Caenorhabditis elegans RBX1 is essential for meiosis, mitotic chromosomal condensation and segregation, and cytokinesis. Genes Cells *8*, 857-872.

Sattlegger, E., and Hinnebusch, A. G. (2000). Separate domains in GCN1 for binding protein kinase GCN2 and ribosomes are required for GCN2 activation in amino acid-starved cells. Embo J *19*, 6622-6633.

Saucedo, L. J., and Edgar, B. A. (2002). Why size matters: altering cell size. Curr Opin Genet Dev *12*, 565-571.

Savitsky, K., Sfez, S., Tagle, D. A., Ziv, Y., Sartiel, A., Collins, F. S., Shiloh, Y., and Rotman, G. (1995). The complete sequence of the coding region of the ATM gene reveals similarity to cell cycle regulators in different species. Hum Mol Genet *4*, 2025-2032.

Schackwitz, W. S., Inoue, T., and Thomas, J. H. (1996). Chemosensory neurons function in parallel to mediate a pheromone response in C. elegans. Neuron *17*, 719-728.

Schalm, S. S., Fingar, D. C., Sabatini, D. M., and Blenis, J. (2003). TOS motif-mediated raptor binding regulates 4E-BP1 multisite phosphorylation and function. Curr Biol *13*, 797-806.

Scheid, M. P., Marignani, P. A., and Woodgett, J. R. (2002). Multiple phosphoinositide 3-kinase-dependent steps in activation of protein kinase B. Mol Cell Biol *22*, 6247-6260.

Schisa, J. A., Pitt, J. N., and Priess, J. R. (2001). Analysis of RNA associated with P granules in germ cells of C. elegans adults. Development *128*, 1287-1298.

Schmelzle, T., and Hall, M. N. (2000). TOR, a central controller of cell growth. Cell *103*, 253-262.

Schmid, S. R., and Linder, P. (1992). D-E-A-D protein family of putative RNA helicases. Mol Microbiol *6*, 283-291.

Schmidt, A., Beck, T., Koller, A., Kunz, J., and Hall, M. N. (1998). The TOR nutrient signalling pathway phosphorylates NPR1 and inhibits turnover of the tryptophan permease. Embo J *17*, 6924-6931.

Schmidt, A., Kunz, J., and Hall, M. N. (1996). TOR2 is required for organization of the actin cytoskeleton in yeast. Proc Natl Acad Sci U S A *93*, 13780-13785.

Schmidt, M., Fernandez de Mattos, S., van der Horst, A., Klompmaker, R., Kops, G. J., Lam, E. W., Burgering, B. M., and Medema, R. H. (2002). Cell cycle inhibition by FoxO forkhead transcription factors involves downregulation of cyclin D. Mol Cell Biol *22*, 7842-7852.

Schmoll, D., Walker, K. S., Alessi, D. R., Grempler, R., Burchell, A., Guo, S., Walther, R., and Unterman, T. G. (2000). Regulation of glucose-6-phosphatase gene expression by protein kinase Balpha and the forkhead transcription factor FKHR. Evidence for insulin response unit-dependent and -independent effects of insulin on promoter activity. J Biol Chem *275*, 36324-36333.

Schumacher, B., Hanazawa, M., Lee, M. H., Nayak, S., Volkmann, K., Hofmann, R., Hengartner, M., Schedl, T., and Gartner, A. (2005). Translational repression of C. elegans p53 by GLD-1 regulates DNA damage-induced apoptosis. Cell *120*, 357-368.

Schumacher, B., Hofmann, K., Boulton, S., and Gartner, A. (2001). The C. elegans homolog of the p53 tumor suppressor is required for DNA damage-induced apoptosis. Curr Biol *11*, 1722-1727.

Scott, P. H., Brunn, G. J., Kohn, A. D., Roth, R. A., and Lawrence, J. C., Jr. (1998). Evidence of insulin-stimulated phosphorylation and activation of the mammalian target of rapamycin mediated by a protein kinase B signaling pathway. Proc Natl Acad Sci U S A *95*, 7772-7777.

Seydoux, G., and Dunn, M. A. (1997). Transcriptionally repressed germ cells lack a subpopulation of phosphorylated RNA polymerase II in early embryos of Caenorhabditis elegans and Drosophila melanogaster. Development *124*, 2191-2201.

Seydoux, G., and Schedl, T. (2001). The germline in C. elegans: origins, proliferation, and silencing. Int Rev Cytol *203*, 139-185.

Shamji, A. F., Nghiem, P., and Schreiber, S. L. (2003). Integration of growth factor and nutrient signaling: implications for cancer biology. Mol Cell *12*, 271-280.

Sheikh, M. S., Rochefort, H., and Garcia, M. (1995). Overexpression of p21WAF1/CIP1 induces growth arrest, giant cell formation and apoptosis in human breast carcinoma cell lines. Oncogene *11*, 1899-1905.

Shen, X., Mizuguchi, G., Hamiche, A., and Wu, C. (2000). A chromatin remodelling complex involved in transcription and DNA processing. Nature *406*, 541-544.

Shi, X., Chang, M., Wolf, A. J., Chang, C. H., Frazer-Abel, A. A., Wade, P. A., Burton, Z. F., and Jaehning, J. A. (1997). Cdc73p and Paf1p are found in a novel RNA polymerase II-containing complex distinct from the Srbp-containing holoenzyme. Mol Cell Biol *17*, 1160-1169.

Shi, X., Finkelstein, A., Wolf, A. J., Wade, P. A., Burton, Z. F., and Jaehning, J. A. (1996). Paf1p, an RNA polymerase II-associated factor in Saccharomyces cerevisiae, may have both positive and negative roles in transcription. Mol Cell Biol *16*, 669-676.

Shiloh, Y. (2003). ATM and related protein kinases: safeguarding genome integrity. Nat Rev Cancer *3*, 155-168.

Shiloh, Y., and Kastan, M. B. (2001). ATM: genome stability, neuronal development, and cancer cross paths. Adv Cancer Res *83*, 209-254.

Shima, H., Pende, M., Chen, Y., Fumagalli, S., Thomas, G., and Kozma, S. C. (1998). Disruption of the p70(s6k)/p85(s6k) gene reveals a small mouse phenotype and a new functional S6 kinase. Embo J *17*, 6649-6659.

Shinagawa, H., and Iwasaki, H. (1996). Processing the holliday junction in homologous recombination. Trends Biochem Sci *21*, 107-111.

Shinagawa, H., Makino, K., Amemura, M., Kimura, S., Iwasaki, H., and Nakata, A. (1988). Structure and regulation of the Escherichia coli ruv operon involved in DNA repair and recombination. J Bacteriol *170*, 4322-4329.

Shull, S., Heintz, N. H., Periasamy, M., Manohar, M., Janssen, Y. M., Marsh, J. P., and Mossman, B. T. (1991). Differential regulation of antioxidant enzymes in response to oxidants. J Biol Chem *266*, 24398-24403.

Siegers, K., Bolter, B., Schwarz, J. P., Bottcher, U. M., Guha, S., and Hartl, F. U. (2003). TRiC/CCT cooperates with different upstream chaperones in the folding of distinct protein classes. Embo J *22*, 5230-5240.

Siegert, R., Leroux, M. R., Scheufler, C., Hartl, F. U., and Moarefi, I. (2000). Structure of the molecular chaperone prefoldin: unique interaction of multiple coiled coil tentacles with unfolded proteins. Cell *103*, 621-632.

Sigler, P. B., Xu, Z., Rye, H. S., Burston, S. G., Fenton, W. A., and Horwich, A. L. (1998). Structure and function in GroEL-mediated protein folding. Annu Rev Biochem *67*, 581-608.

Smith, G. C., Cary, R. B., Lakin, N. D., Hann, B. C., Teo, S. H., Chen, D. J., and Jackson, S. P. (1999). Purification and DNA binding properties of the ataxia-telangiectasia gene product ATM. Proc Natl Acad Sci U S A *96*, 11134-11139.

Sogame, N., Kim, M., and Abrams, J. M. (2003). Drosophila p53 preserves genomic stability by regulating cell death. Proc Natl Acad Sci U S A *100*, 4696-4701.

Solari, F., and Ahringer, J. (2000). NURD-complex genes antagonise Ras-induced vulval development in Caenorhabditis elegans. Curr Biol *10*, 223-226.

Sommers, C. H., Miller, E. J., Dujon, B., Prakash, S., and Prakash, L. (1995). Conditional lethality of null mutations in RTH1 that encodes the yeast counterpart of a mammalian 5'- to 3'-exonuclease required for lagging strand DNA synthesis in reconstituted systems. J Biol Chem *270*, 4193-4196.

Sparagana, S. P., and Roach, E. S. (2000). Tuberous sclerosis complex. Curr Opin Neurol *13*, 115-119.

Squazzo, S. L., Costa, P. J., Lindstrom, D. L., Kumer, K. E., Simic, R., Jennings, J. L., Link, A. J., Arndt, K. M., and Hartzog, G. A. (2002). The Paf1 complex physically and functionally associates with transcription elongation factors in vivo. Embo J *21*, 1764-1774.

Steger, R. W., Bartke, A., and Cecim, M. (1993). Premature ageing in transgenic mice expressing different growth hormone genes. J Reprod Fertil Suppl *46*, 61-75.

Stergiou, L., and Hengartner, M. O. (2004). Death and more: DNA damage response pathways in the nematode C. elegans. Cell Death Differ *11*, 21-28.

Stevens, C., and La Thangue, N. B. (2004). The emerging role of E2F-1 in the DNA damage response and checkpoint control. DNA Repair (Amst) *3*, 1071-1079.

Stevenson, J. B., and Gottschling, D. E. (1999). Telomeric chromatin modulates replication timing near chromosome ends. Genes Dev *13*, 146-151.

Stillman, B. (1989). Initiation of eukaryotic DNA replication in vitro. Annu Rev Cell Biol *5*, 197-245.

Stocker, H., Radimerski, T., Schindelholz, B., Wittwer, F., Belawat, P., Daram, P., Breuer, S., Thomas, G., and Hafen, E. (2003). Rheb is an essential regulator of S6K in controlling cell growth in Drosophila. Nat Cell Biol *5*, 559-565.

Stolinski, L. A., Eisenmann, D. M., and Arndt, K. M. (1997). Identification of RTF1, a novel gene important for TATA site selection by TATA box-binding protein in Saccharomyces cerevisiae. Mol Cell Biol *17*, 4490-4500.

Strasser, K., Masuda, S., Mason, P., Pfannstiel, J., Oppizzi, M., Rodriguez-Navarro, S., Rondon, A. G., Aguilera, A., Struhl, K., Reed, R., and Hurt, E. (2002). TREX is a

conserved complex coupling transcription with messenger RNA export. Nature *417*, 304-308.

Sulston, J. E., and Horvitz, H. R. (1977). Post-embryonic cell lineages of the nematode, Caenorhabditis elegans. Dev Biol *56*, 110-156.

Sutterluty, H., Chatelain, E., Marti, A., Wirbelauer, C., Senften, M., Muller, U., and Krek, W. (1999). p45SKP2 promotes p27Kip1 degradation and induces S phase in quiescent cells. Nat Cell Biol *1*, 207-214.

Suzuki, A., Kusakai, G., Kishimoto, A., Lu, J., Ogura, T., and Esumi, H. (2003a). ARK5 suppresses the cell death induced by nutrient starvation and death receptors via inhibition of caspase 8 activation, but not by chemotherapeutic agents or UV irradiation. Oncogene *22*, 6177-6182.

Suzuki, A., Kusakai, G., Kishimoto, A., Lu, J., Ogura, T., Lavin, M. F., and Esumi, H. (2003b). Identification of a novel protein kinase mediating Akt survival signaling to the ATM protein. J Biol Chem *278*, 48-53.

Swann, M. M. (1957). The control of cell division; a review. I. General mechanisms. Cancer Res *17*, 727-757.

Swanson, M. J., Qiu, H., Sumibcay, L., Krueger, A., Kim, S. J., Natarajan, K., Yoon, S., and Hinnebusch, A. G. (2003). A multiplicity of coactivators is required by Gcn4p at individual promoters in vivo. Mol Cell Biol *23*, 2800-2820.

Szabo, J., Heath, B., Hill, V. M., Jackson, C. E., Zarbo, R. J., Mallette, L. E., Chew, S. L., Besser, G. M., Thakker, R. V., Huff, V., and et al. (1995). Hereditary hyperparathyroidism-jaw tumor syndrome: the endocrine tumor gene HRPT2 maps to chromosome 1q21-q31. Am J Hum Genet *56*, 944-950.

Takahashi, Y., Kadowaki, H., Momomura, K., Fukushima, Y., Orban, T., Okai, T., Taketani, Y., Akanuma, Y., Yazaki, Y., and Kadowaki, T. (1997). A homozygous kinase-defective mutation in the insulin receptor gene in a patient with leprechaunism. Diabetologia *40*, 412-420.

Takanami, T., Mori, A., Takahashi, H., and Higashitani, A. (2000). Hyper-resistance of meiotic cells to radiation due to a strong expression of a single recA-like gene in Caenorhabditis elegans. Nucleic Acids Res *28*, 4232-4236.

Takata, H., Kanoh, Y., Gunge, N., Shirahige, K., and Matsuura, A. (2004). Reciprocal association of the budding yeast ATM-related proteins Tel1 and Mec1 with telomeres in vivo. Mol Cell *14*, 515-522.

Taniguchi, T., Garcia-Higuera, I., Xu, B., Andreassen, P. R., Gregory, R. C., Kim, S. T., Lane, W. S., Kastan, M. B., and D'Andrea, A. D. (2002). Convergence of the fanconi anemia and ataxia telangiectasia signaling pathways. Cell *109*, 459-472.

Tatar, M., Kopelman, A., Epstein, D., Tu, M. P., Yin, C. M., and Garofalo, R. S. (2001). A mutant Drosophila insulin receptor homolog that extends life-span and impairs neuroendocrine function. Science *292*, 107-110.

Taub, J., Lau, J. F., Ma, C., Hahn, J. H., Hoque, R., Rothblatt, J., and Chalfie, M. (1999). A cytosolic catalase is needed to extend adult lifespan in C. elegans daf-C and clk-1 mutants. Nature *399*, 162-166.

Tax, F. E., Yeargers, J. J., and Thomas, J. H. (1994). Sequence of C. elegans lag-2 reveals a cell-signalling domain shared with Delta and Serrate of Drosophila. Nature *368*, 150-154.

Tee, A. R., Manning, B. D., Roux, P. P., Cantley, L. C., and Blenis, J. (2003). Tuberous sclerosis complex gene products, Tuberin and Hamartin, control mTOR signaling by acting as a GTPase-activating protein complex toward Rheb. Curr Biol *13*, 1259-1268.

Temin, H. M. (1971). Stimulation by serum of multiplication of stationary chicken cells. J Cell Physiol *78*, 161-170.

Thomas, G., and Hall, M. N. (1997). TOR signalling and control of cell growth. Curr Opin Cell Biol *9*, 782-787.

Thompson, S. R., Goodwin, E. B., and Wickens, M. (2000). Rapid deadenylation and Poly(A)-dependent translational repression mediated by the Caenorhabditis elegans tra-2 3' untranslated region in Xenopus embryos. Mol Cell Biol *20*, 2129-2137.

Timmons, L., Court, D. L., and Fire, A. (2001). Ingestion of bacterially expressed dsRNAs can produce specific and potent genetic interference in Caenorhabditis elegans. Gene *263*, 103-112.

Timmons, L., and Fire, A. (1998). Specific interference by ingested dsRNA. Nature *395*, 854.

Ting, N. S., and Lee, W. H. (2004). The DNA double-strand break response pathway: becoming more BRCAish than ever. DNA Repair (Amst) *3*, 935-944.

Tishkoff, D. X., Filosi, N., Gaida, G. M., and Kolodner, R. D. (1997). A novel mutation avoidance mechanism dependent on S. cerevisiae RAD27 is distinct from DNA mismatch repair. Cell *88*, 253-263.

Tissenbaum, H. A., and Guarente, L. (2002). Model organisms as a guide to mammalian aging. Dev Cell *2*, 9-19.

Tissenbaum, H. A., and Ruvkun, G. (1998). An insulin-like signaling pathway affects both longevity and reproduction in Caenorhabditis elegans. Genetics *148*, 703-717.

Todone, F., Weinzierl, R. O., Brick, P., and Onesti, S. (2000). Crystal structure of RPB5, a universal eukaryotic RNA polymerase subunit and transcription factor interaction target. Proc Natl Acad Sci U S A *97*, 6306-6310.

Tong, A. H., Evangelista, M., Parsons, A. B., Xu, H., Bader, G. D., Page, N., Robinson, M., Raghibizadeh, S., Hogue, C. W., Bussey, H*., et al.* (2001). Systematic genetic analysis with ordered arrays of yeast deletion mutants. Science *294*, 2364-2368.

Tran, H., Brunet, A., Grenier, J. M., Datta, S. R., Fornace, A. J., Jr., DiStefano, P. S., Chiang, L. W., and Greenberg, M. E. (2002). DNA repair pathway stimulated by the forkhead transcription factor FOXO3a through the Gadd45 protein. Science *296*, 530-534.

Tsaneva, I. R., Muller, B., and West, S. C. (1993). RuvA and RuvB proteins of Escherichia coli exhibit DNA helicase activity in vitro. Proc Natl Acad Sci U S A *90*, 1315-1319.

Tsaneva, I. R., and West, S. C. (1994). Targeted versus non-targeted DNA helicase activity of the RuvA and RuvB proteins of Escherichia coli. J Biol Chem *269*, 26552-26558.

Tsang, W. Y., Sayles, L. C., Grad, L. I., Pilgrim, D. B., and Lemire, B. D. (2001). Mitochondrial respiratory chain deficiency in Caenorhabditis elegans results in developmental arrest and increased life span. J Biol Chem *276*, 32240-32246.

Tsutsui, S., Inoue, H., Yasuda, K., Suzuki, K., Higashi, H., Era, S., and Mori, M. (2005). Reduced Expression of PTEN Protein and Its Prognostic Implications in Invasive Ductal Carcinoma of the Breast. Oncology *68*, 398-404.

Umar, A., and Kunkel, T. A. (1996). DNA-replication fidelity, mismatch repair and genome instability in cancer cells. Eur J Biochem *238*, 297-307.

Unger, M. W., and Hartwell, L. H. (1976). Control of cell division in Saccharomyces cerevisiae by methionyl-tRNA. Proc Natl Acad Sci U S A *73*, 1664-1668.

Usui, T., Ogawa, H., and Petrini, J. H. (2001). A DNA damage response pathway controlled by Tel1 and the Mre11 complex. Mol Cell *7*, 1255-1266.

Vainberg, I. E., Lewis, S. A., Rommelaere, H., Ampe, C., Vandekerckhove, J., Klein, H. L., and Cowan, N. J. (1998). Prefoldin, a chaperone that delivers unfolded proteins to cytosolic chaperonin. Cell *93*, 863-873.

Valenzuela, L., Aranda, C., and Gonzalez, A. (2001). TOR modulates GCN4-dependent expression of genes turned on by nitrogen limitation. J Bacteriol *183*, 2331-2334.

van Haaften, G., Plasterk, R. H., and Tijsterman, M. (2004). Genomic instability and cancer: scanning the Caenorhabditis elegans genome for tumor suppressors. Oncogene *23*, 8366-8375.

van Slegtenhorst, M., de Hoogt, R., Hermans, C., Nellist, M., Janssen, B., Verhoef, S., Lindhout, D., van den Ouweland, A., Halley, D., Young, J.*, et al.* (1997). Identification of the tuberous sclerosis gene TSC1 on chromosome 9q34. Science *277*, 805-808.

Vanfleteren, J. R., and De Vreese, A. (1995). The gerontogenes age-1 and daf-2 determine metabolic rate potential in aging Caenorhabditis elegans. Faseb J *9*, 1355-1361.

Vattem, K. M., and Wek, R. C. (2004). Reinitiation involving upstream ORFs regulates ATF4 mRNA translation in mammalian cells. Proc Natl Acad Sci U S A *101*, 11269-11274.

Vazquez de Aldana, C. R., Wek, R. C., Segundo, P. S., Truesdell, A. G., and Hinnebusch, A. G. (1994). Multicopy tRNA genes functionally suppress mutations in yeast eIF-2 alpha kinase GCN2: evidence for separate pathways coupling GCN4 expression to unchanged tRNA. Mol Cell Biol *14*, 7920-7932.

Vellai, T., Takacs-Vellai, K., Zhang, Y., Kovacs, A. L., Orosz, L., and Muller, F. (2003). Genetics: influence of TOR kinase on lifespan in C. elegans. Nature *426*, 620.

Vowels, J. J., and Thomas, J. H. (1992). Genetic analysis of chemosensory control of dauer formation in Caenorhabditis elegans. Genetics *130*, 105-123.

Waga, S., Bauer, G., and Stillman, B. (1994). Reconstitution of complete SV40 DNA replication with purified replication factors. J Biol Chem *269*, 10923-10934.

Walker, J. E., Saraste, M., Runswick, M. J., and Gay, N. J. (1982). Distantly related sequences in the alpha- and beta-subunits of ATP synthase, myosin, kinases and other ATP-requiring enzymes and a common nucleotide binding fold. Embo J *1*, 945-951.

Wang, L., Eckmann, C. R., Kadyk, L. C., Wickens, M., and Kimble, J. (2002). A regulatory cytoplasmic poly(A) polymerase in Caenorhabditis elegans. Nature *419*, 312-316.

Ward, S., and Carrel, J. S. (1979). Fertilization and sperm competition in the nematode Caenorhabditis elegans. Dev Biol *73*, 304-321.

Wedaman, K. P., Reinke, A., Anderson, S., Yates, J., 3rd, McCaffery, J. M., and Powers, T. (2003). Tor kinases are in distinct membrane-associated protein complexes in Saccharomyces cerevisiae. Mol Biol Cell *14*, 1204-1220.

Wei, W., Gu, J. X., Zhu, C. Q., Sun, F. Y., Dorjsuren, D., Lin, Y., and Murakami, S. (2003). Interaction with general transcription factor IIF (TFIIF) is required for the suppression of activated transcription by RPB5-mediating protein (RMP). Cell Res *13*, 111-120.

Weigmann, K., Cohen, S. M., and Lehner, C. F. (1997). Cell cycle progression, growth and patterning in imaginal discs despite inhibition of cell division after inactivation of Drosophila Cdc2 kinase. Development *124*, 3555-3563.

Weinkove, D., Neufeld, T. P., Twardzik, T., Waterfield, M. D., and Leevers, S. J. (1999). Regulation of imaginal disc cell size, cell number and organ size by Drosophila class I(A) phosphoinositide 3-kinase and its adaptor. Curr Biol *9*, 1019-1029.

Weisman, R., and Choder, M. (2001). The fission yeast TOR homolog, tor1+, is required for the response to starvation and other stresses via a conserved serine. J Biol Chem *276*, 7027-7032.

Wek, S. A., Zhu, S., and Wek, R. C. (1995). The histidyl-tRNA synthetase-related sequence in the eIF-2 alpha protein kinase GCN2 interacts with tRNA and is required for activation in response to starvation for different amino acids. Mol Cell Biol *15*, 4497-4506.

Wendel, H. G., De Stanchina, E., Fridman, J. S., Malina, A., Ray, S., Kogan, S., Cordon-Cardo, C., Pelletier, J., and Lowe, S. W. (2004). Survival signalling by Akt and eIF4E in oncogenesis and cancer therapy. Nature *428*, 332-337.

Wera, S., and Hemmings, B. A. (1995). Serine/threonine protein phosphatases. Biochem J *311 (Pt 1)*, 17-29.

Werner, M., Hermann-Le Denmat, S., Treich, I., Sentenac, A., and Thuriaux, P. (1992). Effect of mutations in a zinc-binding domain of yeast RNA polymerase C (III) on enzyme function and subunit association. Mol Cell Biol *12*, 1087-1095.

West, S. C. (1996). DNA helicases: new breeds of translocating motors and molecular pumps. Cell *86*, 177-180.

West, S. C. (1997). Processing of recombination intermediates by the RuvABC proteins. Annu Rev Genet *31*, 213-244.

Wienecke, R., Konig, A., and DeClue, J. E. (1995). Identification of tuberin, the tuberous sclerosis-2 product. Tuberin possesses specific Rap1GAP activity. J Biol Chem *270*, 16409-16414.

Wolkow, C. A., Kimura, K. D., Lee, M. S., and Ruvkun, G. (2000). Regulation of C. elegans life-span by insulinlike signaling in the nervous system. Science *290*, 147-150.

Wolkow, C. A., Munoz, M. J., Riddle, D. L., and Ruvkun, G. (2002). Insulin receptor substrate and p55 orthologous adaptor proteins function in the Caenorhabditis elegans daf-2/insulin-like signaling pathway. J Biol Chem *277*, 49591-49597.

Wood, M. A., McMahon, S. B., and Cole, M. D. (2000). An ATPase/helicase complex is an essential cofactor for oncogenic transformation by c-Myc. Mol Cell *5*, 321-330.

Woychik, N. A. (1998). Fractions to functions: RNA polymerase II thirty years later. Cold Spring Harb Symp Quant Biol *63*, 311-317.

Woychik, N. A., Liao, S. M., Kolodziej, P. A., and Young, R. A. (1990). Subunits shared by eukaryotic nuclear RNA polymerases. Genes Dev *4*, 313-323.

Wu, X., Braithwaite, E., and Wang, Z. (1999a). DNA ligation during excision repair in yeast cell-free extracts is specifically catalyzed by the CDC9 gene product. Biochemistry *38*, 2628-2635.

Wu, X., Ranganathan, V., Weisman, D. S., Heine, W. F., Ciccone, D. N., O'Neill, T. B., Crick, K. E., Pierce, K. A., Lane, W. S., Rathbun, G.*, et al.* (2000). ATM phosphorylation of Nijmegen breakage syndrome protein is required in a DNA damage response. Nature *405*, 477-482.

Wu, X., Wilson, T. E., and Lieber, M. R. (1999b). A role for FEN-1 in nonhomologous DNA end joining: the order of strand annealing and nucleolytic processing events. Proc Natl Acad Sci U S A *96*, 1303-1308.

Xu, B., Kim, S., and Kastan, M. B. (2001a). Involvement of Brca1 in S-phase and G(2)-phase checkpoints after ionizing irradiation. Mol Cell Biol *21*, 3445-3450.

Xu, B., O'Donnell, A. H., Kim, S. T., and Kastan, M. B. (2002). Phosphorylation of serine 1387 in Brca1 is specifically required for the Atm-mediated S-phase checkpoint after ionizing irradiation. Cancer Res *62*, 4588-4591.

Xu, L., Paulsen, J., Yoo, Y., Goodwin, E. B., and Strome, S. (2001b). Caenorhabditis elegans MES-3 is a target of GLD-1 and functions epigenetically in germline development. Genetics *159*, 1007-1017.

Yang, D. Q., and Kastan, M. B. (2000). Participation of ATM in insulin signalling through phosphorylation of eIF-4E-binding protein 1. Nat Cell Biol *2*, 893-898.

Yart, A., Gstaiger, M., Wirbelauer, C., Pecnik, M., Anastasiou, D., Hess, D., and Krek, W. (2005). The HRPT2 tumor suppressor gene product parafibromin associates with human PAF1 and RNA polymerase II. Mol Cell Biol *25*, 5052-5060.

Yazdi, P. T., Wang, Y., Zhao, S., Patel, N., Lee, E. Y., and Qin, J. (2002). SMC1 is a downstream effector in the ATM/NBS1 branch of the human S-phase checkpoint. Genes Dev *16*, 571-582.

Yochem, J., and Greenwald, I. (1989). glp-1 and lin-12, genes implicated in distinct cell-cell interactions in C. elegans, encode similar transmembrane proteins. Cell *58*, 553-563.

Yu, H., and Larsen, P. L. (2001). DAF-16-dependent and independent expression targets of DAF-2 insulin receptor-like pathway in Caenorhabditis elegans include FKBPs. J Mol Biol *314*, 1017-1028.

Zaragoza, D., Ghavidel, A., Heitman, J., and Schultz, M. C. (1998). Rapamycin induces the G0 program of transcriptional repression in yeast by interfering with the TOR signaling pathway. Mol Cell Biol *18*, 4463-4470.

Zarr, R., Heitman, E., Delclos, G., and Dinh, T. A. (1998). Tuberculosis in Texas: trends and issues in surveillance. Tex Med *94*, 50-56.

Zhang, B., Gallegos, M., Puoti, A., Durkin, E., Fields, S., Kimble, J., and Wickens, M. P. (1997). A conserved RNA-binding protein that regulates sexual fates in the C. elegans hermaphrodite germ line. Nature *390*, 477-484.

Zhang, H., Stallock, J. P., Ng, J. C., Reinhard, C., and Neufeld, T. P. (2000). Regulation of cellular growth by the Drosophila target of rapamycin dTOR. Genes Dev *14*, 2712-2724.

Zhang, P., McGrath, B. C., Reinert, J., Olsen, D. S., Lei, L., Gill, S., Wek, S. A., Vattem, K. M., Wek, R. C., Kimball, S. R.*, et al.* (2002). The GCN2 eIF2alpha kinase is required for adaptation to amino acid deprivation in mice. Mol Cell Biol *22*, 6681-6688.

Zhang, Y., Gao, X., Saucedo, L. J., Ru, B., Edgar, B. A., and Pan, D. (2003). Rheb is a direct target of the tuberous sclerosis tumour suppressor proteins. Nat Cell Biol *5*, 578-581.

Zheng, X. F., Florentino, D., Chen, J., Crabtree, G. R., and Schreiber, S. L. (1995). TOR kinase domains are required for two distinct functions, only one of which is inhibited by rapamycin. Cell *82*, 121-130.

Zheng, X. F., and Schreiber, S. L. (1997). Target of rapamycin proteins and their kinase activities are required for meiosis. Proc Natl Acad Sci U S A *94*, 3070-3075.

Zhou, B. B., and Elledge, S. J. (2000). The DNA damage response: putting checkpoints in perspective. Nature *408*, 433-439.

Zhu, S., Sobolev, A. Y., and Wek, R. C. (1996). Histidyl-tRNA synthetase-related sequences in GCN2 protein kinase regulate in vitro phosphorylation of eIF-2. J Biol Chem *271*, 24989-24994.

Zhu, S., and Wek, R. C. (1998). Ribosome-binding domain of eukaryotic initiation factor-2 kinase GCN2 facilitates translation control. J Biol Chem *273*, 1808-1814.

Zou, L., Cortez, D., and Elledge, S. J. (2002). Regulation of ATR substrate selection by Rad17-dependent loading of Rad9 complexes onto chromatin. Genes Dev *16*, 198-208.

Zou, L., and Elledge, S. J. (2003). Sensing DNA damage through ATRIP recognition of RPA-ssDNA complexes. Science *300*, 1542-1548.

Zuk, D., and Jacobson, A. (1998). A single amino acid substitution in yeast eIF-5A results in mRNA stabilization. Embo J *17*, 2914-2925.

Curriculum vitae

Seestrasse 565

8038 Zürich, Switzerland

Phone: +41 (0) 78 717 56 60

E-mail: christine.parusel@cell.biol.ethz.ch

Name:	Christine Tanja Parusel
Birth date:	08.06.1975
Birthplace:	Frankfurt am Main, Germany
Citizenship:	German
Marital status:	Single

Education

Since 05/2001	**PhD in the field of cancer and metabolic disease** Title: "Functional analysis of the prefoldin URI-1 in *Caenorhabditis elegans*" Friedrich Miescher Institute for Biomedical Research, Basel and Institute of Cell Biology, Eidgenössische Technische Hochschule, Zürich, with Prof. Dr. Wilhelm Krek Expected date of PhD examination: September 2005
09/2000-02/2001	**Diploma thesis in the field of tumour biology** Title: "Regulation of prolactin- and Stat5-dependent genes in mammary epithelial cells" Chemotherapeutic Research Institute Georg-Speyer-Haus, Frankfurt am Main, Germany, with Prof. Dr. Bernd Groner and Prof. Dr. Carrie Shemanko
08/2000	**Diploma degree** in Biochemistry, Biophysical Chemistry and Pharmacy (Grade: 1.0 "with Honours")
10/1995-07/2000	**University studies** in Biochemistry, Pharmacy and Biology, Johann Wolfgang Goethe-University in Frankfurt am Main, Germany
06/1995	High school grade for university entry (Grade 2,2)
09/1986-06/1995	High school, Ziehengymnasium, Frankfurt am Main, Germany

Professional development

Since 04/2005	Postgraduate studies, Economics for scientists, Distance-University Hagen, Germany
05/2002-04/2003	Mentoring programme WIN (Women Into Industry), University of Basel and Novartis AG
07/2002-08/2002	Cold Spring Harbor Laboratory Course on *Caenorhabditis elegans*, Cold Spring Harbor, New York, USA
09/2001	31st Wellcome Trust Course on Genetic, Molecular and Bioinformatic Methods for *Caenorhabditis elegans*, Sanger Center, Cambridge, England

Professional skills

2001-2005	Independent establishment and successful application of a new model system (*Caenorhabditis elegans*) in the host laboratory
2001-2005	Presentation and discussion of scientific results at national and international conferences and seminars
2002-2005	Tutoring of university students in biology and supervision of student practical work using mammalian tumour cell cultures
2003-2005	Technical support and teaching for the Zeiss Axiovision Apotome microscope and computer system

Publications

Parusel CT, Kritikou EA, Hengartner MO, Krek W, and Gotta M: *Caenorhabditis elegans* URI-1 is required for genomic stability (in revision in Development)

Shemanko CS, **Parusel CT**, Liu R, Böcher N, Schultz J, Bor P, Pfitzner E and Groner B: Prolactin-Stat5 induces the expression of the heat shock protein 90α (HSP90α) gene, which sensitizes mammary epithelial cells to apoptosis (manuscript in preparation)

Work experience

1996-2001 **Customer Service in the banking sector**
SEB Card Service GmbH, Frankfurt am Main, Germany
part time (40%) during my university studies

Languages

German (mother tongue)
English (speaking excellent, writing fluent)
Spanish (speaking and writing fluent)
French (speaking and writing intermediate)

Computer skills

Proficiency with MS Office, graphic manipulation software (Adobe Photoshop, Adobe Illustrator, Corel Draw), database software (Endnote) and online scientific databases (Wormbase, PubMed, NCBI)

Zürich, Aug. 25, 2005